

**DEFINING HOW INTESTINAL MUCUS AND MUCUS-DEGRADING COMMENSAL
BACTERIA PROMOTE *CITROBACTER RODENTIUM* PATHOGENESIS**

by

Qiaochu Liang

B.Sc., Acadia University, 2017

A THESIS SUBMITTED IN PARTIAL FULFILLMENT OF
THE REQUIREMENTS FOR THE DEGREE OF

DOCTOR OF PHILOSOPHY

in

THE FACULTY OF GRADUATE AND POSTDOCTORAL STUDIES
(Experimental Medicine)

THE UNIVERSITY OF BRITISH COLUMBIA
(Vancouver)

August 2023

© Qiaochu Liang, 2023

The following individuals certify that they have read, and recommend to the Faculty of Graduate and Postdoctoral Studies for acceptance, the dissertation entitled:

Defining how intestinal mucus and mucus-degrading commensal bacteria promote *Citrobacter rodentium* pathogenesis

submitted by Qiaochu Liang in partial fulfillment of the requirements for

the degree of Doctor of Philosophy

in Experimental Medicine

Examining Committee:

Dr. Bruce A. Vallance, Professor, Pediatrics, UBC

Supervisor

Dr. Dirk Lange, Associate Professor, Urologic Sciences, UBC

Supervisory Committee Member

Dr. Kayla King, Professor, Zoology, UBC

University Examiner

Dr. Wesley Zandberg, Associate Professor, Biochemistry and Molecular Biology, UBC

University Examiner

Additional Supervisory Committee Members:

Dr. Carolina Tropini, Assistant Professor, Microbiology and Immunology, UBC

Supervisory Committee Member

Dr. Theodore S. Steiner, Professor, Department of Medicine, UBC

Supervisory Committee Member

Abstract

The intestinal mucus layer is an essential structure that is well recognized, not only as a key physiochemical barrier that limits direct contact between noxious agents within the intestinal lumen and the underlying epithelium, but also as an important interface between the resident gut microbiota and the host. Mucus is primarily comprised of the mucin (Muc)-2 protein, that is heavily *O*-glycosylated by five major sugar monomers, including sialic acid. To establish infections, enteric pathogens must evolve strategies to adapt to the intestinal environment, overcome the mucus barrier and microbiota-mediated colonization resistance to successfully infect their hosts. I investigated the interactions between the pathogen and mucus, as well as the mucus-degrading commensals during *Citrobacter rodentium* infection. *C. rodentium* is an attaching and effacing pathogen that must cross the colonic mucus layer to infect intestinal epithelial cells (IEC). I demonstrated that upon entering the host, *C. rodentium* localized to the colonic mucus layer and required mucin-derived sialic acid to fuel its growth and virulence. A *C. rodentium* strain deficient in sialic acid uptake ($\Delta nanT$) was dramatically impaired in infecting mice. Sensing of sialic acid also enabled the pathogen to migrate towards mucus and promoted *C. rodentium*'s virulence by inducing the secretion of two key virulence factors, which enhanced the translocation across the mucus layer and increased adhesion to the epithelium. Mucus-degrading commensal bacteria mediated *C. rodentium*'s access to sialic acid by releasing sialic acid from mucin glycans. Correspondingly, the intestines of germ-free (GF) mice contained very low levels of free sialic acid and in line with this, *C. rodentium* displayed impaired virulence when infecting them. However, mice mono-colonized with the commensal bacterium *Bacteroides thetaotaomicron* that can readily degrade mucin glycans displayed increased susceptibility to *C. rodentium* colonic infection. Overall, my research contributes to a better

understanding of how enteric bacterial pathogens interact with mucin glycans, and further emphasizes the crucial role played by mucin-degrading microbiota in enabling these interactions.

Lay Summary

Diarrheal disease-causing bacteria can invade our bodies via contaminated food and water, and upon reaching the gut, they need to reproduce and overcome the immune system's defenses to cause infection. Our gut contains non-disease-causing bacteria (the gut microbiota) and a sticky mucus layer that defend against these invaders. We have discovered that pathogens related to *Escherichia coli* bacteria can use the mucus-degrading capabilities of certain gut microbiota members to access nutrients and grow better, particularly a sugar called sialic acid. This sugar not only provides fuel for the pathogen's growth but also enhances its ability to overcome the mucus barrier and attach to the cells in our gut. This research provides insights into how harmful bacteria can exploit our body's natural defenses to promote infections and may inform the development of alternative treatments beyond antibiotics.

Preface

The research presented herein were conducted in the laboratory of Dr. Bruce A. Vallance at the University of British Columbia, located at the BC Children's Hospital Research Institute. Ethical approval for this research was obtained by the University of British Columbia Animal Care Committee (Protocol A19-0254).

Portions of Chapter 1 has been published: [Liang, Q., & Vallance, B. A. (2021). What's for dinner? How *Citrobacter rodentium*'s metabolism helps it thrive in the competitive gut. *Current Opinion in Microbiology*, 63, 76–82. <https://doi.org/10.1016/j.mib.2021.06.004>]. Text and figures are used with permission from the source. I conducted the literature review, composed the manuscript, created the figures, and contributed to revision of the article. Prof. Bruce A. Vallance helped conceptualize, refine and revise the article.

A version of Chapters 2 and 3 has been accepted for publication: [Liang, Q., Ma, C., Crowley, S. M., Allaire, J. M., Han, X., Chong, R. W. W., Packer, N. H., Yu, H. B., & Vallance, B. A. (2023). Sialic acid plays a pivotal role in licencing *Citrobacter rodentium*'s transition from the intestinal lumen to a mucosal adherent niche. *PNAS in press*.]. I was the lead investigator, responsible for designing and performing the experiments, analyzing the results and writing the manuscript. Caixia Ma assisted in bacteria mutant generation and mouse experiments. Shauna M. Crowley and Nestor Solis assisted in proteomic analysis. Joannie M. Allaire collected mouse intestinal mucus for glycan analysis. Shauna M. Crowley, Xiao Han and Bruce A. Vallance conducted histopathological scoring. Raymond W. W. Chong and Nicolle H. Packer performed Muc2 glycosylation profile analysis. Claire Sie helped quantify virulence gene expression. Bruce

A. Vallance and Hong Bing Yu were the supervisory authors and were involved in study design, data interpretation and manuscript edits.

I was the lead investigator for the work in Chapter 4. I was responsible for all major areas of study design, data collection and analysis, as well as manuscript composition. Joannie M. Allaire conducted the initial experiments on germ-free mice. Joannie M. Allaire, Larissa Celiberto and Hyungjun Yang assisted in gnotobiotic mouse experiments. Gnotobiotic mice mono-colonized with *Bacteroides thetaotaomicron* were generated and obtained from the laboratory of Dr. Carolina Tropini. Shauna M. Crowley assisted in histopathological scoring. Larissa Celiberto performed the infection on GF *Muc2*^{-/-} mice and GF *Muc2*^{+/+} mice. Claire Sie assisted in qPCR and staining. Bruce A. Vallance was the supervisory author and was involved throughout the project in study design, result discussion and manuscript edits. A version of this chapter will be submitted for publication.

Table of Contents

Abstract.....	iii
Lay Summary	v
Preface.....	vi
Table of Contents	viii
List of Tables	xiv
List of Figures.....	xv
List of Symbols	xviii
List of Abbreviations	xix
Acknowledgements	xxii
Dedication	xxiv
Chapter 1: Introduction	1
1.1 Attaching and effacing enteric pathogens.....	1
1.1.1 <i>C. rodentium</i> virulence factors.....	2
1.1.1.1 Type III secretion system.....	2
1.1.1.2 Non-T3SS virulence factors.....	4
1.1.2 <i>C. rodentium</i> infection cycle.....	7
1.1.3 Microbiota impacting <i>C. rodentium</i> virulence.....	10
1.2 Intestinal mucus	12
1.2.1 Properties of intestinal mucus.....	12
1.2.2 Muc2 <i>O</i> -glycosylation	13
1.3 Microbial interactions with the intestinal mucus	14

1.3.1	The influence of gut microbiota on mucus synthesis and integrity	15
1.3.2	Mucus as attachment sites and nutrient sources for commensal microbes	17
1.3.3	Pathogen interactions with mucus	20
1.4	Sialic acids in the gut - an important mucus-derived sugar	23
1.4.1	Sialylation affects mucus integrity, microbiota, and gut inflammation.....	26
1.4.2	Sialic acid metabolism in bacteria	27
1.4.2.1	Sialic acid metabolism in gut microbiota.....	27
1.4.2.2	Sialic acid metabolism in pathogens.....	32
1.5	Nutrient acquisition and metabolism by <i>C. rodentium</i>	34
1.5.1	Phase 1: Overcoming colonization resistance.....	34
1.5.2	Phase 2A: Luminal establishment and crossing the mucus layer	36
1.5.3	Phase 2B: Early expansion and survival at the colonic epithelial surface.....	37
1.5.4	Phase 3: Inflammation, microbial dysbiosis and parasitizing the intestinal epithelium	39
1.5.5	Phase 4: clearance from the mucosal surface	40
1.5.6	Potential targeting of pathogen metabolism	41
1.6	Research objectives.....	45
Chapter 2: Sialic acid metabolism is essential for the fitness of A/E pathogens.....		46
2.1	Synopsis	46
2.2	Introduction.....	46
2.3	Results.....	48
2.3.1	A/E enteric pathogens reside within the colonic mucus layer and can catabolize mucus-derived monosaccharides.	48

2.3.2	Sialic acid is widely expressed in the colon at baseline and during infection	51
2.3.3	A/E pathogens require the NanT transporter to utilize sialic acid	53
2.3.4	Sialic acid utilization is important for the metabolic fitness of <i>C. rodentium</i> in vivo	54
2.3.5	<i>C. rodentium</i> requires NanT to successfully colonize and expand in the large intestine	56
2.3.6	$\Delta nanT$ <i>C. rodentium</i> failed to elicit colitis in a competitive environment	59
2.3.7	Exogenous administration of sialic acid exacerbated <i>C. rodentium</i> -induced colitis	61
2.4	Discussion	62
2.5	Materials and Methods	67
2.5.1	Bacterial strains and growth conditions	67
2.5.2	Mutant construction	67
2.5.3	Bacterial growth curve	68
2.5.4	Murine colonic mucin isolation, purification, and characterization	68
2.5.5	Quantification of free sialic acid	69
2.5.6	Mouse infections	69
2.5.7	Histopathological scoring	70
2.5.8	Immunofluorescence and lectin staining	71
2.5.9	RNA extraction and quantitative real-time PCR for host cytokine responses	71

Chapter 3: Sialic acid metabolism plays a key role in promoting the virulence of A/E pathogens **73**

3.1	Synopsis	73
-----	----------------	----

3.2	Introduction.....	73
3.3	Results.....	75
3.3.1	Sialic acid is sensed by <i>C. rodentium</i> for migration via NanT.....	75
3.3.2	Sialic acid enhances <i>C. rodentium</i> 's ability to degrade mucins.....	76
3.3.3	Sialic acid enhances epithelial adherence of A/E pathogens.....	79
3.3.4	Sialic acid exerts minimal effect on <i>C. rodentium</i> T3SS transcription.....	81
3.3.5	Sialic acid induces the secretion of Pic and EspC proteins in <i>C. rodentium</i>	82
3.3.6	Pic mediates sialic acid-enhanced mucin degradation by <i>C. rodentium</i>	85
3.3.7	Sialic acid enhances the adherence of <i>C. rodentium</i> to IEC by inducing EspC secretion.....	86
3.4	Discussion.....	88
3.5	Materials and Methods.....	95
3.5.1	Chemotaxis assay.....	95
3.5.2	Mucinolytic activity assay.....	96
3.5.3	Mucin transmigration assay.....	96
3.5.4	<i>In vitro</i> bacterial adherence assay.....	97
3.5.5	Immunofluorescence staining.....	97
3.5.6	Detection of <i>ler</i> expression.....	98
3.5.7	Protein secretion assay.....	98

Chapter 4: Gut microbiota promotes nutrient availability and pathogenesis of *C.*

<i>rodentium</i>	100
4.1 Synopsis	100
4.2 Introduction.....	100

4.3	Results.....	103
4.3.1	Sialic acid utilization is not required for <i>C. rodentium</i> colonization and pathogenesis in microbiota-depleted hosts	103
4.3.2	<i>C. rodentium</i> 's access to sialic acid <i>in vivo</i> is dependent on commensal bacteria	105
4.3.3	<i>C. rodentium</i> is impaired in infecting colonic epithelium in GF mice	106
4.3.4	Intestinal mucus limits <i>C. rodentium</i> colonization of colonic epithelium in GF mice	110
4.3.5	Microbiota-derived signals are required for <i>C. rodentium</i> to colonize colonic mucosa	112
4.3.6	<i>Bacteroides thetaiotaomicron</i> enhances <i>C. rodentium</i> 's access to mucin-derived nutrients for growth.....	114
4.3.7	Mice mono-colonized with <i>Bacteroides thetaiotaomicron</i> showed increased susceptibility to <i>C. rodentium</i> infection in the colon.....	116
4.3.8	<i>C. rodentium</i> showed increased epithelial adherence in the colons of <i>B. theta</i> mono-colonized mice.....	117
4.3.9	<i>C. rodentium</i> showed increased T3SS expression in <i>B.theta</i> mono-colonized mice	119
4.4	Discussion.....	121
4.5	Materials and Methods.....	128
4.5.1	Bacterial strains and culture conditions	128
4.5.2	Animals	129
4.5.3	Mouse infections.....	129

4.5.4	Quantification of free sialic acid.....	130
4.5.5	RNA extraction and quantitative real-time PCR for host cytokine responses....	130
4.5.6	Measurement of virulence expression by <i>C. rodentium</i>	131
4.5.7	Fluorescence <i>in situ</i> hybridization (FISH).....	131
4.5.8	<i>C. rodentium</i> growth in <i>B. thetaiotaomicron</i> treated mucins.....	132
4.5.9	<i>C. rodentium</i> and <i>B. thetaiotaomicron</i> mucin co-culture assay.....	133
Chapter 5: Conclusion		134
5.1	Summary and contribution to the field	134
5.2	Limitations and future directions	139
5.3	Final remarks	144
Bibliography		146
Appendices.....		163
Appendix A : Supplementary Figures and Tables		163
A.1	Supplementary Information for Chapter 1	163
A.2	Supplementary Figures and Tables for Chapter 2	163
A.3	Supplementary Figures and Tables for Chapter 3	166
A.4	Supplementary Figures and Tables for Chapter 4	169

List of Tables

Table 3.1 Virulence proteins secreted by <i>C. rodentium</i> in sialic acid-induced culture identified by LC-MS/MS.	84
Table A.2.1 Primers for mutant construction.....	165
Table A.2.2 Primers for qPCR analysis for host cytokine responses	166
Table A.3.1 Primers for qPCR analysis for <i>C. rodentium</i> virulence gene expression.....	168

List of Figures

Figure 1.1 A/E pathogens interact with the colonic epithelium through their T3SS.....	6
Figure 1.2 Phases of <i>C. rodentium</i> infection in C57BL/6 mice.....	9
Figure 1.3 Structures and linkages of sialic acid and sialylated <i>O</i> -glycans on Muc2.	25
Figure 1.4 Representative sialic acid metabolism pathways identified in gut bacteria.	29
Figure 1.5 Metabolic strategies utilized by <i>C. rodentium</i> at different phases of infection.....	43
Figure 1.6 Potential therapeutic approaches to target pathogen nutrition and prevent infections (<i>C. rodentium</i> as an example).	44
Figure 2.1 A/E pathogens reside within the colonic mucus and catabolizes mucus-derived monosaccharides.	50
Figure 2.2 Sialic acid in the colon is mainly derived from mucus produced by goblet cells and widely expressed before and during <i>C. rodentium</i> infection.	53
Figure 2.3 NanT is required for metabolism of sialic acid in <i>C. rodentium</i> and EPEC.	54
Figure 2.4 $\Delta nanT$ <i>C. rodentium</i> is delayed in colonizing mice at a 2.5×10^8 CFU infection dose.	55
Figure 2.5 $\Delta nanT$ <i>C. rodentium</i> is significantly impaired in its ability to colonize mice at a $1 \times$ 10^7 CFU infection dose.	58
Figure 2.6 $\Delta nanT$ <i>C. rodentium</i> failed to elicit colitis and induce an overt inflammatory response.	60
Figure 2.7 Exogenous administration of free sialic acid exacerbated <i>C. rodentium</i> infection.	62
Figure 3.1 NanT is required for <i>C. rodentium</i> chemotaxis towards sialic acid.	76
Figure 3.2 Sialic acid promotes <i>C. rodentium</i> mucin penetration.	78
Figure 3.3 Sialic acid promotes <i>C. rodentium</i> and EPEC epithelial adherence.....	80

Figure 3.4 Sialic acid does not significantly alter <i>C. rodentium</i> T3SS expression.....	82
Figure 3.5 Sialic acid induces secretion of autotransporters Pic and EspC by <i>C. rodentium</i>	84
Figure 3.6 Sialic acid induces Pic mucinase in <i>C. rodentium</i> to accelerate degradation and penetration of the mucus layer.....	86
Figure 3.7 Sialic acid promotes <i>C. rodentium</i> adherence to epithelial cells through EspC.....	87
Figure 3.8 Sialic acid plays a key role in promoting <i>C. rodentium</i> pathogenesis within the gut.	95
Figure 4.1 $\Delta nanT$ <i>C. rodentium</i> displayed comparable pathogenicity to WT <i>C. rodentium</i> in antibiotic pre-treated C57BL/6 mice.	105
Figure 4.2 <i>C. rodentium</i> is dependent on the gut microbiota to liberate sialic acid from intestinal mucins.	106
Figure 4.3 <i>C. rodentium</i> caused minor pathology in GF mouse colons compared to ceca, despite carrying high bacterial burdens at both sites.....	109
Figure 4.4 <i>C. rodentium</i> is impaired in penetrating the mucus layer in the colon of GF mice...	111
Figure 4.5 <i>C. rodentium</i> pre-induced in DMEM containing glucose or GF cecal content showed accelerated infection at the GF cecum but remained resistant in infecting the GF colon.	113
Figure 4.6 <i>B. theta</i> otaomicron-mediated liberation of nutrients from mucins provides substrates for the growth of <i>C. rodentium</i>	115
Figure 4.7 <i>B. theta</i> otaomicron mono-colonized mice showed higher pathogen burdens and more severe pathological damage in their colons compared to GF mice during <i>C. rodentium</i> infection.	117
Figure 4.8 <i>C. rodentium</i> increased colonization of colonic crypts in <i>B. theta</i> mono-associated mice compared to GF mice.	119

Figure 4.9 Virulence expression of <i>C. rodentium</i> in <i>B. theta</i> mono-colonized mice versus GF mice.....	121
Figure 5.1 Proposed model for the interactions between enteric pathogens, the intestinal mucus, and mucus-degrading commensal bacteria.	139
Figure A.2.1 Expression of sialytransferase genes in mouse cecal and colonic tissues before and during <i>C. rodentium</i> infection.....	163
Figure A.2.2 Deletion of the <i>nanT</i> gene does not cause any growth defects in <i>C. rodentium</i> or EPEC when provided with sugars other than sialic acid.	164
Figure A.2.3 $\Delta nanT$ <i>C. rodentium</i> colonizes the mouse intestines at similarly low levels as WT in the early stage of infection.....	165
Figure A.3.1 Sialic acid induces protein secretion by EPEC.....	166
Figure A.3.2 Expression of virulence genes in WT and $\Delta nanT$ in the absence and presence of sialic acid.	167
Figure A.3.3 Migration of WT <i>C. rodentium</i> towards mucin sugars.....	167
Figure A.3.4 The sialometabolic regulon in <i>C. rodentium</i> chromosome.....	168
Figure A.4.1 $\Delta nanT$ <i>C. rodentium</i> was able to spread systematically and induce inflammatory responses in mice deplete of microbiota.	169
Figure A.4.2 <i>B. theta</i> displayed enhanced growth in mucins in the presence of <i>C. rodentium</i> . .	170
Figure A.4.3 Colonization of <i>B. theta</i> remained stable in gnotobiotic mice during <i>C. rodentium</i> infection.	170

List of Symbols

α	Alpha
β	Beta
γ	Gamma
μ	Micro
$<$	Less than
$>$	Greater than
$^{\circ}$	Degree
C	Celsius
-/-	Deficient
\pm	Plus-minus
Δ	Deletion

List of Abbreviations

A/E	Attaching and effacing
ATCC	American Type Culture Collection
<i>B. theta</i>	<i>Bacteroides thetaiotaomicron</i>
BHI	Brain Heart Infusion
BSM	Bovine submaxillary mucins
CAZymes	Carbohydrate-active enzymes
CFU	Colony forming unit
<i>Cr</i>	<i>Citrobacter rodentium</i>
CD	Crohn's disease
CDC	Centers for Disease Control and Prevention
CMAH	Cytidine monophospho- <i>N</i> -acetylneuraminic acid hydroxylase
CRP	cyclic AMP receptor protein
CTRL	Control
DAPI	4',6-diamidino-2-phenylindole
DMEM	Dulbecco's Modified Eagle Medium
DNA	Deoxyribonucleic acid
DPI	Days post-infection
DSS	Dextran sulphate sodium
DTT	Dithiothreitol
<i>E.g.</i>	<i>Exempli gratia</i> (for example)
EAEC	Enterogastric <i>E. coli</i>
EPEC	Enteropathogenic <i>E. coli</i>
Fuc	Fucose
FBS	Fetal bovine serum
FISH	Fluorescence <i>in situ</i> hybridization
FMT	Fecal microbiota transplantation
Gal	Galactose
GalNAc	N-acetylgalactosamine
GCs	Goblet cells
GF	Germ-free
GH	Glycoside hydrolases
GI	Gastrointestinal
GlcNAc	<i>N</i> -acetylglucosamine
h	Hours
H ₂ O ₂	Hydrogen peroxide
H&E	Hematoxylin and eosin
<i>i.e.</i>	<i>id est</i> "in other words"
IAA	Indoleacetic acid
IBD	Inflammatory bowel diseases
IEC	Intestinal epithelial cells
IFN	Interferon
IL	Interleukin
LEE	Locus of enterocyte effacement

LGP	Large undigested glycoproteins
LB	Lysogeny broth
LC-MS/MS	Liquid-chromatography-tandem mass spectrometry
LPS	Lipopolysaccharide
MALII	<i>Maackia amurensis</i> lectin II
MALII ⁺	<i>Maackia amurensis</i> lectin II positive
MFS	Major facilitator superfamily
MOI	Multiplicity of infection
n.s.	Not significant
NADPH	Nicotinamide adenine dinucleotide phosphate
Neu5Ac	<i>N</i> -acetylneuraminic acid
Neu5Gc	<i>N</i> -glycolylneuraminic acid
NI	Non-infected
NOX1	NADPH oxidase 1
OD	Optical density
PAMPs	Pathogen-associated molecular patterns
PBS	Phosphate-buffered saline
PCR	Polymerase chain reaction
PHAC	Public Health Agency of Canada
PMN	Polymorphonuclear neutrophil
PUL	Polysaccharide utilization locus
qPCR	Quantitative polymerase chain reaction
RCF	Relative centrifugal force
RNA	Ribonucleic acid
SCFA	Short-chain fatty acids
SDS-PAGE	Sodium dodecyl sulfate-polyacrylamide gel electrophoresis
SEM	Standard error of mean
SGP	Smaller digested glycoproteins
SNFG	Symbol nomenclature for glycans
Spp	Species
Sia	Sialic acid
SNA	<i>Sambucus nigra</i> agglutinin
SPATE	Serine protease autotransporter of the Enterobacteriaceae
SPF	Specific-pathogen-free (SPF)
ST3GAL4	β -galactoside α 2,3-sialyltransferase 4
ST3GAL6	β -galactoside α 2,3-sialyltransferase 6
ST6GAL1	β -galactoside α 2,6-sialyltransferase 1
ST6/ST6GALNAC1	<i>N</i> -acetylgalactosaminide alpha-2,6-sialyltransferase 1
Strep	Streptomycin
Sus	Starch utilization system
T3SS	Type III secretion system
T6SS	Type VI secretion system
TLR	Toll-like receptor
TSA	Tryptic soy agar
TTC	2,3,5-triphenyltetrazolium chloride

UC
WT

Ulcerative colitis
Wildtype

Acknowledgements

I would like to convey my enduring gratitude to many exceptional people who have supported my PhD studies. I am deeply grateful to Bruce for taking me in as a graduate student, creating an environment that encouraged creativity and flexibility, and allowing me to pursue my research interests. Thanks to Bruce for his tremendous patience, enthusiasm and unwavering support in guiding me throughout my study, and his care for his students' well-being. I could not have asked for a better mentor. I also owe a huge debt of gratitude to the past and current members of the Vallance lab. Thanks, in particular to Caixia Ma, the most amazing lab manager I have ever had, for generously sharing her knowledge of mouse handling and molecular biology, and for always being willing to lend a helping hand when needed. Thanks to my lab mentors, Hong Bing Yu, Shauna Crowley and Joannie Allaire: conversations with them helped me stay motivated and directed through the highs and lows of my projects; and to my student mentees, Mackenzie Gutierrez and Claire Sie, who were always willing to venture into uncharted territory with me and made me immensely proud. Thanks also to Xiao Han and Yan Chen, for making the grad school experience full of fun. And of course, I would like to acknowledge the rest of the Vallance lab members, including Larissa Celiberto, Hyungjun Yang, Kevin Tsai, Andy Sham, Catherine Chan, Irvin Ng, Mariana Hill, Franziska Gräf, Jocelyn Chan, Ashley Gilliland, and Julia Lee. I had great pleasure of working with all of these intelligent and enthusiastic individuals.

I would like to extend my deepest gratitude to my committee members, Dr. Theodore Steiner, Dr. Carolina Tropini, and Dr. Dirk Lange, for their invaluable feedback and guidance throughout my study. I also thank Dr. Nestor Solis for his assistance in proteomic analysis and Dr. Nicki

Packer for her help with Muc2 glycan analysis. In addition, I am grateful to have had the privilege of interacting with numerous exceptional scientists throughout my academic journey. In particular, I am thankful to the inspiring women in science who generously shared their valuable insights and offered me encouragement that helped me overcome obstacles and stay motivated.

I would like to express my deepest appreciation to my dearest friends, Doris, Ada, and Yixian, who have stood by me through thick and thin. They have cheered me on through the many successes and failures in my life, always offering a listening ear and wise advice whenever it is needed. I also want to extend my heartfelt thanks to my housemates, Sunny, Reuben, and Louisa, for their moral support and for creating a warm and welcoming home for me. Last but certainly not least, I am deeply grateful to my family, without whom I could not have accomplished any of this. My parents' unconditional love and support have been the foundation of my success. Their unwavering belief in me, even during times when I doubted myself, has been a constant source of motivation. Looking back, I realize how apprehensive they must have been 11 years ago when they sent their only child to study in a foreign country halfway across the world. Their willingness to take a risk and support my dreams has been truly inspiring. I am truly blessed to have them in my life. I love you very much.

To my parents. Thank you for being my rock and my inspiration, and for your unconditional love and support.

Chapter 1: Introduction

1.1 Attaching and effacing enteric pathogens

Enteric bacterial infections are a growing global health concern and impose a significant burden on society, with their threat increasing in concert with a rise in antibiotic resistance. The clinically important bacterial pathogens, enteropathogenic *Escherichia coli* (EPEC) and enterohemorrhagic *E. coli* (EHEC) both cause acute gastroenteritis in humans. These pathogenic *E. coli* are ranked third (by PHAC and the CDC) in terms of contributing to hospitalizations (following *Salmonella* and *Campylobacter*) and deaths caused by foodborne bacterial infections in both Canada and the US (Collins, 2022; Thomas *et al.*, 2015). Since EPEC and EHEC are specific to humans and poorly pathogenic in mice, their murine specific relative *Citrobacter rodentium* is used as an important tool to model clinically significant *E. coli* infections *in vivo*. *C. rodentium* shares many pathogenic mechanisms with EPEC and EHEC, such as the formation of attaching and effacing (A/E) lesions, through intimate attachment to the intestinal epithelium, effacement of the epithelial brush border, and the formation of elevated pedestal-like structures underneath the adherent bacteria (Collins *et al.*, 2014). Therefore, these three highly related pathogens belong to the family of A/E pathogens.

A/E pathogens belong to the family of Enterobacteriaceae, which are Gram-negative rods that grow rapidly under both aerobic and anaerobic conditions (Ryan, 2017). Over the past decades, *C. rodentium* has contributed significantly to our understanding of the virulence mechanisms employed by bacterial pathogens to colonize the gastrointestinal (GI) tract as well as the host responses that are triggered during infection, including innate and adaptive immunity. Interest in using *C. rodentium* to elucidate pathogen-host-microbiota interactions *in vivo* is steadily

increasing as it is a natural murine pathogen that requires no antibiotic pre-treatment to colonize the mouse GI tract. Thus, studying *C. rodentium* infection in mice offers great potential to lead to the development of novel preventative and therapeutic strategies. This is particularly significant in addressing the growing challenge of antibiotic resistance in enteric bacterial infections and the rising incidence of other intestinal disorders.

1.1.1 *C. rodentium* virulence factors

1.1.1.1 Type III secretion system

The formation of A/E lesions by A/E pathogens is mediated through the type III secretion system (T3SS), which is encoded by genes carried on a pathogenicity island known as the locus of enterocyte effacement (LEE). The LEE T3SS is a complex apparatus that actively delivers bacterial effector proteins directly into the cytoplasm of host intestinal epithelial cells (IEC) (Caballero-Flores *et al.*, 2021). The LEE is conserved among A/E pathogens and encompasses five operons, namely *LEE1-5* that encode the structural components and effectors of the T3SS, as well as chaperones and gene regulators. The master regulator gene *ler* is located in *LEE1*, which encodes Ler (LEE-encoded regulator), a DNA binding protein that promotes the transcription of the five *LEE* operons (Franzin & Sircili, 2015). Ler is therefore essential for the expression of T3SS-related virulence genes, and accordingly, Δler mutants are defective in the formation of A/E lesions (Elliott *et al.*, 2000).

The T3SS injectisome comprises more than 20 proteins that assemble into a syringe-shaped structure protruding above the bacterial surface. The structure of the T3SS can be divided into five parts, starting from the site of contact with the host cell membrane: the translocon, needle,

basal body, export apparatus, and cytoplasmic complex (Figure 1.1B). The translocon, consisting of the EspB and EspD proteins, inserts into the host cell membrane for direct translocation of effectors into the host cytoplasm. The needle is a hollow structure made with repeated copies of the EscF protein that sits on an adaptor formed by EspA filaments which connects the translocon and the needle. The basal body, export apparatus and cytoplasmic complex together serve as the base of the needle assembly, anchoring the T3SS into the inner and outer membranes of the bacterial cell. The basal body spans across both bacterial membranes, with a lower ring attached to the inner membrane and an upper ring extended to the periplasm and outer membrane. The export apparatus is located in the lower ring of the basal body, functioning as the entry portal for effector proteins and a filter that determines the order of secretion. The cytoplasmic complex contains an ATPase called EscN, which is the energy source that powers the secretion system (Hotinger *et al.*, 2021). Deletion of *escN* abolishes the assembly of a functional T3SS, which hinders *C. rodentium*'s capacity to establish its mucosal niche (Deng *et al.*, 2010; Kamada *et al.*, 2012).

The intimate attachment of A/E pathogens to the host's epithelial surface is mediated by the interactions between the outer membrane adhesin intimin and its receptor Tir (translocated intimin receptor). Tir is secreted as an effector and translocated into the host cell plasma membrane by the T3SS. Tir has a loop-like structure that projects into the extracellular space after being inserted into the host cell. Intimin on the bacterial membrane binds the loop region of Tir, thus tightly anchoring the bacterium onto the host cell. Following the binding of intimin, Tir triggers dynamic polymerization of host actin in the cytoplasm, resulting in the accumulation of

actin beneath the attached bacteria that forms a pedestal-like structure rising above the plasma membrane (Figure 1.1A) (Vallance & Finlay, 2000).

While LEE effectors are major contributors for intimate bacterial attachment to the epithelium, non-LEE effectors (Nle) encoded outside the LEE have been shown to aid A/E lesion formation by EPEC *in vitro* (Cepeda-Molero *et al.*, 2017). However, the main role of non-LEE effectors appears to be subverting the host cell signaling pathways to dampen the host inflammatory response through multiple mechanisms (Cepeda-Molero *et al.*, 2020). Deletion of some non-LEE effector genes, such as *nleA* (also named *espl*) (Gruenheid *et al.*, 2004) and *nleB* (Kelly *et al.*, 2006) has been found to highly attenuate the virulence of *C. rodentium in vivo*.

Attachment to the epithelium plays a pivotal role in the pathogenicity of A/E pathogens as these extracellular invaders exert their pathologic effects by adhering to the mucosal surface and translocating effector molecules into the host cells, leading to the induction of host histopathological changes. Hence, the expression of T3SS, bacterial attachment, and pedestal formation are key parameters for assessing the virulence of *C. rodentium*.

1.1.1.2 Non-T3SS virulence factors

In contrast to the T3SS, limited research has been conducted on other virulence factors and mechanisms employed by A/E pathogens to colonize and reach the epithelium before T3SS-mediated adherence. To date, only a few non-T3SS virulence factors have been characterized. Similar to the type IV bundle forming pilus (BFP) of EPEC that facilitates the initial adherence to the epithelium, a type IV pilus termed CFC (colonization factor *Citrobacter*) has been shown

to help *C. rodentium* colonize the mouse colon (Mundy *et al.*, 2003). LifA (lymphocyte inhibitory factor A), a nonfimbrial adhesin also expressed by EPEC and EHEC, has also been found to promote *C. rodentium* colonization (Klapproth *et al.*, 2005). Additional adhesins, including AdcA (adhesin involved in diffuse *Citrobacter* adhesion) and Kfc (K99-like factor involved in *Citrobacter* colonization), which is encoded by a homolog of K99 fimbrial adhesin of enterotoxigenic *E. coli* strains, do not play important roles in *C. rodentium* colonization of mice (Hart *et al.*, 2008). Whether these adhesins contribute to the overall *C. rodentium* infection cycle, such as involvement in initial adherence prior to A/E lesions or conferring tissue tropism, remains unclear (Collins *et al.*, 2014).

C. rodentium harbors two functional type VI secretion systems (T6SSs), T6SS-1 and T6SS-2, encoded by the *cts1* and *cts2* gene clusters respectively (Petty *et al.*, 2010). T6SSs are known to aid in inter-bacterial competition by delivering cytotoxic effectors into target bacterial cells. The T6SS-1 in particular targets commensal Enterobacteriaceae and helps *C. rodentium* outcompete them, thus facilitating *C. rodentium* establishment in the gut during the early phase of infection (Serapio-Palacios *et al.*, 2022). *C. rodentium* also contains 20 putative type V secretion systems or autotransporters, according to a genomic sequence analysis. The majority were identified as putative autotransporter adhesins, although not functionally studied (Petty *et al.*, 2010). Notably, three of these autotransporters belong to the serine protease autotransporter of Enterobacteriaceae (SPATE) family, one being AdcA (described above as an adhesin), and the other two being homologs to the Pic mucinase found in enteroaggregative *E. coli* (EAEC) and EspC secreted by EPEC respectively. Pic (protein involved in intestinal colonization) is a class 2 SPATE that has previously been shown to degrade mucins *in vitro*. The EspC homolog is a class

1 SPATE with predictive cytotoxic effects, but did not cause epithelial cytotoxicity on human Hep-2 epithelial cells. Both are encoded by genes on the large plasmid pCROD1. Interestingly, single deletion mutants of both proteins in *C. rodentium* exhibited a hypervirulent phenotype compared to the wildtype strain, suggesting a novel immunomodulatory role of these SPATEs that remains undefined (Bhullar *et al.*, 2015; Vijayakumar *et al.*, 2014).

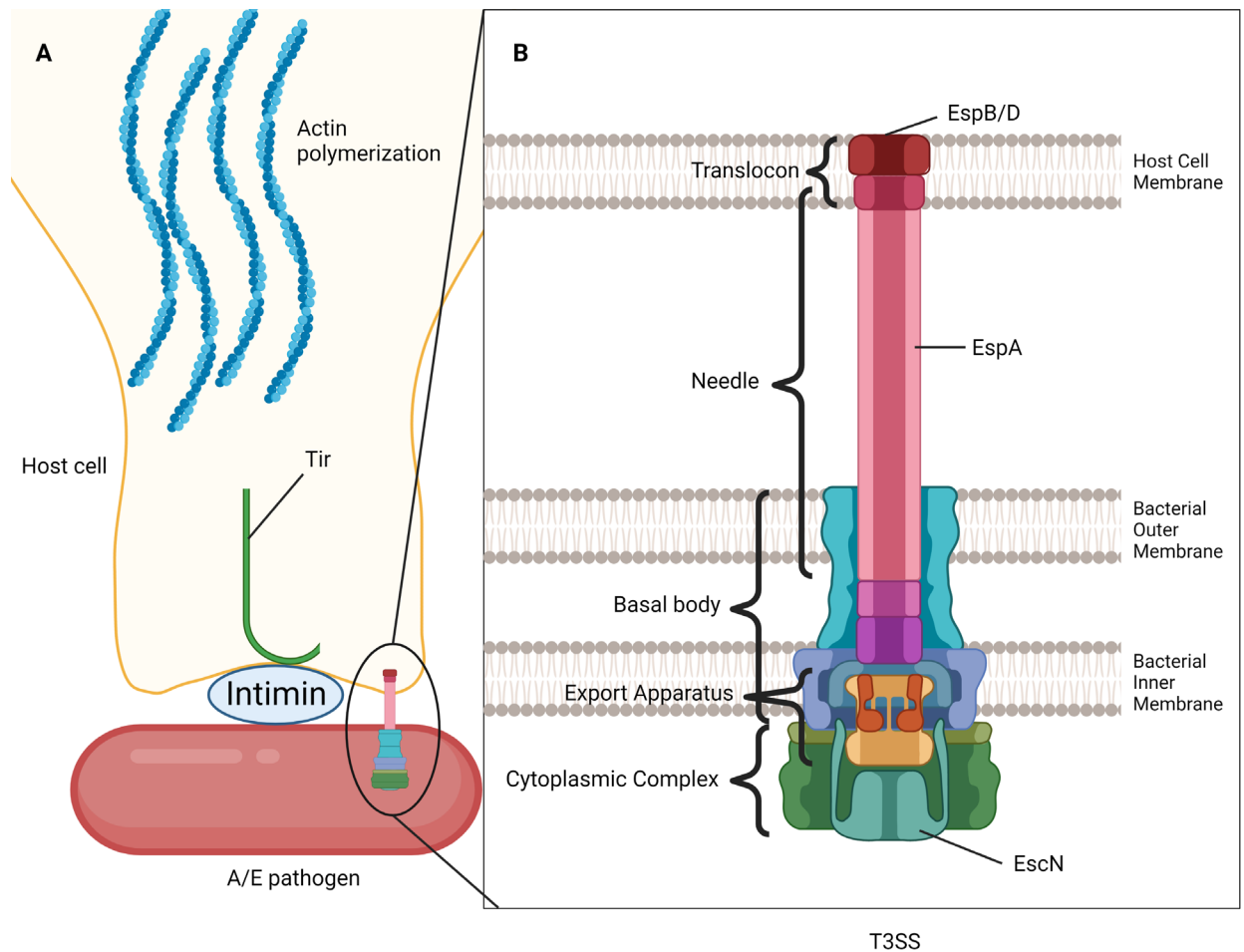


Figure 1.1 A/E pathogens interact with the colonic epithelium through their T3SS.

(A) A/E pathogens localize near the epithelial surface, inject effector proteins in host cells through their T3SS, including the translocated intimin receptor Tir. The adhesion protein, intimin, binds to Tir to firmly attach the bacterium to the host cell. The intracellular domain of Tir invokes actin polymerization, forming a pedestal-like structure beneath the attached pathogen. (B) Structure of the T3SS of A/E pathogens, divided into five parts: the translocon, needle, basal body, export apparatus, and cytoplasmic complex. Figure generated with Biorender.com.

1.1.2 *C. rodentium* infection cycle

C. rodentium, like other foodborne-disease-causing pathogens, is transmitted via the oral-fecal route. It is often modelled in C57BL/6 mice, given through an oral inoculation of laboratory-grown bacterial culture (Bosman *et al.*, 2016). The infection cycle of *C. rodentium* in C57BL/6 mice can be divided into the following four stages (Figure 1.2):

1. Phase 1 (≤ 3 days post infection (DPI)): adaptation and overcoming colonization resistance.
2. Phase 2 (4-6 DPI): establishment and early expansion, crossing the mucus layer and reaching the colonic epithelial surface.
3. Phase 3 (7-12 DPI): onset of host inflammation.
4. Phase 4 (>12 DPI): clearance.

After inoculation, *C. rodentium* first colonizes the cecal patch, a lymphoid tissue in the cecum, where it adapts to the microenvironment of the gut (≤ 3 DPI). At this stage, luminal *C. rodentium* must compete with the gut microbiota and overcome colonization resistance to prevent its removal from the gut. *C. rodentium* then migrates to the distal colon, where it attaches intimately to intestinal epithelial cells (IEC) and rapidly expands, causing substantial microbial dysbiosis in the colon (4-6 DPI). In order to establish, *C. rodentium* needs to coordinate its growth and expression of virulence factors that facilitate penetration of the mucus layer and adherence to the epithelium. During the peak of infection, *C. rodentium* comprises nearly 10% of the luminal population and up to 90% of the mucosal-associated bacteria in the colon. The expression of virulence factors by *C. rodentium* also reprograms host signaling pathways, promoting infection, which leads to widespread inflammation that involves excessive epithelial cell regeneration as an

attempt to replenish IEC infected by the pathogen and subsequently shed (7-12 DPI) (Mullineaux-Sanders *et al.*, 2019). Notably, *C. rodentium* shed at this stage are ‘hyperinfectious’ with high expression of virulence genes, making them capable of infecting naïve mice with a much smaller dose, bypassing the primary adaptation phase at the cecal patch and colonizing the colonic mucosa directly (Wiles *et al.*, 2005).

The host response to *C. rodentium* infection is characterized by colonic crypt elongation (hyperplasia), goblet cell depletion, and immune cell infiltration. Measurements of pathogen burden and histological damage often correlate with the severity of disease (Bhinder *et al.*, 2013). In most mouse strains, including C57BL/6, the infection is self-limiting and clears within 3-4 weeks post-infection. However, C3H strains, such as C3H/HeJ, C3H/HeOuJ, and C3H/HeN mice, are highly susceptible to *C. rodentium* infection and have high infection-induced mortality rates. This susceptibility is mainly due to over-activation of Wnt signaling, which induces excessive expansion of immature, poorly differentiated colonic IEC that are unable to carry out normal intestinal functions (Papapietro *et al.*, 2013).

To initiate the formation of the characteristic A/E lesions, A/E pathogens such as *C. rodentium* must transition from the luminal compartment to a mucosal adherent niche. However, during this process, they encounter multiple barriers, including the resident gut microbiota that provides colonization resistance and the intestinal mucus that prevents bacterial access to the epithelium. The mechanisms by which A/E pathogens overcome these barriers are not yet fully understood.

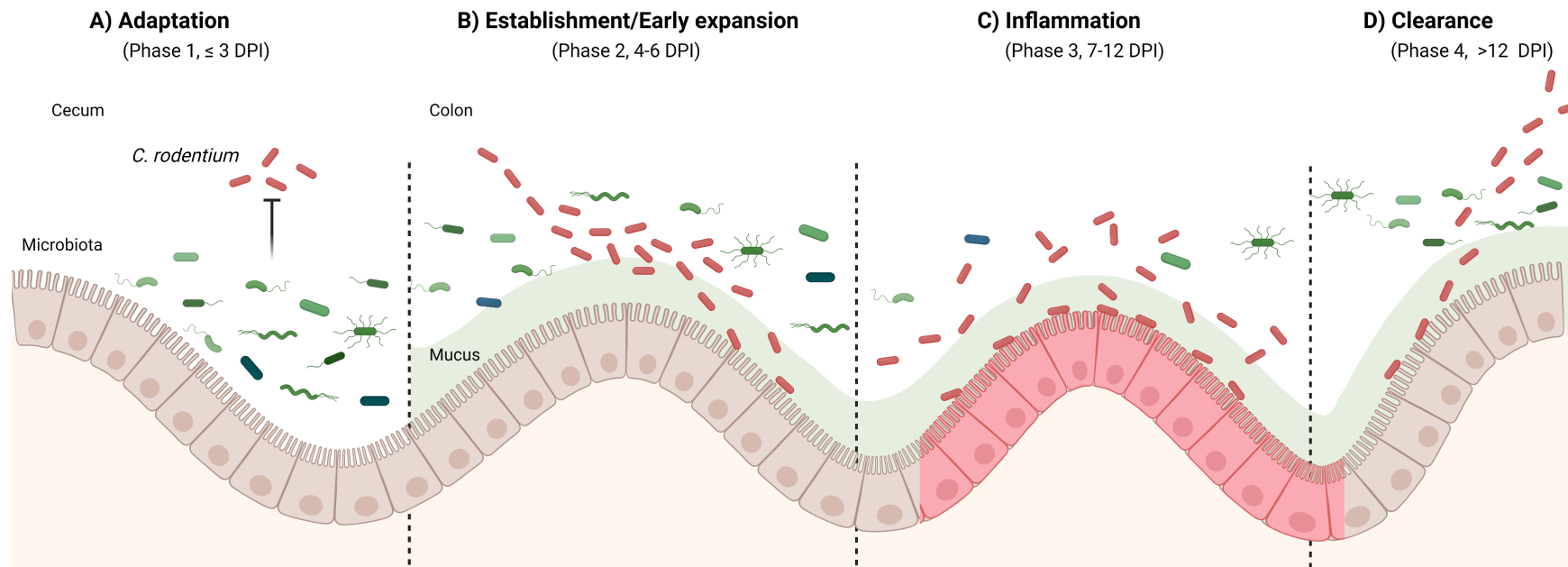


Figure 1.2 Phases of *C. rodentium* infection in C57BL/6 mice.

A) In the adaptation phase (phase 1; ≤ 3 DPI), *C. rodentium* enters the host through the oral-fecal route and mainly colonizes the cecum. *C. rodentium* encounters colonization resistance from the gut microbiota and competes for resources for survival in the lumen. B) In the establishment phase (phase 2; 4-6 DPI), *C. rodentium* expresses virulence factors to overcome the mucus barrier, colonizes the colonic mucosa and expands. C) In the inflammation phase (phase 3; 7-12 DPI), *C. rodentium* triggers intestinal inflammation, causing an increase in luminal oxygen levels. Increased oxygen leads to microbial dysbiosis and further expansion of *C. rodentium* through aerobic respiration. D) In the clearance phase (phase 4, > 12 DPI), *C. rodentium* was displaced from the mucosa by the host's immune response and cleared because it is outcompeted for nutrients/space by commensal bacteria.

1.1.3 Microbiota impacting *C. rodentium* virulence

The "hyperinfectious" phenotype of host-adapted *C. rodentium*, demonstrated during the peak of infection, was found to be lost after overnight passage in laboratory media (Wiles *et al.*, 2005). Host-adapted *C. rodentium* was found to adhere more efficiently to IEC *in vitro* than laboratory-grown cultures (Bishop *et al.*, 2007), and a transcriptomic analysis revealed elevated expression levels of key T3SS effector genes, such as *tir*, *escN*, and several other genes located on the LEE, which are involved in the formation of A/E lesions (Smith *et al.*, 2016). Collectively, these findings suggest that laboratory-grown *C. rodentium* acquires signals from the gut microbiota and/or the host to regulate pathogenesis and achieve the 'hyperinfectious' state, allowing it to establish its niche in the colonic environment. Furthermore, Mullineaux-Sanders *et al.* (2017) found that disrupting commensal bacteria with the antibiotic kanamycin in mice infected with kanamycin-resistant *C. rodentium* at 6 DPI hindered *C. rodentium*'s ability to colonize the colonic mucosa and led to the pathogen persisting avirulently in the cecal lumen. In contrast to kanamycin, treatment with other antibiotics, including vancomycin and metronidazole, did not prohibit colonic colonization by *C. rodentium*. Importantly, this kanamycin-mediated effect was repeated using a *C. rodentium* strain constitutively expressing *ler*, indicating that commensals have a role in altering the pathogenesis of *C. rodentium* beyond regulating LEE expression. These findings highlight the dependence of *C. rodentium* on specific members of the gut microbiota for colonic colonization (Mullineaux-Sanders *et al.*, 2017).

Studies conducted on germ-free (GF) mice provided further insights into the interactions between *C. rodentium* and the gut microbiota during infection. It was found that due to the

absence of colonization resistance, GF mice were highly susceptible to infection even with a low dose of 10^2 colony forming units (CFU), whereas specific-pathogen-free (SPF) mice were fully protected even when given a higher dose of 10^4 CFU. *C. rodentium* also showed rapid colonization and reached a high density in the intestinal lumen of GF mice as early as 1 DPI, regardless of the inoculum dose. However, the population of *C. rodentium* reached a plateau early on in GF mice, which was shown to be constrained by the host's innate immune response (Buschor *et al.*, 2017). Furthermore, another study found that unlike in SPF mice, the T3SS was not required for the expansion of *C. rodentium* in GF mice, as both Δler and $\Delta escN$ mutants without a functional T3SS grew robustly in GF mice. Even so, the T3SS was still necessary for the pathogen to establish a niche at the mucosal surface as Δler *C. rodentium* only localized to the intestinal lumen and not on the epithelial surface. *C. rodentium* persisted long-term in the lumen of GF mice, and could not be cleared except by being outcompeted by gut microbiota members that shared a preference for common carbon nutrients, such as *E. coli*. However, *Bacteroides thetaiotaomicron* which favors the catabolism of polysaccharides and possibly increased the availability of simple sugars, was ineffective in reducing the burden of *C. rodentium* (Kamada *et al.*, 2012), and in some cases, it even increased the mortality of C3H/HeJ mice upon infection (Curtis *et al.*, 2014). This was associated with enhanced expression of virulence genes by *C. rodentium*, such as Pic mucinase, as well as a few LEE-encoded and non-LEE encoded genes (Curtis *et al.*, 2014). Although future studies are needed to elucidate how the virulence factors increased in expression facilitate the infection of *C. rodentium* in the complex gut environment, the results of these studies suggest that metabolites or by-products from the gut microbiota may act as signals to regulate virulence gene expression within *C. rodentium* (discussed in section 1.5).

1.2 Intestinal mucus

1.2.1 Properties of intestinal mucus

The mucus layer overlying the inner surface of the mammalian GI tract is a frontline defender that keeps various hazards away from the epithelium, including co-existing/resident microorganisms, digestive enzymes, food particles and toxins. The organization of mucus varies depending on the intestinal region, with mucus at each site serving unique functions. In the small intestine, which is the primary site for food digestion, there is a loose, single layer of mucus that is permeable to allow nutrient absorption by the underlying epithelium. At the same time, this mucus contains antimicrobials released by underlying Paneth cells to repel bacteria (Gustafsson & Johansson, 2022; Herath *et al.*, 2020). In the mouse ceca, the mucus is discontinuous and predominantly covers the bottom of cecal crypts, leaving the top of the crypts and cecal patch exposed for active antigen sampling, but also leaving it prone to pathogen colonization. Due to its discontinuous morphology, the mucus layer in the cecum is significantly thinner than the mucus layers found in both the small intestine and the colon (Furter *et al.*, 2019). On the other hand, the proximal colon produces the majority of luminal mucus in the GI tract, which encapsulates fecal pellets as they start to form at the distal part of the proximal colon (Bergstrom *et al.*, 2020; Kamphuis *et al.*, 2017). Moving towards the distal colon, the density and abundance of mucus increases, and a region-specific mucus subtype develops, marked by the presence of mucus positively stained by the *Maackia amurensis* lectin II (MALII). As fecal pellets transition from the proximal colon to the distal colon, they undergo a secondary encapsulation by MALII⁺ mucus (Bergstrom *et al.*, 2020). This, in addition to the proximal colon-derived mucus that previously encapsulated them, strengthens the barrier between the luminal material and the host epithelium. This barrier provides significant protection to the underlying IEC as the bacterial

load drastically increases and the fecal content becomes more compact in the distal colon. These barriers are necessary to segregate the microbiota from the epithelium and reduce mechanical damage to the colonic mucosa.

Intestinal mucus is produced by goblet cells (GCs), a specific secretory subtype of IEC. Mucin-2 (MUC2 in human, Muc2 in mice; the murine nomenclature will be used in this dissertation), the predominant core protein that forms the secreted mucus, is densely glycosylated and crosslinked within the Golgi apparatus of GCs. After being released from the GC vesicles, Muc2 unfolds into net-like sheets and expands to at least 1000 times its initial volume (Gustafsson & Johansson, 2022). The colonic mucus comprises two layers, an inner barrier layer that is virtually sterile and impenetrable to the microbiota, and a less defined outer niche layer that harbors bacteria. The outer layer is solely derived from the proximal colon. The inner barrier layer consists of mucus derived from both the proximal colon and the distal colon, presumably to provide adequate protection for the underlying epithelium (Bergstrom & Xia, 2022).

1.2.2 Muc2 *O*-glycosylation

Muc2, the major constituent of mucus, is extensively *O*-glycosylated through the modification of threonine and serine residues with *N*-acetylgalactosamine (GalNAc) at the proline, threonine and serine-rich (PTS) domains that make up the core of the Muc2 protein. These glycans are further elongated by various combinations of monosaccharides, giving rise to a dense carbohydrate-rich matrix that constitutes over 80% of the molecular weight of Muc2 and provides mucus with its viscous properties (Hansson, 2019).

The Muc2 *O*-glycans are composed of five major monosaccharides: *N*-acetylgalactosamine (GalNAc), *N*-acetylglucosamine (GlcNAc), galactose (Gal), sialic acid (Sia), and fucose (Fuc). The precursor of the Muc2 *O*-glycan, GalNAc-Ser/Thr, is referred to as the Tn antigen. The addition of Gal, GlcNAc, or GalNAc on the 3-OH or 6-OH groups of the initiating GalNAc residue results in the primary “core” *O*-glycan structures core 1-4. These oligosaccharides are further extended and often terminated by Sia and Fuc (Arike & Hansson, 2016). Sulfate groups can be added to the 6-OH position of GlcNAc (6S-GlcNAc) and the 3-, 4- or 6-OH positions of Gal (3S-, 4S- and 6S-Gal, respectively) to terminate the glycosylation (Holmén Larsson *et al.*, 2013; Robbe *et al.*, 2003; Thomsson *et al.*, 2012). The biosynthesis of Muc2 *O*-glycans is mediated through a large array of glycosyltransferases and sulfotransferase, with the expression of these enzymes varying in different regions of the gastrointestinal tract and altered under different physiological conditions, such as inflammation (Arike *et al.*, 2017). The varied expression of glycosyltransferases results in differences in mucin glycosylation along the GI tract, with a decreasing gradient of fucosylation and an increasing gradient of sialylation from ileum to rectum in humans (Robbe *et al.*, 2004) and a reverse gradient in mice (Holmén Larsson *et al.*, 2013). Thus, Muc2 glycosylation pattern is differentially and dynamically regulated.

1.3 Microbial interactions with the intestinal mucus

The mammalian GI tract is a complex environment that contains a vast number of commensal microbes. These microbes are largely confined to the lumen of the large intestine by physiochemical barriers, such as the epithelium and the overlying mucus layer. Over the course of the host’s development, the resident bacteria and other microbes colonize unique biogeographical niches within the colon, reflecting their ability not only to withstand local

environmental conditions but also to obtain nutrients from their hosts or nearby microbes (Donaldson *et al.*, 2016; Tropini *et al.*, 2017). Such a complex web of microbe-host interactions is typically beneficial to both the microbes and their hosts (Allaire *et al.*, 2018; Lee *et al.*, 2022; Soderholm & Pedicord, 2019). However, the gut is also the primary route for bacterial pathogens to enter their host (*i.e.* through ingested food or water) (Rogers *et al.*, 2022). To successfully infect their hosts, invading pathogens must subvert host defenses and overcome colonization resistance by competing with the resident microbiota for limited nutrients and space (Nguyen *et al.*, 2021; Rogers *et al.*, 2022). The intestinal mucus layer, which sits between host tissues and the vast microbiota, serves as the interface where interactions between invading pathogens, the gut microbiota and the host immune system take place (Bergstrom & Xia, 2022).

1.3.1 The influence of gut microbiota on mucus synthesis and integrity

The composition and thickness of mucus, which is made up of highly glycosylated mucin proteins, depends on the status of the host and its microbiota (Johansson & Hansson, 2016). The gut microbiota influences mucin gene expression, glycosylation, and secretion, and the regional-specific glycosylation characteristics of intestinal mucus are acquired only after birth, in parallel with the establishment of the gut microbiota. The sialic acid-fucose gradient is not present in the fetal intestine, but it develops during weaning (Robbe-Masselot *et al.*, 2009). Similarly, in GF mice, the inner mucus layer in the colon appears to be far more permeable than that of conventionally raised mice (Johansson *et al.*, 2015). This is accompanied by shorter mucin *O*-glycans on GF intestinal mucins, and glycosyltransferases involved in *O*-glycan elongation were found to be less abundant in GF mice (Arike *et al.*, 2017). The maturation/normalization of the mucus layer of GF mice to the typical thick and impermeable mucus layer requires at least five

weeks after microbial colonization (Johansson *et al.*, 2015), and it depends on the structure of the microbial community, as different microbiota give rise to distinct mucus phenotypes (Jakobsson *et al.*, 2015).

Specific gut bacteria have been shown to shape mucin glycosylation. For instance, *Bacteroides thetaiotaomicron* (*B. theta*), a common member of the intestinal flora in both rodents and humans, induces fucosylation in the mouse ileum, enabling it to forage on fucosylated glycans as a nutrient source (Bry *et al.*, 1996; Hooper *et al.*, 1999). *B. theta* has also been shown to induce mucin-related gene expression in rat colons, enhancing mucin synthesis and sialylation (Wrzosek *et al.*, 2013). *Bifidobacterium longum*, a commonly used probiotic, is capable of restoring mucus defects caused by a Western style diet, such as a lower mucus growth rate and increased mucus penetrability (Schroeder *et al.*, 2018).

The intestinal mucus undergoes rapid turnover to maintain its optimal protective function, which is strictly regulated to ensure that it remains effective in protecting the intestinal epithelium from harmful pathogens while allowing beneficial bacteria to thrive. The inner mucus layer found in the colon of a healthy mouse expands at a rate of approximately 2 $\mu\text{m}/\text{min}$ (Gustafsson *et al.*, 2012). In Crohn's Disease (CD) patients, their intestinal mucus can be thicker than that of healthy individuals, even in the absence of inflammation. The overproduction of mucus can impair the quality of the mucus barrier, as the post-translational glycosylation process may fall behind, resulting in reduced *O*-glycan chains that would otherwise contribute to the viscoelastic properties of mucus. Conversely, in Ulcerative Colitis (UC) patients, their mucus layer is often thinner, causing attrition of mucus and exposing the underlying epithelium to commensal

bacteria and pathogens (Sun *et al.*, 2016). Therefore, mucus digestion by mucus-degrading commensal bacteria (discussed in section 1.3.2) at a rate that does not exceed mucus renewal by the host is essential to promote appropriate mucus turnover and establish a symbiotic relationship between the host and commensal bacteria.

1.3.2 Mucus as attachment sites and nutrient sources for commensal microbes

The symbiotic relationship between the gut microbiota and their host is vital for disease prevention and promoting their well-being. To maintain the health of the gut microbiota, host innate defense develops tolerance towards symbionts, with the intestinal mucus barrier function playing a significant role in this. The multi-layered structure of the intestinal mucus, with an outer layer colonized by microbes and an inner barrier layer that is largely impenetrable, keeps microbes that thrive in mucus nourished but spatially separated from the colonic epithelium. Mice genetically deficient in Muc2 (*Muc2*^{-/-}) have been found to develop spontaneous colitis (Van der Sluis *et al.*, 2006) and are more susceptible to enteric infections than wildtype mice (Bergstrom *et al.*, 2010; Cornick *et al.*, 2017; Zarepour *et al.*, 2013). The microbiota in *Muc2*^{-/-} mice is in direct contact with the intestinal epithelium and localize deep in the crypts, suggesting that the loss of segregation between the microbiota and colonic tissues may contribute to gut inflammation (Johansson *et al.*, 2008). As noted earlier, defective mucus has been observed in human patients with active UC. Mucus in these patients is thinner, altered in glycosylation, and more penetrable to bacteria than patients in remission, indicating a potential role for mucus in IBD pathogenesis (Johansson *et al.*, 2014; Johansson & Hansson, 2016).

The microbial populations in the GI tract are organized both longitudinally and along a cross-sectional axis. Bacterial densities and diversities are much higher in the cecum and colon. The lack of readily available simple carbon sources in the cecum and colon facilitates the growth of polysaccharide-degrading anaerobes, which forage either the dietary polysaccharides that are not digested in the small intestine by the host, or the carbohydrate-rich mucins. The intestinal mucus creates a distinct habitat for specific bacterial ecosystems. Multiple mouse and human studies have shown that the composition of microbial communities in the central luminal compartment is significantly different from those residing near the colonic crypts (Donaldson *et al.*, 2016; Li *et al.*, 2015). By providing attachment sites and nutrient sources to the mucosa-associated microbiota, the intestinal mucus maintains the coexistence of certain species in close proximity to the host tissue.

Mucin glycans are binding sites for those gut microbes containing adhesins that recognize mucin carbohydrates. For instance, *Lactobacillus*, *Ruminococcus gnavus*, and *Bacteroides fragilis* have been shown to directly bind to intestinal mucins or mucin *O*-glycans, occupying a unique niche that protects them from being washed out following infections or antibiotic disturbance (Bergstrom & Xia, 2022). The binding of these beneficial bacteria to intestinal mucus potentially saturates niches that are required for pathogens or pathobionts to colonize, thus providing a possible mechanism of colonization resistance (Lee *et al.*, 2013).

Commensal bacteria possessing functional Carbohydrate-Active enZymes (CAZymes) that cleave complex mucin glycans are considered mucin degraders, and these include *Bacteroides* (e.g., *B. thetaiotaomicron*, *B. fragilis*), *Akkermansia muciniphila*, and *Ruminococcus* (e.g., *R.*

gnavus, *R. torques*). These species are enriched in the colons of mice and humans (Berry *et al.*, 2013; Png *et al.*, 2010). A variety of glycoside hydrolases (GHs, a subset of CAZymes) and sulfatases encoded by mucus degraders are involved in the sequential release of mucin glycans. In *Bacteroides*, these GHs are organized in polysaccharide utilization loci (PULs), consisting of sets of co-regulated genes (GHs, sugar transporters, sensors, regulatory proteins *etc.*) responsible for utilizing a single glycan or glycans similar in structure (Grondin *et al.*, 2017). *A. muciniphila* possesses extracellular and intracellular GHs, working in coordination to hydrolyze up to 85% of mucin structures (Derrien, 2007). While traditional models of mucin glycan degradation have largely proposed the sequential trimming of terminal monosaccharides by exo-acting GHs, the characterization of an endo-acting *O*-glycanase from the GH16 family has introduced an additional mechanism for commensals to access oligosaccharides from *O*-glycan chains, import them into the periplasm to allow further degradation by other CAZymes. Interestingly, these endo *O*-glycanase activities require the prior removal of the capping sialic acids (Crouch *et al.*, 2020). Furthermore, sulfatases and sulfoglycosidases, which remove the sulfate groups or sulphated saccharides, have been shown to enhance the accessibility of other GHs to colonic *O*-glycans and further contribute to the fitness of commensals that encode them in the gut (Luis *et al.*, 2021; Katoh *et al.*, 2023). The liberated monosaccharides or oligosaccharides are subsequently harvested by mucus degraders for their own metabolism, through the starch utilization system (Sus)-like system in *Bacteroidota* (formerly *Bacteroidetes*) and sugar transporters in other bacteria to establish their own nutrient-providing niche (Koropatkin *et al.*, 2012). Mucin glycans are rich endogenous sources of energy, making the commensal bacteria that feed on them more resistant to perturbations such as diet fluctuations and antibiotic administration (Donaldson *et al.*, 2016).

Mucin glycans also benefit other bacteria that lack GHs but express relevant sugar metabolism pathways, exemplifying bacterial cross-feeding. The most significant outcome of microbial cross-feeding is the production of short-chain fatty acids (SCFA): acetate, butyrate, and propionate. Butyrate, which is the primary energy source for colonocytes and plays a key role in maintaining mucosal health, is generally produced by bacteria belonging to the phylum Bacillota (previously known as Firmicutes). Mucus degraders produce acetate and propionate from mucin glycans, which are subsequently converted to butyrate by butyrate producers (Berkhout *et al.*, 2021). Butyrate then diffuses through the mucus, is absorbed and used by IEC via SCFA oxidation, a process that consumes oxygen, thereby promoting anaerobiosis which is favored by many commensal bacteria. Therefore, mucus sustains the mutualistic symbiosis between the gut microbiota and their hosts. However, further evidence focusing on the mucus-associated microbiota is required to elucidate the role of this microbial community in regulating intestinal homeostasis.

1.3.3 Pathogen interactions with mucus

The mucus layer is an important site for host-pathogen interactions, as many pathogens use mucus as an initial site to adhere/adapt to their host. As such, pathogens presumably adapt to the mucus environment to not only overcome the mucus barrier but also prepare to interact with the underlying epithelial cells to cause disease. Availability of nutrients in the mucus layer can affect the metabolism and virulence of infecting pathogens. While most enteric bacterial pathogens are unable to digest intact mucus because they do not encode mucin-degrading GHs (Pruss *et al.*, 2021), they do appear to exploit the sugars that commensal microbes cleave from mucins, using

them as a source of nutrition. *Salmonella enterica* serovar Typhimurium, *E. coli*, and *Clostridioides difficile* consume sialic acids released by *Bacteroides* within the gut, to expand during colitis (discussed in 1.4.2.2) (Huang *et al.*, 2015; Ng *et al.*, 2013). Strains of *Campylobacter jejuni* encode fucose metabolism genes that allow them to scavenge liberated fucose, with the fucose facilitating its colonization and pathogenesis (Dwivedi *et al.*, 2016; Stahl *et al.*, 2011). EHEC can efficiently use multiple mucin-related monosaccharides as carbon sources for growth (Fabich *et al.*, 2008). Pathogens can also use favorable nutrients derived from mucins as chemoattractants to stimulate their migration towards mucus, as demonstrated by *C. difficile* (Engevik *et al.*, 2021) and *C. jejuni* (Dwivedi *et al.*, 2016).

To reach the epithelium and disrupt their target cell's functions, pathogens must also develop strategies to subvert the protective barrier functions of the mucus layer. Motility is important for *S. Typhimurium* (Furter *et al.*, 2019) and *C. jejuni* (Stahl *et al.*, 2016) to penetrate the mucus layer. Non-flagellated *S. Typhimurium* loses its motility, rendering it unable to penetrate the inner mucus layer and reach the colonic epithelium (Furter *et al.*, 2019). In contrast, the helical shape of *C. jejuni* allows it to propel efficiently through the viscous environment of the mucus (Stahl *et al.*, 2016). Pathogens have also evolved an array of proteases to degrade intestinal mucus. Mucin-degrading enzymes, collectively termed mucinases, include GHs that cleave mucin oligosaccharides, and proteases that break down the mucin protein backbone. The majority of our understanding on pathogen mucinases is centered on proteases as the expression of GHs in pathogens is very limited (Sjögren & Collin, 2014). In contrast, the expression of mucin proteases is much lower in commensal bacteria than in pathogens, demonstrated by a comparative study that evaluated the secretion level of the metalloprotease YghJ in pathogenic *E.*

coli and commensal *E. coli* (Luo *et al.*, 2014). Therefore, pathogens utilize a strategic approach to exploit commensal bacteria's capacity to degrade mucin glycans, using them as a source of nutrients for their own survival, while cleaving the mucin peptide backbone using proteases to disassemble the mucin polymeric network, enabling their penetration of intestinal mucus.

A/E pathogens colonize the intestinal mucosa of their respective hosts by transiting across the intestinal mucus layer through as yet unknown mechanisms, then adhering to the intestinal epithelium and forming A/E lesions on their mucosal surface. The mechanisms by which A/E pathogens overcome the intestinal mucus barrier is not fully understood, however there are three proteases encoded by A/E pathogens, SslE found in EPEC and EHEC (Nesta *et al.*, 2014), StcE in EHEC (Hews *et al.*, 2017; In *et al.*, 2015), and Pic in *C. rodentium* (Bhullar *et al.*, 2015), that have been associated with mucin degradation. The exact roles they play in helping these pathogens to navigate through mucus remain controversial due to the lack of *in vivo* evidence, as well as the additional immunomodulatory effects that these proteases demonstrated (Bhullar *et al.*, 2015). In addition, EPEC and EHEC have flagella that exhibit adhesive properties against mucins (Erdem *et al.*, 2007). It is unclear whether their motility, provided by flagella, aids in their ability to cross the mucus layer.

In conclusion, the interactions that occur between commensal gut microbes and intestinal mucus are usually mutually beneficial for both the host and the resident commensals. Disrupted mucus–gut microbiota interactions can lead to mucus dysfunction and an imbalanced gut microbiota, increasing the susceptibility to intestinal disorders, such IBD and colorectal cancer (Johansson &

Hansson, 2016). Enteric pathogens have evolved various strategies to subvert the mucus barrier, enabling them to escape the gut lumen and reach their target host cells.

1.4 Sialic acids in the gut - an important mucus-derived sugar

Sialic acids are a family of nine-carbon-backbone acidic monosaccharides that are derivatives of neuraminic acids. In the gut, mucins are the primary source of sialic acid (Bell *et al.*, 2023).

Many of the glycans identified in mucins from the mouse intestine (Holmén Larsson *et al.*, 2013) and human colonic biopsies (Holmén Larsson *et al.*, 2009) are mono-, di-, or tri-sialylated. Sialic acid is crucial for maintaining both mucus integrity and intestinal homeostasis (discussed below). Sialic acid is located at the terminal position of mucin glycans, making its release the initial step in the sequential degradation of mucin glycans from their non-reducing ends (Juge *et al.*, 2016).

Sialylation of mucins varies regionally throughout the GI tract, with an increasing gradient of sialic acid from the ileum to the rectum in humans (Robbe *et al.*, 2004), whereas the gradient is reversed in mice (Holmén Larsson *et al.*, 2013). The most common form of sialic acid in the mammalian GI tract is *N*-acetylneuraminic acid (Neu5Ac) (Lin *et al.*, 2022). Neu5Ac, with an acetyl group on the fifth carbon (C-5), can be converted to the second most abundant form, *N*-glycolylneuraminic acid (Neu5Gc) by hydroxylation of the acetyl group to a glycolyl group (Figure 1.3A). However, Neu5Gc exists in only trace amounts in humans due to the absence of the CMP-*N*-acetylneuraminic acid hydroxylase (CMAH) enzyme that catalyzes the hydroxylation (Altman & Gagneux, 2019).

Sialic acid residues (Neu5Ac) are attached to Muc2 *O*-glycans via an α 2,3 linkage to Gal, or α 2,6 linkage to Gal or GalNAc, through the action of sialyltransferases. The main sialyltransferases identified in the mouse IEC are ST3GAL4, ST3GAL6, and ST6GAL1 (Figure 1.3B). Among them, ST3GAL4 shows the highest expression in the small intestine, whereas ST3GAL6 and ST6GAL1 are most highly expressed in the colon. Bacterial colonization increases the expression of sialyltransferases, aligning with the higher abundance of sialylated glycans in the colons of conventionally raised mice as compared to GF mice (Arike *et al.*, 2017). Neu5Ac can be further modified by *O*-acetyl groups at C-4, 7, 8, 9 positions. In mice, the colon shows the highest levels of *O*-acetylation, representing approximately 17% of sialic acid being *O*-acetylated at one or more positions. The primary *O*-acetylation location is at the C-9 position, forming 9-*O*-Ac sialic acid. The *O*-acetyl groups then spontaneously migrate between C-7 to 9, leaving C-9 available again for *O*-acetylation to generate multi-acetylated sialic acid (Barnard *et al.*, 2020).

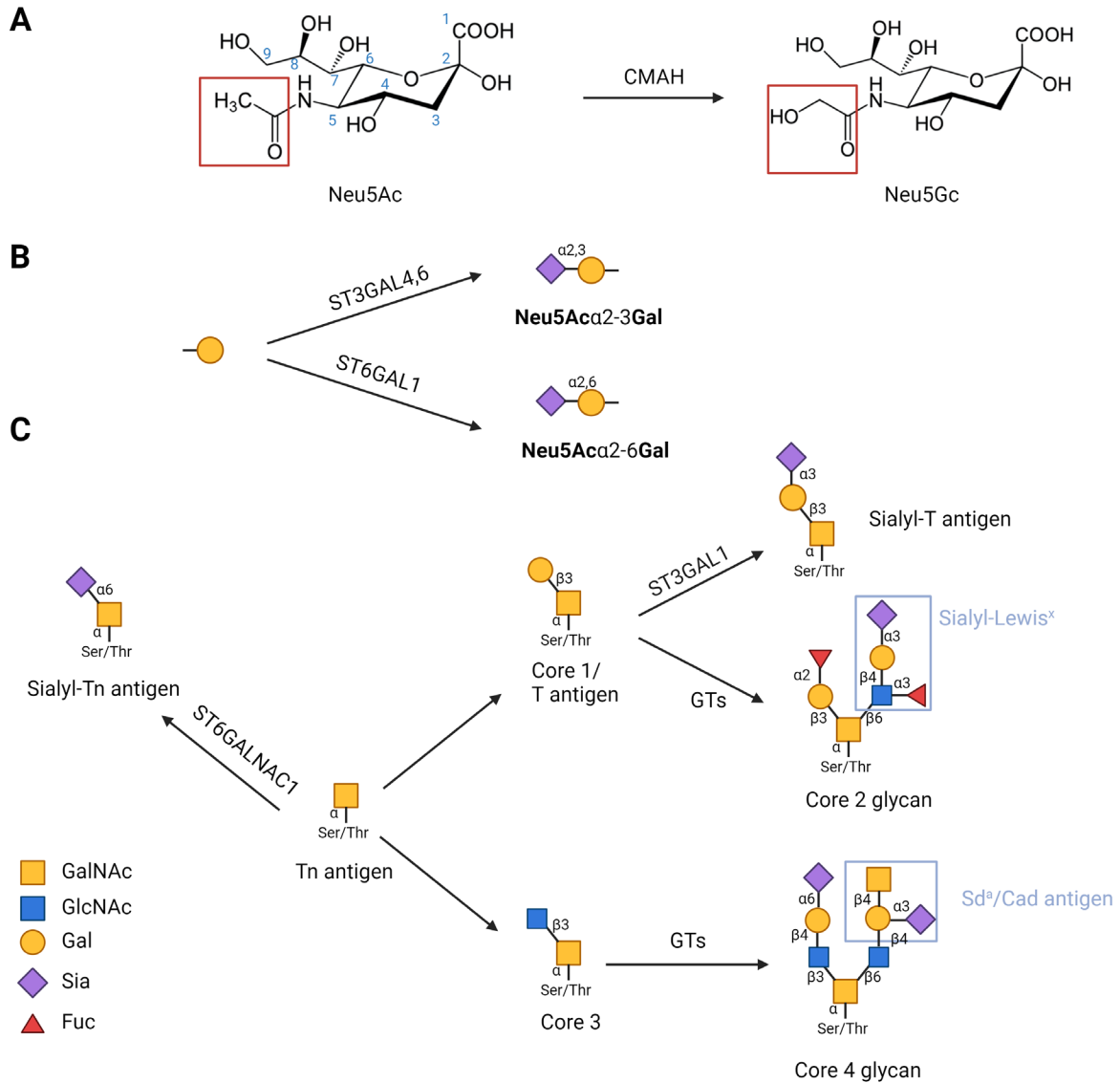


Figure 1.3 Structures and linkages of sialic acid and sialylated O-glycans on Muc2.

(A) Structures of two main forms of sialic acid: *N*-acetylneuraminic acid (Neu5Ac) and *N*-glycolylneuraminic acid (Neu5Gc). (B) Examples of sialic acid linkages on Muc2 *O*-glycans and main sialyltransferases in the mouse intestine. (C) Examples of sialylated Muc2 *O*-glycans, including sialylated mucin glycan epitopes shown in blue boxes. Monosaccharide units are represented according to the symbol nomenclature for glycans (SNFG) recommended by the Consortium for Functional Glycomics (Neelamegham *et al.*, 2019). CMAH, CMP-*N*-acetylneuraminic acid hydroxylase. GTs, glycosyltransferases. ST3GAL4, β -galactoside α 2,3-sialyltransferase 4. ST3GAL6, β -galactoside α 2,3-sialyltransferase 6. ST6GAL1, β -galactoside α 2,6-sialyltransferase 1. ST6GALNAC1, *N*-Acetylgalactosaminide α 2,6-sialyltransferase 1. ST3GAL1, β -galactoside α 2,3-sialyltransferase 1. Figure generated with Biorender.com.

1.4.1 Sialylation affects mucus integrity, microbiota, and gut inflammation

Sialylation of intestinal mucus has been shown to affect mucus homeostasis, gut microbiota functionality, and the development of inflammation in the gut. Recent research has highlighted the importance of sialylation by demonstrating that mice deficient in the sialyltransferase ST6GALNAC1 (ST6) have a compromised mucus layer, as well as a dysbiotic gut microbiota, and are highly susceptible to intestinal inflammation. ST6GALNAC1, which is specifically expressed by goblet cells, is currently known to catalyze the addition of sialic acid to GalNAc via an α -2,6 linked. Mucus generated from a ST6-deficient colonic epithelial cell line was found to be more prone to digestion by microbial proteases. This was found to correspond to the thinner colonic mucus found in ST6-deficient mice that was more penetrable by gut microbiota. Although the mutation of ST6 in mice did not contribute to pathology at baseline, ST6 deficiency did predispose them to intestinal inflammation, leading to more severe dextran sulphate sodium (DSS)-induced colitis. Furthermore, their exacerbated colitis was linked to changes in the gut microbiota and an elevated level of butyrate produced by symbiotic bacteria, which potentially impaired cell proliferation and compromised IEC repair during the disease (Yao *et al.*, 2022).

The Muc2 *O*-glycan precursor, known as the Tn antigen (GalNAc α -*O*-Ser/Thr), is typically elongated and modified with other sugars (Bergstrom *et al.*, 2016). In the healthy human colon, mucin *O*-glycans are typically highly complex and heavily sialylated (Holmén Larsson *et al.*, 2009). However, in pathological situations, such as active IBD, mucin *O*-glycans are often truncated, characterized by increased levels of shorter glycans. In the colon of these patients, the MUC2 *O*-glycans were found to have increased abundance of sialylated Tn antigen (sialyl-Tn antigen, Neu5Ac α -GalNAc α -*O*-Ser/Thr) (Figure 1.3C), which inhibits the extension of the Tn

glycan (Holmén Larsson *et al.*, 2011). Interestingly, ST6, the enzyme that governs the synthesis of sialyl-Tn antigen, was found to be expressed at higher levels in GCs from IBD patients with colitis as compared to GCs from healthy donors. However, patients with a loss-of-function mutation in ST6 demonstrated early onset of IBD (< 6-year-old) (Yao *et al.*, 2022). Moreover, lower sialic acid *O*-acetylation was reported in patients with UC and colorectal carcinoma, although healthy individuals lacking *O*-acetylation of sialic acid do not demonstrate any overt consequences (Corfield *et al.*, 1999; Robertson & Corfield, 1999). Depletion of sialic acid *O*-acetylation potentially predisposes mucins to degradation by bacterial flora, disrupting the barrier function of mucus in patients with GI disorders.

1.4.2 Sialic acid metabolism in bacteria

The initial step leading to mucin degradation involves the release of sialic acid, as the terminal sialic acids on mucin glycans can impede the action of other GHs. Therefore, many enteric bacteria, including both commensals and pathogens, have evolved to use sialic acid as a nutrient source. In bacteria, genes involved in sialic acid metabolism are found in clusters, known as the *nan* clusters (Almagro-Moreno & Boyd, 2009).

1.4.2.1 Sialic acid metabolism in gut microbiota

Phylogenetic analysis revealed that sialic acid metabolism is highly prevalent among members of the gut microbiota, finding approximately 5.9% of species contain a *nan* cluster to potentially utilize sialic acid as an energy source. These bacteria include species from the phyla of Actinomycetota, Bacteroidota, Bacillota, Fusobacteriota, Pseudomonadota, among others, and

are mainly found colonizing the mucus in regions of the gut where sialic acid is abundant (Haines-Menges *et al.*, 2015).

The *nan* cluster was first described in commensal *E. coli* and is the canonical sialic acid metabolism pathway shared by most bacteria (Figure 1.4A). This pathway comprises a transporter NanT, a Neu5Ac lyase (NanA), a *N*-acetyl-mannosamine kinase (NanK), and a *N*-acetyl-mannosamine epimerase (NanE), thus termed the *nanAKE* cluster. An alternative pathway was first discovered in *Bacteroides fragilis* (Figure 1.4B) and has been identified in many other species from the Bacteroidiota phylum. The Bacteroidota paradigm pathway relies on a transporter NanT, a non-orthologous Neu5Ac lyase (NanL), a GlcNAc epimerase (NanE-II), and a glucokinase (RokA), hereby called the *nanLE2T* gene cluster (Coker *et al.*, 2021). Both pathways convert sialic acid into GlcNAc-6-phosphate. This compound is further processed by GlcNAc-6-P deacetylase (NagA) and glucosamine-6-P deaminase (NagB) to yield fructose-6-phosphate, which then enters the glycolysis pathway (Bell *et al.*, 2023).

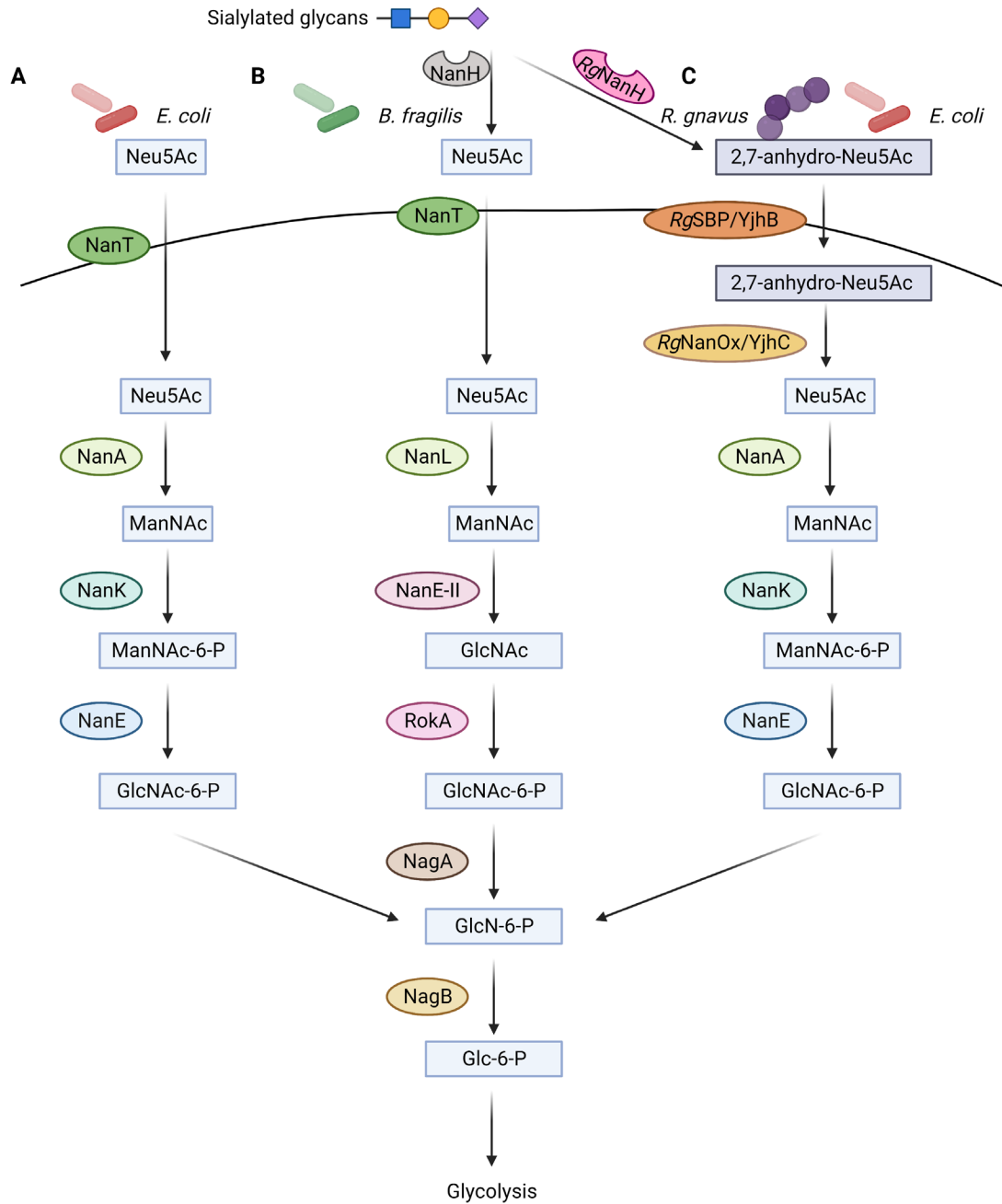


Figure 1.4 Representative sialic acid metabolism pathways identified in gut bacteria.

Metabolism of sialic acid derived from mucin glycans is a multi-step process. Sialidases, such as NanH from *Bacteroides*, release sialic acids from sialylated glycans. Liberated Neu5Ac is transported into the cell by sialic acid transporters, such as NanT and enter: (A) the canonical pathway first observed in *E. coli*, or (B) *B. fragilis* utilization pathway. (C) *R. gnavus* releases 2,7-anhydro-Neu5Ac instead of Neu5Ac with its IT-sialidase. The transporters, RgSBP in *R. gnavus* or YjhB in *E. coli*, take up 2,7-anhydro-Neu5Ac into the cell, which is further converted to Neu5Ac by an oxidoreductase, RgNanOx or YjhC. Generated Neu5Ac then enters the canonical pathway described in (A). NanH, Neuraminidase; RgNanH, intramolecular trans-sialidase; Neu5Ac, *N*-acetylneuraminic acid, sialic acid; NanT, sialic acid transporter; RgSBP, ATP-binding cassette (ABC) transporter (solute binding protein) specific for 2,7-anhydro-Neu5Ac in *R. gnavus*; YjhB, major facilitator superfamily (MFS) transporter in *E. coli*; RgNanOx,

oxidoreductase in *R. gnavus*; YjhC, oxidoreductase in *E. coli*; NanA, *N*-acetylneuraminic acid lyase; ManNAc, *N*-acetylmannosamine; NanK, *N*-acetylmannosamine kinase; ManNAc-6-P, *N*-acetylmannosamine-6-phosphate; NanE/NanE-II, *N*-acetylmannosamine-6-P epimerase; GlcNAc-6-P, *N*-acetylglucosamine-6-phosphate; NagA, *N*-acetylglucosamine-6-phosphate deacetylase; GlcN-6-P, Glucosamine-6-phosphate; NagB, Glucosamine-6-phosphate deaminase; RokA, hexokinase. Figure generated with Biorender.com.

Sialidases are enzymes that release sialic acid from glycoconjugates (Juge *et al.*, 2016). Gut bacterial sialidases involved in the breakdown of mucin glycans are typically found in the GH33 family of CAZymes. A study that analyzed the distribution of sialidase genes among human gut bacteria revealed that 40% of strains encoding a sialic acid utilization pathway also encode a GH33 sialidase, including bacteria from the *Akkermansia*, *Bacteroides*, *Bifidobacterium*, *Clostridium*, *Flavonifractor*, *Parabacteroides*, and *Prevotella* genera (Coker *et al.*, 2021). A newly discovered sialidase family, GH156, has recently been identified in poorly studied phyla, including Planctomycetes and Verrucomicrobiota (Mann *et al.*, 2022). Sialidases expressed by different bacteria vary in terms of their substrate specificity and enzymatic reactions. Most sialidases are hydrolytic sialidases, which cleave α 2,3 or α 2,6 linkages to release the terminal sialic acids on glycoproteins or glycolipids. Hydrolytic sialidases have been studied in *Bacteroides*, *Bifidobacterium*, *Clostridium* and *Akkermansia*, but only a limited number have been characterized using mucin as a substrate (Tailford *et al.*, 2015). A minority of these sialidases also display additional enzymatic activities, such as transglycosylation activity by SiaBb2 from *B. bifidum* that transfers sialic acids to 1-alkanols (Kiyohara *et al.*, 2011) and hydrolytic activity by NanI from *Clostridium perfringens* that hydrates the inhibitor Neu5Ac2en to Neu5Ac *in vitro* (Newstead *et al.*, 2008). Another class of sialidases found in the gut microbiota is the intramolecular *trans*-sialidase (IT-sialidase), which releases 2,7-anhydro-Neu5Ac instead of Neu5Ac, specifically targeting α 2,3-linkages. The IT-sialidase RgNanH from *Ruminococcus gnavus* ATCC 29149 strain is the first functionally characterized IT-sialidase

encoded by the gut microbiota. The action of *RgNanH* on sialylated mucin glycans results in 2,7-anhydro-Neu5Ac, which is utilized directly by *R. gnavus* for growth, and is then converted to Neu5Ac intracellularly by the enzyme *RgNanOx* (Figure 1.4C). This unique metabolic pathway of *R. gnavus* is important for its colonization of the mucus niche (Bell *et al.*, 2019). A similar catabolism pathway for 2,7-anhydro-Neu5Ac was found in the human commensal *E. coli* K-12 substrain BW25113 (Figure 1.4C), though *E. coli* lacks the IT-sialidase to obtain the precursor from glycans (Bell *et al.*, 2020). Bioinformatics analysis revealed that the presence of IT-sialidases is restricted to Bacillota, particularly Clostridiales and Lactobacillales (Tailford *et al.*, 2015).

O-acetylation on sialic acid provides resistance against cleavage by sialidases. When the action of sialidases is blocked by *O*-acetylation, esterases are required to remove the acetyl group. Similar to sialidases, sialic acid *O*-acetyl esterases are widely expressed among gut bacteria (Corfield *et al.*, 1992). However, not all bacteria encoding a sialidase have an esterase, e.g., *B. thetaiotaomicron*, which only possesses a sialidase, while *B. fragilis* possesses both a sialidase and an esterase. *B. fragilis* *O*-acetyl esterase EstA has been shown to remove 9-*O*-acetyl esterification, allowing sialidases to subsequently release Neu5Ac (Robinson *et al.*, 2017). Interestingly, *B. bifidum* encodes a bifunctional sialidase (SiaBb1) with esterase activity that removes the 9-*O*-acetyl group prior to the sialidase activity (Ashida *et al.*, 2018).

Complete metabolism of sialic acid requires both a sialidase and the *nan* cluster. However, some bacteria encode an incomplete package for utilizing sialic acid. Many symbionts, such as *Escherichia*, *Eubacterium*, *Faecalibacterium*, and a number of opportunistic pathogens,

including *Clostridioides*, lack a sialidase but can utilize sialic acid. Others possess a sialidase but lack the *nan* operon to consume the liberated sialic acid for energy, including many *Bacteroides* strains (e.g. *B. faecis*, *B. intestinalis*, *B. thetaiotaomicron*) (Coker *et al.*, 2021). The released sialic acid becomes available to serve as a substrate for other microorganisms through cross-feeding. For instance, *B. breve* can use the sialic acid released by *B. bifidum* for growth (Egan *et al.*, 2014; Nishiyama *et al.*, 2018). These intricate interactions between mucin glycans and gut bacteria highlight the critical role of sialic acid in sustaining a harmonious metabolic network within the microbial communities.

1.4.2.2 Sialic acid metabolism in pathogens

Sialic acid provides colonization advantages for several enteric pathogens. It plays a significant role in both pathogenicity and as a nutrient to pathogenic bacteria.

While sialidases are not commonly expressed by gut pathogens, they appear to primarily function to decrypt binding sites for pathogen adhesins or toxins rather than being used to acquire substrates for growth, as seen in *Vibrio cholerae* and *C. perfringens* (Lewis & Lewis, 2012). For instance, sialidases in *V. cholerae* facilitate binding of cholera toxin to intestinal epithelial cells (Kaisar *et al.*, 2021), while in *C. perfringens*, sialidases enhance the binding and toxicity of its epsilon toxin (Li *et al.*, 2011). Moreover, *Salmonella* Typhimurium sialidases were shown to be induced during an infection of Caco-2 IECs, potentially degrading the glycocalyx on the epithelial membrane to mediate invasion (Arabyan *et al.*, 2016). Although *E. coli* strains also encode a sialic acid transport and catabolism pathway, they do not encode sialidases that act on host sialic acids *in situ* (Robinson *et al.*, 2017).

Sialic acid has been shown to provide growth advantages to enteric pathogens by serving as a carbon and energy source. Ng *et al.* demonstrated that antibiotic treatment led to a spike of free sialic acids in mouse ceca, which *S. Typhimurium* and *C. difficile* accessed to promote pathogen expansion. Thus, mutant strains of *S. Typhimurium* and *C. difficile* deficient in sialic acid utilization were significantly compromised in attaining high densities in the gut (Ng *et al.*, 2013). Another study showed that during DSS-induced acute colitis, free sialic acid levels are elevated, promoting the outgrowth of commensal *E. coli* that exacerbate the concurrent inflammation (Huang *et al.*, 2015).

As enteric pathogens lack sialidases, the gut microbiota plays a crucial role in mediating the interplay between pathogens and host sialylated glycans. For example, the colonization of wildtype *B. thetaiotaomicron*, but not a sialidase-deficient mutant, contributed to the availability of free sialic acids, increasing the density of *C. difficile* (Ng *et al.*, 2013). Intestinal inflammation-induced gut dysbiosis causes an increase in the abundance of *Bacteroides vulgatus* and its sialidase activity, resulting in enhanced exposure of *E. coli* to sialic acid (Huang *et al.*, 2015). Additionally, microbiota-encoded *O*-acetyl esterases, such as EstA from *B. fragilis*, augment the liberation of mucin-derived sialic acids by removing acetyl groups on sialic acids, enhancing the release of sialic acid by sialidases, thus promoting the expansion of pathogenic *E. coli*, at least *in vitro* (Robinson *et al.*, 2017). Although sialic acid metabolism has been shown to have pronounced effects on the outgrowth of pathogenic bacteria under post-antibiotic and inflammatory conditions, where the composition and function of the gut microbiota is significantly altered, the role of sialic acid in a naturally occurring infection in the context of an

intact microbiota has not been elucidated. *C. rodentium*, as a natural murine pathogen that colonizes the mouse colon and causes colitis without antibiotic pre-treatment, provides a robust model to address this question.

1.5 Nutrient acquisition and metabolism by *C. rodentium*

The increasing concerns regarding the rising incidence of antibiotic resistance has led to a growing interest in targeting pathogen nutrition and metabolism as novel antimicrobial approaches. In the last several years, many of the greatest advances in the field of pathogen metabolism have come from the study of *C. rodentium*. During the course of infection, *C. rodentium* targets the metabolic landscape of both the host and the microbiota, accessing new nutritional niches that are not accessible by commensals. *C. rodentium* also induces host responses that deplete competing commensals, taking over those nutritional niches left vacant. Thus, the strategies used by pathogens (such as *C. rodentium*) to source nutrients for growth are likely key to their success within the competitive environment of the GI tract. *C. rodentium* modifies its metabolic processes to adapt to the challenges that it encounters during the four stages of infection outlined in section 1.1.2 (Figure 1.2).

1.5.1 Phase 1: Overcoming colonization resistance

Overcoming colonization resistance is a particular challenge for *C. rodentium* at the early stages of infection (< 3 DPI) due to the nutritional competitiveness of other microbes within the gut lumen (Figure 1.5A). As mentioned in section 1.1.3, in SPF mice, competition with the microbiota is so great that *C. rodentium* at an infectious dose of $< 10^4$ CFU are unable to establish and are rapidly lost from the host. In contrast, in GF mice, *C. rodentium* rapidly

colonizes the gut, regardless of the challenge dose (Buschor *et al.*, 2017), highlighting the microbiota's impact on host defense. Recent technical advances in microbiota analysis have enabled researchers to develop mechanistic insights into how particular microbiota populations (Ghosh *et al.*, 2011; Lupp *et al.*, 2007; Willing *et al.*, 2011) and their metabolic pathways contribute to colonization resistance.

Using genetically identical mouse lines, Osbelt *et al.* demonstrated that naturally occurring variations in microbiota composition led to distinct *C. rodentium* colonization kinetics. Mice carrying a greater abundance and diversity of Bacillota showed increased resistance to *C. rodentium*, due to the protective effects of the short-chain fatty acids (SCFA) produced by Bacillota (Osbelt *et al.*, 2020). Moreover, Stacy *et al.* demonstrated that prior GI infections led to the expansion of microbiota species that utilize the sulfur-containing compound, taurine. Metabolism of taurine generated the by-product hydrogen sulfide, which impeded *C. rodentium*'s aerobic respiration and its colonization of hosts (Stacy *et al.*, 2021).

The gut microbiota also hinders pathogen metabolism by restricting access to essential nutrients. Two independent studies identified significantly lower amino acid levels in the colonic contents of conventionally housed mice as compared to GF mice (Barroso-Batista *et al.*, 2020; Caballero-Flores *et al.*, 2020). These data suggest that the resident gut microbiota limits amino acid availability, thus prompting *C. rodentium* to heighten its own amino acid biosynthesis (Caballero-Flores *et al.*, 2020). Another study using RNA sequencing found that amino acid biosynthesis was upregulated in *C. rodentium* isolated from the mouse ceca at 3 DPI as compared to *C. rodentium* grown *in vitro* (Connolly *et al.*, 2018), confirming the important role

that amino acids play during *in vivo* infection. Thus, outcompeting commensals is key to *C. rodentium*'s pathogenesis, with *C. rodentium* more easily bypassing this barrier when the host's diet is replete with favored nutrients, such as proteins (Caballero-Flores *et al.*, 2020) and fructose (Montrose *et al.*, 2021).

1.5.2 Phase 2A: Luminal establishment and crossing the mucus layer

During the establishment phase of infection, nutrients are acquired by *C. rodentium*, both as growth substrates as well as signals for virulence gene expression. For example, galacturonic acid derived from dietary pectin enhances *C. rodentium* growth up to 2 DPI in highly susceptible C3H/HeJ mice. Moreover, sensing of galacturonic acid reduces *C. rodentium*'s expression of its LEE genes (including those encoding the T3SS), thereby relieving some of its metabolic burden (Jimenez *et al.*, 2020). Other metabolized nutrients do not yield a growth benefit *in vivo*, but solely regulate *C. rodentium*'s virulence. These include the amino acids arginine (Menezes-Garcia *et al.*, 2020), tryptophan (Kumar & Sperandio, 2019) and cysteine (Pifer *et al.*, 2018), as well as microbiota-derived metabolites such as 1,2-propanediol (Connolly *et al.*, 2018) and succinate (Curtis *et al.*, 2014). Other nutrients can modulate virulence without the pathogen's capacity to metabolize them, such as SCFA at concentrations not inhibitory to growth (Nakanishi *et al.*, 2009).

As part of its pathogenesis, luminal *C. rodentium* must cross the intestinal mucus barrier to reach and infect IEC. Increasing attention is being paid to non-T3SS dependent virulence factors, such as SPATEs, including *C. rodentium*'s Pic mucinase (Bhullar *et al.*, 2015; Harrington *et al.*, 2009; Liu *et al.*, 2020). Surprisingly, Pic is not an essential virulence factor, nor is it clear if Pic's

ability to degrade mucus affects nutrient availability (Flores-Sanchez *et al.*, 2020; Harrington *et al.*, 2009), however metabolites produced by commensals, e.g. *B. thetaiotaomicron* do appear to enhance Pic expression, accelerating bacterial penetration of mucus, correlating with worsened epithelial damage (Curtis *et al.*, 2014).

Unfortunately, the mechanisms used by *C. rodentium* to migrate through colonic mucus and the nutrient(s) that fuels the pathogen during this process remains ill-defined. It seems that A/E pathogens benefit from mucin-derived monosaccharides released by commensals, as *C. rodentium* densely colonizes the colonic mucus layer (Bergstrom *et al.*, 2010) despite the layer's rapid turnover rate (Johansson, 2012). Similarly, fucose released from the mucus by commensal microbes represses overexpression of LEE in EHEC, alleviating its energy burden for optimal fitness (Pacheco *et al.*, 2012). When *C. rodentium* does not use fucose for growth (Kamada *et al.*, 2012), it likely senses fucose (as previously shown for EHEC (Pacheco *et al.*, 2012) and acquires other mucus-derived nutrients as it crosses this barrier. Thus, as it adapts to the gut, *C. rodentium* metabolism intertwines with virulence gene expression to subvert the mucus layer and initiate epithelial attachment (Figure 1.5B). Further research exploring how *C. rodentium* reprograms its metabolism at the mucus-lumen interface should be illuminating.

1.5.3 Phase 2B: Early expansion and survival at the colonic epithelial surface

As *C. rodentium* expands throughout the colon (4-6 DPI) in search of nutrient-rich niches, several cellular processes involved in nitrogen and monosaccharide metabolism, as well as energy generation are upregulated (Connolly *et al.*, 2018). Among the variety of nutrients that could feed *C. rodentium*'s massive expansion, the prevalence of carbohydrate substrates in the

gut lumen suggests monosaccharides are likely crucial to its pathogenesis (Kamada *et al.*, 2012). Several studies have shown that pathogenic *E. coli* prefer simple sugars as carbon sources for growth (Chang *et al.*, 2004; Fabich *et al.*, 2008). Moreover, *in vitro* growth of EHEC exposed to the luminal contents of cow intestines was found to be largely dependent on mucus-derived monosaccharides (Bertin *et al.*, 2013; Segura *et al.*, 2018). Such dependence could change towards proteinaceous substrates as *C. rodentium* spreads from the lumen and towards the mucosal surface, since carbohydrate metabolism appears to be reduced in those microbiota populations residing closer to the intestinal epithelium (Albenberg *et al.*, 2014).

In addition, adherence to IEC, through the T3SS, provides *C. rodentium* access to epithelial derived hydrogen peroxide (H_2O_2). Prior to the onset of inflammation, when oxygen and nitrate levels are low, H_2O_2 generated from the NADPH oxidase NOX1 in colonic IEC (Matziouridou *et al.*, 2018) fuels the growth of *C. rodentium*. Correspondingly, *C. rodentium* is impaired in colonizing Nox1 deficient mice (with low colonic H_2O_2 concentrations) (Miller *et al.*, 2020). *C. rodentium* exploits H_2O_2 as a terminal electron acceptor for anaerobic respiration, creating a unique metabolic niche that promotes its survival and competition against microbiota prior to the onset of inflammation. Exactly how H_2O_2 grants *C. rodentium* a competitive advantage is unclear, as is how other metabolic pathways (Kitamoto *et al.*, 2020) and virulence factor expression (Pircalabioru *et al.*, 2016) are regulated in the presence of H_2O_2 . Moreover, nitrate present in the intestine (mainly diet-derived prior to inflammation (Lundberg *et al.*, 2004)) could support *C. rodentium* expansion through anaerobic respiration (Bueno *et al.*, 2018), especially when intestinal pH is elevated (e.g. in GF or antibiotic-treated mice (Shimizu *et al.*, 2021)). Thus, prior to the onset of infection induced gut inflammation, *C. rodentium* expands its

population by acquiring several nutrient sources while also accessing nitrate and IEC-derived H₂O₂ for anaerobic respiration (Figure 1.5B).

1.5.4 Phase 3: Inflammation, microbial dysbiosis and parasitizing the intestinal epithelium

As *C. rodentium* infection progresses, it induces widespread, albeit only moderate intestinal inflammation (7-12 DPI), in concert with an increase in luminal oxygen levels. Under homeostatic conditions, mature colonic IEC obtain energy through mitochondrial based β -oxidation of the SCFA butyrate, a process that consumes oxygen, leaving the gut lumen anaerobic. Correspondingly, the majority of the resident gut microbiota are obligate anaerobes, with butyrate produced by specific members (*i.e.* Clostridia) (Rivera-Chávez *et al.*, 2016). Secretion of T3SS effectors into host IEC causes damage to their mitochondria, and together with *C. rodentium*-induced expansion of undifferentiated colonocytes, changes the metabolism of the epithelium to aerobic glycolysis, which converts glucose to lactate without consuming oxygen, thereby elevating luminal oxygen levels. Increased oxygen availability is critical for the expansion of *C. rodentium*. Correspondingly, mucosa-associated *C. rodentium* exhibit higher oxidative metabolic activities than the population residing in the lumen (Lopez *et al.*, 2016).

Access to oxygen enables *C. rodentium* to generate energy more efficiently through aerobic respiration, thus making anaerobic respiration dispensable (Lopez *et al.*, 2016). Moreover, aerobic respiration also benefits the pathogen in competing against microbes that rely on anaerobic respiration, since the elevated oxygen levels cause overt microbial dysbiosis, characterized by a depletion of obligate anaerobes and an expansion of facultative anaerobic

bacteria (e.g., Enterobacteriaceae such as *C. rodentium*). Consequently, during this phase, *C. rodentium* comprises only 10% of luminal bacteria but up to 90% of mucosal-associated bacteria (Berger *et al.*, 2017; Hopkins *et al.*, 2019). Since obligate anaerobes are key players in degrading complex glycans, such as dietary fibers and mucus glycans, their depletion should lead to a reduction in monosaccharide availability. Kitamoto *et al.* suggested this could promote the metabolism of alternative nutrient sources, including the amino acid L-serine. Correspondingly, a *C. rodentium* L-serine catabolism mutant shows colonization defects from 8 DPI onward and induces less severe colitis (Kitamoto *et al.*, 2020).

It is currently unclear where A/E pathogens obtain nutrients such as L-serine while intimately adhering to the apical surface of IEC, since this site is distant from any commensals that could cross-feed them. An *in vitro* study demonstrated that the T3SS injectisome not only injects bacterial proteins into host IEC, but it also permits A/E pathogens to directly extract nutrients, such as amino acids from the host cytoplasm (Figure 1.5C). However, the extent to which this ‘host nutrient extraction’ sustains *C. rodentium*’s fitness *in vivo* remains to be explored (Pal *et al.*, 2019).

1.5.5 Phase 4: clearance from the mucosal surface

During the late phase of infection (> 12 DPI), host antibody responses lead to downregulation of *C. rodentium* LEE gene expression, resulting in its displacement from the epithelial surface to the lumen. Correspondingly, based on the nutrients found in the lumen, pathways involved in monosaccharide metabolism are upregulated in *C. rodentium* during this late phase of infection (Connolly *et al.*, 2018). Even so, in most cases, *C. rodentium* is eventually cleared from the

lumen by microbiota that outcompete it for key nutrients, such as monosaccharides (Kamada *et al.*, 2012). Interestingly, a study has shown that when luminal glucose levels remain high, *C. rodentium* can persistently colonize the host's intestinal lumen without causing disease (Sanchez *et al.*, 2018). Similarly, *C. rodentium* can persist in the gut lumen of GF mice since they have no microbial competition for host or diet-derived nutrients. Ethanolamine, a cell membrane phospholipid component, is available from the turnover of IEC and serves as a nitrogen source for *C. rodentium*, facilitating its persistence in the gut (Figure 1.5D) (Rowley *et al.*, 2020).

In conclusion, *C. rodentium* employs distinct metabolic strategies in varying spatiotemporal niches. While significant attention has been paid to specific pathogen virulence factors, in fact the ability of pathogens to adapt their metabolism to match their environment is key to their success, and this involves acquiring available nutrients to generate the energy needed during their different phases of infection. Identifying and targeting those nutrients found essential for bacterial pathogenesis is an attractive anti-microbial approach in the new post-antibiotic era.

1.5.6 Potential targeting of pathogen metabolism

The study of the complex pathogen–host–microbiota metabolic network during *C. rodentium* infection has shed light on the development of novel therapeutics to control enteric infections. This could be pursued through the use of dietary interventions to limit key nutrients, such as L-serine, or by administering dietary components with inhibitory effects, such as SCFA, taurine, and pectin. One could also promote commensal microbiota-mediated approaches by increasing the populations of important players in colonization resistance to outcompete pathogens for essential resources. Additionally, the discovery of crucial metabolic pathways for pathogen

survival could lead to the synthesis of small molecule inhibitors that target pathogen uptake of nutrients, or prevent the release of accessible nutrients by enzymes of the gut microbiota (Figure 1.6).

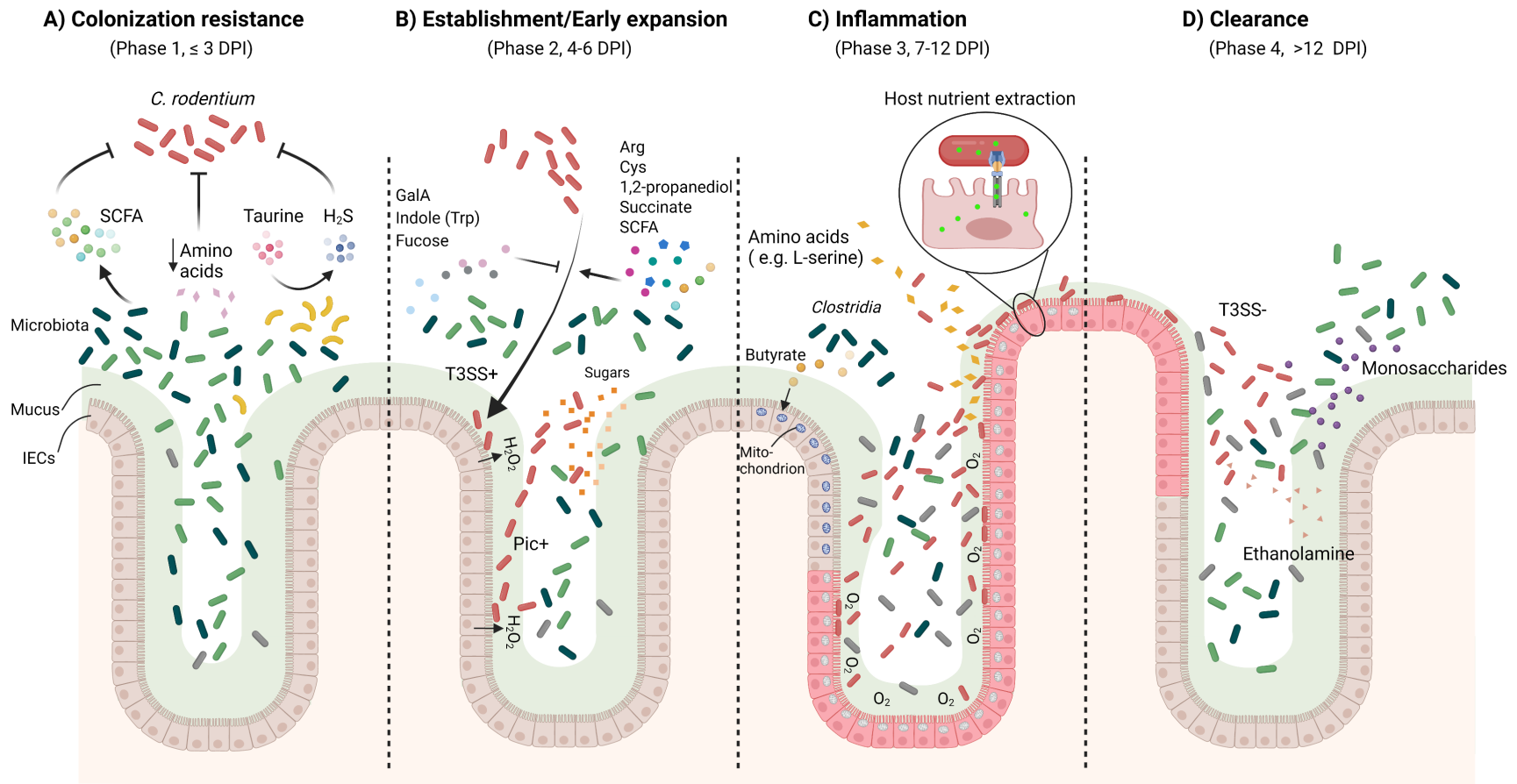


Figure 1.5 Metabolic strategies utilized by *C. rodentium* at different phases of infection.

(A) Phase 1: *C. rodentium* overcoming colonization resistance conferred by the gut microbiota. B) Phase 2: Nutrients that facilitate early expansion of *C. rodentium* and/or regulate virulence expression, enabling *C. rodentium* to cross the mucus layer and initiate attachment to the epithelium. C) Phase 3: Inflammation promotes further expansion of *C. rodentium* through aerobic respiration, leading to microbial dysbiosis. *C. rodentium* resorts to amino acid utilization and extracts nutrients from the infected epithelium (see enlargement). D) Phase 4: *C. rodentium* persists in the intestinal lumen through its access to ethanolamine, or is outcompeted by microbiota for key nutrients, such as monosaccharides. H₂S, hydrogen sulfide. GalA, galacturonic acid. Trp, tryptophan. Arg, arginine. Cys, cysteine. Figure generated with Biorender.com.

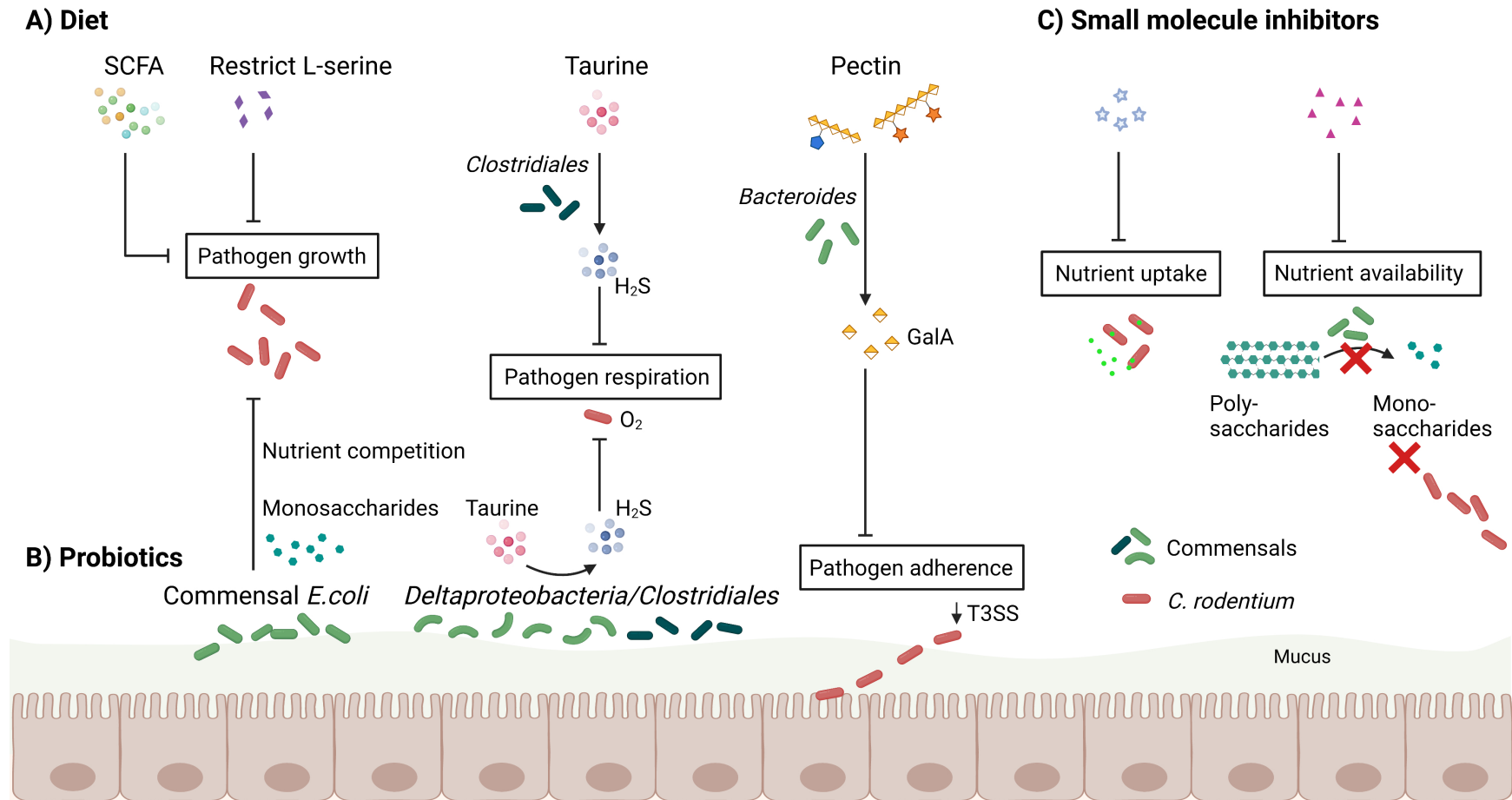


Figure 1.6 Potential therapeutic approaches to target pathogen nutrition and prevent infections (*C. rodentium* as an example).

(A) Dietary supplementation of nutrients with inhibitory effects (such as SCFA, pectin, taurine) on *C. rodentium*, or diet-based limitation of *C. rodentium*'s favored nutrients (such as L-serine). B) Administration of probiotics (such as commensal *E. coli*) that outcompete *C. rodentium* for essential nutrients, or probiotics that produce inhibitory metabolites (such as taurine-metabolizing commensals). C) small molecule inhibitors that prevent nutrient uptake by *C. rodentium* (such as inhibitors for nutrient sensors/transporters/catabolic enzymes), or those that reduce nutrient availability (e.g., by blocking cleavage of monosaccharides from polysaccharides). GalA, galacturonic acid. Figure generated with Biorender.com.

1.6 Research objectives

As outlined above, A/E pathogens must overcome colonization resistance from the gut microbiota, penetrate the intestinal mucus layer, and reach IEC to cause disease. However, the mechanism by which A/E pathogens reach the colonic mucosal surface is not yet fully understood. While sialic acid, a sugar located at the terminus of mucin glycans has been demonstrated to promote the growth of other enteric pathogens in the aftermath of antibiotic treatment or chemical-induced colitis, its contribution to naturally occurring infections, including those caused by A/E pathogens, has not been thoroughly explored.

The overall objective of this thesis is thus to investigate the interactions of the A/E enteric pathogen *C. rodentium* with intestinal mucus and mucus-degrading commensals. I hypothesized that *C. rodentium* utilizes sialic acid liberated by commensals from mucin for both its own growth and to regulate its expression of virulence factors, which licenses its transition from the luminal to the mucosal niche. This hypothesis will be tested through the following objectives:

- 1: Investigate how sialic acid metabolism affects the fitness of *C. rodentium*.
- 2: Examine the impact of sialic acid on the virulence of *C. rodentium*.
- 3: Explore how mucus-degrading commensals facilitate interactions between *C. rodentium* and the intestinal mucus.

Together, these objectives will further elucidate pathogen-host-microbiota interactions at the mucus layer, thereby enhancing our understanding of A/E pathogenesis.

Chapter 2: Sialic acid metabolism is essential for the fitness of A/E pathogens

2.1 Synopsis

Enteric bacterial pathogens face a significant challenge of competing with the gut microbiota for nutrient sources in the highly competitive environment of the gut. A/E pathogens, which cause severe diarrheal disease by colonizing the host's intestinal mucosal surface and forming attaching/effacing (A/E) lesions, must closely interact with the intestinal mucus. This mucus, composed primarily of the highly glycosylated protein Muc2, provides a potentially rich source of nutrients for these pathogens. Sialic acid, the most common terminal sugar on Muc2 glycans, is actively released and presented to bacteria or pathogens localizing at or near the mucus layer. Here we show sialic acid is expressed widely in the GI tracts of mice, primarily in the colonic mucus layer and by intestinal goblet cells. We observed that both EPEC and *C. rodentium* take up and metabolize sialic acid via the transporter NanT. Our findings demonstrate that sialic acid utilization is essential for establishing pathogen colonization and maintaining metabolic fitness in *C. rodentium*. A *C. rodentium* strain deficient in sialic acid uptake ($\Delta nanT$) was significantly impaired in colonizing the intestines of mice and was rapidly cleared.

2.2 Introduction

A/E pathogens are primarily known for their intimate attachment to IEC via their T3SS (Collins *et al.*, 2014; Gaytán *et al.*, 2016a). Once attached, *C. rodentium* can leverage IEC-derived H₂O₂ to establish its own niche and promote its respiration (Miller *et al.*, 2020). However, prior to this phase of infection, ingested A/E pathogens reside within the gut lumen (Liang & Vallance, 2021). We hypothesize that successful infection by A/E pathogens requires metabolic adaptation to the luminal environment, allowing them to acquire nutrients and energy to reach their target

mucosal niche. The colonic mucus layer is likely key to this adaptation, as it provides a rich source of endogenous nutrients within the mammalian colon (Koropatkin *et al.*, 2012; Marcobal *et al.*, 2013). Colonic mucus predominantly consists of the heavily *O*-glycosylated mucin Muc2, which forms two layers: a sterile compact inner mucus layer and a detached outer mucus layer harboring mucus-dwelling bacteria (Hansson, 2020). The terminal position of these *O*-glycans is frequently occupied by sialic acid (Neu5Ac) (Bergstrom & Xia, 2022; Johansson *et al.*, 2011).

Several studies have shown that the catabolism of sialic acid contributes to bacterial overgrowth in the gut when the host is exposed to certain chemicals or antibiotics. For example, DSS-induced colitis was shown to increase sialidase activity by the resident microbiota, leading to increased availability of sialic acid and the outgrowth of commensal *E. coli* species (Huang *et al.*, 2015). Additionally, it was demonstrated that the dramatic post-antibiotic expansion of *S. Typhimurium* and *C. difficile* in infected mice involves the catabolism of microbiota-liberated sialic acid by these pathogens (Ng *et al.*, 2013). These studies suggest that prior exposure to antibiotics or colitis-inducing chemicals may be necessary to increase the availability of sialic acid and promote the expansion of enteric pathogens. However, it is unclear whether other enteric pathogens, such as *C. rodentium*, can use sialic acid to expand even in the absence of chemical or antibiotic-driven microbiota disruption. Here, we investigate the ability of A/E pathogens to use mucin-derived sialic acid as a nutrient source and explore its role in the metabolic fitness of A/E pathogens *in vivo* using *C. rodentium* as a model.

2.3 Results

2.3.1 A/E enteric pathogens reside within the colonic mucus layer and can catabolize mucus-derived monosaccharides.

A/E pathogens are known to colonize their host's intestinal mucosal surface, forming A/E lesions, and causing severe diarrheal disease. Based on their location at the mucosal surface, they must closely interact with the intestinal mucus. The mouse A/E pathogen, *C. rodentium*, is known to initially colonize the colonic lumen and then spread to the mucosal epithelial surface during its infection of the murine GI tract (Khan *et al.*, 2006). To define the biogeography of *C. rodentium in vivo*, in relationship to colonic mucus, we collected colonic tissues from mice at 6 days post *C. rodentium* infection (DPI), and co-stained them with antibodies recognizing *C. rodentium* and the mucin Muc2. Staining found populations of *C. rodentium* that were heavily colonizing the outer mucus layer, or adherent to the colonic epithelium. In particular, a smaller subpopulation of *C. rodentium* was localized to the inner colonic mucus layer, in some cases appearing to traverse this barrier (arrowheads) (Figure 2.1A).

This close association between *C. rodentium* populations and mucus led us to hypothesize that A/E pathogens utilize mucus and its glycans as nutrient sources. To test this hypothesis, we cultured *C. rodentium* and EPEC in minimal medium supplemented with either whole mucins or one of the five monosaccharides that make up the Muc2 O-glycans. As expected, *C. rodentium* and EPEC were unable to metabolize whole mucins (Figure 2.1B and C) as they lack the glycoside hydrolase enzymes necessary to cleave complex glycans (Drula *et al.*, 2022; Popov *et al.*, 2019). However, they could grow on several sugar monomers, including galactose (Gal), N-acetylglucosamine (GlcNAc), and sialic acid (Sia, Neu5Ac). In contrast, no growth was observed

when *C. rodentium* was cultured with *N*-acetylgalactosamine (GalNAc) or fucose (Fuc) (Figure 2.1B), while EPEC could metabolize Fuc but not GalNAc (Figure 2.1C). These data suggest that A/E pathogens can utilize monosaccharides derived from mucin glycans as nutrient sources. Thus, access to these monosaccharides may affect the pathogenesis of A/E pathogens *in vivo*.

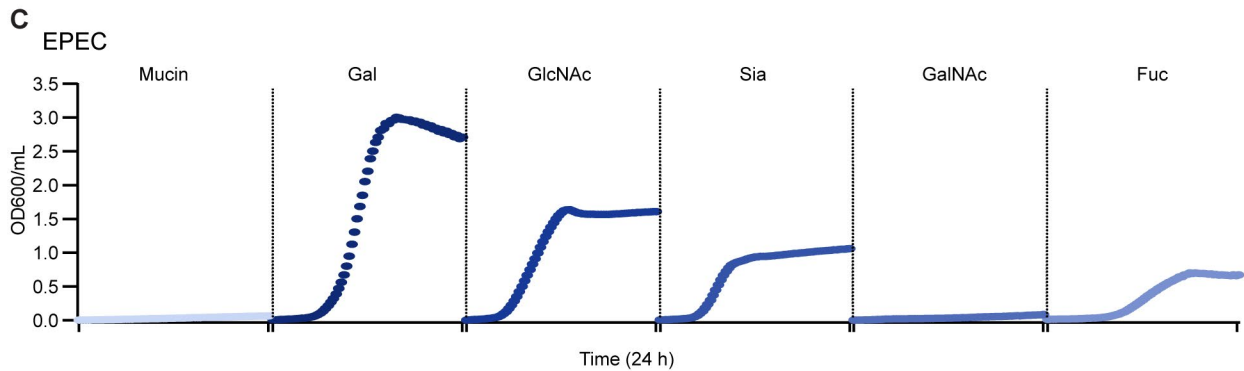
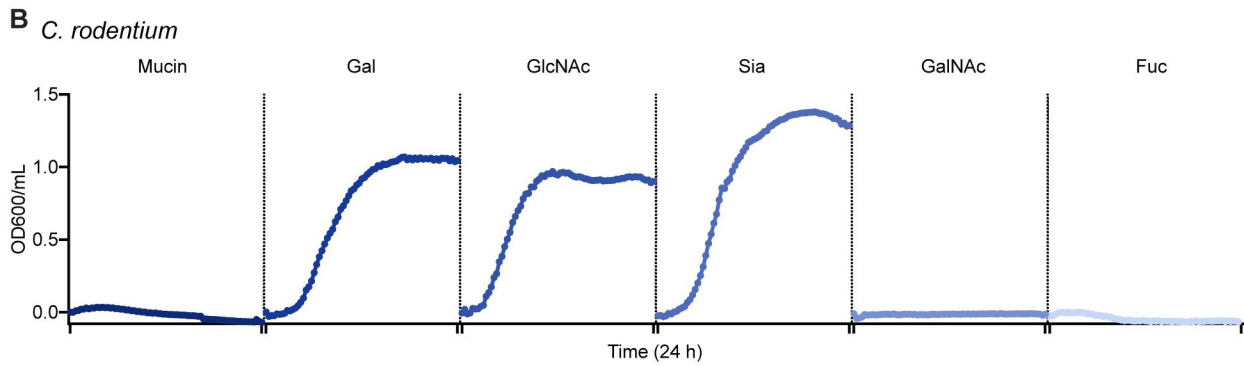
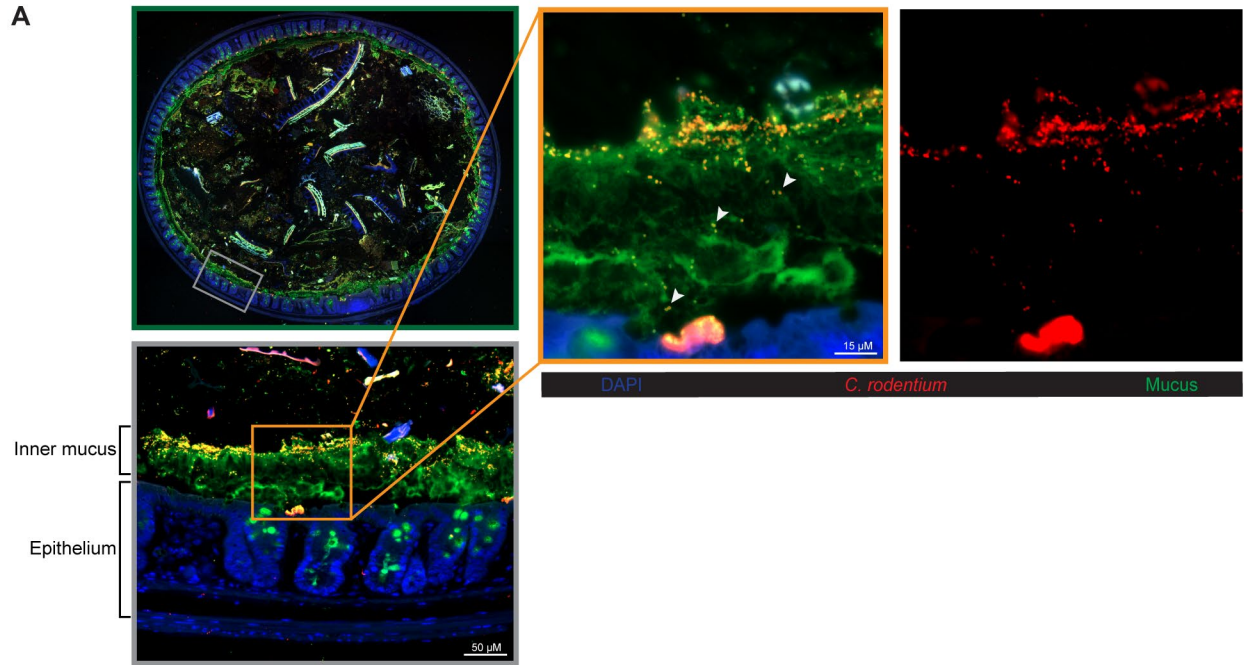


Figure 2.1 A/E pathogens reside within the colonic mucus and catabolizes mucus-derived monosaccharides. (A) *C. rodentium* localizes to the mucus layer. Representative immunofluorescence staining of mouse colonic tissue infected with *C. rodentium*. A colon cross-section (green panel) was stained with DAPI to detect DNA (blue), anti-*C. rodentium* (red) to visualize *C. rodentium* and anti-Muc2 to visualize mucus (green). Grey panel is the enlarged view of the boxed region within the cross-section, original magnification =200 \times . Orange panel is a magnified image indicating a subpopulation of *C. rodentium* localized to the inner mucus and traversing the mucus (arrowheads), with a separate image showing *C. rodentium* staining independently (red channel), original magnification =630 \times .

Scale bar = 15 μm . (B, C) *C. rodentium* (B) and EPEC (C) use mucus-derived monosaccharides as sole carbon sources for growth. Bacterial growth was measured by optical density (OD600) at 20-minute intervals over 24 hours at 37°C in M9 minimal medium supplemented with 0.2% purified mucins, galactose (Gal), *N*-acetylglucosamine (GlcNAc), *N*-acetylneuraminic acid (sialic acid, Sia), *N*-acetylgalactosamine (GalNAc), or fucose (Fuc). Data are presented as averages of cell growth ($n=9$) from three independent experiments.

2.3.2 Sialic acid is widely expressed in the colon at baseline and during infection

Among the different glycan sugars that decorate mucin proteins, sialic acid, which is commonly found at the terminus of mucin *O*-glycans, is frequently cleaved by bacterial enzymes, and can be utilized by bacterial pathogens to facilitate host infection (Holmén Larsson *et al.*, 2013).

In the mouse colon, sialic acid residues on these glycans are α 2,3-linked with Gal and α 2,6-linked with Gal or GalNAc. To evaluate the origin and availability of sialic acid in the mouse colon, mouse colonic tissues were stained with two sialic acid specific lectins, *Maackia amurensis* lectin II (MALII, recognizing α 2,3-linked sialylated and sulfated glycans) and *Sambucus nigra* agglutinin (SNA, α 2,6- sialic acid binding). Both types of sialic acids were present in mouse colons. Both these lectins stained the mature GCs in the epithelium as well as the mucus, indicating that mucus is the major source of sialic acid in the intestine. Widespread positive staining of both lectins was observed in healthy mice as well as during infection (Figure 2.2A).

Since mucin *O*-glycosylation is known to be dynamic, the patterns of which can be altered in response to enteric infections (Arike & Hansson, 2016), the degree of sialylation in secreted Muc2 mucin before and during *C. rodentium* infection was measured by analyzing its *O*-linked glycan profiles using liquid-chromatography-tandem mass spectrometry (LC-MS/MS). High levels of sialylated glycans were detected in colonic mucus from both uninfected and 6 DPI mice (Figure 2.2B). Staining by lectins suggests that *C. rodentium* infection leads to a moderate

increase in sialic acid detected in the secreted mucus (Figure 2.2A), potentially due to the stimulation of overall mucus secretion by the infection. This is supported by the slight increase in the percentage sialylation during infection shown in the LC-MS/MS analysis, although the increase is not statistically significant (Figure 2.2B).

The sialylated mucus glycans are subject to cleavage by bacterial sialidases, which release free sialic acids that subsequently become accessible to *C. rodentium*. We further quantified the levels of free sialic acids in the fecal contents and detected similar levels under both uninfected and infected conditions (Figure 2.2C). These findings indicate that sialic acid is abundant in the colon under both uninfected and infected conditions, but *C. rodentium* infection does not significantly change its availability.

In the host, mucin *O*-glycosylation is catalyzed by enzymes called glycosyltransferases. Sialyltransferases are glycosyltransferases that are responsible for biosynthesis of sialylated glycoproteins, adding sialic acid to the terminal portions of mucin glycans. To determine whether infection led to changes in host sialylation, the gene transcript levels of all three sialyltransferases present in mouse colons (Arike *et al.*, 2017) were quantified. Among the three sialyltransferases, β -galactoside α 2,6-sialyltransferase 1 (ST6GAL1) adds sialic acid to the 6-position of galactose while ST3GAL4 and ST3GAL6 contribute to α 2,3-sialylation. It appears that the levels of all three sialyltransferase enzymes were reduced upon infection (Figure A.2.1), suggesting the host may be limiting the synthesis of sialic acid in GCs in an effort to control the infection.

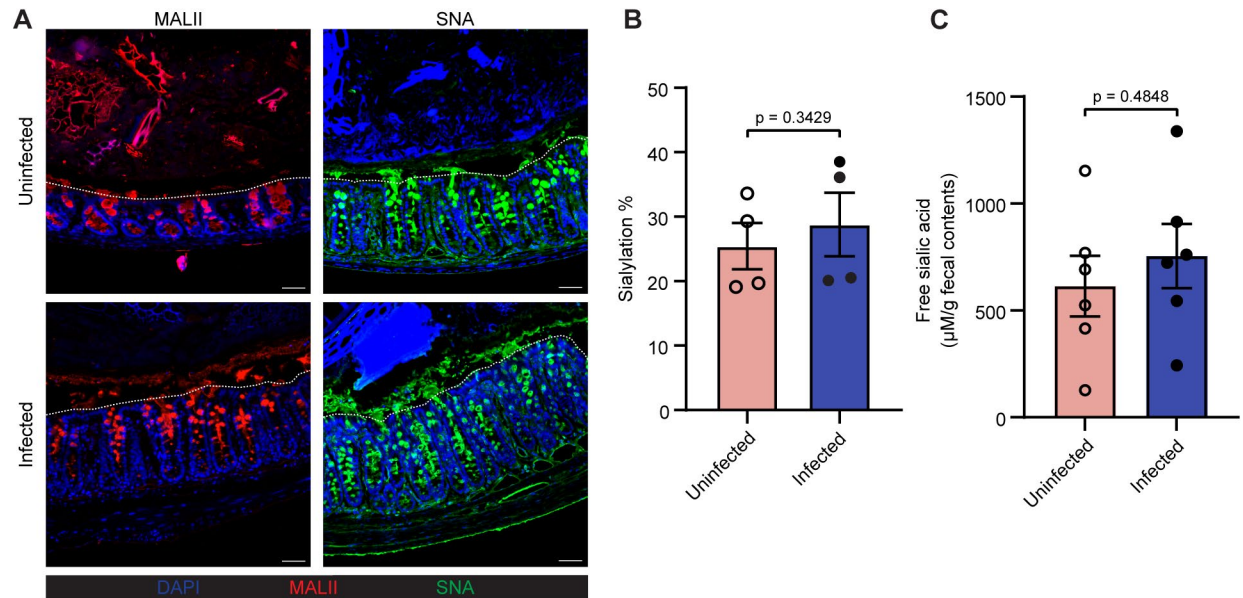


Figure 2.2 Sialic acid in the colon is mainly derived from mucus produced by goblet cells and widely expressed before and during *C. rodentium* infection.

(A) Representative immunofluorescence staining of sialic acid on murine colonic sections with and without infection of *C. rodentium*. Sections were stained with DAPI to detect DNA (blue), MALII lectin (recognizing α 2,3-linked sialylated and sulfated glycans), and SNA lectin (recognizing α 2,6-sialic acid) to visualize sialic acid. Dotted lines indicate the apical side of the epithelium. Original magnification = 200 \times . Scale bar = 50 μ m. (B) Degree of sialylation on Muc2 *O*-glycans of colonic mucus with ($n = 4$) and without ($n = 4$) infection with *C. rodentium* for 6 days. Released *O*-glycans from distal intestine were analyzed on PGC-LC-MS/MS. (C) Levels of free sialic acid in fecal contents of mice with ($n = 6$) and without ($n = 6$) infection of *C. rodentium* for 6 days.

2.3.3 A/E pathogens require the NanT transporter to utilize sialic acid

Due to the terminal position of sialic acid residues on Muc2 glycan chains, many commensals, as well as pathogens, have evolved sialic acid transport systems to exploit sialic acid as a nutrient source. In Enterobacteriaceae, the predominant sialic acid transporter is NanT, a major facilitator superfamily (MFS)-type transporter (North *et al.*, 2018; Thomas, 2016). Although sialic acid uptake in *C. rodentium* has not been previously characterized, our search of *C. rodentium*'s genome indicated the presence of the *nan* operon responsible for sialic acid catabolism, including a NanT homolog (Popov *et al.*, 2019). We generated an in-frame deletion mutant of the *nanT* gene in *C. rodentium*, termed the Δ *nanT* *C. rodentium* strain. Notably, this mutant displayed a clear defect in utilizing sialic acid (Neu5Ac) as a sole carbon source (Figure 2.3A), but showed

no impairment in using other mucin sugars or glucose for growth (Figure A.2.2). Similarly, deletion of *nanT* in EPEC ($\Delta nanT$ EPEC) also abolished its ability to use sialic acid as a sole carbon source (Figure 2.3B), but did not affect its growth in other mucin sugars (Figure A.2.2). These findings suggest that NanT is the sole sialic acid transporter expressed by *C. rodentium* and EPEC, which is required for the uptake of sialic acid in these A/E pathogens.

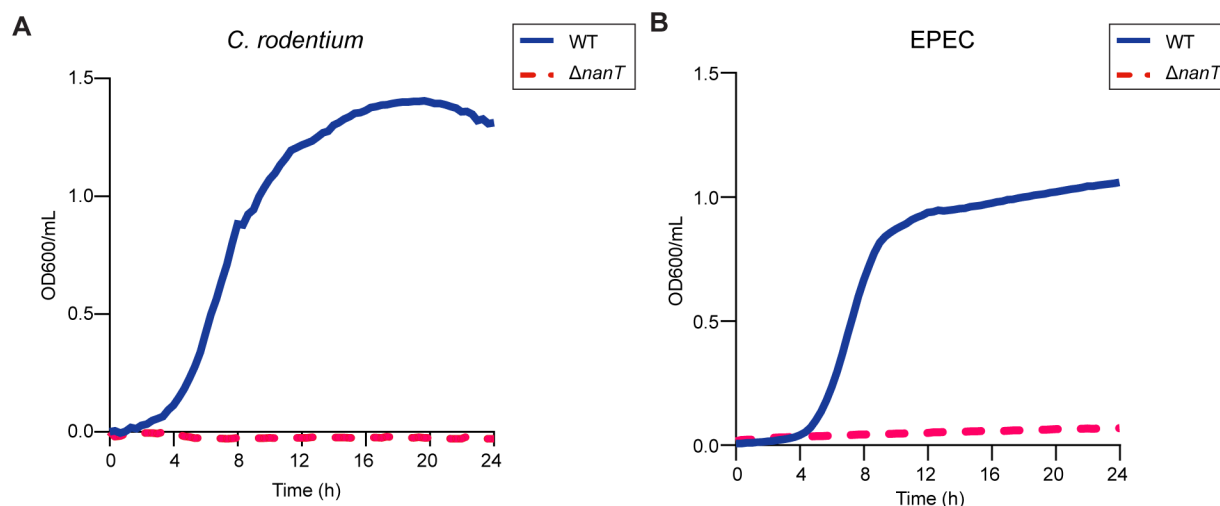


Figure 2.3 NanT is required for metabolism of sialic acid in *C. rodentium* and EPEC.

Growth analysis of $\Delta nanT$ *C. rodentium* (A) and $\Delta nanT$ EPEC (B) in M9 minimal medium supplemented with 0.2% sialic acid (Neu5Ac), in comparison to WT. Cultures were tracked with OD₆₀₀ readings at 20-minute intervals over 24 hours at 37°C. Data are presented as averages of cell growth ($n=9$) from three independent experiments.

2.3.4 Sialic acid utilization is important for the metabolic fitness of *C. rodentium* *in vivo*

To address the impact of NanT and sialic acid on *C. rodentium*'s *in vivo* pathogenesis, C57BL/6 mice were infected with a dose of $\sim 2.5 \times 10^8$ CFU of WT or $\Delta nanT$ *C. rodentium*. To monitor the colonization of each strain, pathogen burdens were enumerated from fecal samples over the course of infection. It was noticed that the $\Delta nanT$ mutant displayed a delay in colonizing mice at this infection dose, indicated by significantly lower burdens in mice infected $\Delta nanT$ at 3 days post-infection (DPI) compared to WT infected mice (Figure 2.4A). Impairment of $\Delta nanT$ in colonizing the colonic tissues was also observed at 8 DPI upon euthanizing the mice, with the

most significant difference appearing in the colons (Figure 2.4B). Macroscopically, $\Delta nanT$ caused less intestinal damage (*i.e.*, severely shrunken and inflamed ceca and shortened colons) (Figure 2.4C). Collectively, the above data suggested that at this infection dose, $\Delta nanT$ was delayed by several days in its ability to expand and heavily infect the colon as compared to WT *C. rodentium*. A competition experiment performed using equal amounts of WT and $\Delta nanT$ at a final dose of 2.5×10^8 CFU inoculum also found $\Delta nanT$ was outcompeted by WT in the cecum (CI = 0.92 ± 0.53), colon (CI = 0.56 ± 0.31), and intestinal lumen (CI = 0.59 ± 0.91) (Figure 2.4D), further revealing that $\Delta nanT$ *C. rodentium* displays reduced fitness compared to WT *in vivo*.

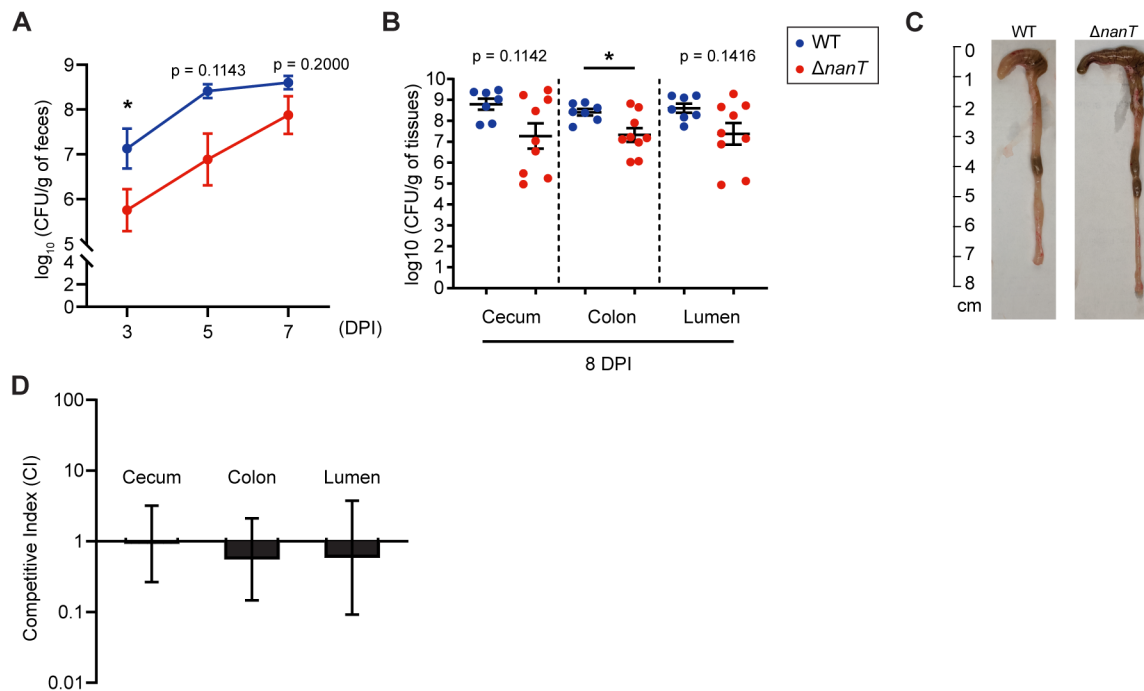


Figure 2.4 $\Delta nanT$ *C. rodentium* is delayed in colonizing mice at a 2.5×10^8 CFU infection dose.

(A-C) C57BL/6 mice were orally infected with 2.5×10^8 CFU of WT ($n = 7$) or $\Delta nanT$ ($n = 9$) *C. rodentium* (n , number of biological replicates), and (A) stools were collected at 3, 5, 7 days post infection (DPI); (B) intestinal tissues and luminal contents were collected at 8 DPI, plated and enumerated for *C. rodentium* CFU. (C) Representative macroscopic images of large intestines at 8 DPI showing an inflamed cecum and shrunken colon in WT infected mice compared to milder inflamed tissues in $\Delta nanT$ infected mice. (D) C57BL/6 mice were WT and $\Delta nanT$ *C. rodentium* in equal amounts and the competitive index (output ratio over input ratio of $\Delta nanT$ /WT) was determined at 6 DPI.

2.3.5 *C. rodentium* requires NanT to successfully colonize and expand in the large intestine

To better simulate the most common scenario of enteric pathogen infections in real life, where the pathogen is ingested in low numbers, but later on expands in the gut after adapting and obtaining available nutrients to expand, we tested the $\Delta nanT$ mutant with a lower dose infection, at 1×10^7 CFU, in C57BL/6CR mice. At this dose, WT and $\Delta nanT$ *C. rodentium* were found to colonize the mouse GI tract at similarly low levels in the early stages of infection (3 DPI) (Figure 2.5A, Figure A.2.2). Over the following days, we observed a rapid expansion of WT *C. rodentium* from $\sim 10^3$ CFU/g (at 3 DPI) to a level of $\sim 10^7$ CFU/g at 7 DPI (Figure 2.5A). In contrast, the $\Delta nanT$ *C. rodentium* strain appeared unable to expand over this time, remaining at CFU burdens (at 7 DPI), similar to those seen at 3 DPI (Figure 2.5A).

In the absence of an expansion of $\Delta nanT$, we euthanized infected mice at 8 DPI. Large numbers of WT *C. rodentium* were recovered from cecal and colonic tissues as well as from the luminal contents of infected mice (Figure 2.5B). In contrast, $\Delta nanT$ *C. rodentium* was either completely cleared from the intestines of most mice by 8 DPI, or otherwise remained at very low numbers ($< 10^4$ CFU/g) (Figure 2.5B). We also examined the colonization dynamics of $\Delta nanT$ in each individual mouse by enumerating their stool burdens throughout the infection. We confirmed that the $\Delta nanT$ mutant was able to colonize the intestines of all mice, but the timing of colonization, and clearance varied (Figure 2.5C). Such rapid clearance exhibited in $\Delta nanT$ infected mice suggests that the $\Delta nanT$ mutant is not only severely impaired in expanding its niche within the murine colon, but in many cases unable to maintain its niche in the absence of a functional sialic acid utilization pathway. Further, we tested the pathogenicity of $\Delta nanT$ with this

lower dose in the highly susceptible C3H/HeJ mouse strain in which a normal dose infection by *C. rodentium* is fatal. Similarly, $\Delta nanT$ *C. rodentium* showed reduced colonization, most significantly in the distal colon (Figure 2.5E). $\Delta nanT$ *C. rodentium* was also impaired in spreading systemically into mesenteric lymph nodes, liver and spleen (Figure 2.5F).

In line with the reduced burdens observed in C57BL/6 mice infected with $\Delta nanT$, WT *C. rodentium* was also found to heavily colonize the colonic mucosal surface at the time when the mice were euthanized (8 DPI), with many bacteria found intimately attached to the colonic epithelium whereas $\Delta nanT$ *C. rodentium* were too few in number to detect by immunostaining (Figure 2.5D).

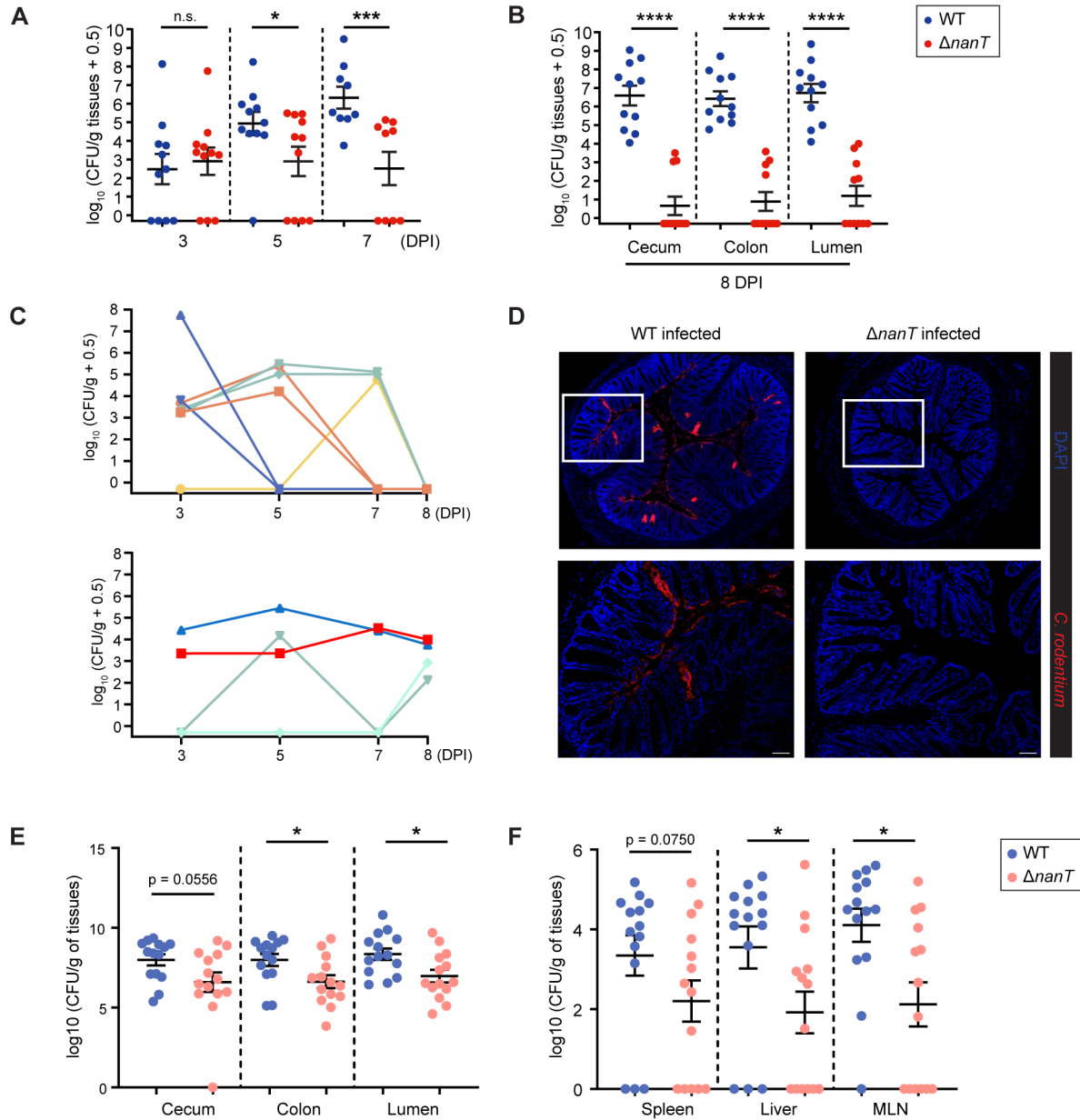


Figure 2.5 *ΔnanT C. rodentium* is significantly impaired in its ability to colonize mice at a 1×10^7 CFU infection dose.

(A-D) C57BL/6 mice were orally infected with 1×10^7 CFU of WT ($n = 11$) or *ΔnanT* ($n = 11$) *C. rodentium* (n , number of biological replicates), and (A) stools were collected at 3, 5, 7 days post infection (DPI); (B) intestinal tissues and luminal contents were collected at 8 DPI, plated and enumerated for *C. rodentium* CFU. (C) Colonization of *ΔnanT* in each individual mouse, enumerated from stools collected on 3, 5 and 7 DPI, shows that *ΔnanT* was able to colonize the intestines of all mice, but the timing of colonization, and clearance varied. Most mice completely cleared by 8 DPI (top), while others remained at very low numbers (bottom). (D) Representative colonic immunostaining for *Citrobacter* LPS (red) and DAPI (blue), showing little to no *C. rodentium* present on the *ΔnanT*-infected colon. Lower panels are expanded images of corresponding boxed regions in panels above. Original magnification = 200 \times . Scale bar = 50 μ m. (E-F) C3H/HeJ mice were orally infected with 1×10^7 CFU of WT or *ΔnanT* *C. rodentium* and (E) intestinal tissues and luminal contents and (F) systemic tissues were collected at 18h post infection (p.i.), plated and

bacterial numbers enumerated. Data are represented as mean \pm SEM from four independent experiments. **** $p < 0.0001$, *** $p < 0.001$, ** $p < 0.01$, * $p < 0.05$. Statistical significance calculated by Mann-Whitney U-test (A, B).

2.3.6 $\Delta nanT$ *C. rodentium* failed to elicit colitis in a competitive environment

Histopathological damage caused by WT and $\Delta nanT$ *C. rodentium* infection at the lower infectious dose was evaluated. Mice infected with WT *C. rodentium* developed significant intestinal inflammation, leading to the disruption of colonic crypt architecture and extensive inflammatory cell infiltration. In contrast, the transient colonization by $\Delta nanT$ *C. rodentium* caused very modest colonic pathology (Figure 2.6A-B).

Upon establishing an infection in the host GI tract, *C. rodentium* and its associated pathogen-associated molecular patterns (PAMPs) trigger inflammation, by activating transcription factors, leading to the production of pro-inflammatory cytokines, such as IL-6 by innate immune cells through Toll-like receptor (TLR) signaling; the production of IL-1 β through inflammasome activation; as well as the production of IFN- γ and IL-17 α cytokines through Th1 and Th17 responses. By measuring gene transcription levels of these key cytokines, we confirmed that mice infected with $\Delta nanT$ showed little inflammatory response to infection as their cytokine expression levels were similar to those of uninfected controls. As expected, upon infection of WT *C. rodentium*, a significant elevation in inflammatory cytokine gene expression was seen within both the cecum and colon (Figure 2.6C). Together, these data suggest that the transient colonization by $\Delta nanT$ *C. rodentium* failed to induce an overt inflammatory response, thus causing very modest colonic pathology.

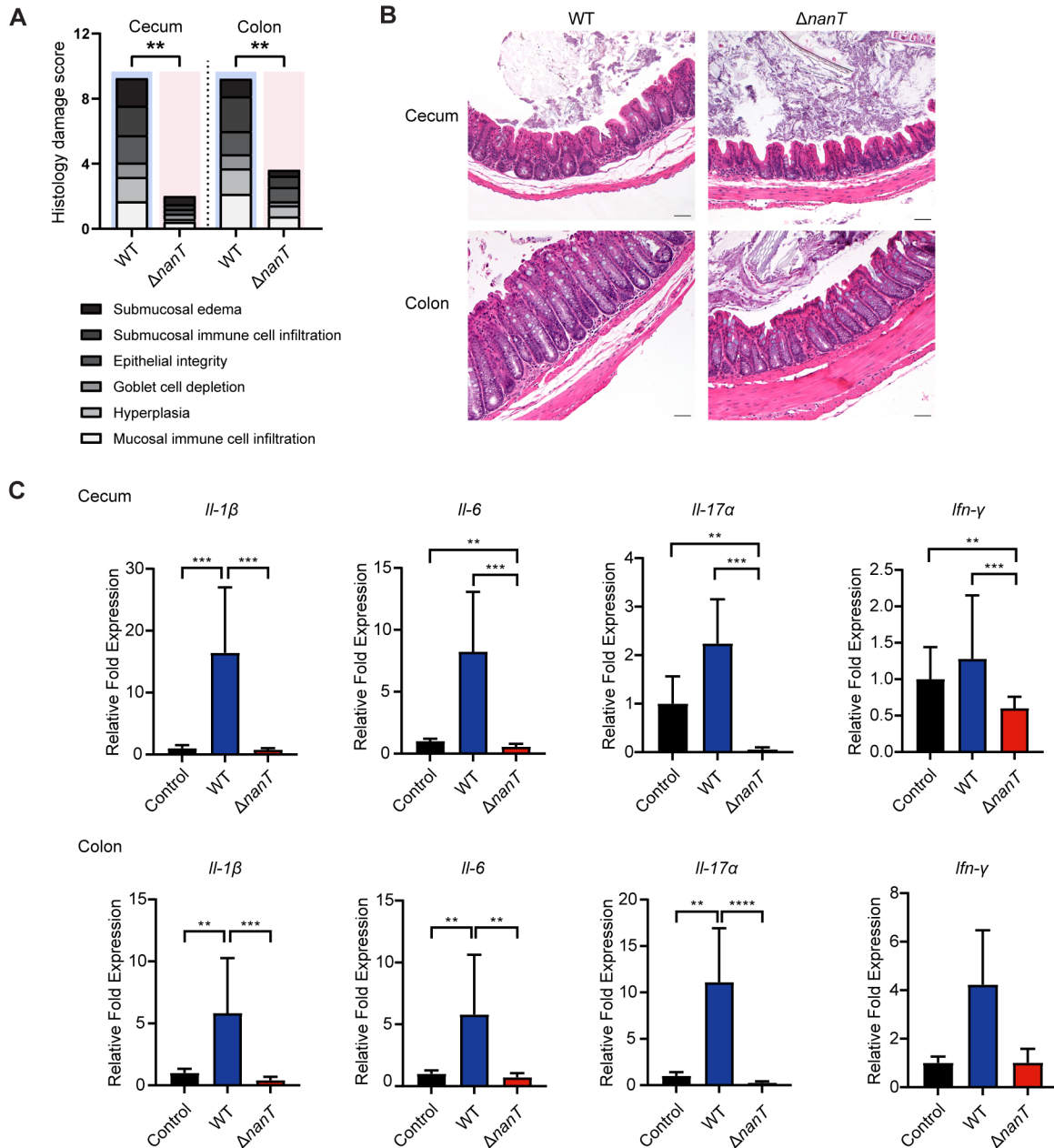


Figure 2.6 $\Delta nanT$ *C. rodentium* failed to elicit colitis and induce an overt inflammatory response.

(A) Blinded histopathological scores of H&E tissue sections of mice infected with WT ($n = 8$) or $\Delta nanT$ ($n = 8$) *C. rodentium* (see Materials and Methods for scoring criteria). Means are indicated. Agreement among raters ensured by Kendall's coefficient of concordance WT = 0.848. (B) Representative H&E-stained cecal and distal colonic sections from WT and $\Delta nanT$ infected mice. Original magnification = 200 \times . Scale bar = 50 μ m. (C) qPCR analysis of inflammatory genes in mouse cecum and colon, expressed as fold change over control uninfected mice. **** $p < 0.0001$, *** $p < 0.001$, ** $p < 0.01$. Statistical significance calculated by Mann-Whitney U-test (A) and one-way ANOVA (C).

2.3.7 Exogenous administration of sialic acid exacerbated *C. rodentium*-induced colitis

The above results demonstrate that *C. rodentium* colonization and virulence are attenuated *in vivo* when the pathogen cannot utilize sialic acid ($\Delta nanT$). Despite sialic acid being abundant in the mouse GI tract, *C. rodentium* faces significant competition from the gut microbiota to access this key nutrient as many commensal bacteria exhibit significant capacity to utilize sialic acid as a metabolic substrate (Bell *et al.*, 2023). Hence, we investigated the impact of exogenous free sialic acid on *C. rodentium* infection. C57BL/6 mice were gavaged with 1mg of sialic acid once a day from 24h prior to infection until 1 DPI, while subsequently being administered with 1% sialic acid in their drinking water throughout the infection. The administration of free sialic acid accelerated the colonization of *C. rodentium*, as evidenced by the higher burdens recovered at 3 DPI (Figure 2.7A). This trend continued until the time of euthanization (6 DPI), with mice given sialic acid carrying higher numbers of *C. rodentium*, although the increase did not reach significance (Figure 2.7A-B).

Interestingly, histopathological analysis revealed that sialic acid administration resulted in a more severely damaged cecal and colonic epithelium, demonstrated by a higher degree of epithelial desquamation and occasional loss of defined crypt architecture (Figure 2.7C-D). In contrast, the control group lacking exogenous sialic acid showed a lesser degree of cell sloughing, hyperplasia, and immune cell infiltration, suggesting less pronounced epithelial damage (Figure 2.7C-D). These data suggest an additional role of sialic acid in *C. rodentium* infection, beyond serving as a nutrient for bacterial expansion, resulting in the exacerbated colitis observed in mice given free sialic acid.

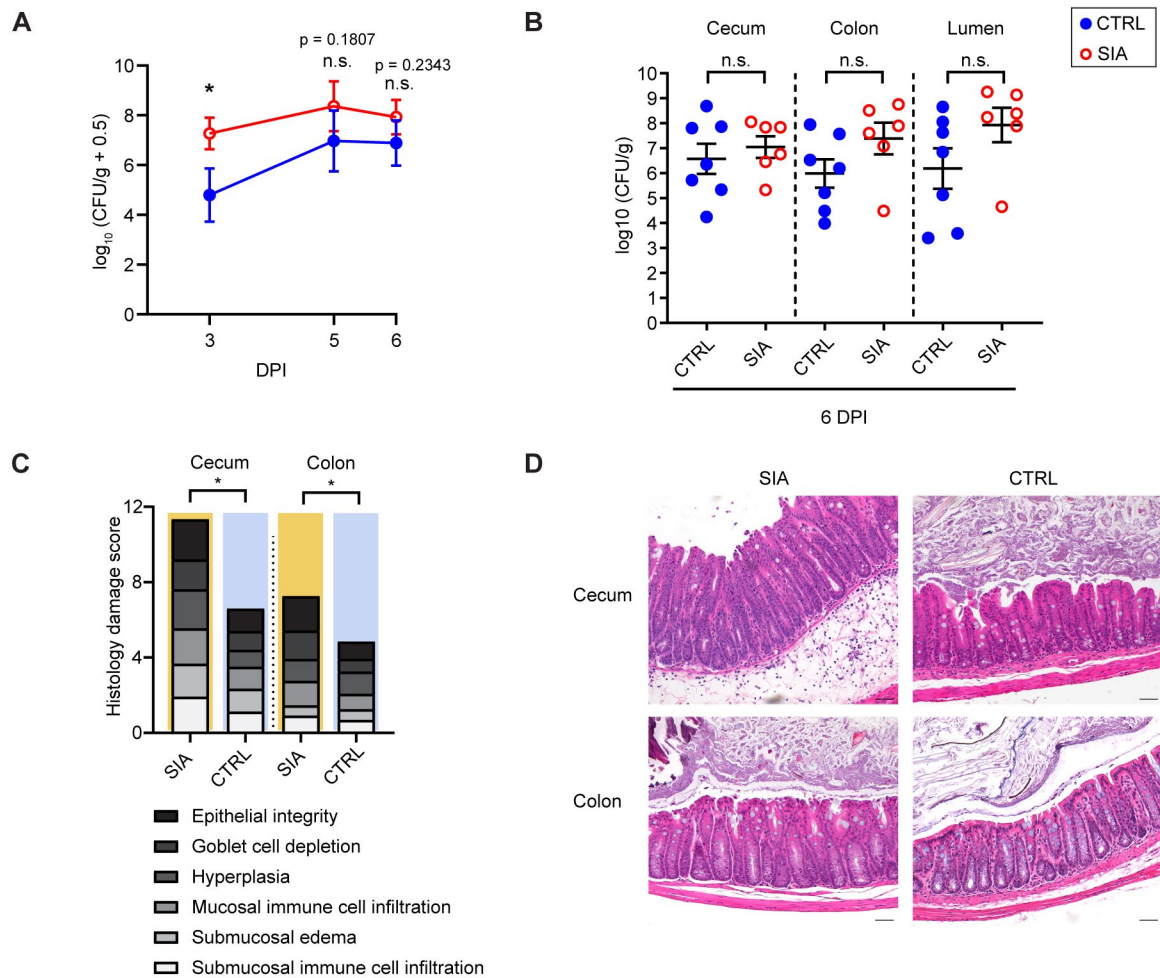


Figure 2.7 Exogenous administration of free sialic acid exacerbated *C. rodentium* infection.

C57BL/6 mice were treated with normal drinking water (CTRL) or exogenous free sialic acid (SIA) before and during *C. rodentium* infection and pathogen colonization was enumerated in (A) fecal contents collected at 3, 5, 6 (DPI) and (B) intestinal tissues and luminal contents collected at 6 DPI. Data are shown in the mean \pm SEM from two independent experiments. (C) Blinded histopathological scores of H&E tissue sections. Means are indicated. (D) Representative H&E-stained cecal and distal colonic sections from control mice and mice supplemented with exogenous free sialic acid. Original magnification = 200 \times . Scale bar = 50 μ m. * $p < 0.05$, n.s. = not significant. Significance levels calculated by Mann-Whitney U-test.

2.4 Discussion

The acquisition of nutrients is a critical factor in the success of bacterial pathogens, particularly those targeting the GI tract, but the nutrient sources utilized by A/E pathogens are still relatively

understudied. A previous study suggested that commensal *E. coli* directly competes with *C. rodentium* for carbon sources during pathogen clearance (Kamada *et al.*, 2012). While knowledge regarding nutrient sources for A/E pathogens is limited, growth analyses of commensal *E. coli* from previous research may provide insights into potential nutrients favored by *C. rodentium*. Both *C. rodentium* and commensal *E. coli* exhibit optimal growth on monosaccharides, but not on polysaccharides, suggesting that monosaccharides are the preferred carbon sources for these bacteria (Kamada *et al.*, 2012). When cultured on mouse cecal mucus, commensal *E. coli* upregulates a spectrum of genes related to catabolic pathways for mucus-derived nutrients. Correspondingly, mutations in carbohydrate metabolism pathways have been shown to affect *in vivo* colonization of *E. coli* (Chang *et al.*, 2004). Moreover, mucin *O*-glycan-derived monosaccharides have been shown to support *E. coli* growth to varying degrees during different stages of its colonization (Chang *et al.*, 2004). We hypothesize that mucin *O*-glycans are also a major source of nutrients for *C. rodentium* during its migration through colonic mucus. My study demonstrated that *C. rodentium* is capable of utilizing three out of the five key sugars that make up the Muc2 *O*-glycans for growth, including sialic acid, galactose and *N*-acetyl glucosamine. Moreover, the pathogen may display a hierarchical utilization of nutrient sources among these sugars, as observed in commensal *E. coli*, wherein the consumption of sugars occurs in a specific order determined by their genetic program for nutritional preferences. In our growth assays, *C. rodentium* appeared to enter log phase in minimal media supplemented with GlcNAc faster than with sialic acid or galactose. Furthermore, the selection of carbohydrates utilized could also be influenced by the intestinal environment, including variations in nutrient availability and sites of colonization. Our *in vivo* data indicate that sialic acid plays a significant

role in the expansion phase of *C. rodentium* infection (from 3 DPI), corresponding with the timing for colonic mucosa colonization.

My findings and others (Arike *et al.*, 2017; Holmén Larsson *et al.*, 2013; Robbe *et al.*, 2003) have demonstrated that sialic acid in the mammalian large intestine is mainly derived from the mucus secreted by GCs, which contains a high proportion of sialylated mucins. In the distal colon, where there is a high microbial burden and an abundance of commensals capable of catabolizing sialic acid, the availability of this nutrient is likely limited. Invading pathogens must compete for it with the resident bacteria. Previous studies have revealed that α 2,6-linked sialic acid is more abundant than α 2,3-linked sialic acid in human and mouse colonic Muc2 glycans through glycomic analysis of mucin *O*-glycans and the proteomic analysis of sialyltransferase expression (Arike *et al.*, 2017; Robbe *et al.*, 2003). My study employed the SNA lectin for the detection of α 2,6-linked sialic acid and the MALII lectin for the recognition of α 2,3-linked sialic acid. Although MALII lectin has been widely used for detecting α 2,3-linked sialic acid, recent evidence suggested that it primarily binds to sulphated glycans rather than sialylated glycans (Bergstrom *et al.*, 2020). Thus, the distribution of α 2,3-linked sialic acid in the GI tract and its response to infection needs further clarification. Furthermore, the varying binding affinities of these lectins present challenges when directly comparing the abundance of different sialic acid linkages through staining (Bojar *et al.*, 2022). A previous proteomic study revealed an increase in sialyltransferase expression and mucus secretion upon microbial colonization of previously GF mice (Arike *et al.*, 2017). My data indicated that the expression of sialyltransferases by IEC was reduced upon *C. rodentium* infection, however, free sialic acid remained present in large amounts both before and after infection. Alterations in microbiota composition during *C.*

rodentium infection could also impact the availability of sialic acid for *C. rodentium*, which needs to be further characterized.

We showed that provision of exogenous sialic acid accelerated the course of *C. rodentium* infection. Correspondingly, the $\Delta nanT$ *C. rodentium* strain proved dramatically attenuated in its ability to infect its hosts when given at a “low” dose. While capable of initially colonizing the mouse colonic lumen, the $\Delta nanT$ strain was unable to expand beyond a very modest level, and in many cases was rapidly cleared from the colon. We suspect this partly reflects an inability of the mutant strain to acquire sufficient nutrients to fuel its passage across the mucus layer and reach the underlying epithelium. Even when given at a higher infectious dose, the $\Delta nanT$ strain was still impaired in colonizing the mouse colon as compared to WT *C. rodentium*, being delayed by several days in its ability to expand and heavily infect the colon. This delay highlights the important role played by sialic acid. It also indicates that given a large enough infectious dose, $\Delta nanT$ *C. rodentium* can eventually overcome its inability to use sialic acid, likely by acquiring other (less preferred) nutrients.

The utilization of intestinal mucus as a nutrient source appears to be a common strategy employed by enteric pathogens and is critical for their survival (McDonald *et al.*, 2016; Ng *et al.*, 2013). However, a previous study from our laboratory demonstrated that mice deficient ($^{-/-}$) in the mucin Muc2, and therefore lacking a mucus layer, are highly susceptible to *C. rodentium* infection. *Muc2* $^{-/-}$ mice carried large pathogen burdens and suffered from exaggerated colitis (Bergstrom *et al.*, 2010). These findings suggest that *C. rodentium* is capable of colonizing and expanding within the mouse colon in the absence of mucus, and therefore, mucus-derived sialic

acid. While the source of alternative nutrients available within the *Muc2*^{-/-} colon remains elusive, earlier research revealed that the A/E pathogen EPEC can extract nutrients from infected IEC in culture, using components of its T3SS. If this mechanism is also true for *C. rodentium*, then in the absence of a mucus barrier, once it infects the colonic epithelium, sialic acid would potentially be redundant if this pathogen could obtain a rich supply of nutrients from the cells it directly infects.

In conclusion, my study revealed that sialic acid is present in mucins produced by goblet cells, as well as in the gut lumen and secreted mucus. Furthermore, I demonstrated that *C. rodentium* can utilize sialic acid as its sole carbon source for growth, via a pathway that is dependent on the sialic acid transporter NanT. I also found that *C. rodentium* lacking the *nanT* gene showed reduced colonization abilities, suggesting the importance of sialic acid in *C. rodentium* colonization *in vivo*. Administration of exogenous free sialic acid to mice resulted in an expedited colonization by WT *C. rodentium* and induced more severe pathology. To further investigate the underlying mechanism, it is crucial to challenge these mice with $\Delta nanT$ *C. rodentium* to confirm if the heightened inflammation observed in WT infection is indeed attributed to the uptake of sialic acid by *C. rodentium*. While previous research has identified the role of sialic acid catabolism in the expansion of enteric bacterial pathogens following antibiotic use (Ng *et al.*, 2013), our study is the first to reveal its role in the absence of antibiotics.

2.5 Materials and Methods

2.5.1 Bacterial strains and growth conditions

C. rodentium strain DBS100 and *E. coli* O127:H6 strain E2348/69 (streptomycin-resistant) were used as the wild-type (WT) bacterial strains in this study. Bacteria were routinely grown on Luria-Bertani (LB) agar plates or in LB broth with shaking (200 rpm) at 37°C overnight. Where appropriate, streptomycin was supplemented at 100 µg/ml, while kanamycin was supplemented at 50 µg/ml. For growth analysis on intestinal mucus and mucosal sugars as sole carbon sources, M9 minimal medium supplemented with 2 mM MgSO₄ and 0.1 mM CaCl₂ was used.

2.5.2 Mutant construction

In-frame deletion mutants of *C. rodentium* DBS100 and EPEC E2348/69 were using overlap extension PCR (Ho *et al.*, 1989) with a suicide vector pRE112 (Edwards *et al.*, 1998). Two PCR fragments, upstream and downstream of each target gene respectively were amplified using DNA extracted from WT strain as a template by primers with flanking KpnI restriction site or primers with flanking SacI restriction sites as detailed in Table A.2.1. The two PCR fragments, sharing an overlapping sequence, were used as the template for a secondary PCR, the product of which was then digested with KpnI and SacI restriction enzymes, and directly cloned into pRE112 (chloramphenicol resistant). The plasmid construct was transformed into *E. coli* SM10 λ pir via electroporation, and introduced into the WT strain by conjugation. Double-crossover mutants were selected by plating onto LB (no sodium chloride) agar plates containing 5% sucrose. The resulting mutants were confirmed by PCR and DNA sequencing with check-Forward and check-Reverse primers (Table A.2.1).

2.5.3 Bacterial growth curve

Overnight bacterial cultures grown (shaking) in LB broth at 37°C were pelleted by centrifugation, washed three times with M9 media, and resuspended in M9 media. Resuspended cultures were then diluted 1:100 in 200 µl M9 media supplemented with either 0.2% of purified porcine stomach mucin (Millipore Sigma), galactose (Fisher Scientific), *N*-acetylgalactosamine, *N*-acetylglucosamine, sialic acid (Millipore Sigma), or fucose (Millipore Sigma) was added to M9 to serve as the carbon source. Cultures were added into a sterile 96-well plate (Costar) and incubated at 37°C with shaking for 24 hours. The optical density at 600 nm (OD₆₀₀) was taken every 20 minutes using a Varioskan LUX microplate reader (Thermo Fisher). Each experiment was performed with at least three biological replicates. Results were confirmed by measuring bacterial densities in CFU per ml of culture in parallel experiments run in test tubes.

2.5.4 Murine colonic mucin isolation, purification, and characterization

Colonic mucus was gently scraped from uninfected C57BL/6 mice (control) and mice infected with *C. rodentium* at 6 DPI. Mucus was partially purified from mucosal scrapings by repeated extraction with 3 × 100 µl aliquots of 6 M guanidine hydrochloride (GuHCl) (Herrmann *et al.*, 1999). The Muc2 containing insoluble fraction was washed with 80% ice cold acetone to remove excess GuHCl and centrifuged at 14,000 relative centrifugal force (RCF) for 10 min to obtain a Muc2 containing pellet. *O*-glycans were released in-solution by reductive beta elimination by the addition of 100 µl of 1 M NaBH₄ in 100 mM KOH and incubation at 50°C for 16 hours. The reaction was quenched with 10 µl glacial acetic acid, then desalted with Dowex AG-50W-X8 cation exchange resin and porous graphitized carbon packed into 100 µl C18 OMIX tips (Agilent). Desalted *O*-linked glycans were analyzed by porous graphitized carbon (PGC)-LC-

MS/MS in negative ion mode (Jensen *et al.*, 2012). Glycan peak areas were processed with Skyline 3.7.0. Peak area of all sialylated glycans were divided by the total peak area of all glycans detected to obtain a relative abundance of sialylated glycans.

2.5.5 Quantification of free sialic acid

Mouse fecal samples were collected and snap-frozen before use. Feces were weighed, reconstituted in distilled water (200 mg/ml) and homogenized for 15 minutes at maximum speed. Clarified supernatants were obtained after centrifugation for 15 minutes at 14,000 *ref* and used to measure free sialic acid levels using QuantiChrom Sialic Acid Assay Kit (BioAssay Systems) according to the manufacturer's protocol.

2.5.6 Mouse infections

C57BL/6CR mice (6–10 weeks old) used in this study were bred under specific pathogen-free conditions at the BC Children's Hospital Research Institute or purchased from Charles River Laboratories. C3H/HeJ mice (6–10 weeks old) were purchased from the Jackson Laboratory. Mice were fed a normal chow diet (Picolab Rodent Diet 20, Cat #5053) for at least two weeks prior to and throughout the infections. Mice were orally gavaged with $5.0 \times 10^6 \sim 2.5 \times 10^8$ CFU of *C. rodentium*. To monitor *C. rodentium* colonization, fecal pellets were collected, homogenized in PBS and plated on LB agar containing streptomycin. At the end of each experiment, mice were anaesthetized with isoflurane and euthanized by cervical dislocation. Colonic tissues were immediately fixed in 10% neutral buffered formalin (Fisher) for 24 h or in Methacarn fixative (60% methanol, 30% chloroform, 10% glacial acetic acid) for 3 to 24 hours

at 4°C. Pathogen burdens within tissues or luminal compartments were enumerated through serial dilutions on selective agar plates.

For sialic acid administration experiments, *N*-acetylneuraminic acid (Calbiochem) was administered in the water at a 1% concentration throughout the infection. Additionally, mice were orally gavaged with 1 mg of sialic acid once a day from 24 h prior to infection until 1 DPI.

2.5.7 Histopathological scoring

Histopathological analysis was performed on hematoxylin-eosin-stained (H&E) cecal and distal colon tissue sections. In brief, tissues previously fixed in 10% neutral buffered formalin were paraffin-embedded and sectioned at 5 µm. These sections were stained with H&E and scored by two blinded observers using previously established criteria (Gibson *et al.*, 2008). Tissue sections were assessed for: (1) submucosal edema (0-no change, 1- mild, 2-moderate, 3- severe), (2) submucosal polymorphonuclear neutrophil (PMN) and mononuclear cell infiltration (per 400x magnification field) (0- < 5, 1- 5-20, 2- 21 to 60, 3- 61 to 100, 4- >100 cells/field), (3) epithelial integrity (0-no pathological changes detectable, 1-epithelial desquamation (few cells sloughed, surface rippled), 2-erosion of epithelial surface (epithelial surface rippled, damaged), 3-epithelial surface severely disrupted/damaged, large amounts of cell sloughing, 4-ulceration), (4) goblet cell depletion (0-no change, 1-mild depletion, 2-severe depletion, 3-absence of goblet cells), (5) crypt hyperplasia (0-no change, 1: 1–50%, 2: 51–100%, 3: >100%), (6) mucosal mononuclear cell infiltration (per 400x magnification field) (0-no change, 1- <20, 2- 20 to 50, 3- >50 cells/field). A maximum score under this scale is 20.

2.5.8 Immunofluorescence and lectin staining

Paraffin-embedded tissue sections (5 μm) were deparaffinized by heating at 60°C for 8 minutes, cleared with xylene, rehydrated with 100%, 95%, and 70% ethanol, followed by dH₂O.

Deparaffinized sections were boiled in sodium citrate buffer (pH 6.0) for 40 minutes, followed by 1 hour blocking with blocking buffer (PBS containing 2 % donkey serum, 0.1% Triton-X100 and 0.05% Tween 20). For visualizing *C. rodentium* localization in the intestinal mucus, Methacarn-fixed mouse distal colons were stained with the following primary antibodies: rat anti-*C. rodentium* Tir (gift from W. Deng), rabbit anti-Muc2 (Boster), rabbit anti-Muc2 (Novus), which were then probed with Alexa Fluor 488-conjugated donkey anti-rabbit IgG (Life Technologies) and Alexa Fluor 568-conjugated donkey anti-rat IgG (Life Technologies). To detect WT and $\Delta nanT$ *C. rodentium* in tissue sections, formalin-fixed sections were stained with antisera against *E. coli* monospecific O152 (rabbit polyclonal, SSI Diagnostica) that recognizes *C. rodentium* O-antigen (Tsai *et al.*, 2022; Vallance *et al.*, 2002), and labeled with Alexa Fluor 568-conjugated donkey anti-rabbit IgG (Life Technologies). To detect the distribution of sialic acid, FITC-*Sambucus nigra* agglutinin (SNA, Vector laboratories) and biotinylated-*Maackia amurensis* lectin II (MALII, Vector laboratories) were used. Stained tissues were mounted using ProLong Gold Antifade reagent containing 4',6-diamidino-2-phenylindole (DAPI, Invitrogen).

2.5.9 RNA extraction and quantitative real-time PCR for host cytokine responses

RNA from mouse cecal and distal colonic tissues was preserved in RNAlater (Qiagen) and extracted using the RNeasy Mini kit (Qiagen) according to the manufacturer's instructions. Total RNA was quantified using a NanoDrop spectrophotometer (Thermo Fisher). Complementary DNA (cDNA) was constructed from reverse transcription of 500 ng RNA using 5X All-In-One

RT MasterMix (Applied Biological Materials) according to the manufacturer's instructions. The cDNA was then diluted 1:5 in RNase/DNase free H₂O and 5 µl was used for 20 µl quantitative PCR (qPCR) reactions that contained primers (300 nM) and 10 µl SsoFast EvaGreen Supermix (Bio-Rad). qPCR reactions were carried out using a Bio-Rad CFX connect Real-time PCR detection system, with the specificity for each of the PCR reactions confirmed by melting point analysis. The expression of genes was normalized to housekeeping gene, *Ribosomal Protein Lateral Stalk Subunit (Rplp0)*. mRNA transcript expression was normalized to the relative expression of the reference genes using the $2^{-\Delta Ct}$. For treatment conditions, mRNA transcript expression was normalized to the control group (untreated condition) using the $2^{-\Delta\Delta Ct}$ method and presented as relative expression values. Primers used for qPCR are listed in Table A.2.2.

Chapter 3: Sialic acid metabolism plays a key role in promoting the virulence of A/E pathogens

3.1 Synopsis

The ability to dynamically regulate the expression of virulence factors is critical for enteric pathogens to adapt to their environment and maximize their fitness. This regulation is often achieved through changes in gene expression in response to environmental cues such as nutrient availability. Nutrients can serve as energy sources for pathogens to fuel their growth, and/or as signaling molecules that guide pathogen virulence strategies for niche adaptation. Here, I highlight the importance of sialic acid, a mucin-derived nutrient, in regulating the virulence of *C. rodentium* at the intestinal lumen-mucus-epithelium interface. My research shows that sialic acid acts as a signal that is sensed by *C. rodentium* to migrate towards intestinal mucus. Furthermore, sialic acid enhances *C. rodentium*'s virulence by inducing the secretion of two important virulence factors, Pic and EspC, which promote the penetration of mucus and increase adhesion to the underlying epithelium.

3.2 Introduction

Access to nutrients is not only crucial for a pathogen's metabolic fitness, but can also drive the expression of virulence factors that contribute to pathogenicity. Precise regulation of virulence expression allows enteric pathogens to adapt to a niche and establish colonization within an extremely competitive environment. The majority of research on the pathogenesis of A/E pathogens to date has focused on their T3SS (Croxen & Finlay, 2010). However, the virulence factors that play a critical role in the initial stages of A/E pathogen infections, prior to A/E lesion

formation, are poorly defined. Pathogens can sense and respond to environmental cues, including nutritional signals, to regulate the expression of virulence genes. For instance, various nutrients derived from the host and the gut microbiota have been associated with T3SS regulation in A/E pathogens, such as the amino acids arginine (Menezes-Garcia *et al.*, 2020), tryptophan (Kumar & Sperandio, 2019) and cysteine (Pifer *et al.*, 2018), as well as microbiota-derived 1,2-propanediol (Connolly *et al.*, 2018) and succinate (Curtis *et al.*, 2014). Furthermore, mucin-derived sugars have been shown to impact the expression of LEE genes in EHEC (Carlson-Banning & Sperandio, 2016; Le Bihan *et al.*, 2015, 2017; Pacheco *et al.*, 2012). As one of the mucin-derived sugars, sialic acid frequently terminates *O*-glycans and is likely recognized by bacteria localized to the mucus layer. Therefore, we hypothesize that sialic acid metabolism in *C. rodentium* may influence *C. rodentium* pathogenesis by modulating the expression of a wide range of virulence factors.

Enteric pathogens have evolved chemosensory mechanisms to search for nutrient sources in the host. The chemotactic sensing pathways further control bacterial motility, such as one driven by flagella, which allow pathogens to move towards areas in the host that are rich in their preferred nutrients (Wadhams & Armitage, 2004). *C. difficile* has been found to chemotax towards the mucin glycan monosaccharides mannose and GlcNAc, which also serve as carbon sources for *C. difficile* growth *in vitro*. Correspondingly, the presence of MUC2 increases *C. difficile*'s expression of genes encoding flagellar components *in vitro* (Engevik *et al.*, 2021). Similarly, flagellated *S. Typhimurium* also exhibit a chemotactic response to the mucin sugar galactose *in vitro*, which may contribute to its higher growth rate in the inflamed gut and increased accumulation at the cecal mucosa as compared to non-flagellated or non-chemotactic *S.*

Typhimurium mutants (Stecher *et al.*, 2008). Unlike *C. difficile* and *S. Typhimurium*, *C. rodentium* does not express flagella. It was not well understood how *C. rodentium* navigates through the intestinal mucus layer before reaching the underlying epithelium. While Chapter 2 highlights the significance of sialic acid as a vital nutrient for *C. rodentium*'s survival and fitness *in vivo*, here, I investigated the role of sialic acid as a signal for *C. rodentium*'s migration through the mucus layer and its function as a regulator of virulence. By elucidating the molecular mechanisms that govern the interplay between sialic acid and virulence factors in *C. rodentium*, we aim to gain insights into how this pathogen adapts to its host environment and identify novel strategies for controlling its virulence.

3.3 Results

3.3.1 Sialic acid is sensed by *C. rodentium* for migration via NanT

The ability to search for preferred nutrients in the competitive gut environment is important for enteric pathogens to establish their niche. We hypothesize that sialic acid could serve as a signal to help direct *C. rodentium* towards the nutrient-rich mucus layer, as a means to escape the highly competitive gut lumen. To examine whether *C. rodentium* is able to sense and actively migrate towards sialic acid, we developed a novel Eppendorf-tube-based chemotaxis assay adapted from the study of *Campylobacter jejuni* chemotaxis (Dwivedi *et al.*, 2016). In this assay, the bacteria underwent upward directional movement through a layer of soft agar when exposed to a chemoattractant placed at the top of the tube (Figure 3.1A). We found that WT *C. rodentium* migrated towards sialic acid or glucose, but not PBS (control), as indicated by the red positive staining of triphenyltetrazolium chloride (TTC) near the top of the tube (Figure 3.1B). In contrast, $\Delta nanT$ *C. rodentium* failed to migrate towards sialic acid but retained its ability to

migrate towards glucose (Figure 3.1B). Thus, the transporter NanT is required for sensing sialic acid and triggering the chemotactic movement of *C. rodentium* towards sialic acid. Sensing of sialic acid in the environment could facilitate *C. rodentium*'s ability to navigate towards the mucus layer and search for sialic acid during its colonization of the GI tract.

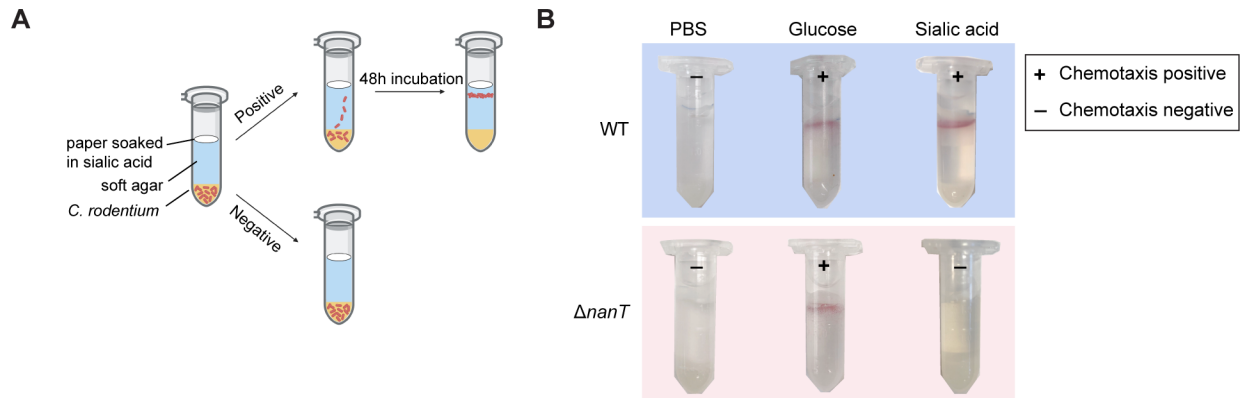


Figure 3.1 NanT is required for *C. rodentium* chemotaxis towards sialic acid.

(A) Schematic of a qualitative chemotaxis assay used. (B) Migration of WT and $\Delta nanT$ *C. rodentium* towards glucose or sialic acid. The “+” and “-” signs indicate the presence or absence of migration towards the stimulants, visualized through the formation of red rings of bacterial cells stained with 0.01% TTC (2,3,5-triphenyltetrazolium chloride). Images are representative of at least three independent experiments.

3.3.2 Sialic acid enhances *C. rodentium*'s ability to degrade mucins

Aside from promoting the growth of bacterial pathogens, nutrients can also function to modulate virulence gene expression during the pathogen's adaptation and/or establishment in the host's intestines (Liang & Vallance, 2021). Considering the dramatic impairment in pathogenesis observed with $\Delta nanT$ *C. rodentium*, we suspected that sialic acid could play a role in regulating *C. rodentium* virulence.

Since *C. rodentium* residing in the colonic lumen or outer mucus layer must penetrate the normally impenetrable inner mucus layer to infect the underlying epithelium, we examined

whether sialic acid would impact *C. rodentium*'s ability to degrade mucins. *C. rodentium* was cultured in Dulbecco's modified Eagle media (DMEM) supplemented with either sialic acid or glucose, with the supernatants collected and concentrated, followed by incubation with purified bovine submaxillary mucins (BSM). After incubation, the BSM was run on a sodium dodecyl sulfate-polyacrylamide gel electrophoresis (SDS-PAGE) gel and stained by periodic acid-Schiff (PAS) to recognize the glycosylated mucin proteins. As shown in Figure 3.2A, in the lane loaded with untreated BSM (mucus control), the majority of staining is seen at the loading site and consists of large undigested glycoproteins (LGP), whereas smaller digested glycoproteins (SGP) are seen to have migrated further down the lane. When the BSM were incubated with supernatant from WT *C. rodentium* grown in glucose, the LGP band disappeared, leaving only the SGP bands (red boxed area), indicating *C. rodentium* was able to partially degrade BSM, as previously reported (Bhullar *et al.*, 2015). Notably, when the BSM were incubated with the supernatant from sialic acid treated WT *C. rodentium*, both the LGP and SGP populations largely disappeared, suggesting sialic acid robustly increased the ability of *C. rodentium* to degrade mucins. Further, NanT plays an essential role in mediating the augmentation of mucin degradation by sialic acid, as BSM incubated with supernatants from sialic acid-cultured $\Delta nanT$ *C. rodentium* showed only partial mucin degradation, similar to the profile seen without sialic acid (red boxed area).

To determine if the enhanced mucinolytic activity induced by sialic acid in WT *C. rodentium* would accelerate the pathogen's penetration through a mucin layer, we employed a mucin transmigration assay (Hayashi *et al.*, 2013), in which *C. rodentium*, previously cultured in DMEM with glucose or sialic acid, was added onto mucins layered in Transwell inserts (3 μm

pores, 6.5 mm diameter, Corning), followed by an incubation at 37°C for 1 h before enumeration of bacteria that passed through the mucin layer and reached the lower chamber (Figure 3.2B). While only 2% of *C. rodentium* grown in glucose containing media were able to penetrate through the mucin layer within 1 h, pre-incubation of *C. rodentium* in sialic acid led to a significant 5-fold increase (11%) in migration through the mucin layer (Figure 3.2B). These findings demonstrate that exposure to sialic acid not only promotes *C. rodentium*'s mucin degradation activity, but also facilitates its ability to penetrate and transit across mucins.

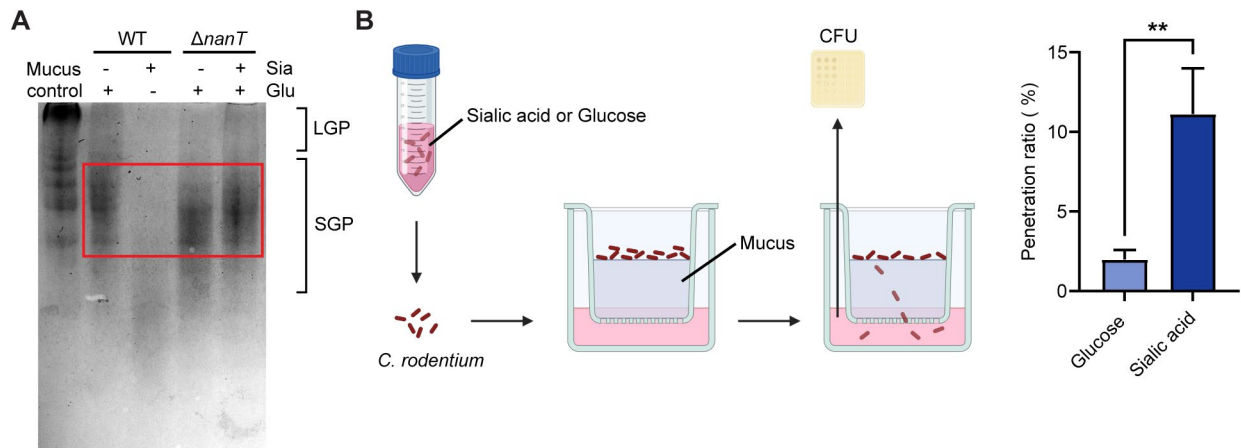


Figure 3.2 Sialic acid promotes *C. rodentium* mucin penetration.

(A) Characterization of mucinolytic activity in secreted proteins of WT and $\Delta nanT$ *C. rodentium* cultured in sialic acid compared to the glucose controls. Proteins secreted from WT cultured in glucose or from $\Delta nanT$ demonstrated moderate mucinolytic activity, indicated by the clearance of large glycoproteins (LGP) in the stacking region of the gel and increased abundance of smaller glycosylated proteins (SGP, boxed area). Secreted proteins collected from WT sialic acid culture demonstrated enhanced mucinolytic activity, cleaving the mucin proteins into significantly lower molecular weights. Image is representative of four independent experiments. (B) Penetration of WT *C. rodentium* through the mucin layer when pre-cultured in sialic acid compared to glucose. *C. rodentium* pre-cultured in Dulbecco's modified Eagle medium (DMEM) with glucose or sialic acid was added to the top of purified mucins layered in the insert of a Transwell. DMEM medium was placed in the lower chamber and collected after 1 hr incubation at 37°C. Bacteria that penetrated the transwells were collected from the lower chamber and plated for CFU. Penetration ratio represents the percentage of bacteria that have penetrated the mucin layer. Data are shown in mean \pm SEM from four independent experiments. ** $p < 0.01$. Significance levels calculated by Mann-Whitney U-test.

3.3.3 Sialic acid enhances epithelial adherence of A/E pathogens

The best-known characteristic of A/E pathogens is their ability to adhere to the gut mucosa and attach intimately to the apical plasma membrane of IECs. We explored whether sialic acid impacted *C. rodentium*'s ability to adhere to IECs by performing an *in vitro* adherence assay with the CMT-93 murine colonic IEC line. Under the standard condition where infections were carried out in regular DMEM media with or without glucose, $\Delta nanT$ displayed similarly low levels of intestinal epithelial adherence and pedestal formation as observed with WT *C. rodentium* (Figure 3A). In contrast, when sialic acid was added and served as the sole carbon source in the media, WT *C. rodentium* showed significantly increased adherence to the IEC (arrows). No increase in adherence was noted with the $\Delta nanT$ strain, however, as it remained at the same adherence level when exposed to sialic acid as it did when exposed to glucose (Figure 3.3A-B). These data demonstrate that sialic acid promotes the adherence of *C. rodentium* to IEC.

A/E lesions are characterized by remodeling of the epithelial cell cytoskeleton and formation of a pedestal-like structure beneath the bacteria. Immunostaining revealed an increase in pedestal formation by WT *C. rodentium* when treated with sialic acid, as evidenced by the accumulation of actin (arrowheads) beneath the majority of adherent bacteria (a typical feature of A/E pathogen infection) (Vallance & Finlay, 2000) (Figure 3.3B). This phenomenon was also observed in the infection of Caco-2 human IEC line by the human pathogen EPEC O127:H6. Similarly, sialic acid increased the attachment of WT EPEC to Caco-2 cells (Figure 3.3C-D). Strikingly, cross-section immunostaining showed a significantly greater number of pedestals formed when infection was performed in the presence of sialic acid (Figure 3.3E). Hence, these

results suggest that the potentiating effect of sialic acid on adherence is shared between EPEC and *C. rodentium*.

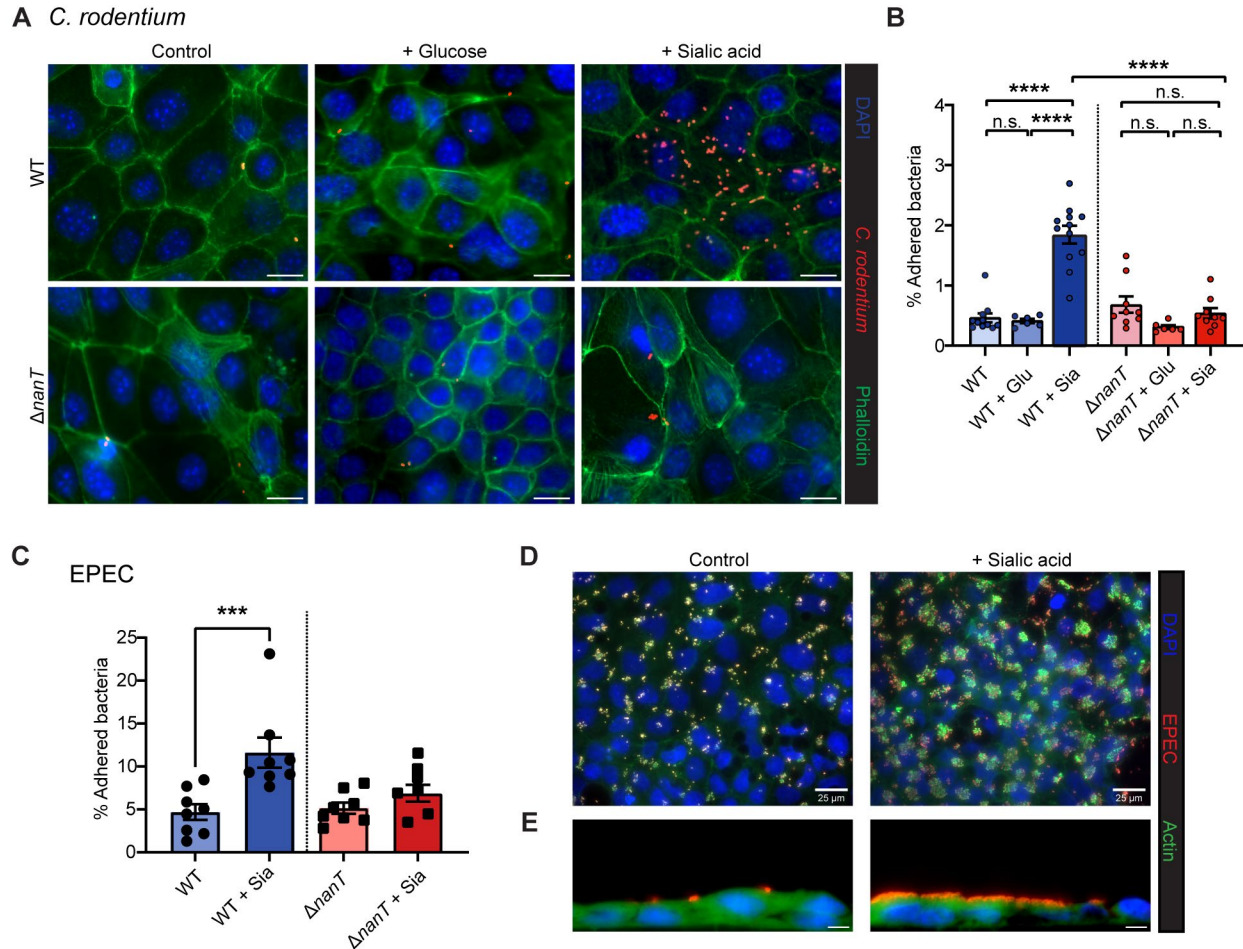


Figure 3.3 Sialic acid promotes *C. rodentium* and EPEC epithelial adherence.

(A) CMT-93 cells were infected with *C. rodentium* WT or $\Delta nanT$ in the presence or absence of sialic acid for 5 h, then washed to remove nonadherent bacteria and stained with phalloidin (green), anti-*C. rodentium* LPS (red) and DAPI to detect DNA (blue). Arrows and arrowheads indicate increased adherence and pedestal formation of WT *C. rodentium* respectively in the presence of sialic acid. Original magnification = 630 \times . Scale bar = 15 μ m. (B) Adherence of *C. rodentium* WT or $\Delta nanT$ to CMT-93 cells. Data represent the percentage of bacteria that adhered after 5 h infection. (C) Adherence of EPEC O127:H6 to Caco-2 cells. Data represent the percentage of bacteria that adhered after 5 h infection. (D) Immunostaining of Caco-2 cells infected with EPEC in the presence or absence of sialic acid, after removal of nonadherent bacteria and staining with phalloidin (green), O127 antiserum (red) and DAPI (blue). Original magnification = 630 \times . Scale bar = 25 μ m. (E) Representative images of infected Caco2 cells at cross-section. Original magnification = 630 \times . Scale bar = 5 μ m. Mean and SEM from three independent experiments are indicated. **** p < 0.0001, *** p < 0.001, n.s. = not significant. Significance levels calculated by Mann-Whitney U-test (B, C).

3.3.4 Sialic acid exerts minimal effect on *C. rodentium* T3SS transcription

The formation of A/E lesions by A/E pathogens requires a functional T3SS, which translocates bacterial effectors into colonocytes. We examined whether sialic acid promotes adherence in a T3SS-dependent manner. The expression of the T3SS is controlled by the master regulator Ler while EscN is a T3SS encoded ATPase required for T3SS function. The intimate attachment of *C. rodentium* is mediated through Tir, a T3SS effector that is injected into host cells and bound by the bacterial surface protein intimin (Gaytán *et al.*, 2016b). We therefore tested the effects of sialic acid on the ability of the T3SS-defective mutants $\Delta escN$ *C. rodentium* and Δtir *C. rodentium* to adhere to intestinal epithelial cells. Interestingly, while $\Delta escN$ and Δtir *C. rodentium* displayed limited ability to attach to IEC at baseline, sialic acid still promoted their adherence to IECs over baseline (Figure 3.4A). These findings indicate that sialic acid enhances *C. rodentium*'s adherence to IEC even in the absence of a functional T3SS, the key machinery promoting intimate cell adherence.

We further examined whether sialic acid would upregulate the transcription of *C. rodentium* T3SS. We employed a bioluminescent reporter strain Cr-P_{ler}-*lux*, in which WT *C. rodentium* carries a plasmid expressing the *luxCDABE* operon of *Photobacterium luminescens* under the control of the *ler* promoter (Winson *et al.*, 1998). Cr-P_{ler}-*lux* exhibited a lower level of bioluminescence per bacterium on average when grown in media containing sialic acid as compared to glucose (Figure 3.4B), although the difference was not statistically significant. This result suggests that sialic acid does not modulate the transcription of T3SS. Taken together, while sialic acid enhances *C. rodentium*'s adherence to IECs, it does not appear to regulate T3SS

transcription. These observations prompted further investigation into alternative virulence pathways influenced by sialic acid.

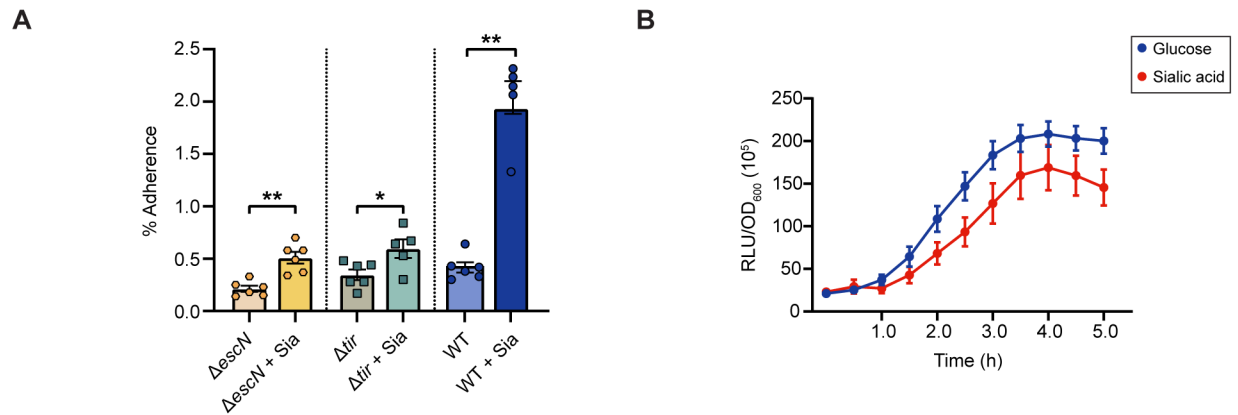


Figure 3.4 Sialic acid does not significantly alter *C. rodentium* T3SS expression.

(A) Adherence of *C. rodentium* $\Delta escN$ or Δtir (T3SS-deficient) strains to CMT-93 cells. Data represent the percentage of bacteria that adhered after 5 h infection. Mean and SEM from three independent experiments are indicated. ** $p < 0.01$, * $p < 0.05$, n.s. = not significant. Significance levels calculated by Mann-Whitney U-test. (B) Expression of *ler* is not significantly altered in response to sialic acid compared to glucose. Bioluminescent reporter strain Pler-*lux* *C. rodentium* was grown in DMEM with sialic acid or glucose under tissue culture conditions (20% O₂, 5% CO₂) for 5 hours. Expression of *ler* over time was measured by luciferase activity (relative luminescence units per optical density, RLU/OD₆₀₀), normalized to media containing no bacteria. Data are shown in the mean \pm SEM from three independent experiments.

3.3.5 Sialic acid induces the secretion of Pic and EspC proteins in *C. rodentium*.

We next delved into the key virulence factors of *C. rodentium* that are regulated in response to sialic acid. Protein secretion is a crucial mechanism used by pathogens to ensure survival and elicit virulence. This includes both T3SS-dependent and independent secretion systems, which deliver bacterial virulence proteins (effectors) to subvert host signaling pathways and immune responses or overcome colonization resistance conferred by the gut microbiota (Deng *et al.*, 2010). To determine whether sialic acid alters protein secretion by *C. rodentium* and EPEC, we cultured the bacteria in DMEM in the absence/presence of sialic acid (compared to glucose) and examined the protein secretion profile. The addition of sialic acid did not appear to affect the

secretion of the T3SS translocon proteins (*i.e.*, EspA, EspB, EspD), which are T3SS effectors that play a critical role in intimate adherence to IEC (Figure 3.5A, Figure A.3.1). In the case of EPEC, sialic acid significantly altered the secretion of a large number of proteins, resulting in a distinct protein profile for WT EPEC in comparison to glucose-treated samples (Figure A.3.1). For *C. rodentium*, sialic acid led to a significant increase in the secretion of proteins with molecular weights close to 115 kDa when compared to glucose-grown *C. rodentium*. These protein bands were also present in sialic acid cultures of the $\Delta escN$ *C. rodentium* strain that lacks a functional T3SS, suggesting the secretion of these proteins is T3SS-independent (Figure 3.5A).

To identify the differentially secreted proteins from *C. rodentium*, we took the supernatants of *C. rodentium* cultured in the presence of sialic acid and precipitated the proteins through the addition of 10% trichloroacetic acid (TCA) as previously described (Deng *et al.*, 2010), followed by analysis using an LC-MS/MS based approach. As expected, many T3SS-secreted proteins were identified, such as EspD, EspB, EspA and Tir (Table 3.1). Notably, we identified two proteins, EspC (EPEC secreted protein C) and Pic (protease involved in intestinal colonization) that showed high abundance, with predicted molecular weights 145.8 kDa and 141.0 kDa, respectively. To confirm the identity of these two proteins, we generated deletion mutants of *C. rodentium* ($\Delta espC$, $\Delta picC$, and $\Delta espC\Delta picC$ ($\Delta\Delta$)), and analyzed their secretion profiles in the presence/ absence of sialic acid. As shown in Figure 3.5B, the deletion of *espC* did not affect sialic acid-induced secretion of Pic, and similarly, the deletion of *picC* did not affect sialic acid-induced secretion of EspC. When both *espC* and *picC* were deleted, the large protein band(s) close to 115kDa typically induced by sialic acid were absent. However, RT-qPCR analysis did not detect a significant increase in expression of either the *picC* and *espC* genes or the T3SS-

related genes (*ler*, *tir*, *espB*) in WT *C. rodentium* grown in sialic acid compared to glucose (Figure A.3.2). Collectively, these data indicate that the secretion of two proteins, EspC and Pic, is induced by sialic acid in *C. rodentium*.

Table 3.1 Virulence proteins secreted by *C. rodentium* in sialic acid-induced culture identified by LC-MS/MS.

Protein ID	Protein description	MW (kDa)	Unique peptides	Sequence coverage (%)
D2TV59	Putative serine protease autotransporter Pic	145.8	91	68.91
D2TV46	Putative serine protease autotransporter EspC	141.0	69	40.60
D2TKE2	T3SS translocator protein EspD	39.6	38	79.21
D2TKE8	Translocated intimin receptor Tir	56.3	34	82.82
D2TKE1	T3SS effector protein EspB	33.4	36	89.41
D2TKE3	T3SS translocator protein EspA	20.5	34	96.87
D2TKD7	T3SS effector protein EspF	30.9	22	71.10

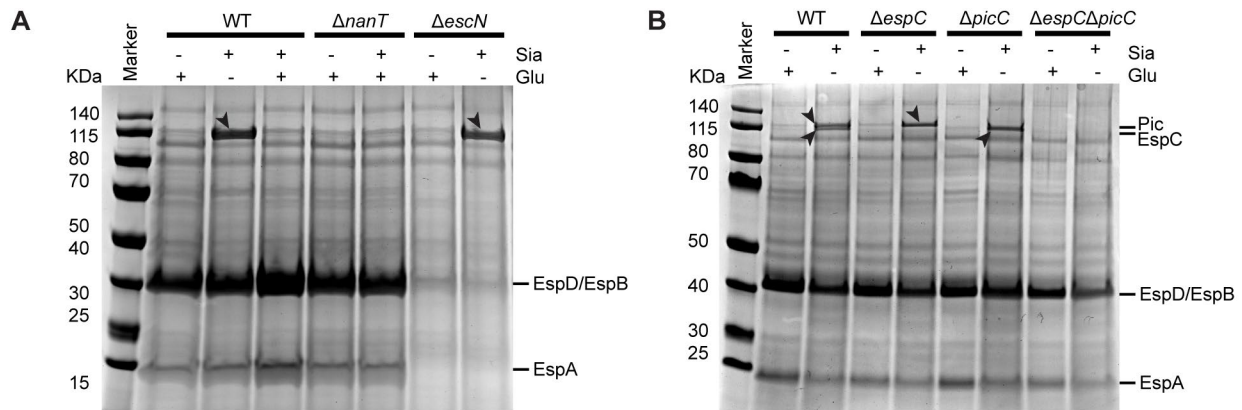


Figure 3.5 Sialic acid induces secretion of autotransporters Pic and EspC by *C. rodentium*.

(A) Protein secretion profiles of WT, $\Delta nanT$ and $\Delta escN$ *C. rodentium* after growth in DMEM with glucose or/and sialic acid as carbon sources. $\Delta escN$ is a negative control strain that is T3SS-deficient. (B) Protein secretion profiles of WT, $\Delta espC$, $\Delta picC$, $\Delta espC\Delta picC$ *C. rodentium* after growth in DMEM with glucose or sialic acid. Secreted proteins in equal amounts of cultures for each strain (normalized by OD_{600}) were analyzed in 4-12% SDS-PAGE and stained by Coomassie G-250. Arrowheads indicate proteins that are differentially secreted under sialic acid conditions.

3.3.6 Pic mediates sialic acid-enhanced mucin degradation by *C. rodentium*

Both EspC and Pic are proteases belonging to the family of serine protease autotransporters of the Enterobacteriaceae (SPATE) (Dautin, 2010; Pokharel *et al.*, 2019). Notably, Pic expressed by EAEC has previously been shown to exhibit mucinolytic activity, potentially aiding the pathogen in penetrating intestinal mucus (Flores-Sanchez *et al.*, 2020; Liu *et al.*, 2020). To address whether sialic acid enhances mucin degradation through the induction of Pic and/or EspC, we characterized the mucinolytic activities of the proteins secreted by WT *C. rodentium*, as well as the $\Delta espC$, $\Delta picC$, and $\Delta\Delta$ strains when cultured in the presence of sialic acid. Notably, while exposure to sialic acid caused the expected increase in mucinolytic activity by the WT and $\Delta espC$ strains, it caused no increase in mucin degradation by the $\Delta picC$ or $\Delta\Delta$ strains (Figure 3.6A). We also examined the ability of these *C. rodentium* strains to transmigrate through a mucin layer after culturing them in sialic acid containing media. Both $\Delta picC$ and the $\Delta\Delta$ strain showed significant impairment in penetrating the mucin layer as compared to WT *C. rodentium* (Figure 3.6B). While the $\Delta\Delta$ strain showed a modestly reduced efficiency at transmigrating through the mucin layer as compared to $\Delta picC$ (Figure 3.6B), the difference was not significant. These findings thus suggest that Pic plays the primary role in enhancing mucin degradation by *C. rodentium* following sialic acid stimulation, likely enhancing the ability of *C. rodentium* to penetrate the inner mucus layer overlying the colonic epithelium.

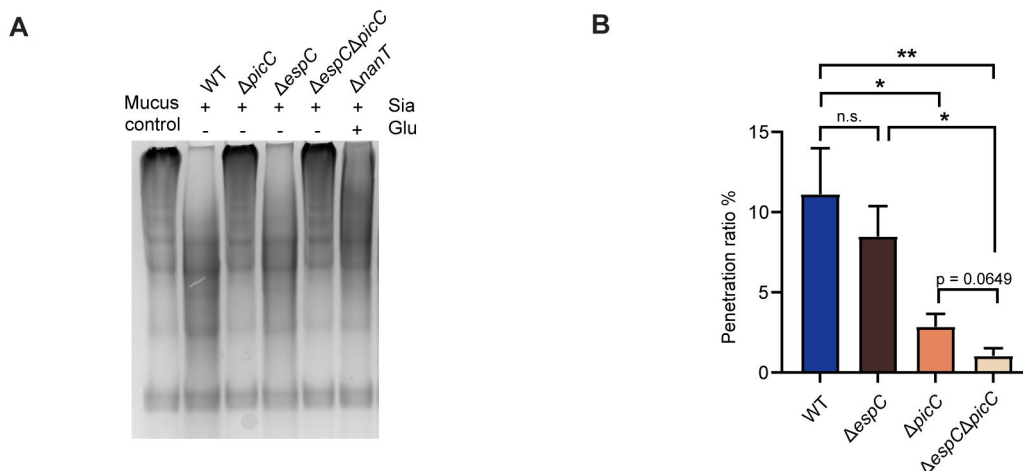


Figure 3.6 Sialic acid induces Pic mucinase in *C. rodentium* to accelerate degradation and penetration of the mucus layer.

(A) Mucinolytic activity in secreted proteins of WT, $\Delta picC$, $\Delta espC$, $\Delta espC\Delta picC$ and $\Delta nanT$ *C. rodentium* after growth in sialic acid. Concentrated proteins were incubated with BSM (control) overnight. *C. rodentium* $\Delta picC$ and $\Delta espC\Delta picC$ mutants are significantly impaired in degrading mucins. (B) Sialic acid's induction of Pic enhances *C. rodentium*'s ability to penetrate mucins. *C. rodentium* WT, $\Delta espC$, $\Delta picC$ and $\Delta espC\Delta picC$ mutants, after growth in sialic acid, were placed on top of Transwell inserts layered with purified mucins. Bacteria that penetrated the transwells were collected from the lower chamber and plated for CFU. Penetration ratio represents the percentage of bacteria that have penetrated the mucin layer. Data are shown in the mean \pm SEM from four independent experiments. ** p < 0.01, * p < 0.05, n.s. = not significant. Significance levels calculated by one-way ANOVA.

3.3.7 Sialic acid enhances the adherence of *C. rodentium* to IEC by inducing EspC secretion

Due to their highly upregulated secretion by *C. rodentium* grown in sialic acid, we next asked if either Pic or EspC contributed to the sialic acid-enhanced adherence of this pathogen to IEC. CMT-93 cells were infected with WT, $\Delta espC$, $\Delta picC$, or $\Delta\Delta$ strains of *C. rodentium*, and the infected cells were fixed for immunostaining to detect *C. rodentium* localization (Figure 3.7A), or homogenized to quantify *C. rodentium* adherence as in Figure 3.3B. Both WT and $\Delta picC$ showed increased adherence to IEC upon sialic acid treatment (Figure 3.7A, B). In contrast, the $\Delta espC$, and the $\Delta\Delta$ strains showed remarkably lower levels of adherence, irrespective of the

presence of sialic acid. These data suggest that sialic acid promotes the adherence of *C. rodentium* to IEC by inducing EspC secretion.

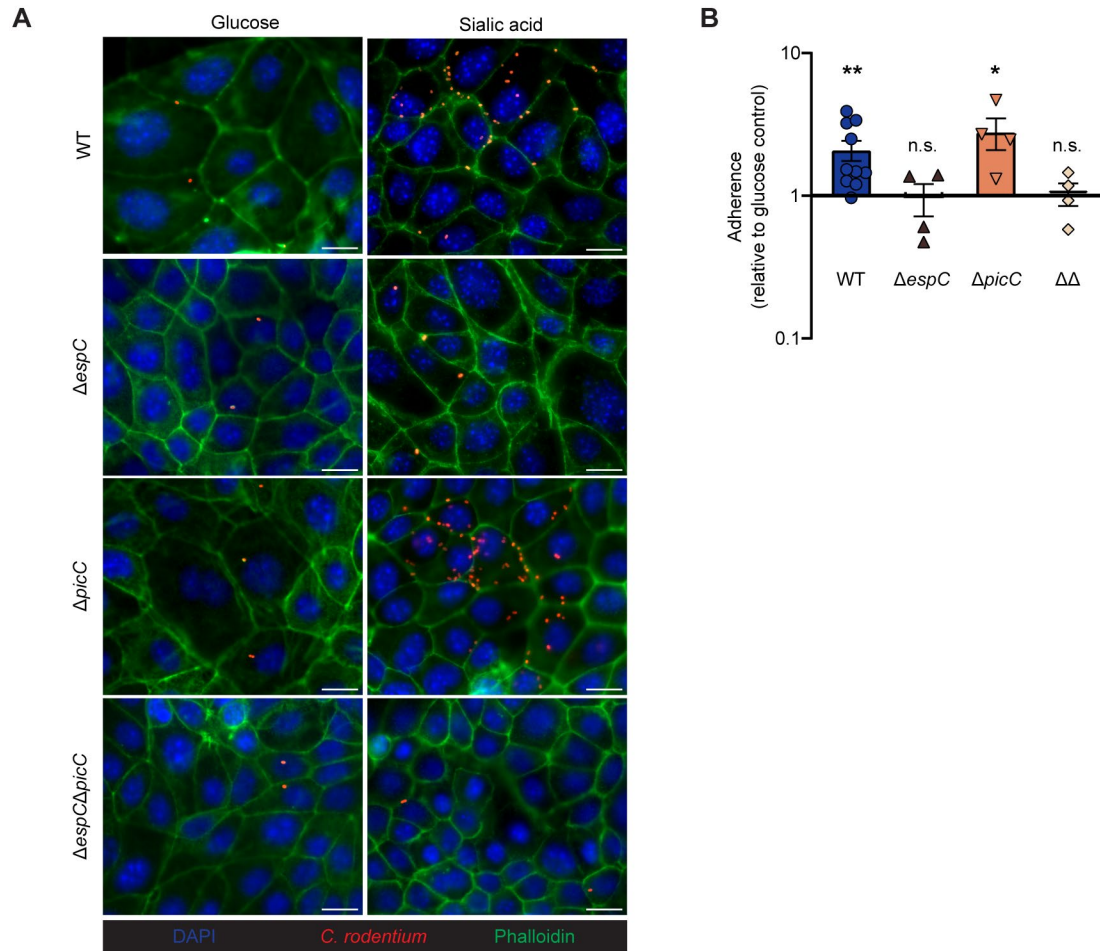


Figure 3.7 Sialic acid promotes *C. rodentium* adherence to epithelial cells through EspC.

(A) CMT-93 cells were infected with *C. rodentium* WT, or $\Delta espC$, $\Delta picC$, $\Delta espC\Delta picC$ mutants in the presence or absence of sialic acid for 5 hours, then washed to remove nonadherent bacteria and stained with phalloidin (green), anti-*C. rodentium* LPS (red) and DAPI to detect DNA (blue). Original magnification = 630 \times . Scale bar = 15 μ m. (B) Relative fold changes in adherence of *C. rodentium* WT, $\Delta espC$, $\Delta picC$, and $\Delta espC\Delta picC$ ($\Delta\Delta$) mutants to CMT-93 cells treated with sialic acid in comparison to glucose. Data are shown in the mean \pm SEM from two independent experiments. ** $p < 0.01$, * $p < 0.05$, n.s. = not significant. Significance levels calculated by Mann-Whitney U-test.

3.4 Discussion

The major impediment for luminal bacterial pathogens to infect the colonic epithelium is the tightly adherent, largely impermeable and thus sterile “inner” mucus layer. Above this “inner” mucus layer lies the loosely adherent “outer” mucus layer that extends into the lumen and is heavily populated by commensal bacteria (Johansson *et al.*, 2011). Among the species that inhabit the mucus layer are mucin degraders such as *Bacteroides* spp. and *Akkermansia muciniphila*, as well as bacterial species that can scavenge mucin-derived sugars released by mucin degraders such as Pseudomonadota (formerly Proteobacteria) (Chassaing & Gewirtz, 2018; Donaldson *et al.*, 2016). However, despite their ability to utilize mucin-derived nutrients, commensal microbes are unable to breach the mucus layer and therefore remain segregated from the host’s colonic mucosal surface (Johansson *et al.*, 2011; Johansson *et al.*, 2014). In contrast, most enteric bacterial pathogens must interact with their host’s IECs to cause disease, requiring the development of strategies to subvert the normally impenetrable inner mucus layer (McGuckin *et al.*, 2011). Correspondingly, mice lacking an intestinal mucus layer appear to have accelerated infections, although the loss of mucus can also lead to abnormal and/or weakened pathogen interactions with the gut epithelium (Bergstrom *et al.*, 2010; Zarepour *et al.*, 2013).

Previous research on A/E pathogenesis has primarily focused on their T3SS (Croxen & Finlay, 2010), with efforts directed towards identifying signals that induce T3SS expression (Caballero-Flores *et al.*, 2021; Furniss & Clements, 2017; Turner *et al.*, 2019) and investigating the ability of T3SS-encoded effectors to subvert host cell functions (Slater & Frankel, 2020; Wong *et al.*, 2011). However, little attention has been paid to the mechanisms employed by these pathogens to colonize their hosts and reach their target cells, prior to T3SS-mediated adherence. Studies

investigating the effect of mucin-derived sugars on the expression of LEE genes in EHEC have yielded inconsistent results. Fucose has been found to inhibit LEE over-expression in EHEC, which helps to maximize the pathogen's fitness by preventing excessive energy expenditure (Pacheco *et al.*, 2012). However, the effects of GlcNAc and sialic acid on LEE expression in EHEC are still under debate. One research group reported that these sugars reduced the expression of LEE in EHEC *in vitro* (Le Bihan *et al.*, 2015, 2017), while another study found that they increased the secretion of the T3SS effector EspB *in vitro* (Carlson-Banning & Sperandio, 2016).

It is intriguing that sialic acid did not affect T3SS expression in *C. rodentium*, but instead strongly and specifically upregulated the secretion of two members of the SPATE family of secreted serine proteases, namely Pic and EspC. SPATEs are large extracellular proteases, primarily secreted by disease causing Gram-negative bacteria (Pokharel *et al.*, 2019). More than 25 SPATEs have been identified, with class 1 SPATEs shown to impact bacterial virulence through cytotoxic effects on IEC, whereas class 2 SPATEs appear to be largely immunomodulatory. Numerous *in vitro* studies have characterized the functions of those SPATEs secreted by enteric pathogens such as *Shigella*, EPEC, EAEC, and uropathogenic *E. coli* (UPEC) (Pokharel *et al.*, 2019). Unfortunately, due to the lack of relevant animal models for many of these pathogens, characterization of most SPATEs has been limited to *in vitro*, *in situ*, or *ex vivo* conditions (Ruiz-Perez & Nataro, 2014). Correspondingly, there is relatively little understanding of how these proteases interact with their hosts to promote disease, or how their expression is regulated *in vivo*.

Our study determined that secretion of Pic by *C. rodentium* largely underlies the increased mucin degradation and mucin penetration demonstrated by *C. rodentium* following exposure to sialic acid. Most prior studies of Pic function have focused on the colonic human pathogen EAEC, with *in vitro* assays showing that Pic exhibits both mucinolytic and mucus secretagogue functions (Flores-Sanchez *et al.*, 2020; Liu *et al.*, 2020; Navarro-Garcia *et al.*, 2010). We previously investigated whether Pic impacts *C. rodentium* pathogenesis *in vivo*, but discovered that loss of the Pic gene ($\Delta picC$) not only reduced mucinolytic activity, but also led to abnormal colony morphology, increased adherence to other bacteria, as well as exaggerated activation of toll-like receptor 2 (Bhullar *et al.*, 2015). Thus, defining the action of these autotransporters through null mutations may prove problematic, whereas defining their actions in response to stimuli (like sialic acid) that upregulate their expression may offer a better approach to interrogate their roles in bacterial pathogenesis.

The other SPATE abundantly secreted by *C. rodentium* following exposure to sialic acid is EspC. EspC is expressed by a number of diarrheagenic *E. coli* pathotypes and has been shown to degrade a variety of substrates, including fodrin (Navarro-Garcia *et al.*, 2014), a ubiquitous protein involved in actin polymerization. However, the effects of EspC on mucins require further assessment (Dautin, 2010). Cell culture studies have shown that purified EspC displays enterotoxic effects on rat jejunal tissues (Mellies *et al.*, 2001), as well as cytotoxic effects when added to IEC *in vitro* (Navarro-Garcia *et al.*, 2014), that were dependent on EspC's protease activity. While studies with EPEC suggest EspC is neither a T3SS effector, nor required for A/E lesion formation (Stein *et al.*, 1996), it does potentially interact with components of the T3SS (Guignot *et al.*, 2015; Vidal & Navarro-García, 2008). EspC has been noted to be the first EPEC

derived protein to insert into host cell membranes (Kenny & Finlay, 1995; Vidal & Navarro-García, 2006), though likely independent of the T3SS. In the current study, when compared to Pic, *C. rodentium*'s EspC played little role in the mucin degradation/penetration exhibited by *C. rodentium*. In contrast, its major role appears to be in promoting bacterial adherence to IEC, even in the absence of a functional T3SS. This could reflect its insertion into the host cell, or alternatively, the previously described ability of EspC to oligomerize into large “rope-like” structures that exhibit adhesive and cytopathic properties (Xicohtencatl-Cortes *et al.*, 2010). Furthermore, it is known that EspC can induce both apoptosis and necrosis in epithelial cells in the context of EPEC infection *in vitro* (Serapio-Palacios & Navarro-Garcia, 2016). While the impact of EspC on cell death was not directly evaluated in our *in vitro* infection assays, the observation of increased cell sloughing in infected mice given exogenous sialic acid (as described in section 2.3.7) suggests that EspC's pro-cell death activity may have contributed to this effect.

The expression of the *nan* operon in *E. coli* is known to be regulated by the transcriptional regulators cAMP receptor protein (CRP) and NanR (Kalivoda *et al.*, 2013). In the presence of sialic acid and in the absence of glucose, the repressor NanR is inactivated, while CRP is activated, leading to increased expression of the *nan* operon. Similar to *E. coli*, the regulatory region of *C. rodentium*'s *nan* operon contains CRP and NanR binding sites (Figure A.3.4), suggesting the *nan* operon of *C. rodentium* and *E. coli* share a conserved regulatory mechanism. CRP binding motifs were also found (124 bp upstream of the start codon for *picC* and 123 bp for *espC*) in the regulatory regions of both the *picC* and *espC* genes in *C. rodentium*. In line with this, Pic and EspC are minimally secreted in WT *C. rodentium* in the presence of glucose

compared to sialic acid (Figure 3.5). Since sialic acid induces the *nan* operon expression through NanR and CRP, we suspect *picC/espC* genes are also repressed by NanR. However, we were unable to identify any notable NanR operators (containing GGTATA repeats) (Kalivoda *et al.*, 2003) in the regulatory regions of *picC/espC*. This suggests that the upregulation of EspC and Pic secretion in response to sialic acid may involve additional regulatory mechanisms, which await further investigation.

Moreover, it would be beneficial to determine if the increased secretion of EspC and Pic is specific to sialic acid. It is well recognized that bacteria have an inherent tendency to prioritize glucose over other available substrates, a phenomenon attributable to catabolite repression (Görke & Stülke, 2008). This preference was underscored in our study when the secretion levels of EspC and Pic by WT *C. rodentium* in a combined glucose/sialic acid environment more closely mirrored those seen in a glucose-only medium, rather than those in a sialic acid-only medium (Figure 3.5A). Such an observation suggests that the active catabolism of sialic acid, rather than just its detection, may play a pivotal role in enhancing secretion. However, a caveat arises with the $\Delta nanT$ mutant, which displayed a limited ability to acquire nutrients and possibly secrete proteins in the exclusive sialic acid medium we utilized. As such, future studies should investigate other carbon sources to discern if the heightened secretion of EspC and Pic is intrinsically linked to sialic acid or a consequence of glucose's suppressive effect.

C. rodentium was believed to be non-motile due to the absence of flagella (Luperchio & Schauer, 2001). However, our results suggest that *C. rodentium* possesses a motility system that enables its chemotactic responses towards glucose and sialic acid. In addition to flagella, pili and other

undefined mechanisms can also facilitate bacterial motility across surfaces (Wadhams & Armitage, 2004). *C. rodentium* contains a type IV pilus, which has been shown to control twitching motility in other bacteria, such as *Pseudomonas aeruginosa* and *Vibrio cholerae* (Mauriello *et al.*, 2010). However, pili primarily function in attaching to surfaces or other cells, as opposed to swimming through liquid, which is more commonly associated with flagella (Shi & Sun, 2002). *C. rodentium* may employ an additional motility apparatus to direct its movement towards a favorable niche in the gut. Although the specific mechanism remains undefined, our results demonstrate that *C. rodentium* is capable of localizing to the colonic mucus layer even without flagella. Understanding how this non-flagellated bacterium achieves this feat could provide important insights into the diverse strategies that bacteria use to navigate and colonize complex environments. Moreover, *C. rodentium*'s chemotaxis towards mucin-derived sugars appears to strongly correlate with their utilization as nutrients. *C. rodentium* demonstrates chemotaxis towards the three mucin *O*-glycan monosaccharides that it can metabolize (Figure A.3.3), but not towards fucose or GalNAc, which are not utilized by *C. rodentium* (observed in section 2.3.1).

In conclusion, we found that in addition to fueling the growth of *C. rodentium* as a substrate, sialic acid also acts as a chemoattractant for the pathogen. This signaling mechanism prompts *C. rodentium* to migrate towards mucus, which is composed of mucin proteins decorated with sialic acid. In addition, sialic acid also induces the secretion of specific virulence factors by *C. rodentium*. These factors include the Pic mucinase, which facilitates the pathogen's ability to traverse mucus barriers by mediating mucin degradation; and the EspC protein, which aids in *C. rodentium*'s initial adherence to the colonic epithelium (Figure 3.8). Our study thus reveals

intriguing insights into how an A/E bacterial pathogen escapes the colonic lumen and ultimately reaches the host's epithelium. Overall, sialic acid plays a key role in promoting *C. rodentium* pathogenesis within the mammalian gut, specifically regarding the poorly defined stages of virulence prior to A/E lesion formation on the intestinal mucosal surface. While some of these sialic acid dependent responses were observed in the human pathogen EPEC, further studies are needed to identify key virulence factors that contribute to sialic acid-related phenotypes observed in this clinically important pathogen. Additionally, it remains uncharacterized whether sialic acid plays a role in the pathogenesis of other enteric pathogens beyond A/E pathogens, since previous studies on other enteric pathogens solely focused on sialic acid's function as an energy source. Nevertheless, our findings highlight the crucial role of mucus-derived nutrients in the pathogenesis of *C. rodentium* and potentially other A/E pathogens. Identifying the key nutrients and environmental signals that contribute to bacterial pathogenesis offers exciting potential for the development of alternative anti-microbial approaches beyond conventional antibiotics.

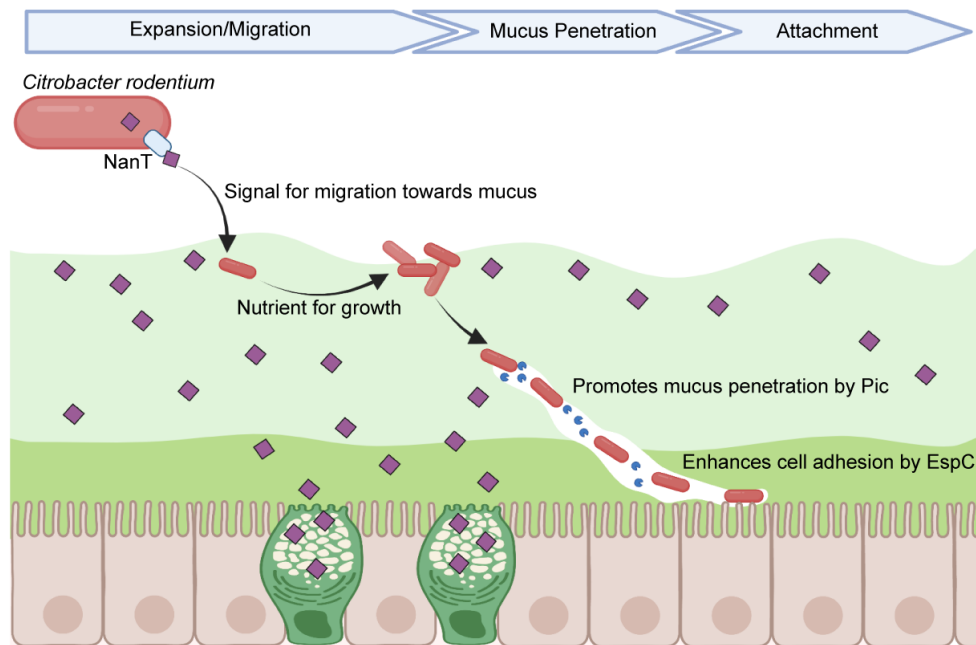


Figure 3.8 Sialic acid plays a key role in promoting *C. rodentium* pathogenesis within the gut.

A proposed model illustrates the effect of sialic acid on *C. rodentium* pathogenesis. Sialic acid is captured from the environment, transported into the cell via *C. rodentium*'s transporter NanT, and thereafter utilized as a growth substrate to promote the expansion of the pathogen within the gut. It also serves as a signal to direct the pathogen towards the mucus layer, and specifically the mucins decorated with sialic acid. Metabolism of sialic acid further induces the secretion of Pic mucinase, thereby enhancing *C. rodentium*'s ability to degrade mucus and overcome this barrier. Upon traversing the mucus layer, sialic acid also induces the expression of the EspC protein that promotes *C. rodentium*'s adhesion to the colonic epithelial surface. Thus, sialic acid plays a pivotal role in licensing *C. rodentium*'s transition from the intestinal lumen to its mucosal adherent niche. Sialic acid is simplified in the illustration as a magenta diamond, representing both a monosaccharide form and a glycosylated form. Figure generated with Biorender.com.

3.5 Materials and Methods

3.5.1 Chemotaxis assay

Bacterial chemotaxis assay was performed in Eppendorf tubes as previously described (Dwivedi *et al.*, 2016). In brief, 4×10^9 CFU of *C. rodentium* were pelleted, resuspended in 500 μ l PBS-based 0.4% agar and transferred to the bottom of a 2 ml Eppendorf tube. Another 1 ml of PBS-based 0.4% agar containing no bacteria was layered on top of the cell suspension. A sterile piece of Whatman paper, soaked with 100 mM solution of glucose, sialic acid (Neu5Ac), or PBS was placed on top. Samples were incubated at 37°C for two days. After incubation, 200 μ l of 0.01%

2,3,5-triphenyltetrazolium chloride (TTC) was added to visualize *C. rodentium* that migrated through the PBS-agar layer towards the compounds added to the Whatman paper. Positive results were presented as formation of red rings of bacterial cells near the top of the tubes stained by TTC after 4 hours of incubation.

3.5.2 Mucinolytic activity assay

Protein secretion was induced in DMEM with or without 0.1% sialic acid as described above. Equal volumes of supernatants (normalized by OD₆₀₀) were collected and filtered through a 0.22 µm filter to remove bacterial cells. Supernatants were then concentrated through Amicon Ultra 4 (50-kDa cutoff; Millipore) filters. Secreted protein concentrates (20 µl) were incubated overnight at 37°C with 6.5 µl of 2% purified bovine submaxillary mucin (BSM; Sigma). Mucin degradation was analyzed on a 3-8% Tris-Acetate gel and visualized by staining with Pierce glycoprotein staining kit (Thermo Scientific).

3.5.3 Mucin transmigration assay

Transwell filters (24-well insert, 3.0-µm pores, Corning) were coated with 100 µl of 30 mg/ml mucin and placed onto 24-well plates containing 250 µl DMEM in the bottom chambers. Next, 10 µl of *C. rodentium* induced in DMEM (5.0×10^6 CFU) was added onto the top of the mucin layers and incubated at 37 °C for 1 hour. Bacteria that were able to transmigrate to the bottom of the well were collected and enumerated through serial dilutions on LB-streptomycin agar plates. The percentage of *C. rodentium* crossing the mucus layers was normalized to control samples from Transwells uncoated with mucin.

3.5.4 *In vitro* bacterial adherence assay

CMT-93 (mouse rectal epithelial) cells (ATCC CCL-223) or Caco-2 (human intestinal epithelial) cells (ATCC HTB-37) were seeded in 24-well plates at a density of 5×10^4 cells/well and grown until reaching >90% confluence (37°C, 5% CO₂). Prior to infection, cells were washed twice with PBS and pre-incubated in DMEM supplemented with 2% fetal bovine serum (FBS; Life Technologies) with or without 0.2% sialic acid for 30 min. Cells were infected with an overnight culture of *C. rodentium* or EPEC O127:H6 E2348/69 at a MOI of 50 for 4 to 5 h. After infection, the supernatants of infected cells were removed and the cell monolayers were washed three times with PBS, and subsequently treated with 200 µl of 0.1% Triton X-100 PBS for 5 min at room temperature to lyse the cells. Adherent bacteria were enumerated by serial dilutions in PBS and plated onto LB-streptomycin plates. The percentage of adhered bacteria was calculated by dividing the number of adhered bacteria by the number of total bacteria.

3.5.5 Immunofluorescence staining

To perform immunofluorescent staining on infected tissue culture cells, sterile coverslips and Transwells (24-well insert, 3.0-µm pores, Corning) were seeded and infected as described above. After post-infection washes in PBS, coverslips and Transwells were fixed in 4% paraformaldehyde (Fisher Scientific) for 15 minutes, rinsed in PBS twice and permeabilized with 0.1% Triton X-100 and 0.05% Tween in PBS for 15 min. To obtain cross-sections for imaging pedestal formation, Transwell membranes containing fixed Caco-2 cells were removed post infection and embedded in parafilm. Coverslips and deparaffinized Transwell cross-sections were stained with *E. coli* monospecific O152 antisera (rabbit polyclonal, SSI Diagnostica) to detect *C. rodentium*, or O127 antisera (Biorad) to detect EPEC for 1 hour, followed by secondary

antibody staining with anti-rabbit Alex Fluor-568 and Alexa Fluor-488 phalloidin for 1 hour, washed and mounted with ProLong Gold Antifade reagent containing DAPI (Invitrogen). Slides were viewed on a Zeiss AxioImager microscope and images taken using an AxioCam HRm camera operating through Zen software.

3.5.6 Detection of *ler* expression

Bioluminescent reporter strain P_{ler} -*lux* *C. rodentium* were diluted 1:40 in DMEM supplemented with 0.1% glucose or sialic acid from overnight LB cultures and grown in sterile 96-well black bottom microplates (Corning) for 5 h to late exponential phase under tissue culture conditions (20% O₂, 5% CO₂) at 37°C. Readings of luminescence and OD₆₀₀ were taken with a Varioskan LUX microplate reader (Thermo Scientific) using the SkanIt software (Thermo Scientific) every 30 min for *ler* expression analysis.

3.5.7 Protein secretion assay

C. rodentium and EPEC O127:H6 E2348/69 strains were grown overnight shaking in LB broth at 37°C and sub-cultured 1:40 into Dulbecco's modified Eagle's medium (DMEM) with or without supplementation of 0.1% sialic acid to induce protein secretion in a tissue culture incubator with 5% CO₂ at 37°C until reaching mid-exponential-phase growth. Secreted proteins in the supernatant of equal amount of cultures (normalized by OD₆₀₀) were obtained as previously described (Deng *et al.*, 2010). Protein secretion was analyzed in 4-12% SDS-PAGE and stained with Coomassie G-250.

For proteomic analysis, protein pellets were reduced with dithiothreitol (DTT) and alkylated with indoleacetic acid (IAA), followed by enzymatic digestion. Proteins were identified through liquid chromatography-tandem MS (LC-MS/MS) analysis with a search against *C. rodentium*'s protein sequence database.

Chapter 4: Gut microbiota promotes nutrient availability and pathogenesis of *C. rodentium*

4.1 Synopsis

The intestinal mucus provides an important source of nutrients for commensal microbes that can thrive on mucus or mucus-derived metabolites. While enteric pathogens have limited mucin glycan-degrading capacities, commensal gut microbes possess a diverse array of enzymes that are able to break down complex mucin glycans into simple monosaccharides. Here, my findings indicate that the presence of a mucin-degrading gut microbiota is necessary for *C. rodentium* to access sialic acid in the gut. We determined that the intestines of GF mice contain very low levels of free sialic acid and correspondingly, *C. rodentium* displays impaired virulence when infecting them. Conversely, the commensal bacterium *B. thetaotaomicron* provides *C. rodentium* access to mucin-derived nutrients. In line with this, mice mono-colonized with *B. thetaotaomicron* demonstrate increased susceptibility to *C. rodentium* colonic infection compared to GF mice. Together, these findings underscore the critical role of the gut microbiota in liberating nutrients from mucin-derived glycans, which are exploited by *C. rodentium* to promote its growth and virulence, highlighting the significance of the interplay between the microbiota and pathogens in determining the outcome of bacterial infections in the gut.

4.2 Introduction

The gut microbiota plays an important role in protecting the GI tract from invading enteric pathogens. Much of this colonization resistance is mediated by limiting nutrient availability. However, enteric pathogens have evolved strategies to subvert this competition, utilizing

commensal metabolites to facilitate their infection. Orally administered laboratory-grown *C. rodentium* initially colonizes the mouse cecal lymphoid patch, where it adapts to the *in vivo* environment by responding to signals from the host and microbiota, inducing the expression of virulence factors (Wiles *et al.*, 2004). After 2 to 3 days, *C. rodentium* progresses to the distal colon, where it adheres to IEC and forms A/E lesions (Wiles *et al.*, 2004). Previous research suggests that *C. rodentium* relies on specific commensal bacteria to colonize the distal colon (Mullineaux-Sanders *et al.*, 2017). Kanamycin treatment at the peak of infection displaced *C. rodentium* from the colonic mucosa, restricting its colonization to the cecal lumen. Interestingly, this effect of kanamycin also occurs in a *C. rodentium* strain engineered to constitutively express the LEE (Mullineaux-Sanders *et al.*, 2017), indicating that additional virulence factors induced by microbiota-derived signals may facilitate the colonization of the colonic mucosa. The cecum and distal colon exhibit two prominent differences: a thicker and multi-layered colonic mucus compared to the loose mucus layer in the cecum, and a higher bacterial load in the distal site of the intestine. As *C. rodentium* moves towards the distal colon, its ability to subvert the mucus barrier and utilize nutrients derived from mucins to avoid competition with luminal commensals becomes increasingly important.

As shown in Chapters 2 and 3, sialic acid is a mucin-derived nutrient that plays a key role in licensing *Citrobacter rodentium*'s transition from the intestinal lumen to its mucosal niche. Notably, sialic acid in the gut is primarily present on glycosylated structures. The release of sialic acid from these glycoconjugates is mediated by the bacterial enzyme sialidase (Juge *et al.*, 2016). Despite our findings demonstrating that *C. rodentium* utilizes sialic acid in its monosaccharide form for growth, we did not identify any sialidase genes in its genome. This

suggests that *C. rodentium* may rely on other microorganisms to release sialic acid from complex glycoproteins and oligosaccharides. Many commensals possess sialidase activity to liberate free sialic acid, including members of the Actinomycetota, Bacteroidota, and Bacillota phyla (Ravcheev & Thiele, 2017). Sialidases are highly prevalent in species of *Bacteroides* within the Bacteroidota phylum, followed by species of *Clostridia* in the Bacillota phylum. While most *Bacteroides* spp. express all the enzymes required to utilize sialic acid, including genes for sialidases and sialic acid catabolism pathways, many members of Bacillota and a few other *Bacteroides* spp., such as *B. thetaiotaomicron*, encode a sialidase, but lack the complete catabolic pathway to fully metabolize sialic acid (Almagro-Moreno & Boyd, 2009). This results in the release of free sialic acid into the gut environment, making it potentially available for other resident bacteria or incoming pathogens to utilize. In gnotobiotic mice mono-associated with WT *B. thetaiotaomicron*, but not its sialidase-deficient mutant, significantly higher levels of free sialic acid were detected in their ceca compared to GF mice. In contrast, mice mono-associated with *B. fragilis*, which can both cleave and catabolize sialic acid, did not show any increase in free sialic acid levels (Ng *et al.*, 2013).

Here, I addressed the role of mucus-degrading gut commensals in mediating the interactions between the enteric pathogen *C. rodentium* and mucin-derived glycans. I demonstrated that *C. rodentium* lacks mucin-degrading glycosidases and is unable to utilize whole mucins for growth. *C. rodentium* also displayed impaired colonization of colonic mucosa in GF mice that contained low levels of free sialic acid in their GI tract. However, *B. thetaotaomicron* released nutrients from mucins that facilitated the growth of *C. rodentium*. Mice mono-colonized with *B. thetaotaomicron* contained increased levels of free sialic acid (Ng *et al.*, 2013) and demonstrated

enhanced and expedited colonic infection by *C. rodentium*, correlated with its heightened virulence in this context.

4.3 Results

4.3.1 Sialic acid utilization is not required for *C. rodentium* colonization and pathogenesis in microbiota-depleted hosts

The successful colonization of the murine intestine by *C. rodentium* requires it to overcome the colonization resistance posed by the vast number of commensal microbes residing in the gut (Kamada *et al.*, 2012). We and others have shown that changes in the gut microbiota, potentially driven by host inflammatory responses, can create an environment that facilitates the expansion of *C. rodentium*'s niche within the gut (Mullineaux-Sanders *et al.*, 2019). A major mechanism of colonization resistance is through direct competition for nutrients utilized by the incoming pathogens. We hypothesize that sialic acid is a key nutrient for *C. rodentium*, particularly in the presence of an intact microbiota with limited alternative nutrient sources.

Others have studied the effect of antibiotic treatment in reducing the total number of resident bacteria and altering microbiota composition (Ng *et al.*, 2013; Ramirez *et al.*, 2020; Sekirov *et al.*, 2008), potentially resulting in a surplus of nutrient sources for invading pathogens to exploit. Our previous study showed that administration of streptomycin 24 h prior to infection led to a 10-20 fold reduction in commensal microbe numbers in the feces of C57BL/6 mice, without inducing any inflammation or pathological damage (Bergstrom *et al.*, 2010). To assess whether antibiotic-induced microbial changes would facilitate the pathogenesis of $\Delta nanT$ *C. rodentium*, C57BL/6 mice were pre-treated with streptomycin and then infected with either WT or $\Delta nanT$ *C.*

rodentium. Notably, streptomycin pretreatment dramatically improved the colonization kinetics of $\Delta nanT$ *C. rodentium*, almost matching that of WT *C. rodentium* (Figure 4.1A), with both $\Delta nanT$ and WT *C. rodentium* reaching intestinal pathogen burdens of $10^7 \sim 10^8$ CFU/g at 8 DPI (Figure 4.1B). Furthermore, mice infected with either strain carried comparable pathogen burdens in systemic tissues (Figure A.4.1A). These results suggest that in microbiota depleted mice, $\Delta nanT$ is as competent as WT *C. rodentium* in its ability to establish an intestinal niche, colonize the colonic mucosa, and spread systemically.

In addition to their similar pathogen burdens, infections from both strains led to comparable levels of inflammation, as indicated by microscopic images (Figure 4.1C), histopathological scores (Figure 4.1D) and inflammatory cytokine responses (Figure A.4.1B). Together, these data indicate that subsequent loss of commensal bacteria following streptomycin pretreatment presumably freed up nutrients other than sialic acid for $\Delta nanT$ *C. rodentium* to use, leading to the establishment and expansion of *C. rodentium* in the gut.

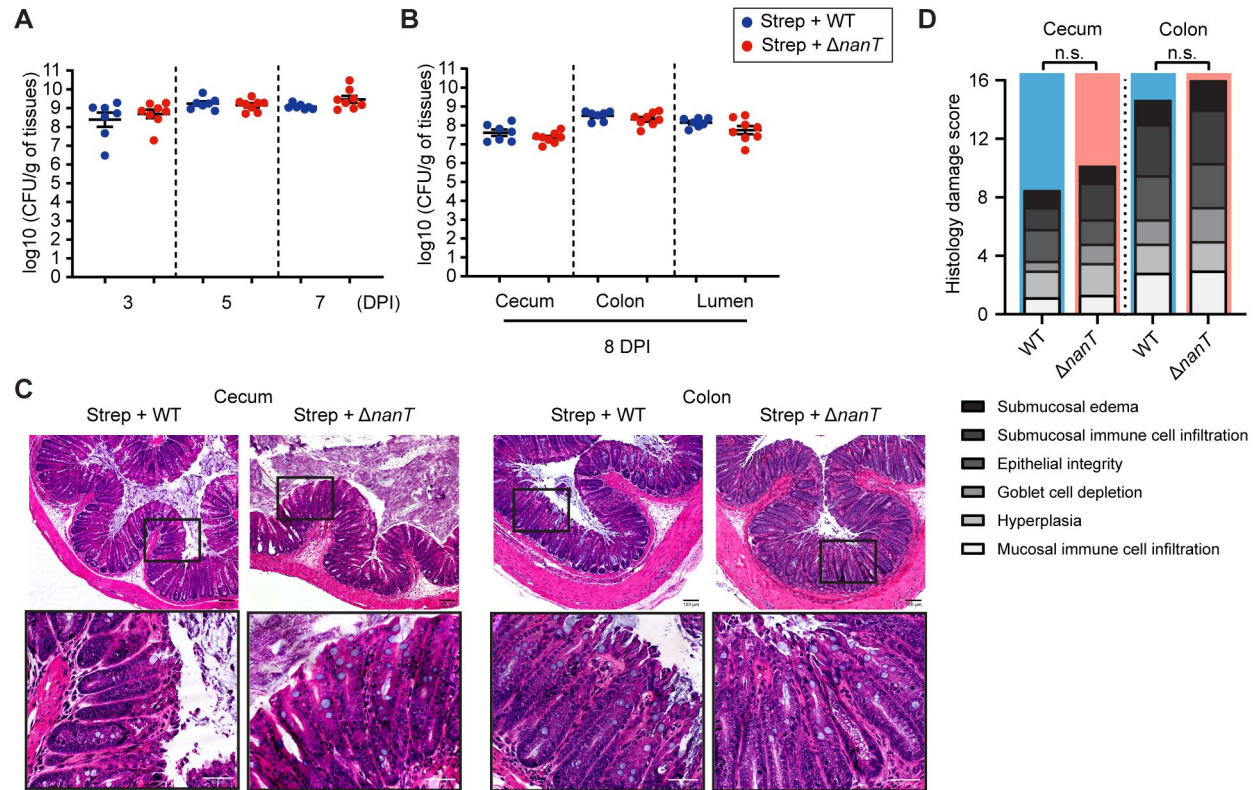


Figure 4.1 $\Delta nanT$ *C. rodentium* displayed comparable pathogenicity to WT *C. rodentium* in antibiotic pre-treated C57BL/6 mice.

C57BL/6 mice were pre-treated with streptomycin 24 h prior to the oral challenge with *C. rodentium* (1×10^7 CFU), WT ($n = 7$) or $\Delta nanT$ ($n = 8$), and (A) stools were collected at 3, 5, 7 days post infection (DPI); (B) intestinal tissues and luminal contents were collected at 8 DPI, plated and enumerated for *C. rodentium* CFU. (C) Representative H&E-stained cecal and distal colonic sections from WT and $\Delta nanT$ infected mice. Lower panels (scale bar = 50 μm) are expanded images of corresponding boxed regions in panels above (scale bar = 100 μm). (D) Blinded histopathological scores of H&E tissue sections of mice infected with WT ($n = 6$) or $\Delta nanT$ ($n = 6$) *C. rodentium* (see Materials and Methods for scoring criteria). Means are indicated, n.s. = not significant. Statistical significance calculated by Mann-Whitney U-test (A, B, D).

4.3.2 *C. rodentium*'s access to sialic acid *in vivo* is dependent on commensal bacteria

Genomic analysis revealed that *C. rodentium* encodes limited glycosidases that can break down glycoconjugates (Drula *et al.*, 2022; Popov *et al.*, 2019). Correspondingly, *C. rodentium* did not exhibit any growth when cultured in a minimal medium containing whole mucins as the sole carbon source (Figure 4.2A).

We suspected that *C. rodentium* would require the assistance of other bacteria to access free sialic acid *in vivo*, particularly commensal bacteria that encode sialidases. We examined the levels of free sialic acid in the fecal samples of GF and SPF mice. As shown in Figure 4.2, free sialic acid levels in GF mice were significantly lower than those in SPF mice. However, in GF mice that received fecal microbiota transplantation (FMT) from SPF mice, the level of free sialic acid significantly increased and reached a level comparable to that found in SPF mice (Figure 4.2B). These results suggest that the gut microbiota plays a crucial role in releasing sialic acid from mucin glycoproteins. In the absence of commensals, *C. rodentium*'s ability to access free sialic acid is restricted.

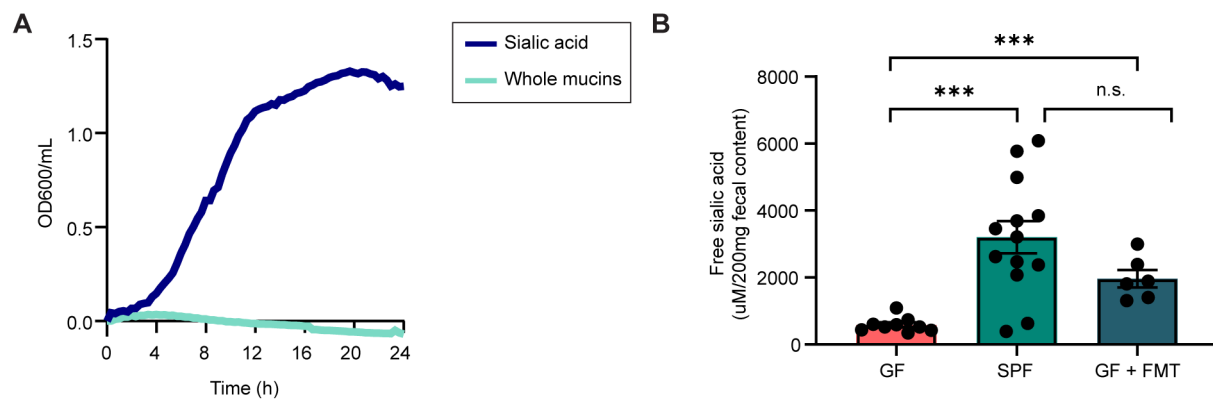


Figure 4.2 *C. rodentium* is dependent on the gut microbiota to liberate sialic acid from intestinal mucins. (A) *C. rodentium* is unable to utilize whole mucins for growth. *C. rodentium* growth was measured by optical density (OD₆₀₀) at 20-minute intervals over 24 hours at 37°C in M9 minimal medium supplemented with 0.2% purified mucins or sialic acid (positive control). Data are presented as averages of cell growth ($n = 9$) from three independent experiments. (B) Levels of free sialic acid in germ-free (GF), specific pathogen-free (SPF), and GF mice received fecal microbiota transplantation (FMT) of SPF mouse fecal samples after three days (GF + FMT). Data are represented as mean \pm SEM. *** $p < 0.001$, n.s. = not significant. Statistical significance calculated by Mann-Whitney U-test.

4.3.3 *C. rodentium* is impaired in infecting colonic epithelium in GF mice

Given the significance of sialic acid in *C. rodentium* pathogenesis as demonstrated in Chapters 2 and 3, we hypothesized that the behavior of *C. rodentium* would differ significantly between GF

and SPF conditions. To test this hypothesis, we assessed the pathogenicity of *C. rodentium* in both GF mice and SPF mice. We infected GF and SPF mice with WT *C. rodentium* for 6 days and compared their pathogen burdens and tissue histopathology. To assess *C. rodentium* densities at various sites, luminal contents from the cecum and colon were collected by gently scraping the dissected tissues to quantify luminal *C. rodentium*. Meanwhile, the tissues, including any adherent mucus were collected and used to quantify both adherent and mucus-associated *C. rodentium*. In GF mice, *C. rodentium* rapidly colonized the gut and reached high pathogen burdens as early as 1 DPI (Figure 4.3A). In contrast, in SPF mice, the pathogen required several days to overcome colonization resistance and expand its population (Figure 4.3A). At 6 DPI, *C. rodentium* continued to colonize GF mice at significantly higher levels than SPF mice, as indicated by the heavy cecal, colonic, and luminal pathogen burdens in GF mice (Figure 4.3B).

To determine whether the higher pathogen burdens in GF mice resulted in more severe tissue damage, we assessed cecal and colonic histopathology caused by *C. rodentium* infection. The ceca of GF mice displayed more significant damage (Figure 4.3C, D), which was accompanied by greater adherence of *C. rodentium* to the mucosal surface as compared to SPF mice (arrowheads in Figure 4.3C). In particular, infected GF ceca exhibited extensive cell sloughing (arrows in Figure 4.3C), resulting in a significant loss of crypt architecture (Figure 4.3C, D). In contrast, the colons of GF mice displayed lower histological scores as compared to SPF mice upon infection (Figure 4.3F), and showed fewer signs of pathogen adherence to the colonic mucosa (arrowheads in Figure 4.3E), despite carrying a significantly higher pathogen burden as quantified in Figure 4.3B. Thus, the high *C. rodentium* densities detected in GF colonic tissues in

Figure 4.3A-B predominantly represent *C. rodentium* population residing within the mucus layer in the absence of commensal bacteria, rather than direct adherence to the mucosa. These results suggest that in GF mice, *C. rodentium* exhibits a reduced ability to infect the mucosa and induce substantial histological damage in the colon while causing more pronounced damage to the cecum when compared to SPF mice.

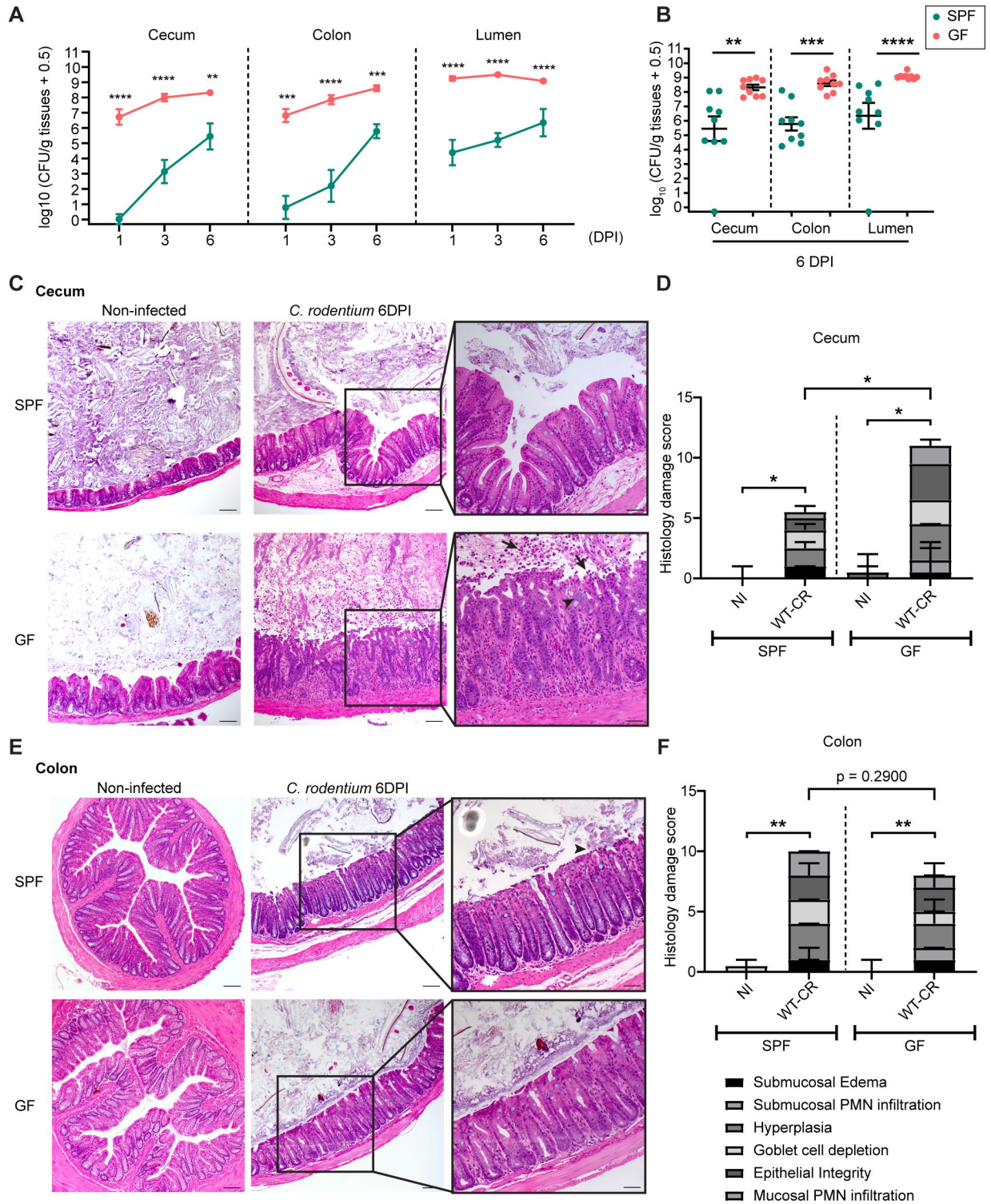


Figure 4.3 *C. rodentium* caused minor pathology in GF mouse colons compared to ceca, despite carrying high bacterial burdens at both sites.

GF and SPF mice were infected with WT *C. rodentium* (2×10^8 CFU). (A) Pathogen burdens in intestinal tissues and luminal contents collected from infected GF and SPF mice at 1, 3, and 6 DPI. (B) Pathogen burdens in intestinal

tissues and luminal contents collected from infected GF and SPF mice at 6 DPI. (C,E) Representative H&E-stained cecal (C) and distal colonic sections (E) from control mice and mice infected with *C. rodentium*. Original magnification = 100×, scale bar = 100 μm. The third column are expanded images of the corresponding boxed regions in the second column, original magnification = 200×, scale bar = 50 μm. Arrows indicate sloughing cells. Arrowheads indicate bacteria adhering to the IEC. (D, F) Blinded histopathological scores of H&E cecal (C) and colonic (E) tissue sections from non-infected (NI) and WT *C. rodentium* (WT-CR) infected mice. Means are indicated. ****p < 0.0001, *** p < 0.001, ** p < 0.01, * p < 0.05. Statistical significance calculated by Mann-Whitney U-test (A, B, D, F).

4.3.4 Intestinal mucus limits *C. rodentium* colonization of colonic epithelium in GF mice

The observed differences in histopathological damage between the cecal and colonic tissues of GF mice following *C. rodentium* infection were intriguing. Surprisingly, although GF mice carried high pathogen burdens in the colon, they did not exhibit more epithelial damage than SPF mice, unlike in the cecum. One possible explanation for this discrepancy could be the difference in mucus architecture between these two regions. Specifically, the mucus layer in the colon is known to be thicker and less permeable as compared to that of the cecum in SPF mice (Furter *et al.*, 2019). To investigate the pathogen-mucus-host epithelium interactions during *C. rodentium* infection in the GF condition, we performed immunofluorescence staining on infected cecal and colonic tissues collected from GF mice. We stained for *C. rodentium*'s T3SS effector protein Tir to identify adherent *C. rodentium*, Muc2 to label the mucus layer, and E-cadherin to recognize epithelial cells. Our immunofluorescence staining (green) confirmed that the distinction in mucus layer organization between cecum and colon remained consistent in GF mice. While the cecal mucus did not form a well-defined layer, the colonic mucus displayed two distinct layers, with an inner layer associated with the IEC and a looser outer layer near the lumen (Figure 4.4A). We also observed more *C. rodentium* (red) adherent to the epithelium in the cecum than in the colon (Figure 4.4A). These results led us to hypothesize that the mucus layer in the colon acts as a barrier that prevents direct access of *C. rodentium* to the colonic epithelium in GF mice, despite

the pathogen's ability to rapidly colonize the lumen and outer mucus layer in the absence of competition from the gut microbiota. To confirm the role of intestinal mucus in restricting *C. rodentium* adherence to the colonic epithelium, we infected GF *Muc2*^{-/-} mice and GF *Muc2*^{+/+} mice, and examined the localization of *C. rodentium* in their colons. As expected, a higher degree of pathogen adherence was observed in the colons of GF *Muc2*^{-/-} mice, which lack the protective mucus barrier, compared to GF *Muc2*^{+/+} mice (Figure 4.4B). This finding supports the hypothesis that the mucus layer largely prevents direct access of *C. rodentium* to the colonic epithelium in GF mice.

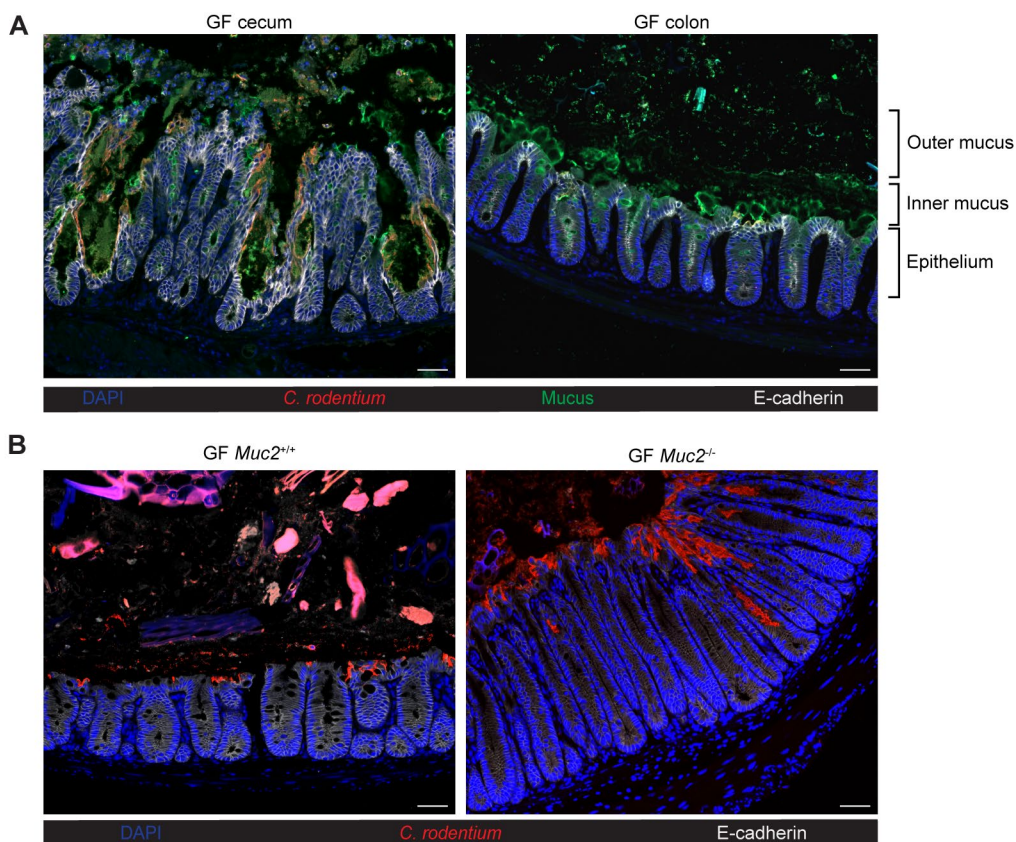


Figure 4.4 *C. rodentium* is impaired in penetrating the mucus layer in the colon of GF mice.

(A) Representative immunostaining of GF cecal and colonic tissues infected with *C. rodentium* (6 DPI) for adherent *C. rodentium* (Tir; red), Muc2 (green), E-cadherin (white) and DAPI (blue). (B) Representative immunostaining of GF *Muc2*^{-/-} and GF *Muc2*^{+/+} mouse colons infected with *C. rodentium* (6 DPI) for *C. rodentium* (red), E-cadherin (white) and DAPI (blue). Original magnification = 200×, scale bar = 50 μm (A, B).

4.3.5 Microbiota-derived signals are required for *C. rodentium* to colonize colonic mucosa

The reduced *C. rodentium* colonization at the colonic mucosal surface in GF mice as compared to SPF mice suggests that the absence of microbiota could potentially impair the expression of virulence factors necessary for *C. rodentium* to breach the mucus layer and adhere to IEC. We further explored whether inducing the expression of *C. rodentium* virulence factors *in vitro* prior to infecting mice would lead to a higher degree of colonic infection. The pre-induction was carried out by subculturing LB-grown *C. rodentium* in either DMEM medium or in a GF cecal content suspension and then incubating it under tissue culture conditions for 3 hours to assess the effect of host-derived signals on *C. rodentium* virulence. DMEM medium containing 0.4% glucose is known to induce the expression and secretion of several T3SS components (Deng *et al.*, 2010). In comparison to LB-grown *C. rodentium* without pre-induction, both DMEM and GF cecal content-induced *C. rodentium* displayed accelerated adherence to cecal tissues in GF mice, as early as 1 DPI (arrowheads in Figure 4.5A). The pre-induced *C. rodentium* also caused rapid damage to GF ceca at 1 DPI, as evidenced by extensive cell sloughing (arrows in Figure 4.5A). Cecitis resulting from pre-induced *C. rodentium* infection progressed from 1 DPI to 3 DPI, as indicated by substantial disruption of epithelial integrity (Figure 4.5B) and deep penetration of *C. rodentium* into intestinal crypts (arrowheads in Figure 4.5B). In contrast, the GF colons remained resistant to infection by pre-induced *C. rodentium*, as similar tissue pathologies were observed between LB-grown *C. rodentium* and pre-induced *C. rodentium* at both 1 and 3 DPI (Figure 4.5A-B). These findings indicate that pre-induction in DMEM and GF cecal content only provides advantages to *C. rodentium* infection at the cecum, but not the distal colon. Therefore, microbiota-derived signals may be necessary to facilitate *C. rodentium* infection of the colon.

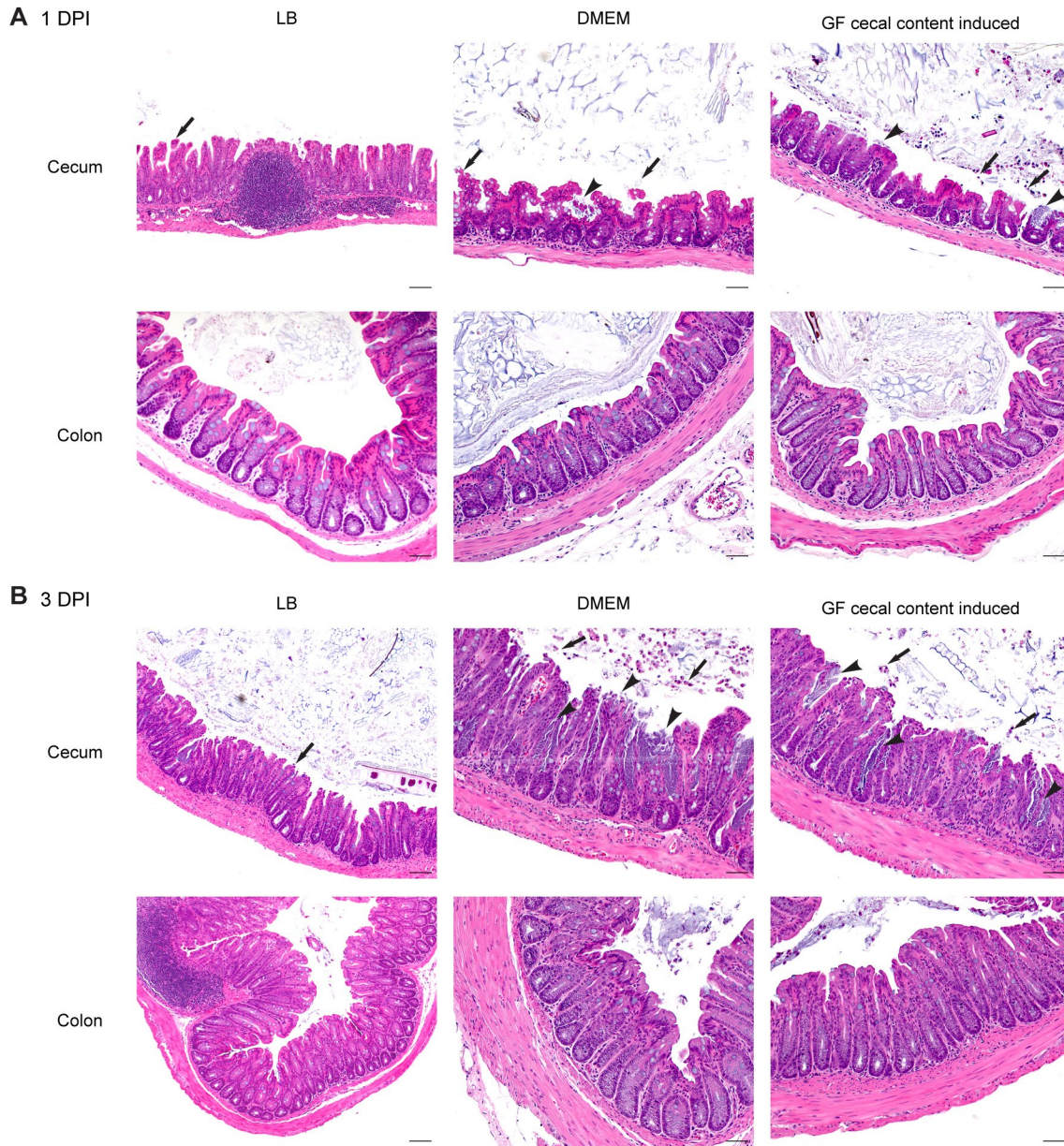


Figure 4.5 *C. rodentium* pre-induced in DMEM containing glucose or GF cecal content showed accelerated infection at the GF cecum but remained resistant in infecting the GF colon.

C. rodentium was sub-cultured to the DMEM medium or GF cecal content suspension for 3 hours for pre-induction and compared the infection to the one performed with LB-grown *C. rodentium*. Cecal and colonic tissues were collected at 1 (A) and 3 (B) DPI. Original magnification = 200 \times . Scale bar = 50 μ m. Arrowheads indicate *C. rodentium* adhered to the epithelium. Arrows indicate sloughed epithelial cells.

4.3.6 *Bacteroides thetaiotaomicron* enhances *C. rodentium*'s access to mucin-derived nutrients for growth

As established in Chapter 3, *C. rodentium* benefits from the metabolism of mucin-derived sialic acid for its penetration of the colonic mucus barrier and attachment to the underlying epithelium. *C. rodentium* may take advantage of the glycan-degrading activities of commensal microbes in the gut to access monosaccharides, including sialic acid from glycosylated mucins. *B. thetaiotaomicron* (*B. theta*), a prominent member of the microbiota in both humans and mice, has been extensively researched for its saccharolytic capacity to break down mucin glycans (Sonnenburg *et al.*, 2005). To determine whether *B. theta* promotes *C. rodentium*'s utilization of mucin-derived nutrients, we conducted an *in vitro* growth assay that simulated the *in vivo* environment in which pathogens enter the gut and interact with intestinal mucus already populated with commensals. We pre-conditioned mucins with *B. theta* and introduced *C. rodentium* subsequently. After inoculating *B. theta* into a minimal medium that contained mucins as the sole carbon source and incubating it anaerobically overnight, we removed live *B. theta* cells through filtration. *C. rodentium* was added to the pre-processed mucins and grown aerobically for 24 hours, and we monitored bacterial cell density using a plate reader (Figure 4.6A). As expected, *C. rodentium* did not show any growth in the control medium that was not pre-conditioned with *B. theta*. However, when the medium was pre-conditioned with *B. theta*, *C. rodentium* was able to grow and expand (Figure 4.6B). The growth pattern of *C. rodentium* in the *B. theta*-processed mucins exhibited as a diauxic curve, suggesting the utilization of multiple carbon sources (Chu & Barnes, 2016).

We further investigated the growth of *C. rodentium* when co-cultured anaerobically with *B. theta* in mucins and enumerated the bacterial density by plating (Figure 4.6C). We observed an increase in *C. rodentium* growth in the presence of *B. theta*. Moreover, we found that the growth of *C. rodentium* was directly proportional to the population of *B. theta* added (Figure 4.6D). These results confirmed that *B. theta*, which possesses mucin glycan-degrading glycosidases, promotes *C. rodentium*'s growth in mucins. Interestingly, the presence of *C. rodentium* also resulted in enhanced growth of *B. theta*, indicating a synergistic relationship between the two bacteria (Figure A.4.2).

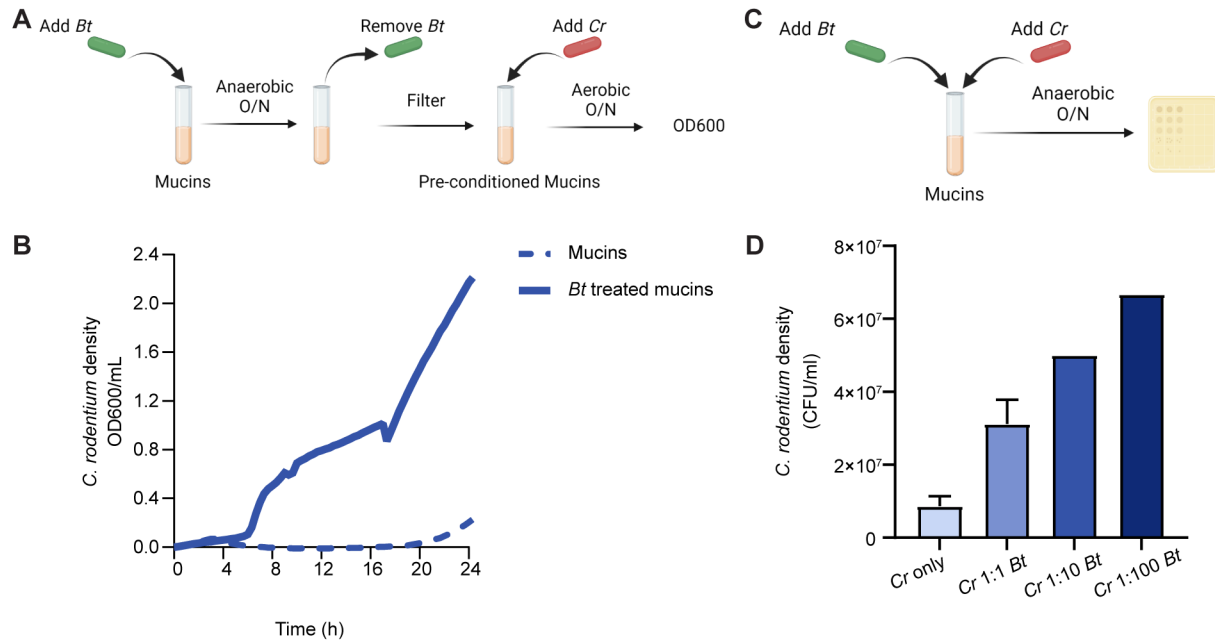


Figure 4.6 *B. theta*-mediated liberation of nutrients from mucins provides substrates for the growth of *C. rodentium*.

(A) Schematic of the experimental set-up to test the growth of *C. rodentium* (*Cr*) in mucins processed by *B. theta* (*Bt*). (B) The growth of *Cr* in whole mucins versus mucins pre-conditioned with *Bt*, measured by optical density (OD600) at 20-minute intervals over 24 hours at 37°C in minimal media supplemented with 0.2% purified mucins. Data are presented as the average cell growth ($n = 3$). (C) A schematic illustration of the experimental set-up for co-culturing *Cr* and *Bt* in minimal media supplemented with 0.2% purified mucins. (D) The endpoint densities of *Cr* in co-cultures with varying starting densities of *Bt*. The growth of *Cr* was proportionally increased with an increasing *Bt* population.

4.3.7 Mice mono-colonized with *Bacteroides thetaiotaomicron* showed increased susceptibility to *C. rodentium* infection in the colon

To explore the interactions between *B. theta* and *C. rodentium* *in vivo*, we used gnotobiotic mice mono-colonized with *B. theta*, and infected them with *C. rodentium* for one to three days to examine early disease progression. Interestingly, *C. rodentium* rapidly colonized the GI tract of *B. theta* mono-colonized mice as early as 1 DPI, a pattern similar to that observed in GF mice, but in striking contrast to SPF mice (Figure 4.7A). Notably, at 1 DPI, *B. theta* mono-colonized mice even carried a higher burden of *C. rodentium* in the colon as compared to GF mice, although the difference did not reach statistical significance (Figure 4.7A). This trend persisted at 3 DPI (Figure 4.7B). Collectively, these findings indicate that *C. rodentium* potentially colonizes the colons of mice mono-associated with *B. theta* faster than GF mice. We assessed whether *C. rodentium* affects the colonization of *B. theta* by monitoring the density of *B. theta* in the mono-colonized mice before and during *C. rodentium* infection. Populations of *B. theta* were found to remain stable before and after *C. rodentium* colonization (Figure A.4.3).

Histopathological analysis revealed that at 3 DPI, infected *B. theta* mono-colonized mice displayed extensive immune cell infiltration, severely damaged epithelial surfaces, and a greater number of sloughed epithelial cells in the colon when compared to GF mice (Figure 4.7C).

However, blinded scorings are required to further validate this observation. Taken together, these preliminary data provide evidence that co-colonization of *B. theta* and *C. rodentium* results in heightened and accelerated colonic inflammation compared to *C. rodentium* infection in GF mice.

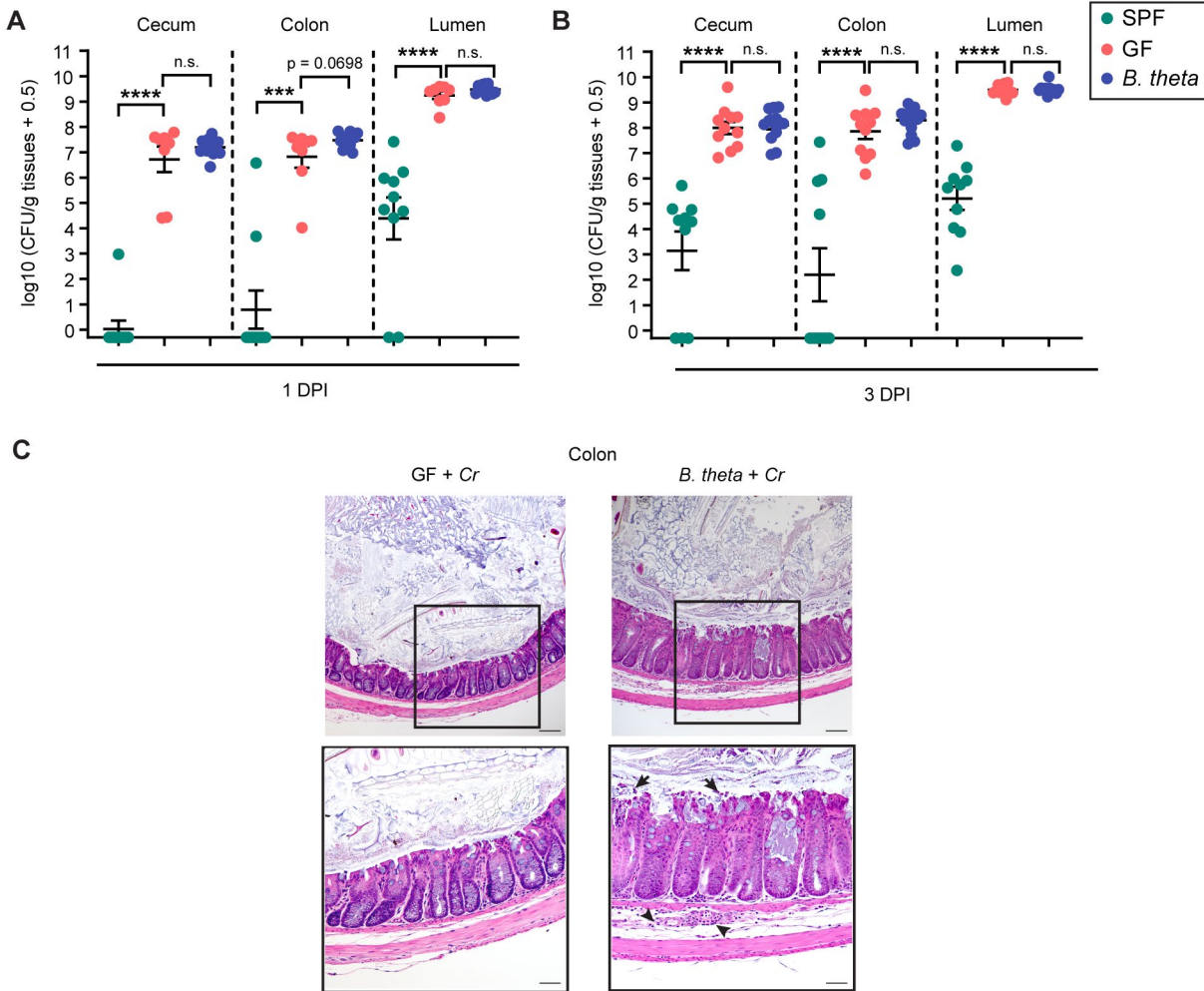


Figure 4.7 *B. theta* mono-colonized mice showed higher pathogen burdens and more severe pathological damage in their colons compared to GF mice during *C. rodentium* infection. *Bt* mono-colonized mice, GF mice, and SPF mice were infected with WT *C. rodentium* (2×10^8 CFU) for 1 or 3 days. (A, B) Pathogen burdens enumerated from intestinal tissues and luminal contents collected at 1 DPI (A) and 3 DPI (B). (C) Representative H&E-stained distal colonic sections at 3 DPI. Upper panel: original magnification = 100 \times , scale bar = 100 μ m. Lower panel: original magnification = 200 \times , scale bar = 50 μ m. Lower panel images are expanded views of corresponding boxed regions in the upper panel. Arrows indicate sloughing IEC. Arrowheads indicate infiltrated immune cells.

4.3.8 *C. rodentium* showed increased epithelial adherence in the colons of *B. theta* mono-colonized mice

To gain a better understanding of the spatial distribution of *B. theta* and *C. rodentium* within the gut, we employed dual Fluorescence *in situ* hybridization (FISH) staining with probes specific to

Bacteroides and γ -Proteobacteria, which recognize *B. theta* and *C. rodentium* respectively. *B. theta* (green), a symbiotic bacterium that is known to feed on dietary polysaccharides or mucus glycans (Sonnenburg *et al.*, 2005), was found primarily in the outer mucus layer of the distal colon or within the luminal compartment of the cecum where mucus was disorganized (Figure 4.8). The presence of *B. theta* had a significant impact on the spatial distribution of *C. rodentium* (red) within the gut. *C. rodentium* appeared to infect fewer cecal crypts in *B. theta* mono-colonized mice as compared to GF mice. However, more *C. rodentium* was found associated with the colonic epithelium, along with deeper penetration into colonic crypts in mice mono-colonized with *B. theta* (Figure 4.8). While additional quantification is required to determine the numbers of infected crypts and the percentage of adherent *C. rodentium*, our current data indicate that *B. theta* alters the localization of *C. rodentium* within the gut, resulting in increased epithelial adherence in the colon but not in the cecum, and dissemination of *C. rodentium* deeper into colonic crypts. The deeper penetration of colonic crypts observed in *B. theta* mono-colonized mice suggests that *C. rodentium* might display heightened pathogenicity in this context.

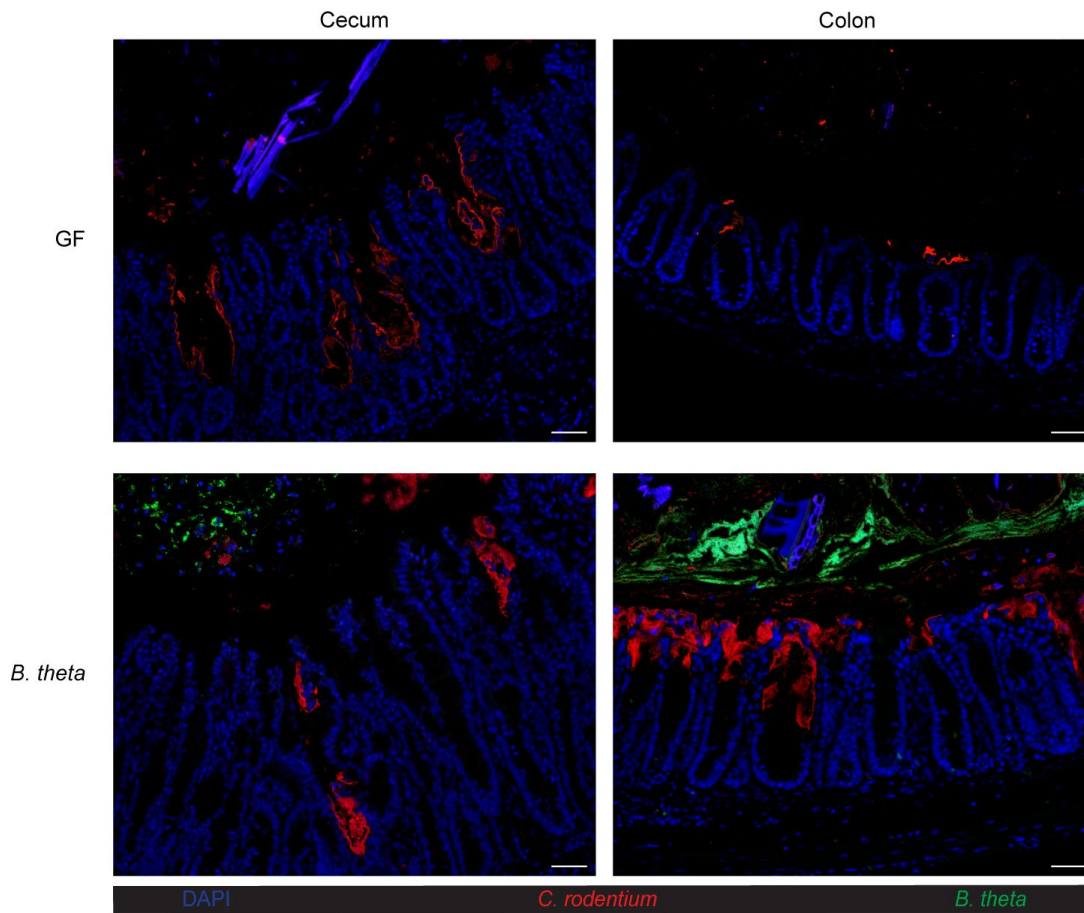


Figure 4.8 *C. rodentium* increased colonization of colonic crypts in *B. theta* mono-associated mice compared to GF mice.

Representative dual Fish staining of cecal and distal colonic tissues using Bac303 probe (green; stains *B. theta*) and Gam42a probe (red; stains *C. rodentium*). Original magnification =200 \times , scale bar =50 μ m.

4.3.9 *C. rodentium* showed increased T3SS expression in *B. theta* mono-colonized mice

The ability of A/E pathogens to reach and adhere to host IEC is a critical step in establishing infection and causing epithelial damage. This process relies on the expression of key virulence factors, particularly the T3SS. To investigate whether virulence genes are highly expressed in *B. theta* mono-colonized mice, we infected them with a bioluminescent reporter strain Cr-Pler-*lux*, and monitored the expression of *ler*, the T3SS master regulator. After removing the luminal contents from the colonic tissues and washing them with PBS, we used bioluminescence imaging

to quantify the level of adherence of *ler*-expressing *C. rodentium* to the cecal and colonic tissues. Strong bioluminescent signals were observed in the colonic tissues of *B. theta* mono-colonized mice as early as 1 DPI (Figure 4.9A), indicating early *ler* expression and rapid epithelial adherence by *C. rodentium* in this region. In contrast, GF mice primarily showed signals in the cecum at this time. By 3 DPI, both groups showed increased bioluminescent signals at both cecum and colon, corresponding to the increased *C. rodentium* densities measured from 1 DPI to 3 DPI (as shown in Figure 4.7A-B). In GF mice, significant signals were not detected in the colon until 3 DPI (Figure 4.9A), and these signals remained approximately five-fold weaker than those detected from *B. theta* mono-colonized mouse colons (Figure 4.9B). At 3 DPI, bioluminescence from the colonic tissues of *B. theta* mono-colonized mice increased extensively and remained the strongest among all sites (Figure 4.9A-B).

Next, the expression of key virulence genes by luminal *C. rodentium* was quantified through qPCR analysis. Luminal contents from the ceca and colons of infected mice were collected to measure the expression of *ler*, as well as the T3SS effector genes *tir* and *espB*. Luminal *C. rodentium* also expressed higher levels of *ler* in *B. theta* mono-colonized mice than in GF mice, in both the cecum and colon. Correspondingly, the expression of *tir* and *espB* was also elevated in *B. theta* mouse colons, with approximately 40-fold and 100-fold differences, respectively (Figure 4.8C). Therefore, pre-inoculation of *B. theta* in the gut significantly enhances the virulence of *C. rodentium* upon infection, leading to changes in the pattern of *C. rodentium* colonization. The interaction with *B. theta* expedited *C. rodentium*'s transition through the mucus-epithelium interface, enabling it to more effectively colonize the colonic mucosa.

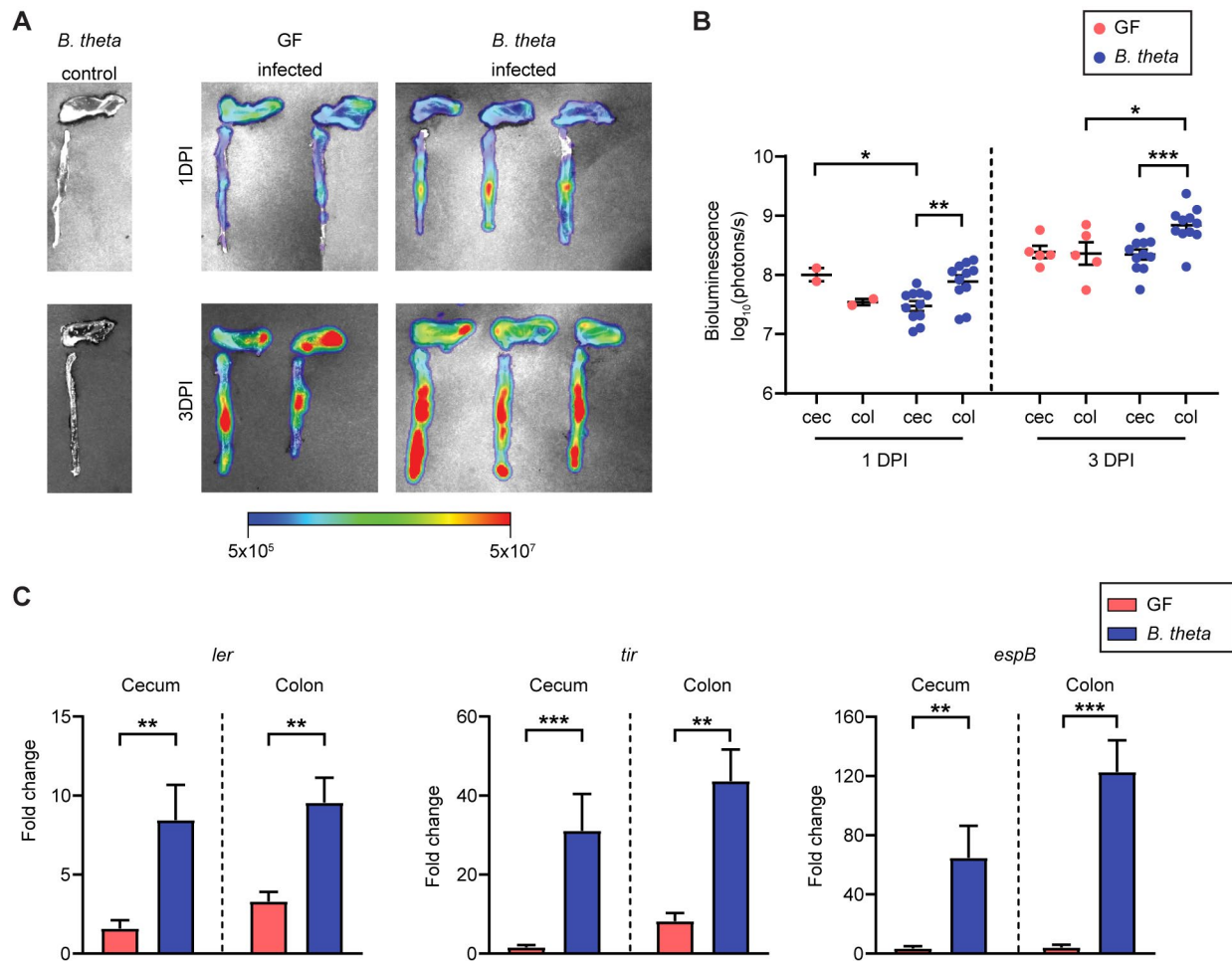


Figure 4.9 Virulence expression of *C. rodentium* in *B. theta* mono-colonized mice versus GF mice.

(A, B) *B. theta* mono-colonized mice and GF mice were infected with a bioluminescent reporter strain *Cr-Pler-lux* for 1 or 3 days to monitor the LEE gene expression by *C. rodentium* in the GI tract. (A) Representative images of bioluminescence signals detected in the large intestines with color representing the densities of *ler*-expressing *C. rodentium* at a given location. The color bar at the bottom indicates the strongest bioluminescence signals in red and the weakest bioluminescence signals in blue. (B) Bioluminescence signals quantified by the software (Aura) associated with the *in vivo* imaging system at specific regions of interest (ceca and colons). The bioluminescence signals correspond to logarithmic units of light measurement (photons/s). (C) Quantification of virulence gene expression in luminal *C. rodentium* from GF and *B. theta* colonized mouse tissues using qPCR.

4.4 Discussion

The gut microbiota co-evolving with its host provides numerous physiological benefits, one of which is protection against pathogen infections. The gut microbiota confers colonization resistance through multiple mechanisms that limit pathogen colonization of the GI tract, while

the host provides nutrients and space to support the growth and survival of beneficial microorganisms. In the gut, the main sources of nutrients for commensal organisms are ingested foods and host secretions, including intestinal mucus. One of the major mechanisms by which the gut microbiota exerts colonization resistance is through direct competition with pathogens for nutrients. Studies on GF mice have demonstrated their heightened susceptibility to enteric infections, such as those caused by *Listeria monocytogenes* (Zachar & Savage, 1979), *Salmonella* spp. (Stecher *et al.*, 2005) and Shiga-like toxin-producing EHEC (Taguchi *et al.*, 2002). Most of these pathogens poorly colonize the mouse GI tract under SPF conditions due to colonization resistance. Unlike many bacterial infection models that require antibiotics to disrupt the intestinal microflora prior to infection, *C. rodentium*, a natural murine bacterial pathogen, can infect the murine GI tract in the presence of an intact microbiota. This suggests that *C. rodentium* has evolved strategies to subvert colonization resistance conferred by the microbiota, potentially by utilizing metabolites produced by commensal bacteria to facilitate its infection. Furthermore, *C. rodentium* has been shown to persist in the colons of GF mice long-term (Kamada *et al.*, 2012). However, whether *C. rodentium* causes significant pathology in GF mice and where the pathogen localizes during its colonization remained undefined.

We showed that *C. rodentium* rapidly colonized the intestines of GF mice, with a high bacterial load present as early as 1 DPI. However, GF mice displayed only minor pathological damage in the colon as compared to the cecum, despite carrying a significantly higher pathogen burden in both sites as compared to SPF mice at 6 DPI. Furthermore, although the high pathogen burden in GF cecum correlated with increased adherence to the cecal epithelium, *C. rodentium* failed to efficiently infect the colonic epithelium of GF mice. These results suggest that there are site-

specific differences in the host response and/or pathogen virulence during *C. rodentium* infection in GF mice that lead to differential tissue pathology between the cecum and colon. We hypothesize that the thicker and multi-layered intestinal mucus in the distal colon provides an additional defense against foreign microorganisms as compared to the cecum, acting as a barrier to prevent *C. rodentium* from infecting the colonic epithelium in the GF condition. This was further supported by our observations that GF *Muc2*^{-/-} mice lacking the protective mucus were more susceptible to *C. rodentium* adherence to the colonic mucosa than GF *Muc2*^{+/+} mice with intact mucus. However, these observations were primarily made through immunostaining images, and further quantification is needed to assess the relative population of *C. rodentium* that reaches the mucosal surface (versus those that remain luminal) under these specific conditions. Nevertheless, our data provides compelling evidence that the absence of microbiota impairs *C. rodentium*'s ability to overcome the mucus barrier in the colon.

My research described in Chapters 2 and 3 demonstrated that access to sialic acid promotes the pathogenicity of *C. rodentium* by inducing key virulence factors that facilitate translocation across the mucus layer and adhesion to the epithelium, expediting disease progression. Sialic acid in the gut is primarily derived from intestinal mucin glycans that have complex structures formed by sugar monomers connected through a number of unique linkages (Tailford *et al.*, 2015). However, most enteric pathogens lack the ability to catabolize these complex polysaccharides (Pacheco & Sperandio, 2015), thus relying on glycosidases produced by the gut microbiota to gain access to the rich source of nutrition from mucus. We hypothesized that the microbiota plays a critical role in facilitating *C. rodentium* infection by making important mucin-derived nutrients, such as sialic acid, available for utilization by the pathogen. We found that GF

mice contain very low levels of free sialic acid in their intestines. However, after receiving fecal contents from SPF mice via FMT, the levels of free sialic acids in GF mice increased significantly and reached a level comparable to that found in SPF mice. The nutrients made available by the gut microbiota can potentially provide a benefit to pathogens as they actively search for energy sources to survive and fuel their expression of virulence factors in the highly competitive intestinal environment. The GF gut, in contrast, since there is no microbial competition, offers abundant host or diet derived nutrients, which support *C. rodentium* growth. Notably, ethanolamine, a cell membrane phospholipid component, has been demonstrated to be available from the turnover of IECs and serve as a nitrogen source for *C. rodentium*, thereby promoting its persistence in the gut (Rowley *et al.*, 2020). However, it is likely that these nutrients do not signal *C. rodentium* to activate virulence mechanisms that allow it to breach the mucus barrier.

We utilized *in vitro* growth assays to investigate the potential cross-feeding relationship between mucin-degrading commensal microbes and the pathogen *C. rodentium* when utilizing mucus as an energy/carbon source. We confirmed that *C. rodentium* is unable to grow on whole mucins without the gut microbiota. We employed a prominent commensal member, *B. thetaiotaomicron*, that is found in both human and mice. *B. theta* possesses an array of glycosidases, including a sialidase, that can readily degrade glycosylated mucins. Notably, it lacks a sialic acid metabolic pathway to consume the liberated sialic acids. We found that *C. rodentium* and *B. theta* grew cooperatively using mucins as the sole carbon source. Previous studies have shown that *Bacteroides* spp. establish a cross-feeding relationship with other resident commensals and pathobionts by liberating mucin-derived sugars in the inflamed gut (Huang *et al.*, 2015; Huus *et*

al., 2021). We demonstrated a similar synergistic growth relationship between *B. theta* and the enteric pathogen *C. rodentium* *in vitro*. Moreover, in mice mono-associated with *B. theta*, *C. rodentium* colonization was comparable to that in GF mice, and the density of *B. theta* remained unchanged upon *C. rodentium* infection, which further supports the concept of a mutualistic interaction between the two species *in vivo*. It is also intriguing that provided mucins pre-inoculated with *B. theta*, *C. rodentium* displayed diauxic growth, a pattern commonly observed in environments with multiple carbon sources where bacteria metabolize the most favorable source first before switching to the second-best source (and so on) and upregulating the corresponding metabolic genes (Chu & Barnes, 2016). Further investigation is needed to characterize the components that mediate the metabolic exchange between *B. theta* and *C. rodentium*. Nonetheless, our findings suggest that *C. rodentium* takes advantage of the glycan degrading capacities of the gut microbiota to access monosaccharides that are liberated from intestinal mucins, which in turn helps promote its growth. These results highlight the complex metabolic network between resident bacteria and incoming pathogens and its potential impact on the course of bacterial infections.

Furthermore, we demonstrated *in vivo* that *B. theta* also promotes the pathogenicity of *C. rodentium* and expedites the infection. It is intriguing that *C. rodentium* infects the colonic epithelium of *B. theta* mono-colonized mice as early as 1 DPI, while it requires approximately 3 days in GF mice and 6~10 days in SPF mice to reach similar levels of pathogen adherence of their colonic tissues. When infecting SPF mice that harbor diverse commensal microbes, *C. rodentium* requires an establishment phase to adapt to the gut environment and subvert colonization resistance. During this early stage of infection, *C. rodentium* has been found largely

confined to the cecum (Mullineaux-Sanders *et al.*, 2019). In mice mono-colonized with *B. theta*, *C. rodentium* did not encounter the overt colonization resistance seen in SPF mice, although this is partially attributed to the absence of other commensal species that could provide colonization resistance. Interestingly, *C. rodentium* appeared to bypass the establishment phase in the cecum and rapidly colonized the colonic mucosa, as demonstrated by higher levels of adherent *C. rodentium* in the colon as compared to the cecum at 1 DPI in *B. theta* mono-colonized mice. Furthermore, in *B. theta* mono-colonized mouse colons, *C. rodentium* did not only show increased adherence but also deeper penetration into the colonic crypts compared to GF colons. However, these observations should be further supported by quantitative data. Our findings suggest the shift in spatial distribution of *C. rodentium* in the presence of *B. theta* could be attributed to the early induction of virulence expression, including the T3SS components that facilitate *C. rodentium* colonization at the colonic mucosa. Further research is also needed to determine if other virulence factors also contribute to this process, particularly those that mediate the transition through mucus layer prior to epithelial adherence, such as the Pic mucinase.

Taken together, these results suggest that the presence of a mucin-degrading commensal can promote the colonization and pathogenicity of *C. rodentium* within the distal colon. Further investigations are required to unravel the underlying mechanisms, as the pre-inoculation of *B. theta* may not only influence the metabolic landscape within the gut but also the host's physiology. The presence of *B. theta in vivo* has been shown to alter the levels of numerous metabolites (Curtis *et al.*, 2014). For instance, *B. theta* has been shown to induce goblet cell differentiation and expression of sialylated mucins in *B. theta* mono-associated rats, through the

production of acetate (Wrzosek *et al.*, 2013). Therefore, it is necessary to further investigate whether the organization of mucus in *B. theta* mono-colonized mice resembles that of GF mice, both before and after *C. rodentium* infection. Moreover, the role of sialic acid in contributing to the increased susceptibility of *B. theta* mono-colonized mice to *C. rodentium* infection needs to be elucidated. Future experiments will be conducted to examine the behaviour of $\Delta nanT$ *C. rodentium* in *B. theta* mono-colonized mice, as well as to assess this strain's colonization and virulence in mice mono-colonized with a *B. theta* sialidase mutant or other mucin degrading commensal bacteria.

In conclusion, we demonstrate that although commensal microbes promote colonization resistance, as an A/E pathogen infection establishes, specific commensal bacteria may function to accelerate infection in the GI tract by releasing important nutrients, such as sialic acid, from mucus. A mucin-degrading commensal *B. theta* *iotaomicron* promotes *C. rodentium* virulence by facilitating its adhesion to the colonic epithelium, thereby expediting disease progression. Our findings shed light on the intricate interplay between mucus-degrading commensals and pathogens, highlighting how the presence of such commensals may promote the pathogenicity of certain enteric pathogens by increasing their access to mucin glycans. Understanding the mechanisms that govern these interactions is essential for the development of targeted interventions to modulate gut microbiota and mitigate the impact of enteric infections.

4.5 Materials and Methods

4.5.1 Bacterial strains and culture conditions

All strains of *C. rodentium* were derived from WT *C. rodentium* strain DBS100 on a streptomycin-resistant background. *C. rodentium* were routinely grown aerobically on Luria-Bertani (LB) agar plates or in LB broth with shaking (200 rpm) at 37°C overnight. Where appropriate, streptomycin was supplemented at 100 µg/ml, kanamycin was supplemented at 50 µg/ml. Bioluminescent reporter strain P_{ler}-lux *C. rodentium* was generated from WT *C. rodentium* carrying the *ler-lux* fusion. The *ler-lux* transcriptional fusion was generated by cloning a fragment spanning the *C. rodentium* *ler* regulatory region in plasmid pCS26-Pac containing the promoterless *Photobacterium luminescens luxCDABE* operon (Winson *et al.*, 1998). The plasmid construct P_{ler}-lux was transformed into wild-type *C. rodentium* by electroporation. To pre-induce *C. rodentium* to prime virulence expression, *C. rodentium* was sub-cultured 1:20 from LB to pre-induction media and incubated statically in cell culture incubator for 3 hours. Pre-induced *C. rodentium* was washed with PBS and normalized to OD₆₀₀ of 1.5.

B. thetaiotaomicron (ATCC 29148, also known as VPI-5482) were grown anaerobically (6% H₂, 20% CO₂, 74% N₂) on Tryptic Soy Agar (TSA) plates supplemented with 0.5% yeast extract, 0.0005% hematin, 0.0001% Vitamin K₃ or in Brain Heart Infusion (BHI) broth supplemented with 0.1% cysteine, 0.0005% hematin, 0.0001% Vitamin K₃. Where appropriate, gentamicin was supplemented at 200µg/ml, kanamycin was supplemented at 50 µg/ml.

4.5.2 Animals

Mice used in this study were all on a C57BL/6 background. Specific pathogen-free (SPF) mice were bred under SPF conditions at the BC Children's Hospital Research Institute, or purchased from Charles River Laboratories. GF mice were obtained from the germ-free facility at the International Microbiome Centre (IMC) of the University of Calgary and the Centre of Disease Modelling (CDM) of the University of British Columbia. Gnotobiotic mice mono-colonized with *B. thetaiotaomicron* were generated from GF mice at CDM by Dr. Carolina Tropini. GF mice were inoculated with *B. thetaiotaomicron* VPI-5482 overnight culture at 4 weeks old and maintained in gnotobiotic isolators. The *B. thetaiotaomicron* mono-colonized mice were transferred to the BC Children's Hospital Research Institute at 10-11 weeks of age for infection. GF and *B. thetaiotaomicron* mono-colonized mice were provided with sterile mouse chow and autoclaved water.

4.5.3 Mouse infections

Mice (6-12 weeks old) were orally gavaged with $1.0 \times 10^7 \sim 2.5 \times 10^8$ CFU of *C. rodentium* grown in LB overnight or pre-induction media described above. To deplete microbiota in SPF mice, 20 mg streptomycin dissolved in water was given by oral gavage 24 hours before infection. Mice were fed a normal chow diet (Picolab Rodent Diet 20, Cat #5053) throughout the infections. To monitor *C. rodentium* colonization, fecal pellets were collected, homogenized in PBS and plated on LB agar containing streptomycin. At the end of each experiment, mice were anaesthetized with isoflurane and euthanized by cervical dislocation. Colonic tissues were immediately fixed in 10% neutral buffered formalin (Fisher) for 24 h or in Methacarn fixative (60% methanol, 30% chloroform, 10% glacial acetic acid) for 3 to 24 hours at 4°C. Pathogen

burdens within tissues or luminal compartments were enumerated through serial dilutions on selective agar plates. Histopathological analysis was performed on hematoxylin-eosin-stained (H&E) cecal and distal colon tissue sections.

4.5.4 Quantification of free sialic acid

Mouse fecal samples were collected and snap-frozen before use. Feces were weighed, reconstituted in distilled water (200 mg/ml) and homogenized for 15 minutes at maximum speed. Clarified supernatants were obtained after centrifuge for 15 minutes at 14,000 rcf and used to measure free sialic acid levels using QuantiChrom Sialic Acid Assay Kit (BioAssay Systems) according to manufacturer's protocol.

4.5.5 RNA extraction and quantitative real-time PCR for host cytokine responses

RNA from mouse cecal and distal colonic tissues was preserved in RNAlater (Qiagen) and extracted using the RNeasy Mini kit (Qiagen) according to the manufacturer's instructions. Total RNA was quantified using a NanoDrop spectrophotometer (Thermo Fisher). Complementary DNA (cDNA) was constructed from reverse transcription of 500 ng RNA using 5X All-In-One RT MasterMix (Applied Biological Materials) according to the manufacturer's instructions. The cDNA was then diluted 1:5 in RNase/DNase free H₂O and 5 µl was used for 20 µl quantitative PCR (qPCR) reactions that contained primers (300 nM) and 10 µl SsoFast EvaGreen Supermix (Bio-Rad). qPCR reactions were carried out using a Bio-Rad CFX connect Real-time PCR detection system, with the specificity for each of the PCR reactions confirmed by melting point analysis. The expression of genes was normalized to housekeeping gene, *Ribosomal Protein Lateral Stalk Subunit P0 (Rplp0)*. mRNA transcript expression was normalized to the relative

expression of the reference genes using the $2^{-(\Delta Ct)}$. For treatment conditions, mRNA transcript expression was normalized to the control group (untreated condition) using the $2^{-(\Delta\Delta Ct)}$ method and presented as relative expression values. Primers used for qPCR are listed in Table A.2.2.

4.5.6 Measurement of virulence expression by *C. rodentium*

For *in vivo* bioluminescence imaging, the large intestines (cecum + colon) were immediately removed from mice infected with $P_{Ier-lux}$ *C. rodentium* after euthanasia. Luminal contents were removed from the tissues and washed quickly in PBS. Washed colonic tissues were placed into the light-tight chamber of an *in vivo* imaging system (Ami-X; Spectral Instruments Imaging, Tucson, AZ, USA). Bioluminescence signals emitted from *lux*-expressing bacteria in the tissue were quantified and analyzed using the software program Aura (Spectral Instruments Imaging).

To measure gene expression by luminal *C. rodentium*, bacterial RNA was extracted from luminal contents of the cecum and colon with the MagMax microbiome nucleic acid ultra-isolation kit and semi-automated Kingfisher Duo Prime (ThermoFisher), followed by a DNase treatment with the TURBO DNA-free kit (Invitrogen). Quantitative PCR for *ler*, *tir* and *espB* was performed as described above. Relative expression of virulence factors was normalized to housekeeping gene, *rpoD* (*the sigma 70 factor subunit of the RNA polymerase*). Primers used are listed in Table A.3.1.

4.5.7 Fluorescence *in situ* hybridization (FISH)

Deparaffinized sections were incubated at 37°C overnight in the dark with a FITC-conjugated GAM42a probe (5'-GCC TTC CCA CAT CGT TT-3') recognizing bacteria belonging to γ -

Proteobacter class (including *C. rodentium*) and a Cy3-conjugated Bac303 probe (5'-CCA ATG TGG GGG ACC TT-3') recognizing the *Bacteroides* genus in hybridization buffer (0.1M Tris-HCl, pH 7.2, 0.9 M NaCl, 0.1% sodium dodecyl sulfate). The sections were rinsed with wash buffer (0.1M Tris-HCl, pH 7.2, 0.9 M NaCl) and PBS, and mounted with ProLong Gold Antifade reagent containing DAPI (Invitrogen).

4.5.8 *C. rodentium* growth in *B. thetaiotaomicron* treated mucins

To pre-condition mucins with *B. thetaiotaomicron*, minimal media containing 0.2% purified Type II Porcine Stomach Mucin (Sigma-Aldrich) was inoculated with *B. thetaiotaomicron* cultures (washed and resuspended in minimal media) at 1:100 ratio and incubated at 37°C anaerobically overnight. Minimal media per 1 L contain: 13.6 g of KH₂PO₄; 0.875g of NaCl; 1.125g of (NH₄)₂SO₄; 1.0 ml CaCl₂ solution (0.8% w/v in water); 1.0 ml MgCl₂ solution (0.1 M in water); 1.0 ml histidine-hematin solution (1.9 mM hematin in 0.2M L-histidine); 1.0 g cysteine; 1.0 ml vitamin K₃ solution (1 mg/ml in ethanol); 1.0 ml FeSO₄ in HCl (0.04% w/v in water) and 0.5 ml vitamin B₁₂ solution (0.01 mg/ml in water). Media pH was adjusted to 7.2 with concentrated NaOH. Media treated with *B. thetaiotaomicron* overnight were filtered and inoculated with *C. rodentium* cultures (washed and resuspended in minimal media) at 1:100 ratio. Cultures were added into a sterile 96-well plate (Costar) and incubated at 37°C with shaking for 24 hours. The optical density at 600 nm (OD₆₀₀) was taken every 20 minutes using a Varioskan LUX microplate reader (Thermo Fisher). Each experiment was performed with at least three biological replicates.

4.5.9 *C. rodentium* and *B. thetaiotaomicron* mucin co-culture assay

Overnight cultures of *C. rodentium* and *B. thetaiotaomicron* were normalized to OD₆₀₀ of 2.0, washed with minimal media for three times. *B. thetaiotaomicron* cells were directly resuspended in minimal media containing 0.2% purified mucin at 1:100, 1:10 or 1:1 ratio. *C. rodentium* was added immediately at 1:100 ratio. Co-cultures were incubated at 37°C anaerobically for 24 hours with shaking. To enumerate the growth of both bacteria, samples were serially diluted in PBS, plated, and grown on LB-Streptomycin agar aerobically at 37°C for 24 hours to quantify *C. rodentium* CFU, on TSA plates containing kanamycin or gentamicin anaerobically to quantify *B. thetaiotaomicron* growth.

Chapter 5: Conclusion

5.1 Summary and contribution to the field

The study of enteric pathogen nutrition has become increasingly important due to the widespread emergence of antibiotic resistance over the last decade. However, this field faces unique challenges due to the complexity of the gut environment and the dynamic metabolic strategies employed by pathogens to overcome the various barriers encountered during different stages of infection. The ability of a pathogen to acquire essential nutrients and overcome barriers such as colonization resistance and the intestinal mucus layer is undoubtedly important to the success of infection. These features also distinguish pathogens from the beneficial microbiota, making it essential to identify key nutrients that pathogens acquire and understand the underlying mechanisms. This knowledge can lead to the development of novel anti-microbial approaches in the post-antibiotic era. The research presented in this thesis demonstrates the remarkable ability of an enteric pathogen to turn challenges into opportunities. They acquire essential nutrients through interactions with the intestinal mucus and mucus-degrading commensal microbes, promoting their growth and virulence to facilitate the establishment of infection.

The intestinal mucus barrier not only acts as a physical barrier between luminal gut microbes and the underlying intestinal epithelium, but also provides a rich nutrient source for microorganisms that reside nearby. In Chapter 2, I explored whether A/E pathogens require mucus-derived nutrients for growth during their infection. I showed that a small population of *C. rodentium* gains the ability to traverse the intestinal mucus layer while most of the pathogen population resides in the lumen or outer mucus layer. I found that colonization of the colonic mucus layer and the ability to utilize mucin-derived sugar sialic acid is critical for *C. rodentium* expansion in

the large intestine. This work is the first to identify a mucin-derived sugar as a key nutrient for A/E pathogens. While many aspects of *C. rodentium* nutrition have been studied (Liang & Vallance, 2021), how the pathogen reprograms its metabolism at the mucus-lumen interface was poorly defined. My data characterizing the colonization dynamics of $\Delta nanT$ *C. rodentium* *in vivo* highlighted the importance of sialic acid during *C. rodentium* infection. The impairment of $\Delta nanT$ *C. rodentium* in expanding its population and early clearance correlates with its limited ability to cause pathology in the infected mice, suggesting the ability to utilize sialic acid determines pathogen success. Although studies have previously identified a role for sialic acid catabolism in the post-antibiotic expansion of enteric bacterial pathogens (Ng *et al.*, 2013), our study is the first to show such a role in the absence of antibiotics.

In Chapter 3, I demonstrated how *C. rodentium* metabolism of sialic acid intertwines with virulence gene expression, enabling the pathogen to cross the mucus layer and initiate epithelial attachment. Previous research has primarily focused on sialic acid's role as a nutrient for pathogen growth. My study represents the first investigation into its impact on virulence expression in enteric pathogens. My data provides evidence showing that sialic acid induces a chemotactic response by *C. rodentium* and enhances secretion of two virulence proteins, Pic and EspC. My study on chemotaxis in *C. rodentium* is unprecedented as chemotaxis is generally linked to flagella-expressing pathogens that exhibit swimming motility. My data demonstrated that sialic acid directs *C. rodentium*'s movement towards the intestinal mucus, potentially seeking mucin-derived nutrients for growth and ways to reach the mucosal surface underneath the mucus. My study then delved deeper into the roles played by two secreted proteins, Pic and EspC, in driving sialic acid-related phenotypes. Interestingly, both proteins belong to the SPATE

family of secreted proteases. My data indicated that secretion of Pic by *C. rodentium* is primarily responsible for increased mucin degradation and penetration in response to sialic acid exposure, while EspC plays a minor role in mucin degradation/penetration but is critical in promoting bacterial adherence to IEC, even in the absence of a functional T3SS. Therefore, my research sheds light on an additional role of sialic acid as a signaling molecule promoting virulence, going beyond its well-established function as a nutrient, and enhances our understanding of how pathogens overcome the mucus barrier. Understanding the contribution of previously underappreciated components in *C. rodentium*'s virulence strategies expands our knowledge of A/E pathogenesis beyond the traditional focus on T3SS.

It is worth highlighting that the role of sialic acid, although largely characterized in the context of *C. rodentium* infection in the thesis, is likely to also contribute to the virulence of clinically significant A/E pathogens and other Enterobacteriaceae, as the sialic acid metabolism pathway is highly conserved among them. The findings from my research suggest that the effect of sialic acid on protein secretion and adherence to IEC is not exclusive to *C. rodentium*, as similar observations were made in EPEC.

Finally, in Chapter 4, I explored the role of mucus-degrading commensal bacteria in facilitating interactions between *C. rodentium* and the colonic mucus. GF animals are generally considered more susceptible to enteric infections due to the lack of symbiotic bacteria in the gut that exert colonization resistance to limit pathogen colonization. As expected, upon inoculation of *C. rodentium*, the pathogen rapidly colonized and reached a high density in the GI tract of GF mice. Interestingly, despite carrying very high *C. rodentium* burdens, GF mice exhibited impaired

passage across the colonic mucus layer and infection of the colonic epithelium as compared to SPF mice. When the spatial distribution of *C. rodentium* was evaluated, it was found that those *C. rodentium* found within the distal colon largely resided in the lumen, with A/E lesion formation at the mucosal surface only rarely observed. This was unexpected, considering the high luminal burden, and correspondingly, the distal colon of GF mice remained relatively undamaged during infection. In fact, a previous study showed that *C. rodentium* persists in the colonic lumen of GF mice long-term (Kamada *et al.*, 2012). My research identified the colonic mucus as the major barrier contributing to the impaired colonization of colonic crypts by *C. rodentium* under GF conditions. To my knowledge, this is the first study that characterizes the interactions between intestinal mucus and enteric pathogens in the absence of intestinal flora. Furthermore, my research revealed that GF mice have significantly lower levels of free sialic acid in their intestines. Since most sialic acid in the gut is present in the form of mucin glycoproteins, this finding emphasized the crucial role of bacterial glycosidases in releasing sialic acids from mucin glycans. It also highlighted the importance of mucin-degrading commensal microbes in facilitating this process since most enteric pathogens, including *C. rodentium*, lack mucin-degrading glycosidases. Our *in vitro* growth assessment supported the idea of metabolic cooperation between mucus-degrading commensal microbes and enteric pathogens in facilitating the pathogens' access to mucin-derived nutrients for growth. To dissect the interactions between mucus-degrading commensals and *C. rodentium*, I employed a simplified gnotobiotic mouse model using mice that were mono-associated with *B. thetaiotaomicron*. *B. thetaiotaomicron* is a member of the well-studied mucus-degrading family Bacteroidaceae, which possesses numerous glycosidases capable of degrading glycosylated mucins. Proteomic analysis revealed that *B. thetaiotaomicron* encodes at least 172 glycosidases,

exceeding the capacity of most other sequenced gut microbiota (Xu *et al.*, 2003). Specially, *B. thetaiotaomicron* only contains a sialidase that liberates sialic acids from mucin glycans, but does not have a sialic acid metabolism pathway to consume this nutrient (Juge *et al.*, 2016). In addition to acquiring mucin-derived sugars liberated by *B. thetaiotaomicron*, *C. rodentium* also displays increased virulence in mice mono-associated with this commensal. My work thus provides a plausible mechanism for how enteric pathogens leverage the enzymatic functions of commensals to acquire energy sources from mucins and enhance their pathogenicity to reach the underlying epithelium.

Taken together, in context of the published literature, I envision the following model for the interactions between enteric pathogens, intestinal mucus, and mucus-degrading commensal bacteria: During the early stages of infection, *C. rodentium* is attracted to the intestinal mucus by sensing the sialic acid decorated mucins that make up the mucus layer. Luminal *C. rodentium* migrates to the mucus layer, where the pathogen encounters mucus-degrading commensals such as *B. thetaiotaomicron*, which thrive by utilizing mucin glycans as a source of nutrients in addition to dietary carbohydrates. Sialidases produced by the mucus-degrading commensals cleave sialic acid residues from mucin glycans, making them available to other microbes, including *C. rodentium*, which captures the liberated sialic acid via its sialic acid transporter NanT and uses it as a growth substrate. Additionally, sialic acid enhances the secretion of the Pic mucinase, which facilitates *C. rodentium*'s ability to penetrate the mucus barriers. Concurrently, sialic acid also triggers an increase in the secretion of the EspC protein, which helps *C. rodentium* to initiate adherence to the underlying colonic epithelium prior to the formation of A/E lesions through its T3SS. These findings improve our understanding of the interactions

between enteric bacterial pathogens and mucin glycans, as well as highlighting the key role of mucin-degrading microbiota in facilitating these interactions.

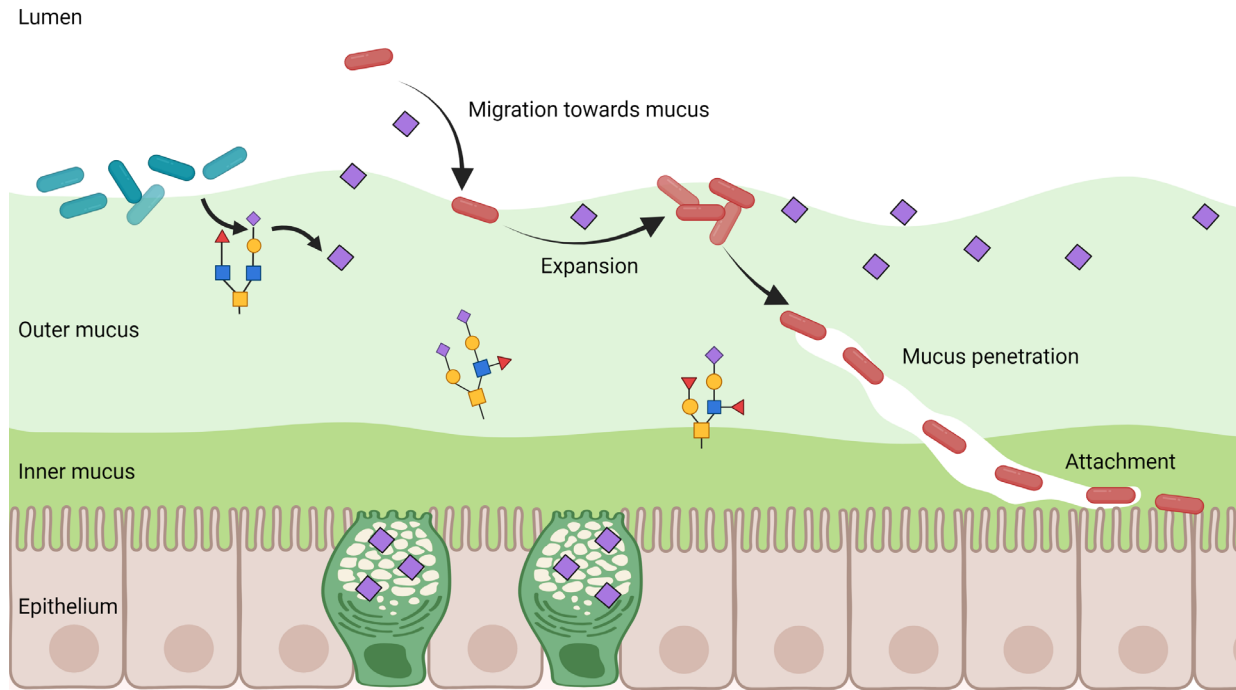


Figure 5.1 Proposed model for the interactions between enteric pathogens, the intestinal mucus, and mucin-degrading commensal bacteria.

The mucus layer harbors commensals that can break down the complex glycans decorating the mucin protein Muc2. Certain bacteria that express sialidases release sialic acid from mucin glycans, making it available to other microbes, including the pathogen *C. rodentium*. Luminal *C. rodentium* senses sialic acid and migrates towards the mucus layer, where it accesses the free sialic acid liberated by commensals. *C. rodentium* uses sialic acid as a nutrient to expand its population. Sialic acid also enhances the virulence of *C. rodentium* by increasing its secretion of Pic and EspC. Pic serves as a mucinase to facilitate *C. rodentium*'s penetration of the mucus barrier. EspC facilitates *C. rodentium*'s initial adhesion to the IEC prior to the formation of T3SS-mediated A/E lesions.

5.2 Limitations and future directions

The work presented in this thesis raises various outstanding questions that need to be addressed by future research. One limitation is the reliance on the *C. rodentium* model and the lack of testing on clinically relevant human pathogens. Although similar effects of sialic acid and the sialic acid transporter NanT on EPEC were observed, it is necessary to examine these effects using human samples. As most enteric pathogens erode the mucus barrier to promote their

adherence or invasion of host IECs, and the sialic acid metabolism pathway is conserved across them, the significance of sialic acid shown in *C. rodentium* may extend to other enteric bacterial pathogens. Future research should include measuring the levels of free sialic acid in fecal samples obtained from patients with enteric bacterial infections and analyzing the expression of genes involved in the sialic acid metabolism pathway by the infecting pathogens, and correlating these findings with disease severity of the patients.

In Chapter 2, several exciting areas regarding the *in vivo* interactions between mucin glycans and *C. rodentium* remain uncharacterized. Obtaining a comprehensive understanding of how *C. rodentium* infection affects host mucin glycosylation is still challenging, as it requires tracking different stages throughout the infection and necessitates a high number of biological replicates. The use of lectin staining in identifying changes in host glycosylation is limited by the quality of tissue preservation and the specificity of lectin binding. For example, MALII lectin was traditionally used to detect α 2,3-sialylation and sulphation, but a recent study showed that it mainly recognizes sulphated mucins (Bergstrom *et al.*, 2020). In-depth analysis of mucin glycosylation profile before and throughout infection, along with a broader range of lectin staining and host glycosylation gene expression analysis, could provide greater insights into the protective mechanisms of the intestinal mucus response against enteric bacterial infections, as well as other intestinal disorders such as IBD. Such research could lead to the discovery of potential therapeutics that strengthen the mucus barrier in treating enteric disorders. To further confirm our findings on the important role of sialic acid in maintaining *C. rodentium* fitness *in vivo*, additional experiments can be conducted to evaluate the susceptibility of mice deficient in colonic mucus sialylation to *C. rodentium* infection. In Chapter 2, we administered exogenous

sialic acid to C57BL/6 mice by oral gavage before and throughout the infection, which resulted in exacerbated colonization and pathological damage. However, it remains unclear whether the administration of sialic acid worsened disease severity by altering host physiology or the pathogenesis of *C. rodentium*. Another outstanding question is to what extent the exogenous sialic acid interacted with the ingested pathogen, as simple sugars are typically absorbed in the small intestine and may not reach the distal portion of the GI tract. Alternatively, we could administer exogenous sialic acid via intrarectal enema using varying doses to assess the response to *C. rodentium* infection.

My work in Chapter 3 expands our understanding of different aspects of A/E pathogenesis, highlighting factors beyond the T3SS. Bacterial chemotaxis and penetration of mucus represent important but understudied aspects of bacterial pathogenesis, in part due to the difficulty of investigating these processes *in vivo*. I consistently relied on *in vitro* assays to decipher the virulence traits altered by sialic acid exposure and to determine the functions of each virulence factor. These *in vitro* phenotypes also require further validation through complementation of all the mutant strains, despite the precision of the gene deletion method I employed. The discovery that *C. rodentium* can actively migrate towards sialic acid *in vitro* is significant, as this bacterium was previously considered non-motile due to its lack of flagella. However, further research is necessary to understand the chemotactic behaviors of *C. rodentium in vivo*. In addition, the mechanisms utilized by non-flagellated bacteria like *C. rodentium* to facilitate their motility need to be elucidated. The roles of Pic and EspC, two proteins highly secreted in response to sialic acid, are explored in this study using *in vitro* mucin penetration assays and IEC adherence assays that I developed. However, the functions of both Pic and EspC remain unclear and contradictory

in the current literature, indicating the need for further investigation. We previously investigated the pathogenesis of ΔpicC *C. rodentium* *in vivo* and found that it not only had reduced mucolytic activity, but displayed abnormal colony morphology and showed exaggerated activation of toll-like receptor 2 (Bhullar *et al.*, 2015). On the other hand, EspC has been shown to degrade a variety of substrates, including host focal adhesion proteins and the cytoskeletal actin-associated protein fodrin, as well as A/E pathogens' own T3SS components. The mechanism by which EspC mediates epithelial adherence should also be further elucidated. It is also worth noting that additional virulence factors other than Pic and EspC can be altered following exposure to sialic acid. It was noticed that sialic acid induced the secretion of several as yet unidentified proteins by EPEC (Figure A.3.1). To discover the identity of additional virulence factors that may be differentially expressed and/or secreted in the presence of sialic acid, valuable approaches would include whole-genome transcriptomic profiling and comparative LC-MS/MS analysis.

Another interesting potential route of investigation to arise from Chapter 3 regards the detailed mechanisms by which *C. rodentium* crosses the multi-layered colonic mucus to attach to the underlying epithelium. A recent study provided new insights into the structural formation of the mucus barrier. The mucus encapsulating the microbial community in the distal colon is comprised of two distinct subtypes, a "b1" layer derived from the proximal colon and a "b2" layer derived from the distal colon that can be differentially recognized by the lectin MALII (Bergstrom *et al.*, 2020). This re-definition of the mucus protective system raises additional questions regarding how *C. rodentium* crosses the mucus barrier. Specifically, whether *C. rodentium* employs mechanisms to avoid encapsulation in the proximal colon or uses different strategies to subvert the "b1" and "b2" layers at the distal site.

Finally, exploring the role of mucus-degrading commensals in mediating the interactions between enteric pathogens and the mucus layer presents another exciting avenue of inquiry. I revealed the essential role played by the gut microbiota in releasing sialic acid from mucin glycans and promoting *C. rodentium* colonization of colonic mucosa by comparing the differences observed between SPF mice and GF mice. However, it is important to exercise caution when interpreting results from GF mice, since aside from lacking a microbiota, they also have impaired development of their innate and adaptive immune responses to bacterial infections. Molecules produced by commensal microorganisms are essential for the stimulation and differentiation of immune cells, as well as lymphatic organs such as Peyer's patches, and IEC (Fiebiger *et al.*, 2016). Exposure to an uneducated mucosal immune system due to the absence of gut microbiota can lead to difficulty interpreting the outcome of infection in GF mice. Dual colonization of *B. thetaiotaomicron* and *C. rodentium* provides a simplified approach to delineate the interactions between enteric pathogens and mucus-degrading commensals *in vivo*. In concert with our *in vitro* growth assessment, *B. thetaiotaomicron* is shown to support the growth of *C. rodentium*, potentially by releasing mucin sugars from colonic mucus. However, additional supportive evidence is required to determine whether sialic acid is the main driver that induces the pathogenicity of *C. rodentium* in *B. thetaiotaomicron* mono-colonized mice. I aim to address this question in future experiments, by infecting these gnotobiotic mice with $\Delta nanT$ *C. rodentium* or performing WT *C. rodentium* infection on gnotobiotic mice mono-colonized with a *B. thetaiotaomicron* strain deficient in sialidase activity. Moreover, it is worth exploring whether *C. rodentium* obtains similar benefits from other mucus-degrading commensal bacteria, such as *B. fragilis* and *Akkermansia muciniphila*, which differ from *B. thetaiotaomicron* in that they

encompass both sialidases and sialic acid metabolism pathways. Expanding to test a broader range of bacterial species will provide more clarity regarding the role of microbial sialidase activity in the intricate metabolic network of the gut ecosystem.

Finally, it is important to further investigate the effects of other mucin sugars on the pathogenesis of *C. rodentium*. In addition to sialic acid, my research showed that *C. rodentium* can grow using GlcNAc and Gal as sole carbon sources. *C. rodentium* also contains a sensor for fucose (FucR), despite having an incomplete pathway to utilize it for energy. Research in our lab is currently seeking to uncover the roles of other mucin sugars in *C. rodentium* pathogenesis. Furthermore, it is crucial to understand how *C. rodentium* prioritizes its nutrient requirements to adapt its metabolism at the mucus layer. Identification of primary nutrients acquired by enteric pathogens could be potential targets for anti-microbials.

Despite the limitations discussed here, the work in this thesis identifies sialic acid as a key mucin-derived nutrient utilized by the A/E pathogen *C. rodentium*, with the necessity of mucus-degrading commensals to liberate the sugar. This work offers exciting potential for targeting pathogen nutrition as an alternative to the use of antibiotics. It sheds light on the development of synthetic small molecule inhibitors to target pathogen uptake of essential nutrients, or enzymatic release of these nutrients by the gut microbiota.

5.3 Final remarks

Enteric bacterial infections pose a significant threat to human health worldwide, with the family of attaching and effacing (A/E) pathogens consistently being identified as one of the most serious

causes of foodborne illness. *C. rodentium*, a natural murine A/E pathogen, is considered an important model organism for the clinically important pathogens EPEC/EHEC and the study of pathogen-host-microbiota interactions. Past decades of investigation in bacterial pathogenesis has left a knowledge gap in understanding how enteric pathogens switch metabolic strategies and regulate the virulence at the mucus layer to subvert the mucus barrier.

In my doctoral thesis, I have taken various approaches to elucidate the interactions of *C. rodentium* with the mucin glycans and mucus-degrading commensals. The findings presented here suggest that sialic acid plays a key role in fueling the expansion of *C. rodentium* in the mammalian gut and promoting the virulence of *C. rodentium* specifically during its transition from the luminal compartment to the intestinal mucosal surface. Further, I reveal the essential role of the gut microbiota possessing glycolytic activities that liberates sialic acid from mucin glycans in promoting the accessibility of sialic acid to the pathogen. Together, this research improves our understanding of the interactions with mucin glycans and mucin-degrading commensal microbes by which enteric pathogens utilize to subvert the mucus barrier, and may inform future therapeutics to treat bacterial infections by targeting pathogen metabolism.

Bibliography

- Albenberg, L., Esipova, T. V., Judge, C. P., Bittinger, K., Chen, J., Laughlin, A., ... Wu, G. D. (2014). Correlation Between Intraluminal Oxygen Gradient and Radial Partitioning of Intestinal Microbiota. *Gastroenterology*, *147*, 1055-1063.e8.
- Allaire, J. M., Crowley, S. M., Law, H. T., Chang, S.-Y., Ko, H.-J., & Vallance, B. A. (2018). The Intestinal Epithelium: Central Coordinator of Mucosal Immunity. *Trends in Immunology*, *39*, 677–696.
- Almagro-Moreno, S., & Boyd, E. F. (2009). Insights into the evolution of sialic acid catabolism among bacteria. *BMC Evolutionary Biology*, *9*, 118.
- Altman, M. O., & Gagneux, P. (2019). Absence of Neu5Gc and Presence of Anti-Neu5Gc Antibodies in Humans—An Evolutionary Perspective. *Frontiers in Immunology*, *10*. Retrieved from <https://www.frontiersin.org/articles/10.3389/fimmu.2019.00789>
- Arabyan, N., Park, D., Foutouhi, S., Weis, A. M., Huang, B. C., Williams, C. C., ... Weimer, B. C. (2016). Salmonella Degrades the Host Glycocalyx Leading to Altered Infection and Glycan Remodeling. *Scientific Reports*, *6*, 29525.
- Arike, L., & Hansson, G. C. (2016). The Densely O-Glycosylated MUC2 Mucin Protects the Intestine and Provides Food for the Commensal Bacteria. *Journal of Molecular Biology*, *428*, 3221–3229.
- Arike, L., Holmén-Larsson, J., & Hansson, G. C. (2017). Intestinal Muc2 mucin O-glycosylation is affected by microbiota and regulated by differential expression of glycosyltransferases. *Glycobiology*. <https://doi.org/10.1093/glycob/cww134>
- Ashida, H., Tanigawa, K., Kiyohara, M., Katoh, T., Katayama, T., & Yamamoto, K. (2018). Bifunctional properties and characterization of a novel sialidase with esterase activity from *Bifidobacterium bifidum*. *Bioscience, Biotechnology, and Biochemistry*, *82*, 2030–2039.
- Barnard, K. N., Alford-Lawrence, B. K., Buchholz, D. W., Wasik, B. R., LaClair, J. R., Yu, H., ... Parrish, C. R. (2020). Modified Sialic Acids on Mucus and Erythrocytes Inhibit Influenza A Virus Hemagglutinin and Neuraminidase Functions. *Journal of Virology*, *94*, e01567-19.
- Barroso-Batista, J., Pedro, M. F., Sales-Dias, J., Pinto, C. J. G., Thompson, J. A., Pereira, H., ... Xavier, K. B. (2020). Specific Eco-evolutionary Contexts in the Mouse Gut Reveal *Escherichia coli* Metabolic Versatility. *Current Biology*, *30*, 1049-1062.e7.
- Bell, A., Brunt, J., Crost, E., Vaux, L., Nepravishta, R., Owen, C. D., ... Juge, N. (2019). Elucidation of a unique sialic acid metabolism pathway in mucus-foraging *Ruminococcus gnavus* unravels mechanisms of bacterial adaptation to the gut. *Nature Microbiology*, *4*, 2393–2404.
- Bell, A., Severi, E., Lee, M., Monaco, S., Latousakis, D., Angulo, J., ... Juge, N. (2020). Uncovering a novel molecular mechanism for scavenging sialic acids in bacteria. *Journal of Biological Chemistry*, *295*, 13724–13736.
- Bell, A., Severi, E., Owen, C. D., Latousakis, D., & Juge, N. (2023). Biochemical and structural basis of sialic acid utilization by gut microbes. *Journal of Biological Chemistry*, 102989.
- Berger, C. N., Crepin, V. F., Roumeliotis, T. I., Wright, J. C., Carson, D., Pevsner-Fischer, M., ... Frankel, G. (2017). *Citrobacter rodentium* Subverts ATP Flux and Cholesterol Homeostasis in Intestinal Epithelial Cells In Vivo. *Cell Metabolism*, *26*, 738-752.e6.

- Bergstrom, K., Liu, X., Zhao, Y., Gao, N., Wu, Q., Song, K., ... Xia, L. (2016). Defective Intestinal Mucin-type O-glycosylation Causes Spontaneous Colitis-associated Cancer in Mice. *Gastroenterology*, *151*, 152-164.e11.
- Bergstrom, K. S. B., Kisson-Singh, V., Gibson, D. L., Ma, C., Montero, M., Sham, H. P., ... Vallance, B. A. (2010). Muc2 Protects against Lethal Infectious Colitis by Disassociating Pathogenic and Commensal Bacteria from the Colonic Mucosa. *PLoS Pathogens*, *6*, e1000902.
- Bergstrom, K., Shan, X., Casero, D., Batushansky, A., Lagishetty, V., Jacobs, J. P., ... Xia, L. (2020). Proximal colon-derived O-glycosylated mucus encapsulates and modulates the microbiota. *Science (New York, N.Y.)*, *370*, 467-472.
- Bergstrom, K., & Xia, L. (2022). The barrier and beyond: Roles of intestinal mucus and mucin-type O-glycosylation in resistance and tolerance defense strategies guiding host-microbe symbiosis. *Gut Microbes*, *14*, 2052699.
- Berkhout, M. D., Plugge, C. M., & Belzer, C. (2021). How microbial glycosyl hydrolase activity in the gut mucosa initiates microbial cross-feeding. *Glycobiology*, *32*, 182-200.
- Berry, D., Stecher, B., Schintlmeister, A., Reichert, J., Brugiroux, S., Wild, B., ... Wagner, M. (2013). Host-compound foraging by intestinal microbiota revealed by single-cell stable isotope probing. *Proceedings of the National Academy of Sciences*, *110*, 4720-4725.
- Bertin, Y., Chaucheyras-Durand, F., Robbe-Masselot, C., Durand, A., de la Foye, A., Harel, J., ... Martin, C. (2013). Carbohydrate utilization by enterohaemorrhagic *Escherichia coli* O157:H7 in bovine intestinal content: Carbon nutrition of EHEC O157:H7 in the bovine intestine. *Environmental Microbiology*, *15*, 610-622.
- Bhinder, G., Sham, H. P., Chan, J. M., Morampudi, V., Jacobson, K., & Vallance, B. A. (2013). The *Citrobacter rodentium* Mouse Model: Studying Pathogen and Host Contributions to Infectious Colitis. *Journal of Visualized Experiments*. <https://doi.org/10.3791/50222>
- Bhullar, K., Zarepour, M., Yu, H., Yang, H., Croxen, M., Stahl, M., ... Vallance, B. A. (2015). The Serine Protease Autotransporter Pic Modulates *Citrobacter rodentium* Pathogenesis and Its Innate Recognition by the Host. *Infection and Immunity*, *83*, 2636-2650.
- Bishop, A. L., Wiles, S., Dougan, G., & Frankel, G. (2007). Cell attachment properties and infectivity of host-adapted and environmentally adapted *Citrobacter rodentium*. *Microbes and Infection*, *9*, 1316-1324.
- Bojar, D., Meche, L., Meng, G., Eng, W., Smith, D. F., Cummings, R. D., & Mahal, L. K. (2022). A Useful Guide to Lectin Binding: Machine-Learning Directed Annotation of 57 Unique Lectin Specificities. *ACS Chemical Biology*, *17*, 2993-3012.
- Bosman, E. S., Chan, J. M., Bhullar, K., & Vallance, B. A. (2016). Investigation of Host and Pathogen Contributions to Infectious Colitis Using the *Citrobacter rodentium* Mouse Model of Infection. *Methods in Molecular Biology (Clifton, N.J.)*, *1422*, 225-241.
- Bry, L., Falk, P. G., Midtvedt, T., & Gordon, J. I. (1996). A Model of Host-Microbial Interactions in an Open Mammalian Ecosystem. *Science*, *273*, 1380-1383.
- Bueno, E., Sit, B., Waldor, M. K., & Cava, F. (2018). Anaerobic nitrate reduction divergently governs population expansion of the enteropathogen *Vibrio cholerae*. *Nature Microbiology*, *3*, 1346-1353.
- Buschor, S., Cuenca, M., Uster, S. S., Schären, O. P., Balmer, M. L., Terrazos, M. A., ... Hafelmeier, S. (2017). Innate immunity restricts *Citrobacter rodentium* A/E

- pathogenesis initiation to an early window of opportunity. *PLOS Pathogens*, *13*, e1006476.
- Caballero-Flores, G., Pickard, J. M., Fukuda, S., Inohara, N., & Núñez, G. (2020). An Enteric Pathogen Subverts Colonization Resistance by Evading Competition for Amino Acids in the Gut. *Cell Host & Microbe*, *28*, 526-533.e5.
- Caballero-Flores, G., Pickard, J. M., & Núñez, G. (2021). Regulation of *Citrobacter rodentium* colonization: Virulence, immune response and microbiota interactions. *Current Opinion in Microbiology*, *63*, 142–149.
- Carlson-Banning, K. M., & Sperandio, V. (2016). Catabolite and Oxygen Regulation of Enterohemorrhagic *Escherichia coli* Virulence. *MBio*, *7*, e01852-16.
- Cepeda-Molero, M., Berger, C. N., Walsham, A. D. S., Ellis, S. J., Wemyss-Holden, S., Schüller, S., ... Fernández, L. Á. (2017). Attaching and effacing (A/E) lesion formation by enteropathogenic *E. coli* on human intestinal mucosa is dependent on non-LEE effectors. *PLoS Pathogens*, *13*, e1006706.
- Cepeda-Molero, M., Schüller, S., Frankel, G., Fernández, L. Á., Cepeda-Molero, M., Schüller, S., ... Fernández, L. Á. (2020). Systematic Deletion of Type III Secretion System Effectors in Enteropathogenic *E. coli* Unveils the Role of Non-LEE Effectors in A/E Lesion Formation. In *E. Coli Infections—Importance of Early Diagnosis and Efficient Treatment*. IntechOpen.
- Chang, D.-E., Smalley, D. J., Tucker, D. L., Leatham, M. P., Norris, W. E., Stevenson, S. J., ... Conway, T. (2004). Carbon nutrition of *Escherichia coli* in the mouse intestine. *Proceedings of the National Academy of Sciences*, *101*, 7427–7432.
- Chassaing, B., & Gewirtz, A. T. (2018). Identification of Inner Mucus-Associated Bacteria by Laser Capture Microdissection. *Cellular and Molecular Gastroenterology and Hepatology*, *7*, 157–160.
- Chu, D., & Barnes, D. J. (2016). The lag-phase during diauxic growth is a trade-off between fast adaptation and high growth rate. *Scientific Reports*, *6*, 25191.
- Coker, J. K., Moyne, O., Rodionov, D. A., & Zengler, K. (2021). Carbohydrates great and small, from dietary fiber to sialic acids: How glycans influence the gut microbiome and affect human health. *Gut Microbes*, *13*. <https://doi.org/10.1080/19490976.2020.1869502>
- Collins, J. P. (2022). Preliminary Incidence and Trends of Infections Caused by Pathogens Transmitted Commonly Through Food—Foodborne Diseases Active Surveillance Network, 10 U.S. Sites, 2016–2021. *MMWR. Morbidity and Mortality Weekly Report*, *71*. <https://doi.org/10.15585/mmwr.mm7140a2>
- Collins, J. W., Keeney, K. M., Crepin, V. F., Rathinam, V. A. K., Fitzgerald, K. A., Finlay, B. B., & Frankel, G. (2014). *Citrobacter rodentium*: Infection, inflammation and the microbiota. *Nature Reviews Microbiology*, *12*, 612–623.
- Connolly, J. P. R., Slater, S. L., O’Boyle, N., Goldstone, R. J., Crepin, V. F., Gallego, D. R., ... Roe, A. J. (2018). Host-associated niche metabolism controls enteric infection through fine-tuning the regulation of type 3 secretion. *Nature Communications*, *9*. <https://doi.org/10.1038/s41467-018-06701-4>
- Corfield, A. P., Myerscough, N., Warren, B. F., Durdey, P., Paraskeva, C., & Schauer, R. (1999). Reduction of sialic acid O-acetylation in human colonic mucins in the adenoma-carcinoma sequence. *Glycoconjugate Journal*, *16*, 307–317.

- Corfield, A. P., Wagner, S. A., Clamp, J. R., Kriaris, M. S., & Hoskins, L. C. (1992). Mucin degradation in the human colon: Production of sialidase, sialate O-acetyltransferase, N-acetylneuraminidase, arylesterase, and glycosulfatase activities by strains of fecal bacteria. *Infection and Immunity*, *60*, 3971–3978.
- Cornick, S., Moreau, F., Gaisano, H. Y., & Chadee, K. (2017). Entamoeba histolytica-Induced Mucin Exocytosis Is Mediated by VAMP8 and Is Critical in Mucosal Innate Host Defense. *MBio*, *8*, e01323-17.
- Crouch, L. I., Liberato, M. V., Urbanowicz, P. A., Baslé, A., Lamb, C. A., Stewart, C. J., ... Bolam, D. N. (2020). Prominent members of the human gut microbiota express endo-acting O-glycanases to initiate mucin breakdown. *Nature Communications*, *11*, 4017.
- Croxen, M. A., & Finlay, B. B. (2010). Molecular mechanisms of Escherichia coli pathogenicity. *Nature Reviews Microbiology*, *8*, 26–38.
- Curtis, M. M., Hu, Z., Klimko, C., Narayanan, S., Deberardinis, R., & Sperandio, V. (2014). The Gut Commensal Bacteroides thetaiotaomicron Exacerbates Enteric Infection through Modification of the Metabolic Landscape. *Cell Host & Microbe*, *16*, 759–769.
- Dautin, N. (2010). Serine Protease Autotransporters of Enterobacteriaceae (SPATEs): Biogenesis and Function. *Toxins*, *2*, 1179–1206.
- Deng, W., de Hoog, C. L., Yu, H. B., Li, Y., Croxen, M. A., Thomas, N. A., ... Finlay, B. B. (2010). A Comprehensive Proteomic Analysis of the Type III Secretome of Citrobacter rodentium*. *Journal of Biological Chemistry*, *285*, 6790–6800.
- Derrien, M. M. N. (2007). *Mucin utilisation and host interactions of the novel intestinal microbe Akkermansia muciniphila*. Retrieved from <https://research.wur.nl/en/publications/mucin-utilisation-and-host-interactions-of-the-novel-intestinal-m>
- Donaldson, G. P., Lee, S. M., & Mazmanian, S. K. (2016). Gut biogeography of the bacterial microbiota. *Nature Reviews. Microbiology*, *14*, 20–32.
- Drula, E., Garron, M.-L., Dogan, S., Lombard, V., Henrissat, B., & Terrapon, N. (2022). The carbohydrate-active enzyme database: Functions and literature. *Nucleic Acids Research*, *50*, D571–D577.
- Dwivedi, R., Nothaft, H., Garber, J., Xin Kin, L., Stahl, M., Flint, A., ... Szymanski, C. M. (2016). L-fucose influences chemotaxis and biofilm formation in Campylobacter jejuni. *Molecular Microbiology*, *101*, 575–589.
- Edwards, R. A., Keller, L. H., & Schifferli, D. M. (1998). Improved allelic exchange vectors and their use to analyze 987P fimbria gene expression. *Gene*, *207*, 149–157.
- Egan, M., O’Connell Motherway, M., Ventura, M., & van Sinderen, D. (2014). Metabolism of Sialic Acid by Bifidobacterium breve UCC2003. *Applied and Environmental Microbiology*, *80*, 4414–4426.
- Elliott, S. J., Sperandio, V., Girón, J. A., Shin, S., Mellies, J. L., Wainwright, L., ... Kaper, J. B. (2000). The Locus of Enterocyte Effacement (LEE)-Encoded Regulator Controls Expression of Both LEE- and Non-LEE-Encoded Virulence Factors in Enteropathogenic and Enterohemorrhagic Escherichia coli. *Infection and Immunity*, *68*, 6115–6126.
- Engevik, M. A., Engevik, A. C., Engevik, K. A., Auchtung, J. M., Chang-Graham, A. L., Ruan, W., ... Versalovic, J. (2021). Mucin-Degrading Microbes Release Monosaccharides That Chemoattract Clostridioides difficile and Facilitate Colonization of the Human Intestinal Mucus Layer. *ACS Infectious Diseases*, *7*, 1126–1142.

- Erdem, A. L., Avelino, F., Xicohtencatl-Cortes, J., & Girón, J. A. (2007). Host Protein Binding and Adhesive Properties of H6 and H7 Flagella of Attaching and Effacing *Escherichia coli*. *Journal of Bacteriology*, *189*, 7426–7435.
- Fabich, A. J., Jones, S. A., Chowdhury, F. Z., Cernosek, A., Anderson, A., Smalley, D., ... Conway, T. (2008). Comparison of Carbon Nutrition for Pathogenic and Commensal *Escherichia coli* Strains in the Mouse Intestine. *Infection and Immunity*, *76*, 1143–1152.
- Fiebiger, U., Bereswill, S., & Heimesaat, M. M. (2016). Dissecting the Interplay Between Intestinal Microbiota and Host Immunity in Health and Disease: Lessons Learned from Germfree and Gnotobiotic Animal Models. *European Journal of Microbiology & Immunology*, *6*, 253–271.
- Flores-Sanchez, F., Chavez-Dueñas, L., Sanchez-Villamil, J., & Navarro-Garcia, F. (2020). Pic Protein From Enteroaggregative *E. coli* Induces Different Mechanisms for Its Dual Activity as a Mucus Secretagogue and a Mucinase. *Frontiers in Immunology*, *11*, 564953.
- Franzin, F. M., & Sircili, M. P. (2015). Locus of Enterocyte Effacement: A Pathogenicity Island Involved in the Virulence of Enteropathogenic and Enterohemorrhagic *Escherichia coli* Subjected to a Complex Network of Gene Regulation. *BioMed Research International*, *2015*, 534738.
- Furniss, R. C. D., & Clements, A. (2017). Regulation of the Locus of Enterocyte Effacement in Attaching and Effacing Pathogens. *Journal of Bacteriology*, *200*, e00336-17.
- Furter, M., Sellin, M. E., Hansson, G. C., & Hardt, W.-D. (2019). Mucus Architecture and Near-Surface Swimming Affect Distinct *Salmonella* Typhimurium Infection Patterns along the Murine Intestinal Tract. *Cell Reports*, *27*, 2665-2678.e3.
- Gaytán, M. O., Martínez-Santos, V. I., Soto, E., & González-Pedrajo, B. (2016a). Type Three Secretion System in Attaching and Effacing Pathogens. *Frontiers in Cellular and Infection Microbiology*, *6*. Retrieved from <https://www.frontiersin.org/articles/10.3389/fcimb.2016.00129>
- Gaytán, M. O., Martínez-Santos, V. I., Soto, E., & González-Pedrajo, B. (2016b). Type Three Secretion System in Attaching and Effacing Pathogens. *Frontiers in Cellular and Infection Microbiology*, *6*. Retrieved from <https://www.frontiersin.org/articles/10.3389/fcimb.2016.00129>
- Ghosh, S., Dai, C., Brown, K., Rajendiran, E., Makarenko, S., Baker, J., ... Gibson, D. L. (2011). Colonic microbiota alters host susceptibility to infectious colitis by modulating inflammation, redox status, and ion transporter gene expression. *American Journal of Physiology-Gastrointestinal and Liver Physiology*, *301*, G39–G49.
- Gibson, D. L., Ma, C., Rosenberger, C. M., Bergstrom, K. S. B., Valdez, Y., Huang, J. T., ... Vallance, B. A. (2008). Toll-like receptor 2 plays a critical role in maintaining mucosal integrity during *Citrobacter rodentium*-induced colitis. *Cellular Microbiology*, *10*, 388–403.
- Görke, B., & Stülke, J. (2008). Carbon catabolite repression in bacteria: Many ways to make the most out of nutrients. *Nature Reviews Microbiology*, *6*, 613–624.
- Grondin, J. M., Tamura, K., Déjean, G., Abbott, D. W., & Brumer, H. (2017). Polysaccharide Utilization Loci: Fueling Microbial Communities. *Journal of Bacteriology*, *199*. <https://doi.org/10.1128/JB.00860-16>
- Gruenheid, S., Sekirov, I., Thomas, N. A., Deng, W., O'Donnell, P., Goode, D., ... Finlay, B. B. (2004). Identification and characterization of NleA, a non-LEE-encoded type III

- translocated virulence factor of enterohaemorrhagic *Escherichia coli* O157:H7. *Molecular Microbiology*, *51*, 1233–1249.
- Guignot, J., Segura, A., & Nhieu, G. T. V. (2015). The Serine Protease EspC from Enteropathogenic *Escherichia coli* Regulates Pore Formation and Cytotoxicity Mediated by the Type III Secretion System. *PLOS Pathogens*, *11*, e1005013.
- Gustafsson, J. K., Ermund, A., Johansson, M. E. V., Schütte, A., Hansson, G. C., & Sjövall, H. (2012). An ex vivo method for studying mucus formation, properties, and thickness in human colonic biopsies and mouse small and large intestinal explants. *American Journal of Physiology - Gastrointestinal and Liver Physiology*, *302*, G430–G438.
- Gustafsson, J. K., & Johansson, M. E. V. (2022). The role of goblet cells and mucus in intestinal homeostasis. *Nature Reviews Gastroenterology & Hepatology*, *19*, 785–803.
- Haines-Menges, B. L., Whitaker, W. B., Lubin, J. B., & Boyd, E. F. (2015). Host Sialic Acids: A delicacy for the pathogen with discerning taste. *Microbiology Spectrum*, *3*, 10.1128/microbiolspec.MBP-0005–2014.
- Hansson, G. C. (2019). Mucus and mucins in diseases of the intestinal and respiratory tracts. *Journal of Internal Medicine*. <https://doi.org/10.1111/joim.12910>
- Hansson, G. C. (2020). Mucins and the Microbiome. *Annual Review of Biochemistry*, *89*, 769–793.
- Harrington, S. M., Sheikh, J., Henderson, I. R., Ruiz-Perez, F., Cohen, P. S., & Nataro, J. P. (2009). The Pic Protease of Enteroaggregative *Escherichia coli* Promotes Intestinal Colonization and Growth in the Presence of Mucin. *Infection and Immunity*, *77*, 2465–2473.
- Hart, E., Yang, J., Tauschek, M., Kelly, M., Wakefield, M. J., Frankel, G., ... Robins-Browne, R. M. (2008). RegA, an AraC-Like Protein, Is a Global Transcriptional Regulator That Controls Virulence Gene Expression in *Citrobacter rodentium*. *Infection and Immunity*, *76*, 5247–5256.
- Hayashi, N., Matsukawa, M., Horinishi, Y., Nakai, K., Shoji, A., Yoneko, Y., ... Gotoh, N. (2013). Interplay of flagellar motility and mucin degradation stimulates the association of *Pseudomonas aeruginosa* with human epithelial colorectal adenocarcinoma (Caco-2) cells. *Journal of Infection and Chemotherapy*, *19*, 305–315.
- Herath, M., Hosie, S., Bornstein, J. C., Franks, A. E., & Hill-Yardin, E. L. (2020). The Role of the Gastrointestinal Mucus System in Intestinal Homeostasis: Implications for Neurological Disorders. *Frontiers in Cellular and Infection Microbiology*, *10*. Retrieved from <https://www.frontiersin.org/articles/10.3389/fcimb.2020.00248>
- Herrmann, A., Davies, J. R., Lindell, G., Mårtensson, S., Packer, N. H., Swallow, D. M., & Carlstedt, I. (1999). Studies on the “insoluble” glycoprotein complex from human colon. Identification of reduction-insensitive MUC2 oligomers and C-terminal cleavage. *The Journal of Biological Chemistry*, *274*, 15828–15836.
- Hews, C. L., Tran, S.-L., Wegmann, U., Brett, B., Walsham, A. D. S., Kavanaugh, D., ... Schüller, S. (2017). The StcE metalloprotease of enterohaemorrhagic *Escherichia coli* reduces the inner mucus layer and promotes adherence to human colonic epithelium ex vivo. *Cellular Microbiology*, *19*, e12717.
- Ho, S. N., Hunt, H. D., Horton, R. M., Pullen, J. K., & Pease, L. R. (1989). Site-directed mutagenesis by overlap extension using the polymerase chain reaction. *Gene*, *77*, 51–59.

- Holmén Larsson, J. M., Karlsson, H., Crespo, J. G., Johansson, M. E. V., Eklund, L., Sjövall, H., & Hansson, G. C. (2011). Altered O-glycosylation profile of MUC2 mucin occurs in active ulcerative colitis and is associated with increased inflammation. *Inflammatory Bowel Diseases*, *17*, 2299–2307.
- Holmén Larsson, J. M., Karlsson, H., Sjövall, H., & Hansson, G. C. (2009). A complex, but uniform O-glycosylation of the human MUC2 mucin from colonic biopsies analyzed by nanoLC/MSn. *Glycobiology*, *19*, 756–766.
- Holmén Larsson, J. M., Thomsson, K. A., Rodríguez-Piñeiro, A. M., Karlsson, H., & Hansson, G. C. (2013). Studies of mucus in mouse stomach, small intestine, and colon. III. Gastrointestinal Muc5ac and Muc2 mucin O-glycan patterns reveal a regiospecific distribution. *American Journal of Physiology-Gastrointestinal and Liver Physiology*, *305*, G357–G363.
- Hooper, L. V., Xu, J., Falk, P. G., Midtvedt, T., & Gordon, J. I. (1999). A molecular sensor that allows a gut commensal to control its nutrient foundation in a competitive ecosystem. *Proceedings of the National Academy of Sciences of the United States of America*, *96*, 9833–9838.
- Hopkins, E. G. D., Roumeliotis, T. I., Mullineaux-Sanders, C., Choudhary, J. S., & Frankel, G. (2019). Intestinal Epithelial Cells and the Microbiome Undergo Swift Reprogramming at the Inception of Colonic *Citrobacter rodentium* Infection. *MBio*, *10*.
<https://doi.org/10.1128/mBio.00062-19>
- Hotinger, J. A., Pendergrass, H. A., & May, A. E. (2021). Molecular Targets and Strategies for Inhibition of the Bacterial Type III Secretion System (T3SS); Inhibitors Directly Binding to T3SS Components. *Biomolecules*, *11*, 316.
- Huang, Y.-L., Chassard, C., Hausmann, M., von Itzstein, M., & Hennet, T. (2015). Sialic acid catabolism drives intestinal inflammation and microbial dysbiosis in mice. *Nature Communications*, *6*. <https://doi.org/10.1038/ncomms9141>
- Huus, K. E., Hoang, T. T., Creus-Cuadros, A., Cirstea, M., Vogt, S. L., Knuff-Janzen, K., ... Finlay, B. B. (2021). Cross-feeding between intestinal pathobionts promotes their overgrowth during undernutrition. *Nature Communications*, *12*, 6860.
- In, J., Foulke-Abel, J., Zachos, N. C., Hansen, A.-M., Kaper, J. B., Bernstein, H. D., ... Kovbasnjuk, O. (2015). Enterohemorrhagic *Escherichia coli* Reduces Mucus and Intermicrovillar Bridges in Human Stem Cell-Derived Colonoids. *Cellular and Molecular Gastroenterology and Hepatology*, *2*, 48-62.e3.
- Jakobsson, H. E., Rodriguez-Pineiro, A. M., Schutte, A., Ermund, A., Boysen, P., Bemark, M., ... Johansson, M. E. (2015). The composition of the gut microbiota shapes the colon mucus barrier. *EMBO Reports*, *16*, 164–177.
- Jensen, P. H., Karlsson, N. G., Kolarich, D., & Packer, N. H. (2012). Structural analysis of N- and O-glycans released from glycoproteins. *Nature Protocols*, *7*, 1299–1310.
- Jimenez, A. G., Ellermann, M., Abbott, W., & Sperandio, V. (2020). Diet-derived galacturonic acid regulates virulence and intestinal colonization in enterohaemorrhagic *Escherichia coli* and *Citrobacter rodentium*. *Nature Microbiology*, *5*, 368–378.
- Johansson, M. E. V., Larsson, J. M. H., & Hansson, G. C. (2011). The two mucus layers of colon are organized by the MUC2 mucin, whereas the outer layer is a legislator of host-microbial interactions. *Proceedings of the National Academy of Sciences*, *108*, 4659–4665.

- Johansson, Malin E. V. (2012). Fast Renewal of the Distal Colonic Mucus Layers by the Surface Goblet Cells as Measured by In Vivo Labeling of Mucin Glycoproteins. *PLoS ONE*, *7*, e41009.
- Johansson, Malin E. V., Ambort, D., Pelaseyed, T., Schütte, A., Gustafsson, J. K., Ermund, A., ... Hansson, G. C. (2011). Composition and functional role of the mucus layers in the intestine. *Cellular and Molecular Life Sciences*, *68*, 3635–3641.
- Johansson, Malin E V, Gustafsson, J. K., Holmén-Larsson, J., Jabbar, K. S., Xia, L., Xu, H., ... Hansson, G. C. (2014). Bacteria penetrate the normally impenetrable inner colon mucus layer in both murine colitis models and patients with ulcerative colitis. *Gut*, *63*, 281–291.
- Johansson, Malin E. V., & Hansson, G. C. (2016). Immunological aspects of intestinal mucus and mucins. *Nature Reviews Immunology*, *16*, 639–649.
- Johansson, Malin E. V., Phillipson, M., Petersson, J., Velcich, A., Holm, L., & Hansson, G. C. (2008). The inner of the two Muc2 mucin-dependent mucus layers in colon is devoid of bacteria. *Proceedings of the National Academy of Sciences*, *105*, 15064–15069.
- Johansson, Malin E.V., Jakobsson, H. E., Holmén-Larsson, J., Schütte, A., Ermund, A., Rodríguez-Piñero, A. M., ... Hansson, G. C. (2015). Normalization of Host Intestinal Mucus Layers Requires Long-Term Microbial Colonization. *Cell Host & Microbe*, *18*, 582–592.
- Juge, N., Tailford, L., & Owen, C. D. (2016). Sialidases from gut bacteria: A mini-review. *Biochemical Society Transactions*, *44*, 166.
- Kaisar, M. H., Bhuiyan, M. S., Akter, A., Saleem, D., Iyer, A. S., Dash, P., ... Bhuiyan, T. R. (2021). *Vibrio cholerae* Sialidase-Specific Immune Responses Are Associated with Protection against Cholera. *MSphere*, *6*, e01232-20.
- Kalivoda, K. A., Steenbergen, S. M., & Vimr, E. R. (2013). Control of the *Escherichia coli* Sialoregulon by Transcriptional Repressor NanR. *Journal of Bacteriology*, *195*, 4689–4701.
- Kalivoda, K. A., Steenbergen, S. M., Vimr, E. R., & Plumbridge, J. (2003). Regulation of Sialic Acid Catabolism by the DNA Binding Protein NanR in *Escherichia coli*. *Journal of Bacteriology*, *185*, 4806–4815.
- Kamada, N., Kim, Y.-G., Sham, H. P., Vallance, B. A., Puente, J. L., Martens, E. C., & Nunez, G. (2012). Regulated Virulence Controls the Ability of a Pathogen to Compete with the Gut Microbiota. *Science*, *336*, 1325–1329.
- Kamphuis, J. B. J., Mercier-Bonin, M., Eutamène, H., & Theodorou, V. (2017). Mucus organisation is shaped by colonic content; a new view. *Scientific Reports*, *7*. <https://doi.org/10.1038/s41598-017-08938-3>
- Katoh, T., Yamada, C., Wallace, M. D., Yoshida, A., Gotoh, A., Arai, M., ... Katayama, T. (2023). A bacterial sulfoglycosidase highlights mucin O-glycan breakdown in the gut ecosystem. *Nature Chemical Biology*, *19*, 778–789.
- Kelly, M., Hart, E., Mundy, R., Marchès, O., Wiles, S., Badea, L., ... Hartland, E. L. (2006). Essential role of the type III secretion system effector NleB in colonization of mice by *Citrobacter rodentium*. *Infection and Immunity*, *74*, 2328–2337.
- Kenny, B., & Finlay, B. B. (1995). Protein secretion by enteropathogenic *Escherichia coli* is essential for transducing signals to epithelial cells. *Proceedings of the National Academy of Sciences of the United States of America*, *92*, 7991–7995.

- Khan, M. A., Ma, C., Knodler, L. A., Valdez, Y., Rosenberger, C. M., Deng, W., ... Vallance, B. A. (2006). Toll-like receptor 4 contributes to colitis development but not to host defense during *Citrobacter rodentium* infection in mice. *Infection and Immunity*, *74*, 2522–2536.
- Kitamoto, S., Alteri, C. J., Rodrigues, M., Nagao-Kitamoto, H., Sugihara, K., Himpfl, S. D., ... Kamada, N. (2020). Dietary l-serine confers a competitive fitness advantage to Enterobacteriaceae in the inflamed gut. *Nature Microbiology*, *5*, 116–125.
- Kiyohara, M., Tanigawa, K., Chaiwangsri, T., Katayama, T., Ashida, H., & Yamamoto, K. (2011). An exo- α -sialidase from bifidobacteria involved in the degradation of sialyloligosaccharides in human milk and intestinal glycoconjugates. *Glycobiology*, *21*, 437–447.
- Klapproth, J.-M. A., Sasaki, M., Sherman, M., Babbin, B., Donnenberg, M. S., Fernandes, P. J., ... Williams, I. R. (2005). *Citrobacter rodentium* lifA/efa1 Is Essential for Colonic Colonization and Crypt Cell Hyperplasia In Vivo. *Infection and Immunity*, *73*, 1441–1451.
- Koropatkin, N. M., Cameron, E. A., & Martens, E. C. (2012). How glycan metabolism shapes the human gut microbiota. *Nature Reviews Microbiology*, *10*, 323–335.
- Kumar, A., & Sperandio, V. (2019). Indole Signaling at the Host-Microbiota-Pathogen Interface. *MBio*, *10*, e01031-19.
- Le Bihan, G., Jubelin, G., Garneau, P., Bernalier-Donadille, A., Martin, C., Beaudry, F., & Harel, J. (2015). Transcriptome analysis of *Escherichia coli* O157:H7 grown in vitro in the sterile-filtrated cecal content of human gut microbiota associated rats reveals an adaptive expression of metabolic and virulence genes. *Microbes and Infection*, *17*, 23–33.
- Le Bihan, G., Sicard, J.-F., Garneau, P., Bernalier-Donadille, A., Gobert, A. P., Garrivier, A., ... Jubelin, G. (2017). The NAG Sensor NagC Regulates LEE Gene Expression and Contributes to Gut Colonization by *Escherichia coli* O157:H7. *Frontiers in Cellular and Infection Microbiology*, *7*, 134.
- Lee, J.-Y., Tsohis, R. M., & Bäumlner, A. J. (2022). The microbiome and gut homeostasis. *Science*, *377*, eabp9960.
- Lee, S. M., Donaldson, G. P., Mikulski, Z., Boyajian, S., Ley, K., & Mazmanian, S. K. (2013). Bacterial colonization factors control specificity and stability of the gut microbiota. *Nature*, *501*, 426–429.
- Lewis, A. L., & Lewis, W. G. (2012). Host sialoglycans and bacterial sialidases: A mucosal perspective: Mucosal sialoglycans and bacterial sialidases. *Cellular Microbiology*, *14*, 1174–1182.
- Li, H., Limenitakis, J. P., Fuhrer, T., Geuking, M. B., Lawson, M. A., Wyss, M., ... Macpherson, A. J. (2015). The outer mucus layer hosts a distinct intestinal microbial niche. *Nature Communications*, *6*, 8292.
- Li, J., Sayeed, S., Robertson, S., Chen, J., & McClane, B. A. (2011). Sialidases Affect the Host Cell Adherence and Epsilon Toxin-Induced Cytotoxicity of *Clostridium perfringens* Type D Strain CN3718. *PLOS Pathogens*, *7*, e1002429.
- Liang, Q., & Vallance, B. A. (2021). What's for dinner? How *Citrobacter rodentium*'s metabolism helps it thrive in the competitive gut. *Current Opinion in Microbiology*, *63*, 76–82.
- Lin, X., Yao, H., Guo, J., Huang, Y., Wang, W., Yin, B., ... Liu, L. (2022). Protein Glycosylation and Gut Microbiota Utilization Can Limit the In Vitro and In Vivo

- Metabolic Cellular Incorporation of Neu5Gc. *Molecular Nutrition & Food Research*, *66*, 2100615.
- Liu, L., Saitz-Rojas, W., Smith, R., Gonyar, L., In, J. G., Kovbasnjuk, O., ... Ruiz-Perez, F. (2020). Mucus layer modeling of human colonoids during infection with enteroaggregative *E. coli*. *Scientific Reports*, *10*, 10533.
- Lopez, C. A., Miller, B. M., Rivera-Chavez, F., Velazquez, E. M., Byndloss, M. X., Chavez-Arroyo, A., ... Baumler, A. J. (2016). Virulence factors enhance *Citrobacter rodentium* expansion through aerobic respiration. *Science*, *353*, 1249–1253.
- Luis, A. S., Jin, C., Pereira, G. V., Glowacki, R. W. P., Gugel, S., Singh, S., ... Martens, E. C. (2021). A single sulfatase is required to access colonic mucin by a gut bacterium. *Nature*, *598*, 332–337.
- Lundberg, J. O., Weitzberg, E., Cole, J. A., & Benjamin, N. (2004). Nitrate, bacteria and human health. *Nature Reviews Microbiology*, *2*, 593–602.
- Luo, Q., Kumar, P., Vickers, T. J., Sheikh, A., Lewis, W. G., Rasko, D. A., ... Fleckenstein, J. M. (2014). Enterotoxigenic *Escherichia coli* Secretes a Highly Conserved Mucin-Degrading Metalloprotease To Effectively Engage Intestinal Epithelial Cells. *Infection and Immunity*, *82*, 509–521.
- Luperchio, S. A., & Schauer, D. B. (2001). Molecular pathogenesis of *Citrobacter rodentium* and transmissible murine colonic hyperplasia. *Microbes and Infection*, *3*, 333–340.
- Lupp, C., Robertson, M. L., Wickham, M. E., Sekirov, I., Champion, O. L., Gaynor, E. C., & Finlay, B. B. (2007). Host-Mediated Inflammation Disrupts the Intestinal Microbiota and Promotes the Overgrowth of Enterobacteriaceae. *Cell Host & Microbe*, *2*, 119–129.
- Mann, E., Shekarriz, S., & Surette, M. G. (2022). Human Gut Metagenomes Encode Diverse GH156 Sialidases. *Applied and Environmental Microbiology*, *88*, e01755-22.
- Marcobal, A., Southwick, A. M., Earle, K. A., & Sonnenburg, J. L. (2013). A refined palate: Bacterial consumption of host glycans in the gut. *Glycobiology*, *23*, 1038–1046.
- Matziouridou, C., Rocha, S. D. C., Haabeth, O. A., Rudi, K., Carlsen, H., & Kielland, A. (2018). INOS- and NOX1-dependent ROS production maintains bacterial homeostasis in the ileum of mice. *Mucosal Immunology*, *11*, 774–784.
- Mauriello, E. M. F., Mignot, T., Yang, Z., & Zusman, D. R. (2010). Gliding Motility Revisited: How Do the Myxobacteria Move without Flagella? *Microbiology and Molecular Biology Reviews* : *MMBR*, *74*, 229–249.
- McDonald, N. D., Lubin, J.-B., Chowdhury, N., & Boyd, E. F. (2016). Host-Derived Sialic Acids Are an Important Nutrient Source Required for Optimal Bacterial Fitness *In Vivo*. *MBio*, *7*. <https://doi.org/10.1128/mBio.02237-15>
- McGuckin, M. A., Lindén, S. K., Sutton, P., & Florin, T. H. (2011). Mucin dynamics and enteric pathogens. *Nature Reviews Microbiology*, *9*, 265–278.
- Mellies, J. L., Navarro-Garcia, F., Okeke, I., Frederickson, J., Nataro, J. P., & Kaper, J. B. (2001). EspC Pathogenicity Island of Enteropathogenic *Escherichia coli* Encodes an Enterotoxin. *Infection and Immunity*, *69*, 315–324.
- Menezes-Garcia, Z., Kumar, A., Zhu, W., Winter, S. E., & Sperandio, V. (2020). L-Arginine sensing regulates virulence gene expression and disease progression in enteric pathogens. *Proceedings of the National Academy of Sciences*, *117*, 12387–12393.

- Miller, B. M., Liou, M. J., Zhang, L. F., Nguyen, H., Litvak, Y., Schorr, E.-M., ... Bäumlner, A. J. (2020). Anaerobic Respiration of NOX1-Derived Hydrogen Peroxide Licenses Bacterial Growth at the Colonic Surface. *Cell Host & Microbe*, *28*, 789-797.e5.
- Montrose, D. C., Nishiguchi, R., Basu, S., Staab, H. A., Zhou, X. K., Wang, H., ... Dannenberg, A. J. (2021). Dietary Fructose Alters the Composition, Localization, and Metabolism of Gut Microbiota in Association With Worsening Colitis. *Cellular and Molecular Gastroenterology and Hepatology*, *11*, 525–550.
- Mullineaux-Sanders, C., Collins, J. W., Ruano-Gallego, D., Levy, M., Pevsner-Fischer, M., Glegola-Madejska, I. T., ... Frankel, G. (2017). Citrobacter rodentium Relies on Commensals for Colonization of the Colonic Mucosa. *Cell Reports*, *21*, 3381–3389.
- Mullineaux-Sanders, C., Sanchez-Garrido, J., Hopkins, E. G. D., Shenoy, A. R., Barry, R., & Frankel, G. (2019). Citrobacter rodentium–host–microbiota interactions: Immunity, bioenergetics and metabolism. *Nature Reviews Microbiology*, *17*, 701–715.
- Mundy, R., Pickard, D., Wilson, R. K., Simmons, C. P., Dougan, G., & Frankel, G. (2003). Identification of a novel type IV pilus gene cluster required for gastrointestinal colonization of Citrobacter rodentium. *Molecular Microbiology*, *48*, 795–809.
- Nakanishi, N., Tashiro, K., Kuhara, S., Hayashi, T., Sugimoto, N., & Tobe, T. (2009). Regulation of virulence by butyrate sensing in enterohaemorrhagic Escherichia coli. *Microbiology*, *155*, 521–530.
- Navarro-Garcia, F., Gutierrez-Jimenez, J., Garcia-Tovar, C., Castro, L. A., Salazar-Gonzalez, H., & Cordova, V. (2010). Pic, an Autotransporter Protein Secreted by Different Pathogens in the Enterobacteriaceae Family, Is a Potent Mucus Secretagogue. *Infection and Immunity*, *78*, 4101–4109.
- Navarro-Garcia, F., Serapio-Palacios, A., Vidal, J. E., Salazar, M. I., & Tapia-Pastrana, G. (2014). EspC Promotes Epithelial Cell Detachment by Enteropathogenic Escherichia coli via Sequential Cleavages of a Cytoskeletal Protein and then Focal Adhesion Proteins. *Infection and Immunity*, *82*, 2255–2265.
- Neelamegham, S., Aoki-Kinoshita, K., Bolton, E., Frank, M., Lisacek, F., Lütteke, T., ... SNFG Discussion Group. (2019). Updates to the Symbol Nomenclature for Glycans guidelines. *Glycobiology*, *29*, 620–624.
- Nesta, B., Valeri, M., Spagnuolo, A., Rosini, R., Mora, M., Donato, P., ... Serino, L. (2014). SslE Elicits Functional Antibodies That Impair In Vitro Mucinase Activity and In Vivo Colonization by Both Intestinal and Extraintestinal Escherichia coli Strains. *PLOS Pathogens*, *10*, e1004124.
- Newstead, S. L., Potter, J. A., Wilson, J. C., Xu, G., Chien, C.-H., Watts, A. G., ... Taylor, G. L. (2008). The Structure of Clostridium perfringens NanI Sialidase and Its Catalytic Intermediates. *The Journal of Biological Chemistry*, *283*, 9080–9088.
- Ng, K. M., Ferreyra, J. A., Higginbottom, S. K., Lynch, J. B., Kashyap, P. C., Gopinath, S., ... Sonnenburg, J. L. (2013). Microbiota-liberated host sugars facilitate post-antibiotic expansion of enteric pathogens. *Nature*, *502*, 96–99.
- Nguyen, J., Pepin, D. M., & Tropini, C. (2021). Cause or effect? The spatial organization of pathogens and the gut microbiota in disease. *Microbes and Infection*, *23*, 104815.
- Nishiyama, K., Nagai, A., Uribayashi, K., Yamamoto, Y., Mukai, T., & Okada, N. (2018). Two extracellular sialidases from Bifidobacterium bifidum promote the degradation of sialyl-oligosaccharides and support the growth of Bifidobacterium breve. *Anaerobe*, *52*, 22–28.

- North, R. A., Horne, C. R., Davies, J. S., Remus, D. M., Muscroft-Taylor, A. C., Goyal, P., ... Dobson, R. C. J. (2018). "Just a spoonful of sugar...": Import of sialic acid across bacterial cell membranes. *Biophysical Reviews*, *10*, 219–227.
- Osbelt, L., Thiemann, S., Smit, N., Lesker, T. R., Schröter, M., Gálvez, E. J. C., ... Strowig, T. (2020). Variations in microbiota composition of laboratory mice influence *Citrobacter rodentium* infection via variable short-chain fatty acid production. *PLOS Pathogens*, *16*, e1008448.
- Pacheco, A. R., Curtis, M. M., Ritchie, J. M., Munera, D., Waldor, M. K., Moreira, C. G., & Sperandio, V. (2012). Fucose sensing regulates bacterial intestinal colonization. *Nature*, *492*, 113–117.
- Pacheco, A. R., & Sperandio, V. (2015). Enteric Pathogens Exploit the Microbiota-generated Nutritional Environment of the Gut. *Microbiology Spectrum*, *3*, 10.1128/microbiolspec.MBP-0001–2014.
- Pal, R. R., Baidya, A. K., Mamou, G., Bhattacharya, S., Socol, Y., Kobi, S., ... Rosenshine, I. (2019). Pathogenic *E. coli* Extracts Nutrients from Infected Host Cells Utilizing Injectisome Components. *Cell*, *177*, 683–696.e18.
- Papapietro, O., Teatero, S., Thanabalasuriar, A., Yuki, K. E., Diez, E., Zhu, L., ... Gruenheid, S. (2013). R-Spondin 2 signalling mediates susceptibility to fatal infectious diarrhoea. *Nature Communications*, *4*. <https://doi.org/10.1038/ncomms2816>
- Petty, N. K., Bulgin, R., Crepin, V. F., Cerdeño-Tárraga, A. M., Schroeder, G. N., Quail, M. A., ... Thomson, N. R. (2010). The *Citrobacter rodentium* Genome Sequence Reveals Convergent Evolution with Human Pathogenic *Escherichia coli*. *Journal of Bacteriology*, *192*, 525–538.
- Pifer, R., Russell, R. M., Kumar, A., Curtis, M. M., & Sperandio, V. (2018). Redox, amino acid, and fatty acid metabolism intersect with bacterial virulence in the gut. *Proceedings of the National Academy of Sciences*, *115*, E10712–E10719.
- Pircalabioru, G., Aviello, G., Kubica, M., Zhdanov, A., Paclat, M.-H., Brennan, L., ... Knaus, U. G. (2016). Defensive Mutualism Rescues NADPH Oxidase Inactivation in Gut Infection. *Cell Host & Microbe*, *19*, 651–663.
- Png, C. W., Lindén, S. K., Gilshenan, K. S., Zoetendal, E. G., McSweeney, C. S., Sly, L. I., ... Florin, T. H. J. (2010). Mucolytic bacteria with increased prevalence in IBD mucosa augment in vitro utilization of mucin by other bacteria. *The American Journal of Gastroenterology*, *105*, 2420–2428.
- Pokharel, P., Habouria, H., Bessaiah, H., & Dozois, C. M. (2019). Serine Protease Autotransporters of the Enterobacteriaceae (SPATEs): Out and About and Chopping It Up. *Microorganisms*, *7*, 594.
- Popov, G., Fiebig-Comyn, A., Shideler, S., Coombes, B. K., & Savchenko, A. (2019). Complete Genome Sequence of *Citrobacter rodentium* Strain DBS100. *Microbiology Resource Announcements*, *8*, e00421-19.
- Pruss, K. M., Marcobal, A., Southwick, A. M., Dahan, D., Smits, S. A., Ferreyra, J. A., ... Sonnenburg, J. L. (2021). Mucin-derived O-glycans supplemented to diet mitigate diverse microbiota perturbations. *The ISME Journal*, *15*, 577–591.
- Ramirez, J., Guarner, F., Bustos Fernandez, L., Maruy, A., Sdepanian, V. L., & Cohen, H. (2020). Antibiotics as Major Disruptors of Gut Microbiota. *Frontiers in Cellular and*

- Infection Microbiology*, 10. Retrieved from <https://www.frontiersin.org/articles/10.3389/fcimb.2020.572912>
- Ravcheev, D. A., & Thiele, I. (2017). Comparative Genomic Analysis of the Human Gut Microbiome Reveals a Broad Distribution of Metabolic Pathways for the Degradation of Host-Synthesized Mucin Glycans and Utilization of Mucin-Derived Monosaccharides. *Frontiers in Genetics*, 8. Retrieved from <https://www.frontiersin.org/articles/10.3389/fgene.2017.00111>
- Rivera-Chávez, F., Zhang, L. F., Faber, F., Lopez, C. A., Byndloss, M. X., Olsan, E. E., ... Bäumler, A. J. (2016). Depletion of Butyrate-Producing Clostridia from the Gut Microbiota Drives an Aerobic Luminal Expansion of Salmonella. *Cell Host & Microbe*, 19, 443–454.
- Robbe, C., Capon, C., Coddeville, B., & Michalski, J.-C. (2004). Structural diversity and specific distribution of O-glycans in normal human mucins along the intestinal tract. *Biochemical Journal*, 384, 307–316.
- Robbe, C., Capon, C., Maes, E., Rousset, M., Zweibaum, A., Zanetta, J.-P., & Michalski, J.-C. (2003). Evidence of Regio-specific Glycosylation in Human Intestinal Mucins: PRESENCE OF AN ACIDIC GRADIENT ALONG THE INTESTINAL TRACT *. *Journal of Biological Chemistry*, 278, 46337–46348.
- Robbe-Masselot, C., Maes, E., Rousset, M., Michalski, J.-C., & Capon, C. (2009). Glycosylation of human fetal mucins: A similar repertoire of O-glycans along the intestinal tract. *Glycoconjugate Journal*, 26, 397–413.
- Roberton, A. M., & Corfield, A. P. (1999). Mucin degradation and its significance in inflammatory conditions of the gastrointestinal tract. In G. W. Tannock (Ed.), *Medical Importance of the Normal Microflora* (pp. 222–261). Boston, MA: Springer US.
- Robinson, L. S., Lewis, W. G., & Lewis, A. L. (2017). The sialate O-acetyltransferase EstA from gut Bacteroidetes species enables sialidase-mediated cross-species foraging of 9-O-acetylated sialoglycans. *Journal of Biological Chemistry*, 292, 11861–11872.
- Rogers, A. P., Mileto, S. J., & Lyras, D. (2022). Impact of enteric bacterial infections at and beyond the epithelial barrier. *Nature Reviews Microbiology*, 1–15.
- Rowley, C. A., Sauder, A. B., & Kendall, M. M. (2020). The Ethanolamine-Sensing Transcription Factor EutR Promotes Virulence and Transmission during *Citrobacter rodentium* Intestinal Infection. *Infection and Immunity*, 88, e00137-20.
- Ruiz-Perez, F., & Nataro, J. P. (2014). Bacterial serine proteases secreted by the autotransporter pathway: Classification, specificity and role in virulence. *Cellular and Molecular Life Sciences : CMLS*, 71, 745–770.
- Ryan, K. J. (2017). Enterobacteriaceae. In *Sherris Medical Microbiology* (7th ed.). New York, NY: McGraw-Hill Education.
- Sanchez, K. K., Chen, G. Y., Schieber, A. M. P., Redford, S. E., Shokhirev, M. N., Leblanc, M., ... Ayres, J. S. (2018). Cooperative Metabolic Adaptations in the Host Can Favor Asymptomatic Infection and Select for Attenuated Virulence in an Enteric Pathogen. *Cell*. <https://doi.org/10.1016/j.cell.2018.07.016>
- Schroeder, B. O., Birchenough, G. M. H., Ståhlman, M., Arike, L., Johansson, M. E. V., Hansson, G. C., & Bäckhed, F. (2018). Bifidobacteria or Fiber Protects against Diet-Induced Microbiota-Mediated Colonic Mucus Deterioration. *Cell Host & Microbe*, 23, 27-40.e7.

- Segura, A., Bertoni, M., Auffret, P., Klopp, C., Bouchez, O., Genthon, C., ... Forano, E. (2018). Transcriptomic analysis reveals specific metabolic pathways of enterohemorrhagic *Escherichia coli* O157:H7 in bovine digestive contents. *BMC Genomics*, *19*, 766.
- Sekirov, I., Tam, N. M., Jogova, M., Robertson, M. L., Li, Y., Lupp, C., & Finlay, B. B. (2008). Antibiotic-Induced Perturbations of the Intestinal Microbiota Alter Host Susceptibility to Enteric Infection. *Infection and Immunity*, *76*, 4726–4736.
- Serapio-Palacios, A., & Navarro-Garcia, F. (2016). EspC, an Autotransporter Protein Secreted by Enteropathogenic *Escherichia coli*, Causes Apoptosis and Necrosis through Caspase and Calpain Activation, Including Direct Procaspase-3 Cleavage. *MBio*, *7*, e00479-16, /mbio/7/3/e00479-16.atom.
- Serapio-Palacios, A., Woodward, S. E., Vogt, S. L., Deng, W., Creus-Cuadros, A., Huus, K. E., ... Finlay, B. B. (2022). Type VI secretion systems of pathogenic and commensal bacteria mediate niche occupancy in the gut. *Cell Reports*, *39*, 110731.
- Shi, W., & Sun, H. (2002). Type IV Pilus-Dependent Motility and Its Possible Role in Bacterial Pathogenesis. *Infection and Immunity*, *70*, 1–4.
- Shimizu, K., Seiki, I., Goto, Y., & Murata, T. (2021). Measurement of the Intestinal pH in Mice under Various Conditions Reveals Alkalinization Induced by Antibiotics. *Antibiotics*, *10*, 180.
- Sjögren, J., & Collin, M. (2014). Bacterial glycosidases in pathogenesis and glycoengineering. *Future Microbiology*, *9*, 1039–1051.
- Slater, S. L., & Frankel, G. (2020). Advances and Challenges in Studying Type III Secretion Effectors of Attaching and Effacing Pathogens. *Frontiers in Cellular and Infection Microbiology*, *10*. Retrieved from <https://www.frontiersin.org/articles/10.3389/fcimb.2020.00337>
- Smith, A. D., Yan, X., Chen, C., Dawson, H. D., & Bhagwat, A. A. (2016). Understanding the host-adapted state of *Citrobacter rodentium* by transcriptomic analysis. *Archives of Microbiology*, *198*, 353–362.
- Soderholm, A. T., & Pedicord, V. A. (2019). Intestinal epithelial cells: At the interface of the microbiota and mucosal immunity. *Immunology*, *158*, 267–280.
- Sonnenburg, J. L., Xu, J., Leip, D. D., Chen, C.-H., Westover, B. P., Weatherford, J., ... Gordon, J. I. (2005). Glycan Foraging in Vivo by an Intestine-Adapted Bacterial Symbiont. *Science*, *307*, 1955–1959.
- Stacy, A., Andrade-Oliveira, V., McCulloch, J. A., Hild, B., Oh, J. H., Perez-Chaparro, P. J., ... Belkaid, Y. (2021). Infection trains the host for microbiota-enhanced resistance to pathogens. *Cell*, *184*, 615-627.e17.
- Stahl, M., Friis, L. M., Nothhaft, H., Liu, X., Li, J., Szymanski, C. M., & Stintzi, A. (2011). L-Fucose utilization provides *Campylobacter jejuni* with a competitive advantage. *Proceedings of the National Academy of Sciences*, *108*, 7194–7199.
- Stahl, Martin, Frirdich, E., Vermeulen, J., Badayeva, Y., Li, X., Vallance, B. A., & Gaynor, E. C. (2016). The Helical Shape of *Campylobacter jejuni* Promotes *In Vivo* Pathogenesis by Aiding Transit through Intestinal Mucus and Colonization of Crypts. *Infection and Immunity*, *84*, 3399–3407.
- Stecher, B., Barthel, M., Schlumberger, M. C., Haberli, L., Rabsch, W., Kremer, M., & Hardt, W.-D. (2008). Motility allows *S. Typhimurium* to benefit from the mucosal defence. *Cellular Microbiology*, *10*, 1166–1180.

- Stecher, B., Macpherson, A. J., Hapfelmeier, S., Kremer, M., Stallmach, T., & Hardt, W.-D. (2005). Comparison of *Salmonella enterica* Serovar Typhimurium Colitis in Germfree Mice and Mice Pretreated with Streptomycin. *Infection and Immunity*, *73*, 3228–3241.
- Stein, M., Kenny, B., Stein, M. A., & Finlay, B. B. (1996). Characterization of EspC, a 110-kilodalton protein secreted by enteropathogenic *Escherichia coli* which is homologous to members of the immunoglobulin A protease-like family of secreted proteins. *Journal of Bacteriology*, *178*, 6546–6554.
- Sun, J., Shen, X., Li, Y., Guo, Z., Zhu, W., Zuo, L., ... Li, J. (2016). Therapeutic Potential to Modify the Mucus Barrier in Inflammatory Bowel Disease. *Nutrients*, *8*, 44.
- Taguchi, H., Takahashi, M., Yamaguchi, H., Osaki, T., Komatsu, A., Fujioka, Y., & Kamiya, S. (2002). Experimental infection of germ-free mice with hyper-toxigenic enterohaemorrhagic *Escherichia coli* O157:H7, strain 6. *Journal of Medical Microbiology*, *51*, 336–343.
- Tailford, L. E., Crost, E. H., Kavanaugh, D., & Juge, N. (2015). Mucin glycan foraging in the human gut microbiome. *Frontiers in Genetics*, *6*. Retrieved from <https://www.frontiersin.org/articles/10.3389/fgene.2015.00081>
- Tailford, L. E., Owen, C. D., Walshaw, J., Crost, E. H., Hardy-Goddard, J., Le Gall, G., ... Juge, N. (2015). Discovery of intramolecular trans-sialidases in human gut microbiota suggests novel mechanisms of mucosal adaptation. *Nature Communications*, *6*. <https://doi.org/10.1038/ncomms8624>
- Thomas, G. H. (2016). Sialic acid acquisition in bacteria—one substrate, many transporters. *Biochemical Society Transactions*, *44*, 760–765.
- Thomas, M. K., Murray, R., Flockhart, L., Pintar, K., Fazil, A., Nesbitt, A., ... Pollari, F. (2015). Estimates of Foodborne Illness–Related Hospitalizations and Deaths in Canada for 30 Specified Pathogens and Unspecified Agents. *Foodborne Pathogens and Disease*, *12*, 820–827.
- Thomsson, K. A., Holmén-Larsson, J. M., Ångström, J., Johansson, M. E., Xia, L., & Hansson, G. C. (2012). Detailed O-glycomics of the Muc2 mucin from colon of wild-type, core 1- and core 3-transferase-deficient mice highlights differences compared with human MUC2. *Glycobiology*, *22*, 1128–1139.
- Tropini, C., Earle, K. A., Huang, K. C., & Sonnenburg, J. L. (2017). The Gut Microbiome: Connecting Spatial Organization to Function. *Cell Host & Microbe*, *21*, 433–442.
- Tsai, K., Ma, C., Han, X., Allaire, J., Lunken, G. R., Crowley, S. M., ... Vallance, B. A. (2022). Highly Sensitive, Flow Cytometry-Based Measurement of Intestinal Permeability in Models of Experimental Colitis. *Cellular and Molecular Gastroenterology and Hepatology*, *15*, 425–438.
- Turner, N. C. A., Connolly, J. P. R., & Roe, A. J. (2019). Control freaks—Signals and cues governing the regulation of virulence in attaching and effacing pathogens. *Biochemical Society Transactions*, *47*, 229–238.
- Vallance, B. A., & Finlay, B. B. (2000). Exploitation of host cells by enteropathogenic *Escherichia coli*. *Proceedings of the National Academy of Sciences*, *97*, 8799–8806.
- Vallance, Bruce A., Deng, W., Knodler, L. A., & Finlay, B. B. (2002). Mice Lacking T and B Lymphocytes Develop Transient Colitis and Crypt Hyperplasia yet Suffer Impaired Bacterial Clearance during *Citrobacter rodentium* Infection. *Infection and Immunity*, *70*, 2070–2081.

- Van der Sluis, M., De Koning, B. A. E., De Bruijn, A. C. J. M., Velcich, A., Meijerink, J. P. P., Van Goudoever, J. B., ... Einerhand, A. W. C. (2006). Muc2-Deficient Mice Spontaneously Develop Colitis, Indicating That MUC2 Is Critical for Colonic Protection. *Gastroenterology*, *131*, 117–129.
- Vidal, J. E., & Navarro-García, F. (2006). Efficient Translocation of EspC into Epithelial Cells Depends on Enteropathogenic Escherichia coli and Host Cell Contact. *Infection and Immunity*, *74*, 2293–2303.
- Vidal, J. E., & Navarro-García, F. (2008). EspC translocation into epithelial cells by enteropathogenic Escherichia coli requires a concerted participation of type V and III secretion systems. *Cellular Microbiology*, *10*, 1975–1986.
- Vijayakumar, V., Santiago, A., Smith, R., Smith, M., Robins-Browne, R. M., Nataro, J. P., & Ruiz-Perez, F. (2014). Role of Class 1 Serine Protease Autotransporter in the Pathogenesis of Citrobacter rodentium Colitis. *Infection and Immunity*, *82*, 2626–2636.
- Wadhams, G. H., & Armitage, J. P. (2004). Making sense of it all: Bacterial chemotaxis. *Nature Reviews Molecular Cell Biology*, *5*, 1024–1037.
- Wiles, S., Clare, S., Harker, J., Huett, A., Young, D., Dougan, G., & Frankel, G. (2004). Organ specificity, colonization and clearance dynamics in vivo following oral challenges with the murine pathogen Citrobacter rodentium. *Cellular Microbiology*, *6*, 963–972.
- Wiles, S., Dougan, G., & Frankel, G. (2005). Emergence of a “hyperinfectious” bacterial state after passage of Citrobacter rodentium through the host gastrointestinal tract. *Cellular Microbiology*, *7*, 1163–1172.
- Willing, B. P., Vacharaksa, A., Croxen, M., Thanachayanont, T., & Finlay, B. B. (2011). Altering Host Resistance to Infections through Microbial Transplantation. *PLoS ONE*, *6*, e26988.
- Winson, M. K., Swift, S., Hill, P. J., Sims, C. M., Griesmayr, G., Bycroft, B. W., ... Stewart, G. S. A. B. (1998). Engineering the luxCDABE genes from Photobacterium luminescens to provide a bioluminescent reporter for constitutive and promoter probe plasmids and mini-Tn5 constructs. *FEMS Microbiology Letters*, *163*, 193–202.
- Wong, A. R. C., Pearson, J. S., Bright, M. D., Munera, D., Robinson, K. S., Lee, S. F., ... Hartland, E. L. (2011). Enteropathogenic and enterohaemorrhagic Escherichia coli: Even more subversive elements. *Molecular Microbiology*, *80*, 1420–1438.
- Wrzosek, L., Miquel, S., Noordine, M.-L., Bouet, S., Chevalier-Curt, M. J., Robert, V., ... Thomas, M. (2013). Bacteroides thetaiotaomicron and Faecalibacterium prausnitzii influence the production of mucus glycans and the development of goblet cells in the colonic epithelium of a gnotobiotic model rodent. *BMC Biology*, *11*, 61.
- Xicohtencatl-Cortes, J., Saldaña, Z., Deng, W., Castañeda, E., Freer, E., Tarr, P. I., ... Girón, J. A. (2010). Bacterial Macroscopic Rope-like Fibers with Cytopathic and Adhesive Properties. *Journal of Biological Chemistry*, *285*, 32336–32342.
- Xu, J., Bjursell, M. K., Himrod, J., Deng, S., Carmichael, L. K., Chiang, H. C., ... Gordon, J. I. (2003). A Genomic View of the Human-Bacteroides thetaiotaomicron Symbiosis. *Science*, *299*, 2074–2076.
- Yao, Y., Kim, G., Shafer, S., Chen, Z., Kubo, S., Ji, Y., ... Lenardo, M. J. (2022). Mucus sialylation determines intestinal host-commensal homeostasis. *Cell*, *185*, 1172-1188.e28.
- Zachar, Z., & Savage, D. C. (1979). Microbial interference and colonization of the murine gastrointestinal tract by Listeria monocytogenes. *Infection and Immunity*, *23*, 168–174.

Zarepour, M., Bhullar, K., Montero, M., Ma, C., Huang, T., Velcich, A., ... Vallance, B. A. (2013). The Mucin Muc2 Limits Pathogen Burdens and Epithelial Barrier Dysfunction during Salmonella enterica Serovar Typhimurium Colitis. *Infection and Immunity*, 81, 3672–3683.

Appendices

Appendix A : Supplementary Figures and Tables

A.1 Supplementary Information for Chapter 1

There is no supplementary information for Chapter 1. This section is included only to maintain a logical numbering system for supplementary figures.

A.2 Supplementary Figures and Tables for Chapter 2

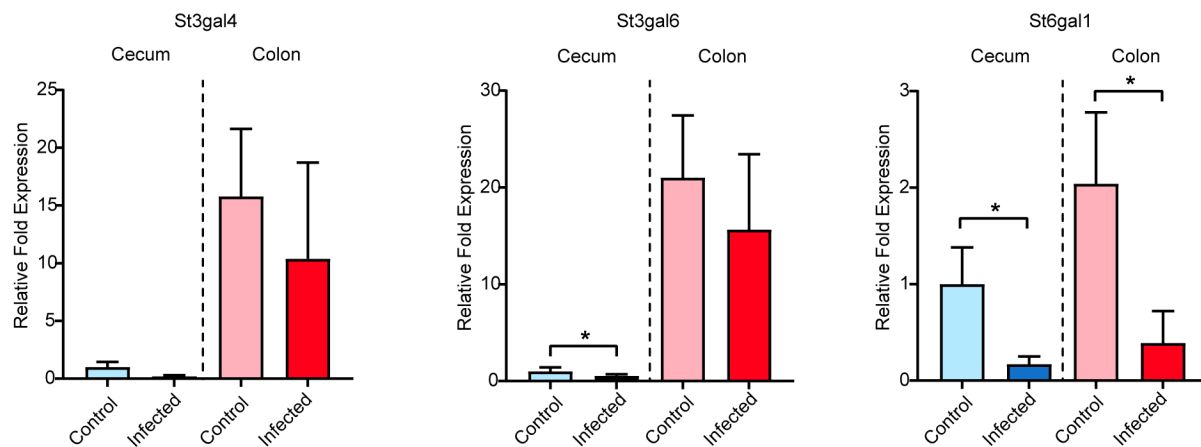


Figure A.2.1 Expression of sialyltransferase genes in mouse cecal and colonic tissues before and during *C. rodentium* infection.

ST3GAL4 and ST3GAL6 contribute to α 2,3-sialylation and ST6GAL1 catalyzes α 2,6-sialylation adds sialic acid. * p < 0.05. Statistical significance calculated by Mann-Whitney U-test.

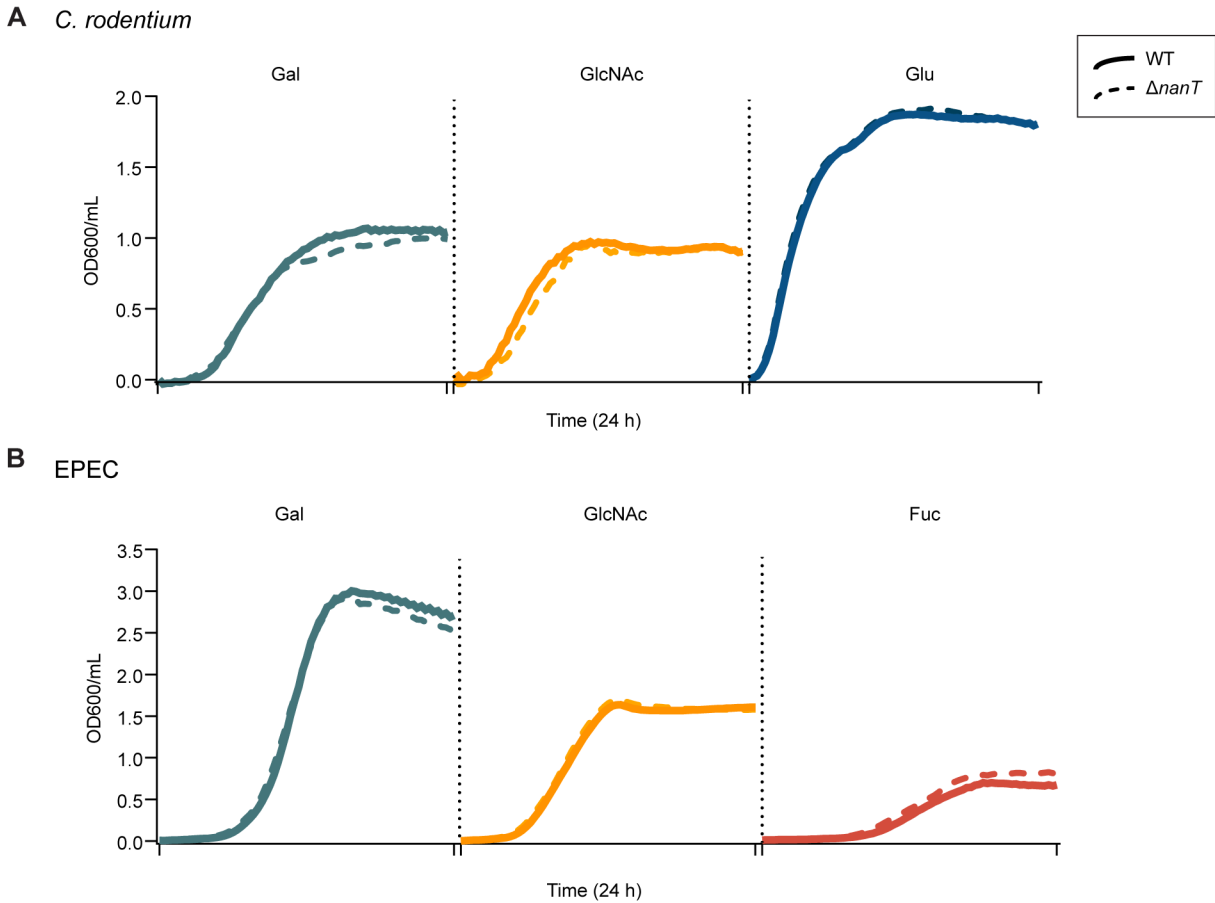


Figure A.2.2 Deletion of the *nanT* gene does not cause any growth defects in *C. rodentium* or EPEC when provided with sugars other than sialic acid.

Growth analysis of WT and $\Delta nanT$ (A) *C. rodentium* and (B) EPEC in M9 minimal medium supplemented with 0.2% galactose (Gal), *N*-acetylglucosamine (GlcNAc), fucose (Fuc) or glucose (Glu). Cultures were tracked with OD₆₀₀ readings at 20-minute intervals over 24 hours at 37°C. Data are presented as averages of cell growth ($n=9$) from three independent experiments.

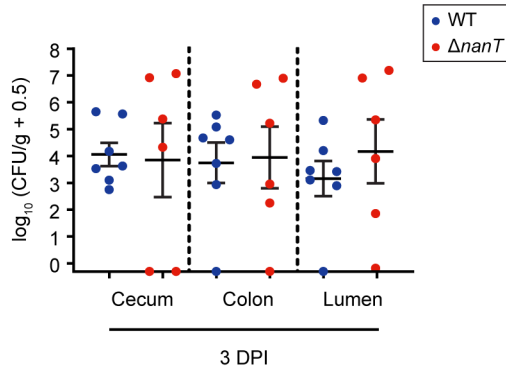


Figure A.2.3 $\Delta nanT$ *C. rodentium* colonizes the mouse intestines at similarly low levels as WT in the early stage of infection.

C57BL/6 mice were orally infected with 1×10^7 CFU of WT ($n = 7$) or $\Delta nanT$ ($n = 6$) *C. rodentium* and intestinal tissues and luminal contents were collected at 3 days post infection, plated and enumerated for *C. rodentium* CFU. Data from two independent experiments were pooled. Mean and SEM are indicated.

Table A.2.1 Primers for mutant construction

Construct and primer designation	Primer sequence (5'-3') (restriction sites are underlined)
<i>C. rodentium nanT</i> deletion mutant	
nanT-P1	GTCTAGGT <u>ACCGCGTAAACTGTCTGGTATAACAGGTA</u> (KpnI site)
nanT-P2	GTTGAGATGGCGATACCACGGGATGCTTTGGGTA
nanT-P3	GTGGTATCGCCATCTCAACGACGCTATTGACGGTAAGCCA
nanT-P4	GACAGT <u>GAGCTCTGCAAATTGCCTTCCTGGATGAT</u> (SacI site)
nanT-check-F	GTGCTGCACTATATGGATGTGGT
nanT-check-R	GATAATCGGTAGCGATACCAC
<i>C. rodentium espC</i> deletion mutant	
espC-P1	GACAGT <u>GAGCTCATTTCGGCTGGGTAAGGATTTGAGTGA</u> (SacI site)
espC-P2	AATGCTGAGATTCATAACAATGTACGCTTT
espC-P3	GAATCTCAGCATTTTGTTCACAGCAAACCCCTCCATG
espC-P4	GTCTAGGTACCATTATTTACAGCTGCTGTGCTAATACCT (KpnI site)
espC-check-F	CACAAGAAAAATGAAGCCCCT
espC-check-R	ACCTCAAAATCCCTGAAGACC
<i>C. rodentium picC</i> deletion mutant	
pic-P1	GTCTAGGTACCAGGATAACGGAGAACGGGATGAGCAG (KpnI site)
pic-P2	TTACGATAAGGACGGCATGAACGCGCAGATAAAGGACAACA
pic-P3	CCGTCCTTATCGTAAACCGGGATATCAGC
pic-P4	GACAGT <u>GAGCTCAACAAATGGACTTAATAAGCAAC</u> (SacI site)
pic-check-F	CTGAAAGGGTCTGTGTGAGTC
pic-check-R	ATGGAGGGTTTGTGTGAATA

<i>EPEC nanT</i> deletion mutant	
EPEC-P1	GTCTAGGTACCCGCATGTGCTTGCAACGGAGAGAC (KpnI site)
EPEC-P2	GCAGCGCCAAAAACGATTTAGTC
EPEC-P3	AATCGTTTTTGGCGCTGCGTTTATTTCCCTCACC
EPEC-P4	GACAGTGAGCTCCAACCTGGATAAAGCGAGTCTGCG (SacI site)
EPEC-check-F	ACAGAGACCGGGCAACAGGA
EPEC-check-R	CGGCAGCACTTACAACATCA

Table A.2.2 Primers for qPCR analysis for host cytokine responses

Target gene	Primer forward	Primer reverse
<i>Il1b</i>	CAGGATGAGGACATGAGCACC	CTCTGCAGACTCAAACCTCCAC
<i>Il6</i>	GAGGATACCACTCCCAACAGACC	AAGTGCACTACTGTTGTTTCATACA
<i>Il17a</i>	GCTCCAGAAGGCCCTCAGA	CTTCCCTCCGCATTGACA
<i>Ifng</i>	TCAAGTGGCATAGATGTGGAAGAA	TGGCTCTGCAGGATTTTCATG
<i>Rplp0</i>	AGATTTCGGGATATGCTGTTGGC	TCGGGCCTAGACCAGTGTTTC

A.3 Supplementary Figures and Tables for Chapter 3

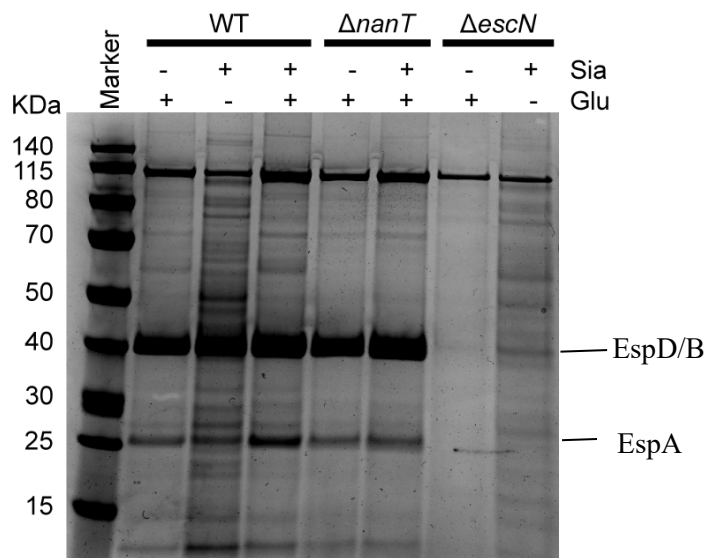


Figure A.3.1 Sialic acid induces protein secretion by EPEC.

(A) Protein secretion profiles of WT, $\Delta nanT$ and $\Delta escN$ EPEC O127:H6 E2348/69 after growth in DMEM with glucose or/and sialic acid as carbon sources. $\Delta escN$ is a negative control strain that is T3SS-deficient. Secreted proteins in equal amounts of cultures for each strain (normalized by OD_{600}) were analyzed in 4-12% SDS-PAGE and stained by Coomassie G-250.

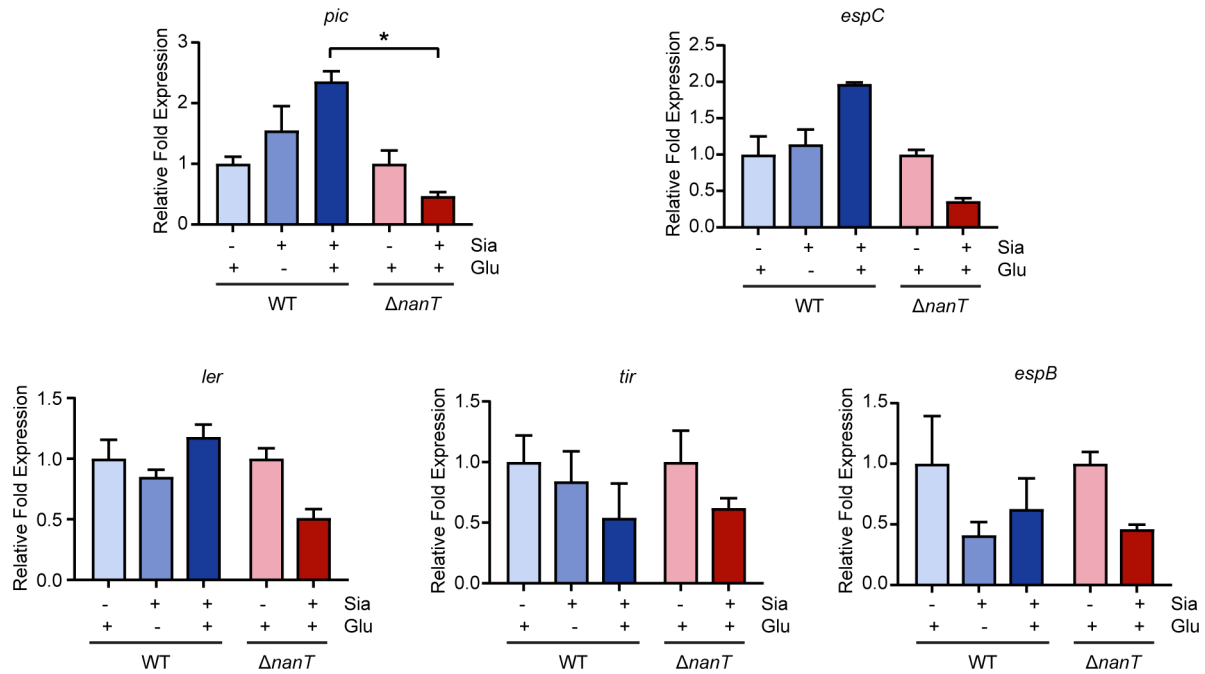


Figure A.3.2 Expression of virulence genes in WT and $\Delta nanT$ in the absence and presence of sialic acid.

Strains were grown in microaerobic conditions at 37°C in DMEM supplemented with corresponding carbon sources. Data were from three independent experiments. Fold changes were calculated relative to *rpoD* as an internal control. The mean and SEM were indicated. * $p < 0.05$. Statistical significance calculated by one-way ANOVA.

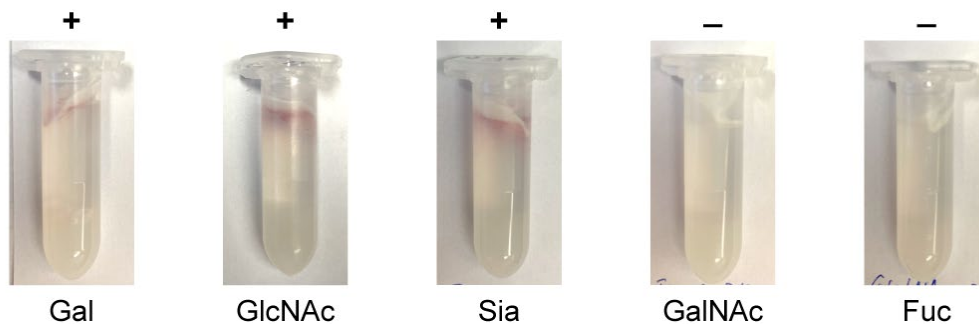


Figure A.3.3 Migration of WT *C. rodentium* towards mucin sugars.

The “+” and “-” signs indicate the presence or absence of migration towards the stimulants, visualized through the formation of red rings of bacterial cells stained with 0.01% TTC (2,3,5-triphenyltetrazolium chloride). Images are representative of at least three independent experiments.

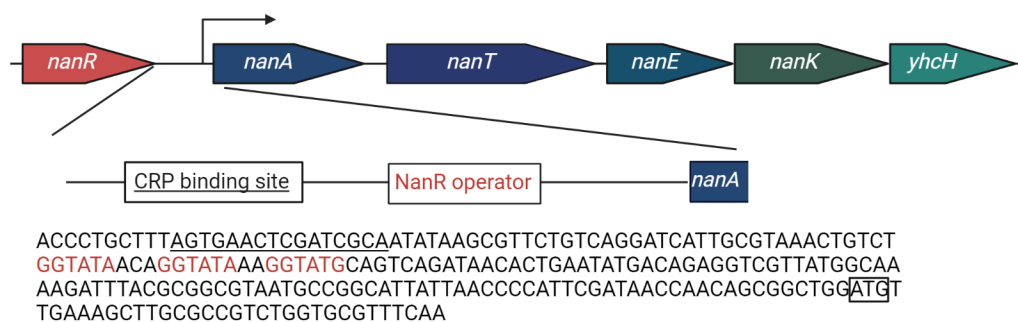


Figure A.3.4 The sialometabolic regulon in *C. rodentium* chromosome.

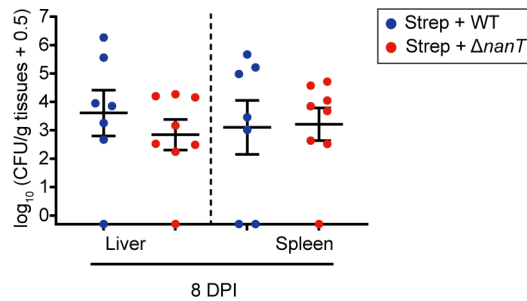
(A) The *nan* operon consists of *nanATEK-yhcH* genes for sialic acid uptake and catabolism. The *nanR* gene encodes a repressor NanR that controls the expression of the *nan* operon. (B) Intergenic region between *nanR* and *nanA*. The nucleotide sequence between the end of *nanR* and the start codon of *nanA* (boxed) is indicated. The CRP binding site is underlined. The NanR operator containing GGTATA repeats is shown in red. Figure generated with Biorender.com.

Table A.3.1 Primers for qPCR analysis for *C. rodentium* virulence gene expression

Target gene	Primer forward	Primer reverse
<i>ler</i>	ACAACAAGCCCATACATTCAGC	TGTTACTTCTTCTTCTGTGTCCTTCA
<i>tir</i>	GCC GAC AGA ACA GAC AAT AGC	ACATCCAACCTTCAGCATACG
<i>espB</i>	AAA CTG ATG CGT GAG ATG GTC	AAA CTG ATG CGT GAG ATG GTC
<i>pic</i>	CTTGCCACTTCCCAGTGCTA	TGAATCTGCCTGGCGGAAAT
<i>espC</i>	GTCCTTCACGGACATCCTGG	AACGCGGAATTCACAACTGC
<i>rpoD</i>	AAGCGAAAGTCCTGCGTATG	GCTTCGATCTGACGGATACG

A.4 Supplementary Figures and Tables for Chapter 4

A



B

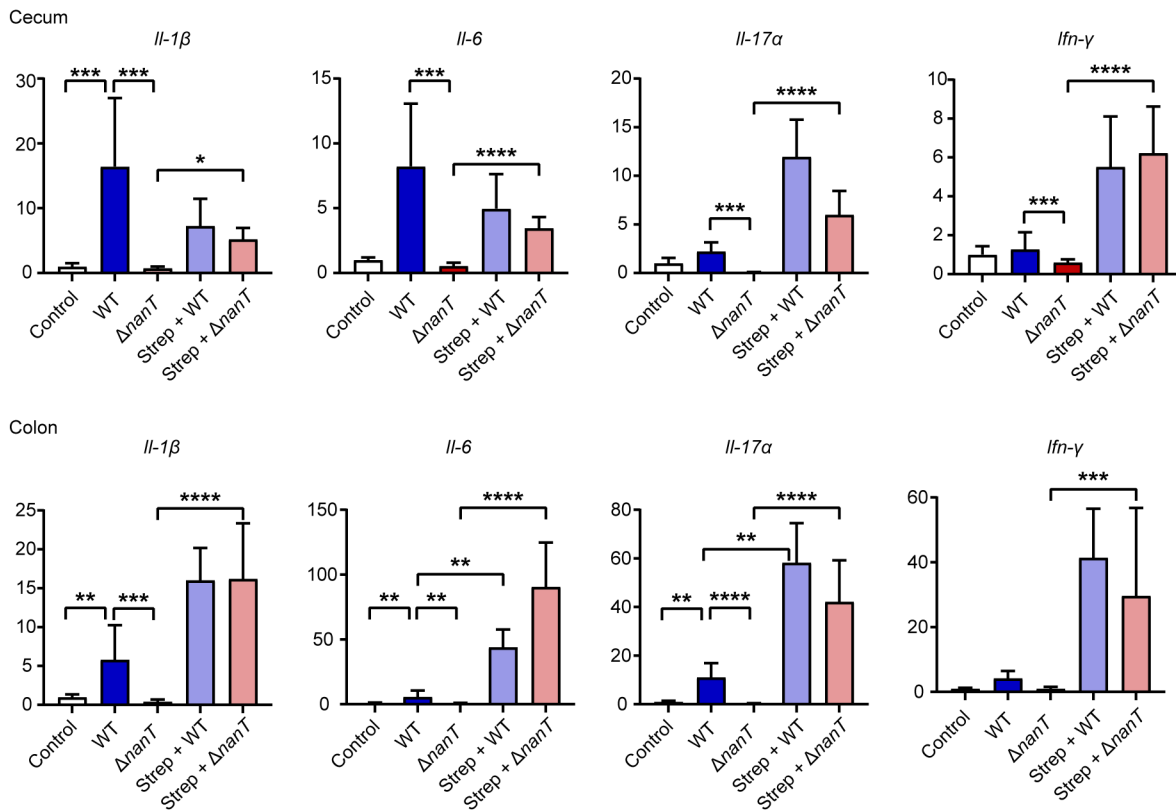


Figure A.4.1 $\Delta nanT$ *C. rodentium* was able to spread systemically and induce inflammatory responses in mice deplete of microbiota.

C57BL/6 mice were pre-treated with streptomycin prior to an infection with 1×10^7 CFU of WT ($n = 7$) or $\Delta nanT$ ($n = 6$) *C. rodentium* and (A) systemic tissues liver and spleen were collected at 8 days post infection, plated and enumerated for *C. rodentium* CFU. (B) qPCR analysis of inflammatory genes in mouse cecum and colon, expressed as fold change over control uninfected mice. **** $p < 0.0001$, *** $p < 0.001$, ** $p < 0.01$, * $p < 0.1$. Statistical significance calculated by one-way ANOVA.

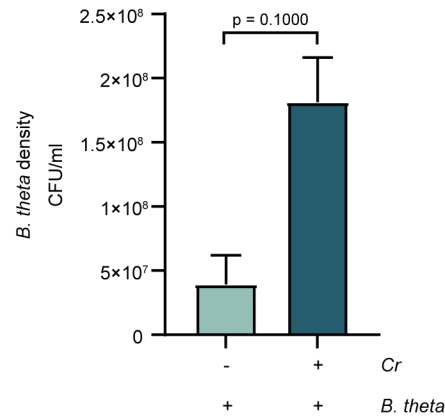


Figure A.4.2 *B. theta* displayed enhanced growth in mucins in the presence of *C. rodentium*.

Endpoint densities of *B. theta* with or without co-culture of *C. rodentium* in minimal media containing mucins as the sole carbon source was enumerated after 24 hours growth with or without *C. rodentium* in mucins under anaerobic conditions.

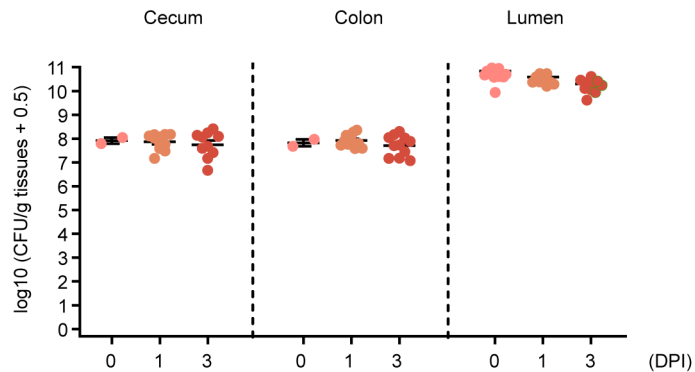


Figure A.4.3 Colonization of *B. theta* remained stable in gnotobiotic mice during *C. rodentium* infection.

Fecal samples were collected from *B. theta* mono-colonized mice before *C. rodentium* infection and at 1, 3 DPI to enumerate for *B. theta* CFU.